UDK 66:54(05) CODEN HMIDA 8 ISSN 0367–598 X

6 Hemijska industrija

Vol. 69

Časopis Saveza hemijskih inženjera

Chemical Industry

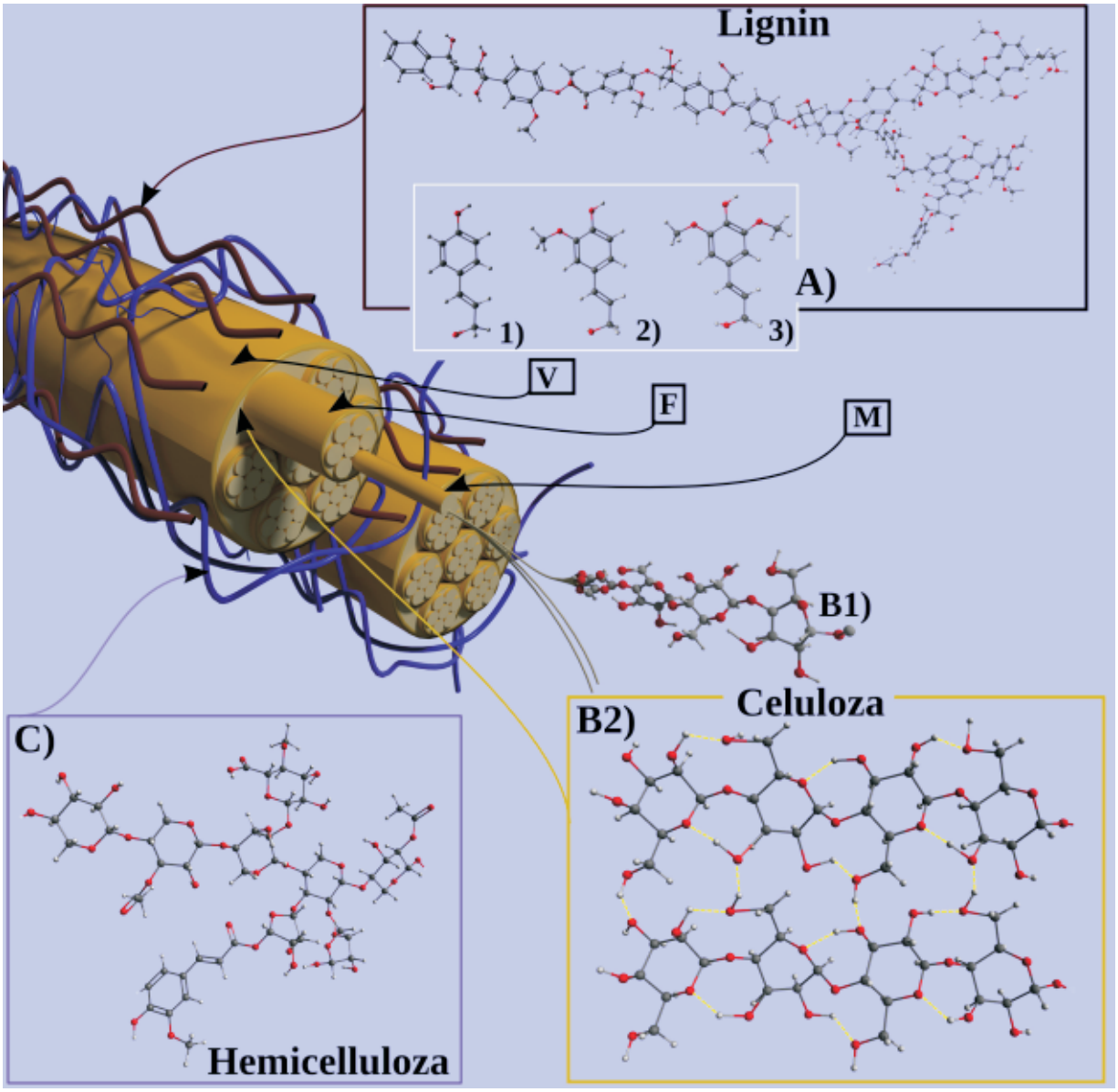

BEOGRAD, NOVEMBAR-DECEMBAR 2015. HMIDA 8, 69 (6) 587-725 (2015)

Beograd Srbija SHI

Chemical Industry
Химическая промышленность

Hemijska industrija

Časopis Saveza hemijskih inženjera Srbije
Journal of the Association of Chemical Engineers of Serbia
Журнал Союза химических инженеров Сербии

VOL. 69 **Beograd, novembar–decembar 2015** **Broj 6**

Izdavač
Savez hemijskih inženjera Srbije
Beograd, Kneza Miloša 9/I

Glavni urednik
Branko Bugarski

Zamenica glavnog i odgovornog urednika
Nevenka Bošković-Vragolović

Urednici
Katarina Jeremić, Ivana Banković-Ilić, Maja Obradović, Dušan Mijin

Članovi uredništva
Milorad Cakić, Željko Čupić, Željko Grbavčić, Katarina Jeremić, Miodrag Lazić, Slobodan Petrović, Milovan Purenović, Aleksandar Spasić, Dragoslav Stoiljković, Radmila Šećerov-Sokolović, Slobodan Šerbanović, Nikola Nikačević, Svetomir Milojević

Članovi uredništva iz inostranstva
Dragomir Bukur (SAD), Jiri Hanika (Češka Republika), Valerij Meshalkin (Rusija), Ljubiša Radović (SAD), Constantinos Vayenas (Grčka)

Likovno-grafičko rešenje naslovne strane
Milan Jovanović

Redakcija
11000 Beograd, Kneza Miloša 9/I
Tel/fax: 011/3240-018
E-pošta: shi@yubc.net
www.ache.org.rs

Izlazi dvomesečno, rukopisi se ne vraćaju

Za izdavača
Tatijana Dudukovi ć

Sekretar redakcije
Slavica Desnica

Izdavanje časopisa pomaže
Republika Srbija, Ministarstvo prosvete, nauke i tehnološkog razvoja

Uplata pretplate i oglasnog prostora vrši se na tekući račun Saveza hemijskih inženjera Srbije, Beograd, broj 205-2172-71, Komercijalna banka a.d., Beograd

Kompjuterska priprema
Vladimir Panić

Štampa
Razvojno-istraživački centar grafičkog inženjerstva, Tehnološko-metalurški fakultet, Univerzitet u Beogradu, Karnegijeva 4, 11000 Beograd

Indeksiranje
Radovi koji se publikuju u časopisu *Hemijska Industrija* ideksiraju se preko *Thompson Reuters Scietific®* servisa *Science Citation Index - Expanded™* i *Journal Citation Report (JCR)*, kao i domaćeg *SCIndeks* servisa Centra za evaluaciju u obrazovanju i nauci

SADRŽAJ/CONTENTS

SADRŽAJ Nastavak
CONTENTS Continued

GENERALNI POKROVITELJ

Hemofarm

HEMOFARM KONCERN

VRŠAC, Beogradski put bb, tel. 013/821-345, 821-027, 821-129
BEOGRAD, Prote Mateje 70, tel. 011/344-26-63, faks: 344-17-87
E-pošta: info@hemofarm.com

IZDAVANJE ČASOPISA POMOGLA JE:

INŽENJERSKA KOMORA SRBIJE
Bulevar vojvode Mišića 37
11000 Beograd

SUIZDAVAČI

Tehnološko-metalurški fakultet
Univerziteta u Beogradu, Beograd

Prirodno-matematički fakultet Univerziteta
u Novom Sadu, Novi Sad

Hemijski fakutet
Univerziteta u Beogradu
Beograd

ITNMS
Institut za tehnologiju nuklearnih i drugih
mineralnih sirovina, Beograd

HIP PETROHEMIJA
HIP Petrohemija a.d. Pančevo

Tehnološki fakultet Univerziteta
u Novom Sadu, Novi Sad

NU Institut za hemiju,
tehnologiju i metalurgiju
Univerziteta u Beogradu,
Beograd

nevena
„Nevena Color“ d.o.o.
Leskovac

Tehnološki fakultet Univerziteta
u Nišu, Leskovac

dcp-hemigal
DCP Hemigal, Leskovac

The influence of the passive evaporative cooling vest on a chemical industry workers and physiological strain level in hot conditions

Radovan M. Karkalic[1], Dalibor B. Jovanovic[2], Sonja S. Radakovic[3], Dusan S. Rajic[4], Biljana V. Petrovic[5], Negovan D. Ivankovic[1], Zeljko B. Senic[6]

[1]*University of Defense, Military Academy, Belgrade, Serbia*
[2]*Technical Test Center, General staff of the SAF, Serbia*
[3]*Medical Faculty of the Military Medical Academy, University of Defense, Belgrade, Serbia*
[4]*University of Belgrade, Innovation Center, Faculty of Technology and Metallurgy, Belgrade, Serbia*
[5]*Faculty of science, University of Kragujevac, Kragujevac, Serbia*
[6]*Military Technical Institute, Belgrade, Serbia*

Abstract

The present study was conducted in order to evaluate efficiency of a personal body cooling system based on passive evaporative technologies and its effects on test subjects and their psycho-physiological suitability during exertional heat stress in hot environment. Performed results are based on conducted tests in climatic chamber in the Military Medical Academy Institute of Hygiene in Belgrade. Ten male test subjects were subjected to exertional heat stress test consisted of walking on motorized treadmill at a speed of 5 km/h in hot environment. Tests were performed with and without cooling system. As a physiological strain indicator the following parameters have been determined: mean skin temperature, tympanic temperature, heart rate and sweat rate. Results confirmed that cooling vest worn over the clothes was able to attenuate the physiological strain levels during exercise, when compared to identical exposure without the cooling system.

Keywords: *chemical industry, heat stress, cooling vest, working uniform, physiological strain*.

Available online at the Journal website: http://www.ache.org.rs/HI/

PROFFESIONAL PAPER

UDC 614.873:66

Hem. Ind. **69** (6) 587–594 (2015)

doi: 10.2298/HEMIND140705079

Thermal insulation of clothing systems mainly depends on the physical activity and the ambiental conditions (temperature and relative humidity). The amount of heat produced by humans depends on the physical activity and can differ from 100 W while resting to over 1000 W during maximum physical performance. At extreme activity, which is often a case with winter sports, the body temperature rises with enhanced heat production. To maintain this increase within a certain limit, the body perspires in order to dissipate thermal energy from the body by evaporative cooling. If the thermal insulation of the clothing is decreased during physical activity, a part of the generated heat can be removed by convection, thus the body doesn't have to perspire so much.

The quality of insulation in a garment in terms of heat and cold will be widely managed by the thickness and density of its component fabrics. High thickness and low density make insulation better. It is observed in many cases that thermal insulation is offered by air gaps between the garment layers. However, the external temperature also influences the effectiveness of the insulation. The more extreme the temperature, be it very high or very low, the less effective the insulation becomes. Thus, a garment designed for its capability to protect against heat or cold is chosen by its wearer on the expectation of the climate in which the garment is to be worn [1].

The accumulation of heat, reflecting the peripheral and body core temperature, occurs during heavy physical exertion or exposure to warm and humid environment. Long-term accumulation of heat in a quantity of about 0.5 W/kg during 1 to 2 h, leads to an increase in body temperature that some people are unable to tolerate. Heat stress can occur in compensated and uncompensated form. Compensed heat stress (CHS) occurs when the heat loss is in balance with its production, so that it can reach the core equilibrium temperature at a given physical activity. It is usually present in most of the activities related to the implementation of dedicated military tasks. Uncompensated heat stress occurs when demands for disclosure of heat (sweat evaporation) overcome the evaporative capacity of the environment. During uncompensed heat stress (UCHS), the body cannot achieve steady state core temperature, so it rises until it reaches physiological limits. Heat exhaustion in terms UCHS occurs at a relatively low internal temperature. Due to inadequate cooling (due to lack of evaporation of sweat) skin temperature remains high. Bloodstream is relocated to expanded vascular in order to remove the heat from inside the body, which

Correspondence: R.M. Karkalic, University of Defense, Military Academy, Pavla Jurisica Sturma 33, 11000 Belgrade, Serbia.
E-mail: rkarkalic@yahoo.com
Paper received: 5 July, 2014
Paper accepted: 22 October, 2014

reduces the minute volume and increases frequency of heart. UCHS extremely reduces physical performance, so that these conditions demand special regimes of work and rest cycles, with the use of active cooling during breaks [2].

Ability to compensate heat stress is primarily determined by biophysical factors (environmental conditions, clothing, the intensity of physical exertion), and moderately by the influence of biological condition (acclimatization to heat and hydration) [3].

Physiological thermoregulation involves activation of mechanism for disclosure of the excess heat and increase blood flow through the skin, which is achieved by enhancing heart rate and simultaneous increasing of sweating [4]. During physical activity in hot conditions, sweat rate raising from 1 to 1,5 l/h is not unusual, and may even reach a value of 2 l/h under extreme efforts, providing a potential loss of excess heat by evaporation of 4500 kJ, or 1 kW (14 W/kg for a person whose body weight is 70 kg). In the absence of adequate rehydration, this process leads to loss of body fluids from all body compartments, including the vascular component. Dehydration causes an increase of body core temperature and cardiovascular strain. For each percent of weight lost, the core temperature additionally raises by 0.15 to 0.2 °C, while heart rate increases by 5 bpm [5].

In long periods of exposure to a hot environment the major mechanism for dissipating heat is sweat evaporation, which is proportional to the effective (exposed) skin area, the water vapor pressure gradient between the skin and the environment, and the water vapor permeability of the clothing. Hence, when protective military clothing is worn, sweat evaporation rates decrease and heat dissipation is reduced [6]. The efficiency of physiological adaptation depends on the heat amount generated in the active muscles, the intensity of the carried external work as well as the level of biophysical heat exchange with environment [7].

Contemporary needs of chemical industry personnel request the best possible physiological suitability and comfort while working in hot conditions (Fig. 1). With this in mind, different systems for body cooling have been developed, with a main purpose to increase comfort as well as to reduce thermal stress. Cooling system industrial application has many other significant valid benefits, such as increased work duration, decrease in hydration needs, improved mental acuity and maintains physical performance of the workers. Although many systems exist today, they generally can be classified in the several basic groups: evaporative cooling products, products based on phase change materials (PCM), liquid circulation systems, compressed air systems and thermoelectric systems [8].

The focus of this study was to investigate the efficiency of the cooling vest based on evaporative principle, combined with working uniform, on physiological suitability during physical effort in hot environment. We hypothesized that vest wearing will alleviate the physiological strain of test subjects and increase ability of industrial personnel to successfully complete any job in extremely hot conditions.

EXPERIMENTAL METHODS AND PROCEDURES

Subjects

The participants involved in examination were 10 male test subjects (27.2±2.6 years), with similar anthropometric parameters (74±7 kg, 184±9 cm). Before exercises started, the subjects were briefed on the nature of the experiment, its purpose, conditions, safety measures and potential medical risks. Each participant read and signed an informed consent form, in accordance to standards of medical safety during examination in extreme hot or cold environment [9]. The protocol for the investigation was approved by competent ethical committee. The procedures performed in the present study corresponded to the standards of thermal strain evaluation by psychological measurements [10].

Performed results are based on exertional heat stress tests (EHST) conducted in climatic chamber in the Military Medical Academy, Institute of Hygiene, Belgrade, Serbia.

Figure 1. Workers exposed to heat stress in chemical industry process.

Body cooling system

The Arctic Heat® cooling system (Fig. 2) tested in this study belongs to the passive evaporative cooling systems. Passive evaporative systems utilize the heat absorbed from the wearer's body to evaporate water that is stored in a gel or specially developed crystals. The gel or crystals are built into a garment that allows the water vapor to be released into the surrounding air. By initial soaking in water (activation), crystals swell into gel form, which has ability to keep constant temperature for a long time.

Figure 2. Arctic Heat® personal cooling vest.

Preparation process comprised the following simple steps: initially soaking in water for 15 min, removing, grabbing top and bottom of vest and gently twisting in opposite directions to remove excess water, then finally hanging to dry. For the cooling effects, vest has to be placed in freezer. Active working time depends of the preparation. If frozen for 2 h or longer it will stay cold up to 2 h. The longer period vest placed in the freezer, the longer it will stay cold. Vest weights 800 g to 1 kg (when correctly activated).

Experimental protocol

Each subject performed two tests, both times wearing working uniform, with and without cooling vest over. In both cases, exercises performed under the same climatic conditions (temperature 40 °C, relative humidity 58%, air speed < 0.3 m/s). Before each test conducted, it was necessary to prepare climatic chamber, treadmill, measurement devices and other equipment. Working uniform consists of textile material (67% cotton, 33% polyester and rip-stop construction). Climatic chamber started minimum one hour before, in order to achieve projected temperature. Each subject was weighed without any equipment, before and after every experiment.

Taking in consideration climatic conditions, each test was initially limited on maximum 45 min. Criteria for termination before the maximal time were: achieving critical value of the tympanic temperature (39 °C), or heart rate (190 beats per min), or participant's subjective feeling of unbearable effort.

All temperature measurements from the subjects during every exposure were automatically monitored and recorded in real-time using a physiological data monitoring system (Biopac Systems, Inc. USA) [12,13]. System consists of MP150 acquisition unit, universal interface module (UIM100C) and five skin temperature amplifier modules (SKT 100C), single channel, differential amplifier designed especially for skin and core temperature monitoring (Fig. 3).

The UIM100C Universal Interface Module (2) is the interface between the MP150/100 and external devices. Typically, the UIM100C is used to input pre-amplified signals (usually greater than ±0.1 volt peak-peak) and/or digital signals to the MP150/100 acquisition unit. Other signals (e.g. those from electrodes or transducers) connect to various signal-conditioning modules.

The Universal Interface Module (UIM100C) is designed to serve as a general-purpose interface to most types of laboratory equipment. The UIM100C consists of sixteen 3.5 mm mini-phone jack connectors for analog inputs, two 3.5 mm mini-phone jack connectors for analog outputs, and screw terminals for the 16 digital lines, external trigger, and supply voltages.

The SKT100C skin temperature amplifier module is a single channel, differential amplifier designed especially for skin and core temperature and respiration flow (rate) monitoring. The SKT100C is designed for general temperature measurement, respiration rate determination, psycho-physiological investigations and sleep studies [11].

Figure 3. Physiological data monitoring system MP150 BIOPAC: MP150/100 Acquisition unit, UIM100C Universal interface module and Skin temperature amplifier modules SKT 100C (a); thermistor transdusers TSD202A (b) and TSD202E (c).

The SKT100C employs any of the BIOPAC TSD202 series thermistor transducers (Fig. 3) to measure temperature. The SKT100C includes a lower frequency response selection switch that permits either absolute (DC) or relative (*via* a 0.05 high-pass filter) temperature measurements [12].

Heart rate was measured and recorded automatically using a Quinton® Q4500 Exercise Test Monitor (Quinton Instruments Company, USA). Continual monitoring was done using monitors that received readings from the heart rate straps that were fastened to each subject (on the chest and bottom of spine). The same device was used for control and handling with treadmill (speed and grade).

Measurement of tympanic temperature

Method used in this study aims to mesuring the tempeature of the tympanic membrane (T_{ty}) whose vascularisation is provided in part by the internal carotid artery, which also supplies the hypothalamus. As the thermal inertia of the eardrum is very low, due to its low mass and high vascularity, its temperature reflects the variations in arterial blood temperature, which influence the centers of thermoregulations [10].

Tympanic temperature was measured by conducting thermo-element TSD202A into the aural channel and investing as close as possible to the eardrum. This measurement was continually, with recording data every 10 s.

Measurement of skin temperature

Skin temperature (T_{sk}) varies widely over the surface of the body, especially during extreme ambiental conditions. Skin temperature is influenced by:

– the thermal exchanges by conduction, convection, radiation and evaporation at the surface of the skin, and

– the variations of skin blood flow and of the temperature of the arterial blood reaching the particular part of the body [10].

In warm and hot enviroment, exept in the precence of the high asymetrial radiation, local skin temperatures tend to be homogeneous, so few measuring points can be used with accuracy [10]. In this study case, the mean body skin temperature (T_{sk}) was determined continually, mesuring of local body temperatures on four points, using transdusers types TSD202E and TS202F.

Skin temperature varies widely over the surface of the body and especially when the ambient conditions are cold. Skin temperature is influenced by:

– the thermal exchanges by conduction, convection, radiation and evaporation at the surface of the skin and

– the variations of skin blood flow and of the temperature of the arterial blood reaching the particular part of the body.

Mean skin temperature (T_{sk}) is obtained from the following formula:

$$T_{sk} = 0.28T_{sk1} + 0.28T_{sk2} + 0.16T_{sk3} + 0.28T_{sk4} \quad (1)$$

where: T_{sk1} – skin temperature measured in the middle of the neck root, T_{sk2} – skin temperature measured in the middle of the right scapula, T_{sk3} – skin temperature measured in the middle of the upper palm side, T_{sk4} – skin temperature measured in the middle of right shin.

Assessment of thermal strain on the basis of heart rate

Heart rate (*HR*) over a time interval *t* (in min) is defined as $HR = n/t$, where *n* is the number of heartbeats observed during this time interval. It is expressed in beats per min (bpm) [10].

At any given time, the heart rate can be considered as the sum of several components, which are not independent of each other:

$$HR = HR_0 + \Delta HR_M + \Delta HR_S + \Delta HR_T + \Delta HR_N + \Delta HR_\varepsilon \quad (2)$$

In the context of this study, only the increase in heart rate connected with the thermal strain experienced by the subject (ΔHR_T), was examined. The other components represent:

– limit of heart rate (HR_0),

– increase in heart rate linked with work metabolism (ΔHR_M),

– increase in heart rate linked with static exertion (ΔHR_S),

– increase in heart rate due to psychological factors (ΔHR_N),

– residual component in heart rate (ΔHR_ε).

Assessment of physiological strain on the basis of body-mass loss due to sweating

The gross body-mass loss (Δm_g) of a person during a given time interval is the sum of the several components:

$$\Delta m_g = \Delta m_{sw} + \Delta m_{res} + \Delta m_0 + \Delta m_{wat} + \Delta m_{sol} + \Delta m_{clo} \quad (3)$$

Hence, total mass loss depends of sweat loss (Δm_{sw}), diference between carbon dioxide and oxigen (Δm_0), evaporation of respiratory tract (Δm_{res}), intake (food) and excretions (stools) of solids (Δm_{sol}), intake and excretions (urine) of water (Δm_{wat}), and sweat accumulation in the chlothing (Δm_{clo}). In the context of this study, only the sweat loss component (Δm_{sw}) are considered and calculated as the rate of sweating (*SwR*), from the difference between pre-test and post-test nude body weights (digital scale Chyo MW-100K). Values expressed to the body surface in the unit time (l m^{-2} h^{-1}) [10].

Subjective assessment of the level of comfort

Thermal comfort is the condition of mind that expresses satisfaction with the thermal environment and is assessed by subjective evaluation. Subjective assessment of the level of comfort was rated by each subject using the McGinnis scale for ergometry testing in the climatic chamber [11]. This scale values range from 1 to 7, where 1 denotes "comfortable" and 7 denotes "extremely intolerable hot":

1) Comfortable
2) Warm but fairly comfortable
3) Uncomfortably warm
4) Hot
5) Very hot
6) Almost as hot as I can stand
7) So hot I am sick and nauseated.

The subjects were asked to point on the scale their subjective assessment every 5 min during the exposure.

RESULTS AND DISCUSSION

During EHST, not one test subjects showed any symptom of the heat stroke, or any disturbances related to serious types of heat illness. Tests lasted a maximum of 45 min, with the only 2 recorded cases of early completion, due to subjective report of intolerable effort (RPE level 7). There were no cases of cancellation owing to achieving limitary values of tympanic temperature (39 °C) or heart rate (190 bpm). Values of the main thermal strain indicators, measured in the last minute of exercises, are shown in Table 1.

In parallel with measuring of the thermal strain parameters, exercises on treadmill were discontinuously recorded by standard and thermal imaging camera (FLIR SC600 640×480 LWIR resolution and 0.03 °C sensitivity), every 5 min. Footage analysis showed the efficiency of the vest cooling features, from start to the end of exercise, based on thermal imaging display of hot and cold zones on the vest and the torso area (Fig. 4).

Table 1. Comparison of the mean values (±SD) for temperature and heart rate during tests; 45th min, 40 °C

Indicator	NoCOOL	ACOOL
Tty	37.73±0.18	37.1±0.24
Tsk	36.05±0.22	35.6±0.16
HR	142±14	130±12

Comparable reviews of tympanic temperature values with a cooling system and without it are displayed in Fig. 5. The mean tympanic temperatures for the whole group without cooling varied from 36.39 to 37.73 °C, considered for the maximum exercise time 45 min. In case with cooling, around the 15th min temperature began to grow noticeably slower, so in 35th min was lower by 0.57±0.08 °C. Maximum diference of 0.69±0.07 °C was recorded at the end of EHST (p < < 0.05).

(a) (b)

Figure 4. Snapshot vest recorded with standard (a) and thermal imaging camera (b), after 30 min of exercise.

Body skin temperature

Figure 6 presents the changes in T_{sk} through the 45 min long heat-stress exposures, with a cooling system and without it.

Body skin temperature was increased in a similar

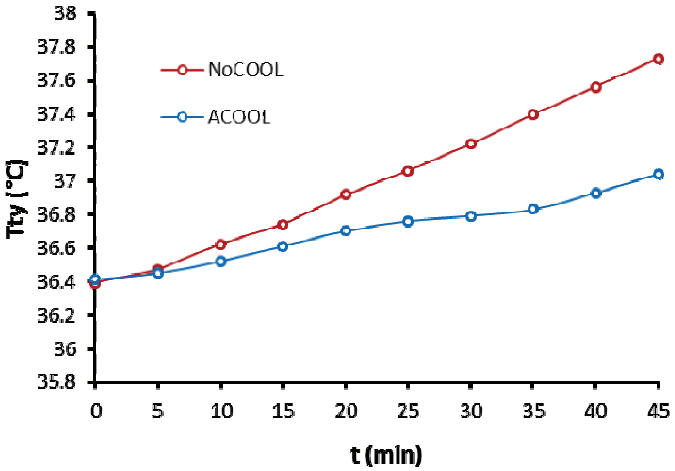

Figure 5. The mean tympanic temperature of all 10 subjects during 45 min without cooling (NoCOOL) and with cooling vest (ACOOL).

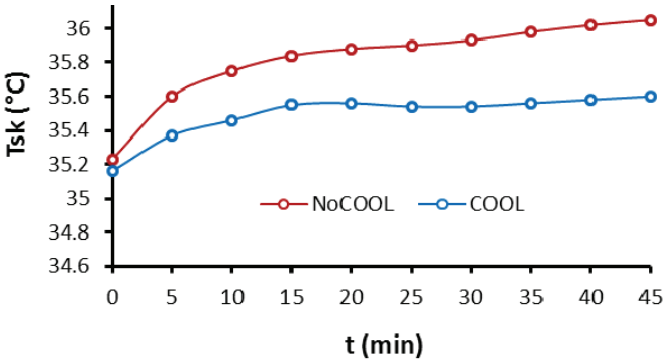

Figure 6. The mean body skin temperature of all 10 subjects during 45 min without cooling (NoCOOL) and with cooling vest (ACOOL).

way in all cases, much faster in the first 15 min, then slowly. Maximum value of T_{sk} was achieved in case NoCOOL in 45th min (36.05 °C), while with cooling vest temperature was at the same time 35.6 °C.

At the two measuring points in the torso area (neck and scapula), significantly lower values of skin temperature were observed in relation to the option ACOOL (an average of 0.8±0.02 °C), as a direct consequence of cooling vests effects. Measured values of T_{sk} at the other two points (leg and arm) did not differ significantly, as expected ($p > 0.05$).

Heart rate

The average measured values of heart rate during laboratory tests are displayed in Fig. 7. No significant differences were observed in values of heart rate during tests. Heart rate in both cases (NoCOOL and ACOOL) increased in similar manner, but limit of 190 bpm was not reached during any single exercise. The heart rate, as an index of cardiovascular strain, was significantly reduced when cooling was provided during exposure to hot conditions. Maximum recorded heart rate was 142 bpm, without vest, in 45th min. During EHST, in case ACOOL, heart rate was lower on average for 8 bpm (maximum difference of 11 bpm noted at the end of the EHST).

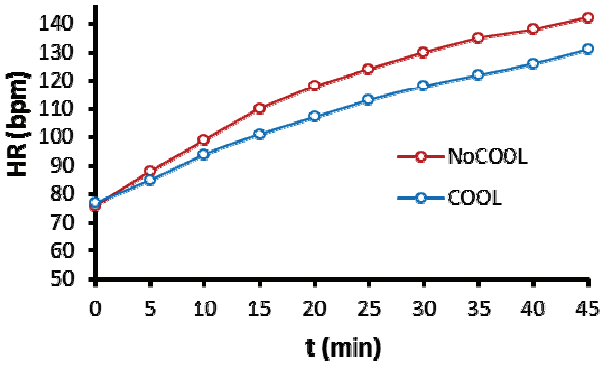

Figure 7. The heart rate of all 10 subjects during 45 min without cooling (NoCOOL) and with cooling vest (ACOOL).

Sweat rate

The average rate of sweating, as expected, achieved a higher value in NoCOOL case (0.48±0.08 l m^{-2} h^{-1}), while using cooling system, value was significantly lower (0.32±0.06 l m^{-2} h^{-1}).

Subjective assessment of comfort

From the 5th to 45th min participants expressed 1–2 levels better feeling of comfort wearing cooling vest, then in cases without it. Subjective assessments of the level of comfort during exercises, with cooling vest and without it, are showed in Fig. 8.

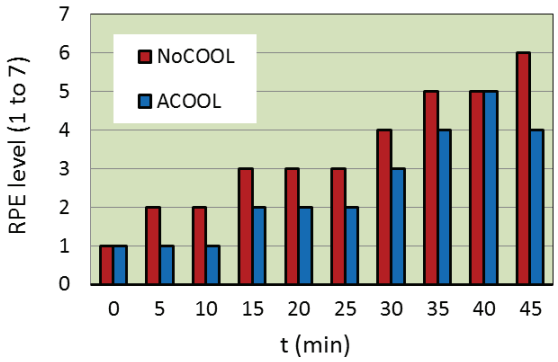

Figure 8. Comparison of the subjective assessment of the level of comfort of all 10 subjects with the cooling system (ACOOL) and without it (NoCOOL).

As the greatest benefit of all cooling systems subjects cited easier breathing and less strain compared to tests without cooling, which is confirmed by the measured lower values of heart rate.

Sweating as a mechanism for disclosure of excess heat has a special importance in the thermal stress caused by physical activity, when it occurs not only as a consequence of thermal factors (increasing of body core and skin temperature), but also non-thermal factors such as central activation, activation of muscle-mechano receptors metabolism and activation of baroreflex due to physical activity. According to test results, the rate of sweating is lower when using the body cooling systems average by 0.16 l m^{-2} h^{-1} ($p < 0.001$).

Because exercises are not lasting equaly long with all subjects, the rate of sweating we expressed per hour.

Our results are consistent with the study of Hadid and Yanovich [6], who carried out the investigation related to effects of the cooling system based on air circulation to the thermal stress caused by physical effort in test subjects.

McLellan [14] obtained similar results exploring the efficacy of an air-cooling vest to reduce thermal strain for light armour vehicle (LAV) personnel. In this study, seven males were exposed to either hot dry – HD (49 °C, 10 % RH) or warm, humid – WH (35 °C, 70 % RH) conditions while either receiving (C) or not receiving (NC) cooling through an air-vest. All subjects completed the 3 h of heat-stress exposure during all conditions but the rise in rectal temperature approached 2 °C during HD with NC. When cooling was provided the rise in rectal temperature was minimal throughout the heat stress. It was concluded that micro-climate conditioning was an effective way to reduce the thermal strain of LAV crew.

CONCLUSION

Methodology used in this study and experimental protocols were carried out in accordance with contemporary standards in area of thermal strain evaluation by physiological measurements (ISO 9886), with respect to prescribed measures of medical supervision of subjects exposed to extreme hot environment (ISO 12894). All laboratory tests were conducted using high performance equipment (Biopac, Quinton®), with technical features that enable to measure, monitor and record necessary physiological parameters in real time. Among other things, validity of results confirming engagement of sufficient number of test subjects (volunteers) with similar anthropometric parameters, selected according to strict criteria from a larger number of potential participants.

The evaluation of the cooling system in this study found two important conclusions: in case of wearing cooling vest covering torso area, body core temperature (measured through tympanic temperature) grows slower, and mean body skin temperature is significantly lower. Moreover, heart rate values and subjective assessment of comfort levels point to the much expressed test subjects physiological stability, which is very important result from the aspect of confidence and efficiency in fulfilling the given professional activities.

The results of this study have clearly identified the benefits of a liquid circulation cooling vest in lowering the thermal strain for the mounted test subjects. Tympanic temperature, as an index of thermal strain, and heart rate, as an index of cardiovascular strain, were reduced when cooling was provided during exposure to hot conditions.

Acknowledgements

Ministry of Education, Science and Technological Development of the Republic of Serbia supported this work, Grant No. TR34034 (2011–2015).

REFERENCES

[1] D. Moran, A. Shitzer, K. Pandolf, A physiological strain index to evaluate heat stress, Am. J. Physiol. **275** (1998) 129–134.

[2] W. Kenney, Heat flux and storage in hot environments, Int. J. Sports. Med. **19** (1998) S92–S95.

[3] I. Mekjavic, E. Banister, J. Morrison, Environmental Ergonomics, Taylor & Francis, London, 1987.

[4] G. Donaldson, W. Keatinge, R. Saunders, Cardiovascular responces to heat stress and their adverse consequences in healthy and vulnerable human populations, Int. J. Hypertermia **19** (2003) 225–235.

[5] C. Cian, P. Barraud, B. Melin, C. Raphael, Effects of fluid ingestion on cognitive function after heat stress or exercise-induced dehydration, Int. J. Psychophysiol. **42** (2001) 243–251.

[6] A. Hadid, R. Yanovich, T. Erlich, G. Khomenok, D. Moran, Effect of a personal ambient ventilation system on physiological strain during heat stress wearing a ballistic vest, Eur. J. Appl. Physiol. **104** (2008) 311–319.

[7] S. Montain, M. Sawka, B. Cadarette, M. Quigley, J. McKay, Physiological tolerance to uncompensable heat sress: effects of exercise intensity, protective clothing, and climate. J. Appl. Physiol. **77** (1994) 216–222.

[8] W. Teal, Microclimate cooling, in Proceedings of Chemical biological individual protection conference, March 7-9, 2006, US Army Natick Solder Center, MA, USA, 2006.

[9] ISO 12894 (E): Ergonomics of the thermal environment - Medical supervision of individuals exposed to extreme hot or cold environment, 2008.

[10] ISO 9886: Ergonomics – evaluation of thermal strain by psychological measurements, 2008.

[11] N. McGinnis, Ergometry testing in the climatic chamber, Sports Med. **25** (1999) 86–89.

[12] MP SYSTEM Hardware Guide, Biopac Systems Inc., pp. 2–10, 26–29, 120–124.

[13] Acq Knowledge® 4 Software Guide, Biopac Systems Inc., www.biopac.com

[14] T. McLellan, The efficacy of an air-cooling vest to reduce thermal strain for light armour vehicle personnel, Technical report, DRDC Toronto, TR 2007-002, 2007.

IZVOD

Uticaj prsluka za hlađenje sa sistemom pasivnog isparavanja na nivo fiziološkog opterećenja radnika hemijske industrije u toploj sredini

Radovan M. Karkalić[1], Dalibor B. Jovanović[2], Sonja S. Radakovic[3], Dušan S. Rajić[4], Biljana V. Petrović[5], Negovan D. Ivanković[1], Željko B. Senić[6]

[1]*Univerzitet odbrane, Vojna akademija, Beograd, Srbija*
[2]*Tehnički opitni centar, Generalštab Vojske Srbije, Beograd, Srbija*
[3]*Medicinski fakultet Vojnomedicinske akademije, Univerzitet odbrane, Beograd, Srbija*
[4]*Univerzitet u Beogradu, Inovacioni centar Tehnološko-metalurškog fakulteta, Beograd, Srbija*
[5]*Prirodno-matematički fakultet, Univerzitet u Kragujevcu, Srbija*
[6]*Vojnotehnički institut, Beograd, Srbija*

(Stručni rad)

Rad predstavlja rezultate naučnih istraživanja na polju efikasnosti sistema za hlađenje tela iz grupe pasivnih sistema na bazi isparavanja i njegov uticaj na fiziološku podobnost ljudi u uslovima izloženosti fizičkom naporu i ekstremno visokim temperaturama. Podaci i dobijeni rezultati zasnovani su na ispitivanjima sprovedenim u klimatskoj komori Instituta za higijenu VMA u Beogradu. Deset ispitanika muškog pola dobrovoljno je podvrgnuto testovima toplotnog opterećenja usled fizičkog napora, izazvanog hodanjem na pokretnoj traci sa brzinom hoda od 5 km/h, u toploj sredini (temperatura vazduha 40 °C). Testovi su realizovani sa ispitanicima srednjih godina (27.2±2.6), sličnih antropometrijskih parametara (74±7 kg, 184±9 cm), u varijanti nošenja radne odeće bez ikakvog rashladnog sistema (opcija NoCOOL) i uz upotrebu rashladnih prsluka za hlađenje tela, model Arctic Heat® (opcija ACOOL). Kao pokazatelji fiziološkog opterećenja određivane su: srednja temperatura kože (T_{sk}), timpanična temperatura (T_{ty}) i frekvencija srčanog rada (*HR*), dok je intenzitet znojenja (*SwR*) izračunat kao pokazatelj vodeno-elektrolitskog statusa. U svim slučajevima izlaganje fizičkom naporu u toploj sredini indukovalo je fiziološki odgovor, manifestovan kroz povećanje timpanične temperature, frekvencije srčanog rada i intenziteta znojenja. U varijantama primene rashladnog prsluka (COOL), timpanična temperatura i srednja temperatura kože su imale značajno niže vrednosti ($p < 0,05$), kao i intenzitet znojenja ($p < 0,001$). Eksperimentalni rezultati dokazali su uticaj rashladnog prsluka, korišćenog preko radne odeće, na snižavanje nivoa fiziološkog opterećenja tokom izlaganja korisnika ekstremnim uslovima, u poređenju sa identičnim testovima u varijanti bez hlađenja tela.

Ključne reči: Hemijska industrija • Toplotni stres • Rashladni prsluk • Radna odeća • Fiziologija napora

Water Kefir grain as a source of potent dextran producing lactic acid bacteria

Slađana Z. Davidović[1], Miona G. Miljković[1], Dušan G. Antonović[2], Mirjana D. Rajilić-Stojanović[1], Suzana I. Dimitrijević-Branković[1]

[1]*University of Belgrade, Faculty of Technology and Metallurgy, Department for Biochemical Engineering and Biotechnology, Belgrade, Serbia*
[2]*University of Belgrade, Faculty of Technology and Metallurgy, Department for Organic Chemistry, Belgrade, Serbia*

Abstract

Water kefir is a beverage fermented by a microbial consortium captured in kefir grains. The kefir grains matrix is composed of polysaccharide, primarily dextran, which is produced by members of the microbial consortium. In this study, we have isolated lactic acid bacteria (LAB) from non-commercial water kefir grains (from Belgrade, Serbia) and screened for dextran production. Among twelve LAB isolates three produced slime colonies on modified MRS (mMRS) agar containing sucrose instead of glucose and were presumed to produce dextran. Three LAB were identified, based on morphological, physiological and biochemical characteristics and 16S rRNA sequencing, as *Leuconostoc mesenteroides* (strains T1 and T3) and *Lactobacillus hilgardii* (strain T5). The isolated strains were able to synthesize a substantial amount of dextran in mMRS broth containing 5% sucrose. Maximal yields (11.56, 18.00 and 18.46 g/l) were obtained after 16, 20 and 32 h for T1, T3 and T5, respectively. Optimal temperature for dextran production was 23°C for two *Leuconostoc mesenteroides* strains and 30 °C for *Lactobacillus hilgardii* strain. The produced dextrans were identified based on paper chromatography, while the main structure characteristics of purified dextran were observed by FT-IR spectroscopy. Our study shows that water kefir grains are a natural source of potent dextran producing LAB.

Keywords: dextran, water kefir grains, *Lc. mesenteroides*, *Lb. hilgardii*.

Available online at the Journal website: http://www.ache.org.rs/HI/

SCIENTIFIC PAPER

UDC 547.458.68:579.66(497.111)

Hem. Ind. **69** (6) 595–604 (2015)

doi: 10.2298/HEMIND140925083D

Water kefir is a beverage produced by fermentation of sucrose solution supplemented with lemon slice and dry fruits, best figs [1]. Beverage is slightly carbonated, with refreshing and moderately sour taste. The fermentation is performed by a consortium of symbiotic microorganisms embedded in kefir grains. The microbiota of kefir grains varies depending on its origin and culture media used for fermentation [2]. The composition of the kefir grains' microbiota has been excessively studied [3–7]. It includes yeasts, acetic acid bacteria and lactic acid bacteria (LAB), with the last being the most abundant [6]. LAB of the kefir grains belong to the following genera: *Lactobacillus*, *Lactococcus* and *Leuconostoc* [3,4,8].

The main component of water kefir grain matrix is dextran [9]. This exopolysaccharide (EPS) is synthesized by indigenous LAB. Different authors reported different bacterial species as the predominant EPS producers in water kefir grains and these include *Lactobacillus casei* (two subspecies) [4], *Leuconostoc mesenteroides*, *Lactobacillus nagelii* and *Lactobacillus hordei* [6], as well as *Lactobacillus hilgardii* [3,8].

Dextran is a high-molecular-mass homopolysaccharide made of glucose. The glucose molecules in the main chain of dextran are linked by alpha 1-6 glycosidic bonds. Branching can occur at positions 2, 3 or 4 [10]. The proportion of branching and the chain length affects the rheological properties of EPS [11].

Due to its relative stability and good solubility, dextran is widely used in different branches of industries, such as medical, pharmaceutical, food, textile and chemical industries [12–16]. Insoluble dextran could be applied as matrix for immobilization of biomolecules [17].

Because dextran is an important polysaccharide that can be applied in various branches of industries, the aim of this study was to isolate LAB which produces dextran from water kefir grains. The present paper describes characteristics of three LAB isolates from water kefir grains that are able to produce dextran in large quantities. We describe conditions for the production of dextran by *Leuconostoc mesenteroides* originating from this source for the first time. Purified dextran samples were preliminary characterized by paper chromatography and FTIR spectroscopy.

Correspondence: S.Z. Davidović, University of Belgrade, Faculty of Technology and Metallurgy, Department for Biochemical Engineering and Biotechnology, Karnegijeva 4, Belgrade, Serbia.
E-mail: sdavidovic@tmf.bg.ac.rs
Paper received: 25 September, 2014
Paper accepted: 28 November, 2014

EXPERIMENTS

Isolation and screening for dextran producing LAB

Non-commercial water kefir grains (from a household in Belgrade, Serbia) were used for isolation of LAB. The grains (1 g) were homogenized in 9mL saline and used as inoculum for two different media: MRS and M17 agar. After two days of incubation at 30 °C, five to ten colonies from each agar plate were inoculated in MRS broth. They were re-streaked and purified strains were routinely propagated in MRS broth at 30 °C in micro-aerofilic condition for further characterization.

The first screening for dextran production was performed on modified MRS (mMRS) agar having 5% sucrose instead of glucose. Selected cultures were streaked on surface of agar plates. Agar media were incubated in micro-aerofilic conditions at 30 °C for 48 h. The slimy colonies were identified and propagated in mMRS broth. The amount of produced dextran was estimated colorimetrically by phenol–sulfuric acid method using glucose as a standard [18]. The absorbance was measured at 490 nm in spectrophotometer (Ultrospec 3300 *pro*Amersham Bioscience).

Identification of dextran-producing isolates

The three selected strains (T1, T3 and T5) were identified by phenotypic and molecular methods. The first tentative identification as LAB was performed according to morphological characteristics (colony morphology, Gram staining and cells shape) and physiological characteristics (catalase test, growth at different temperatures, growth in media with different concentration of NaCl). Further, isolates were examined for fermentation of different carbohydrate using the API 50 CHL system (BioMérieux, France).

The species level identification of selected LAB dextran-producing strains was confirmed by sequencing of the 16S rRNA encoding gene, using the following procedure: the total DNA extraction from pure cultures was done by phenol-chloroform method [19]. The 16S rRNA gene was amplified using the total DNA as template for PCR with primers UNI16SF (5'-GAG AGT TTG ATC CTG GC-3) and UNI16SR (5'-AGG AGG TGA TCC AGC CG-3'). PCR mixture contained 2.5 µL 10xPCR buffer (0.5 M KCl, 0.1 M Tris-HCl, pH 8.8 at 25°C and 0.8% Nonidet P40), 1.5 µL $MgCl_2$ (25 mM), 18.25 µLultrapure double distilled H_2O, 0.25 µLTaq polymerase (Fermentas, Lithuania) and 1 µL genomic DNA of the isolate. The reactions were carried out in GeneAmp 2700 PCR Cycler (Applied Biosystems, Foster City, CA, USA) programmed as follows: the initial denaturation of DNA for 5 min at 96 °C, 30 cycles of 30 s at 96 °C, 30 s at 55 °C, and 30 s at 72 °C; and the extension of incomplete products for 5 min at 72 °C. Resulting PCR amplicons were sequenced at Macrogen in Amsterdam, the Netherlands. The BLAST algorithm (http://www.ncbi.nlm.nih.gov/BLAST) was used to determine the most related sequence in the NCBI nucleotide sequence database.

Production of dextran

Effect of temperature and fermentation time on dextran yield

To evaluate the influence of temperature and incubation time on the growth and dextran production, the three high yield dextran-producing strains (T1, T3 and T5) were grown in 100 mL of mMRS broth containing 50 g/L of sucrose in 300 mL Erlenmeyer flasks at 30 °C for 24 h. This overnight culture was used as inoculum in further experiments.

To study the influence of various temperatures on dextran production the strains were incubated at 23, 30 and 37 °C. Incubation lasted 16h for *Lc. mesentroides* T1, 20 h for *Lc. mesentroides* T3 and 32h for *Lb. hilgardii* T5.

To study the effect of time on dextran production, the culture media were incubated for different time intervals ranging from 0 to 48h. Fermentation was carried out at 23 °C for *Lc. mesenteroides* strains T1 and T3 and 30 °C for *Lb. hilgardii* T5. Dextran concentration, cell biomass and final pH of fermented culture broth were determined.

Isolation and purification of dextran

Samples of the fermented media for dextran quantification were treated in boiling water for 15 min to inactivate bacteria. Bacterial cells were removed by centrifugation at 7000 rpm for 15 min at 4 °C. Dextran was precipitated from the supernatant by addition of double volume ice cold 96% ethanol and kept overnight at –20 °C. The samples were centrifuged at 13500 rpm for 15 min at 4 °C. Dextran pellets were separated from the supernatant and dissolved in hot distilled water. The precipitation procedure was repeated twice. The final precipitate was dissolved in hot distilled water. Dextran samples were additionally purified by dialysis through 10 kDa membrane against distilled water at 4 °C for 48 h with 3–4 changes per day. The purified dextrans were then recovered by spray-drying (BÜCHI Mini Spray Dryer B-290, inlet temperature 140 °C, outlet temperature 80 °C) and stored at room temperature.

Characterization of dextran

Study of monomer composition

Thin layer chromatography (TLC) was performed to determine monomer composition of isolated dextrans. TLC was carried out using paper chromatography of the hydrolyzed polymers according to method described by

Bailer and Oxford [20]. Glucose, fructose and galactose were used as standards.

Study of Fourier-transformed infrared spectroscopy

The major structural groups of the purified dextrans were detected by Fourier-transformed infrared (FTIR) spectroscopy using KBr method.

FT-IR spectroscopy (Bomem MB100, Canada) was performed by mixing the sample, dextran powder (0.6 mg) with 200 mg of KBr. The mixture was tableted under a pressure of 350 MPa, and dried at 110 °C for 48 h before analysis. The analysis was performed at room temperature (27 °C) in the range of wavelengths of 400–4000 cm^{-1}, with a resolution of 4 cm^{-1}.

RESULTS

Identification of dextran-producing isolates

In the present study, 12 lactic acid bacteria were isolated from water kefir grains and were denoted as T1 to T12. Isolated bacteria were able to grow on MRS and M17 plates at 30 °C. All tested strains were catalase-negative and Gram-positive with various shapes ranging from long rods to coccoid rods (Table 1). Three isolates formed mucous colonies on mMRS agar (Fig. 1). They were selected for further studying and dextran production quantification and characterization.

Testing the growth at different temperatures showed that optimal temperature for all three strains was 30 °C. They all could grow at 37 °C but none could grow at 45 °C. The isolate T3 could grow at 15 °C, while T5 showed weak growth at this temperature. The isolate T3 was tolerant to NaCl at all tested concentrations (4, 6.5 and 9.6%), while T1 and T5 grew at 4 and 6.5% NaCl and did not grow in the presence of 9.6% NaCl. All three strains fermented glucose with gas production (Table 1).

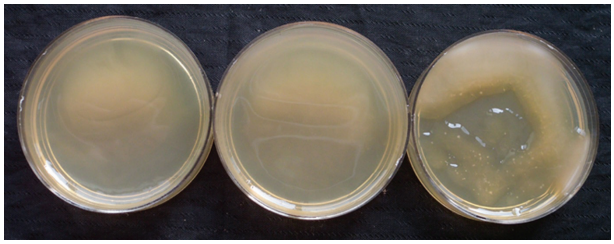

Figure 1. Picture of isolates T1 (left), T3 (middle) and T5 (right) growing on the surface of the mMRS agar with 5% sucrose plates.

API test was used for determination of fermentation pattern of isolates (Table 2).

According to physiological characteristics the isolates T1 and T3 belong to the genus *Leuconostoc*. The sugar fermentation patterns differed for several carbohydrates including arbutin, fructose, galactose, lactose, melibiose, salicin, trechalose, methyl-α-D-glucopyranoside, *N*-acetylglucosamine, gentibiose, inuline and turanose (Table 2). Based on the fermentation profile of the isolate T5 (Table 2), this isolate was preliminarily identified as *Lactobacillus hilgardii* according to Bergey's Manual of Systematic Bacteriology [21]. All three strains could ferment sucrose which is the main carbohydrate available during water kefir preparation.

Based on the 16S rRNA gene encoding sequence of the isolates T1 and T3 were identified as *Leuconostoc mesenteroides* (the isolates shared >99% sequence similarity with *Lc. mesenteroides* strain NCFB 529, acc NR_040817), while the isolate T5 was identified as *Lactobacillus hilgardii* (with 99% 16S rRNA encoding sequence similarity to strain NBRC 15886, acc NR_113817.1). Based on the 16S rRNA gene sequences the isolates and their close relatives, a phylogenetic tree was constructed by the use of ARB software [22] (Fig. 2).

Table 1. Morphological and physiological characteristics of the bacterial isolates; +: positive reaction, –: negative reaction and ±: weakly positive reaction

Characteristic		Isolate		
		T1	T3	T5
Gram reaction		+	+	+
Cell form		Elongated cocci	Elongated cocci	Long rods
Cell size, μm		0.76-0.92	0.86-1.00	15.56-18.30
Catalase		–	–	–
Growth at different temperatures, °C	15	–	+	±
	30	+	+	+
	37	+	+	+
	45	–	–	-
Growth in the present of different concentrations of NaCl, %	4	±	+	±
	6.5	±	±	±
	9.6	–	±	-
Glucose fermentation/gas		+/+	+/+	+/+

Table 2. Carbohydrates fermentation profiles of dextran-producing LAB strains after 48 h of incubation at 30 °C; +: positive reaction, –: negative reaction and ±: weakly positive reaction

Carbohydrate	Bacteria			Carbohydrate	Bacteria		
	Lc. mesenteroides		*Lb. hilgardii*		*Lc. mesenteroides*		*Lb. hilgardii*
	T1	T3	T5		T1	T3	T5
Control	–	–	–	Esculin	+	+	+
Glycerol	–	–	–	Salicin	+	–	–
Erythritol	–	–	–	Cellobiose	+	+	–
D-Arabinose	–	–	–	Maltose	+	+	+
L-Arabinose	–	–	+	Lactose	+	–	–
Ribose	–	w	+	Melibiose	+	–	–
D-Xylose	–	+	+	Sucrose	+	+	+
L-Xylose	–	–	–	Trehalose	–	+	–
Adonitol	–	–	–	Inulin	–	–	–
methyl-β-D-xylopyranoside	+	–	–	Melezitose	–	–	–
Galactose	+	–	–	Raffinose	–	–	–
Glucose	+	+	+	Amidon	w	–	–
Fructose	+	+	+	Glycogen	–	–	–
Mannose	–	+	–	Xylitol	–	–	–
Sorbose	–	–	–	β-Gentibiose	–	w	–
Rhamnose	–	–	–	Turanose	–	+	–
Dulcitol	–	–	–	Lyxose	–	–	–
Inositol	–	–	–	Tagatose	–	–	–
Mannitol	–	w	–	D-Fucose	–	–	–
Sorbitol	–	–	–	L-Fucose	–	–	–
methyl-α-D-mannopyranoside	–	–	–	D-Arabitol	–	–	–
methyl-α-D-glucopyranoside	–	+	–	L-Arabitol	–	–	–
N-Acetylglucosamine	–	+	–	Gluconate	–	w	+
Amygdalin	+	–	–	2-Ketogluconate	–	–	–
Arbutin	–	–	–	5-Ketogluconate	–	–	–

Dextran production

The temperature of incubation significantly influenced the amount of produced dextran during growth of all three isolates (Fig. 3). The isolates were grown on three temperatures of 23, 30 and 37 °C. For *Lb. hilgardii* T5 strain, the amount of synthesized dextran varied between the tested temperatures and was the highest at 30 °C, while both *Lc. mesenteroides* strains showed maximal dextran production at the lowest tested temperature. The maximum dextran amount for *Lc. mesenteroides* T1 and T3 strains was 11.56 and 18.00 g/l, respectively. There was a strong decrease in dextran yield at higher temperatures. T5 strain showed maximal dextran production of 18.46 g/L at the optimal growth temperature (30 °C).

In this study, dextran production by *Lc. mesenteroides* T1 and T3 strains and *Lb. hilgardii* T5 strain was monitored during 48 h in mMRS broth. The T1 and T3 strains were incubated at 23 °C and T5 strain was incubated at 30 °C.The production of dextran increased with time during the exponential growth phase and in the stationary started to decrease (Fig. 4). Dextran yield reached maximum after 16h and 20h of incubation for *Lc. mesenteroides* T1 and T3 strains, respectively. Prolonged time of fermentation had positive effect on dextran yield only for isolate T5 which could be explained by slower growth rate of this bacterium. The maximum dextran production for the isolate T5 was observed after 32 h of fermentation, which was the beginning of stationary phase of growth of this bacterium. The pH of the fermented broth decreased from the initial pH of 7.2 to 4.3 during fermentation (Fig. 4), due to the metabolic activity of isolates, primarily lactic acid production. Common for all three strains was that when the pH value dropped to 4.3, the degradation of dextran started, and the yield was lower.

Characterization of dextran

TLC was performed using paper chromatography with glucose, fructose and galactose as standards. Results show that glucose is monomer unit of poly-

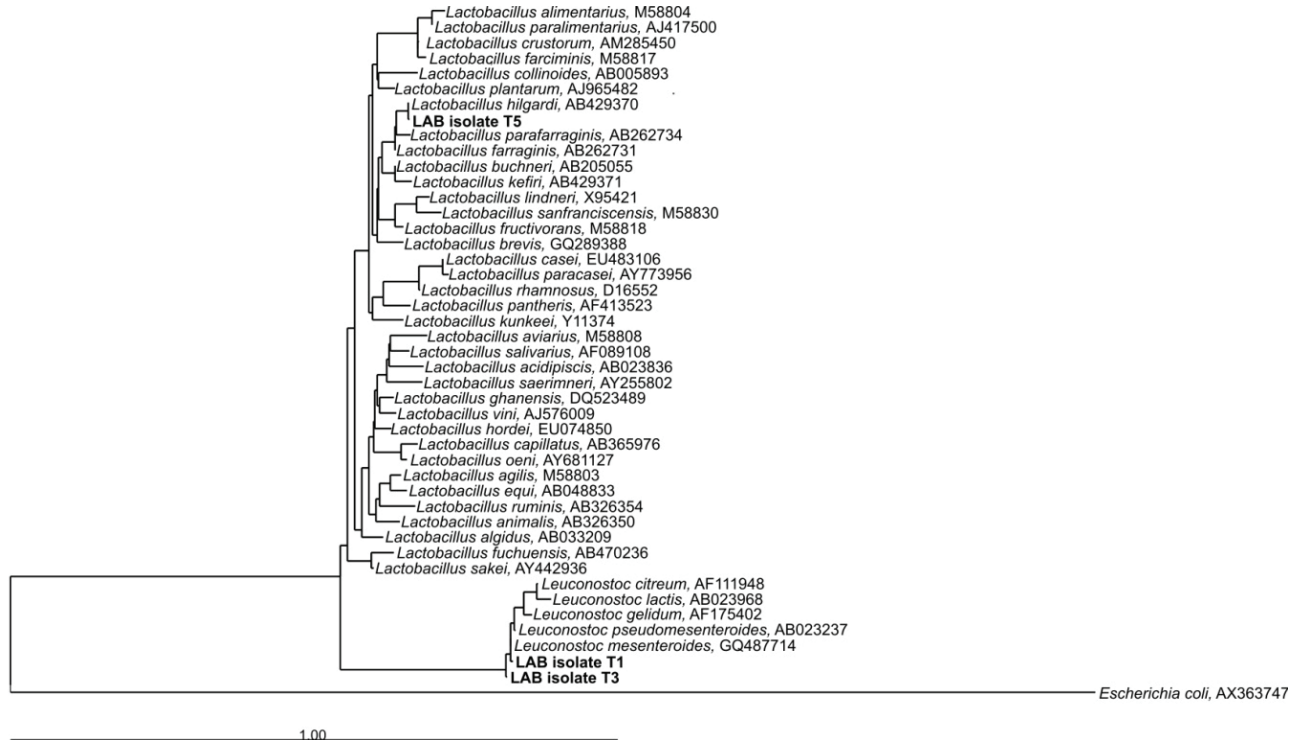

Figure 2. The phylogenetic tree of the LAB strains (T1, T3 and T5) isolated from water kefir grain and other members of Lactobacillus and Leuconostoc genera, constructed using the 16S rRNA gene sequences. The tree was constructed using the neighbor joining algorithm as implemented in ARB software. Escherichia coli is the root of the tree.

saccharides produced by all three studied isolates (T1, T3 and T5).

FTIR spectroscopy analysis confirmed polysaccharide nature of the extracellular material synthesized by the tested isolates (Fig. 5).

All samples analyzed on FT-IR had similar appearance in the area of 2000–4000 cm^{-1}. Intense and broad band in 3200–3500 cm^{-1} originated from the O–H stretching vibrations due to the influence of hydrogen bonds which is characteristic for polysaccharides molecules [23]. Peak around 2927 cm^{-1} is characteristic for the C-H stretching vibration.

There are slight differences in these spectra in the range of 400–2000 cm^{-1}. Broad signal from C–O–C and

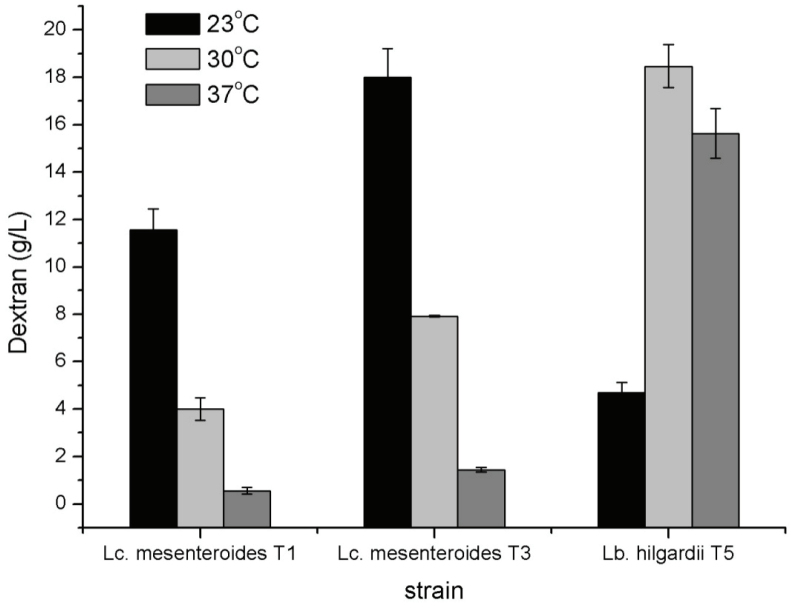

Figure 3. Effect of temperature on dextran production. The bars show the mean value of three replicates, while the vertical lines show the standard deviation of the measurements.

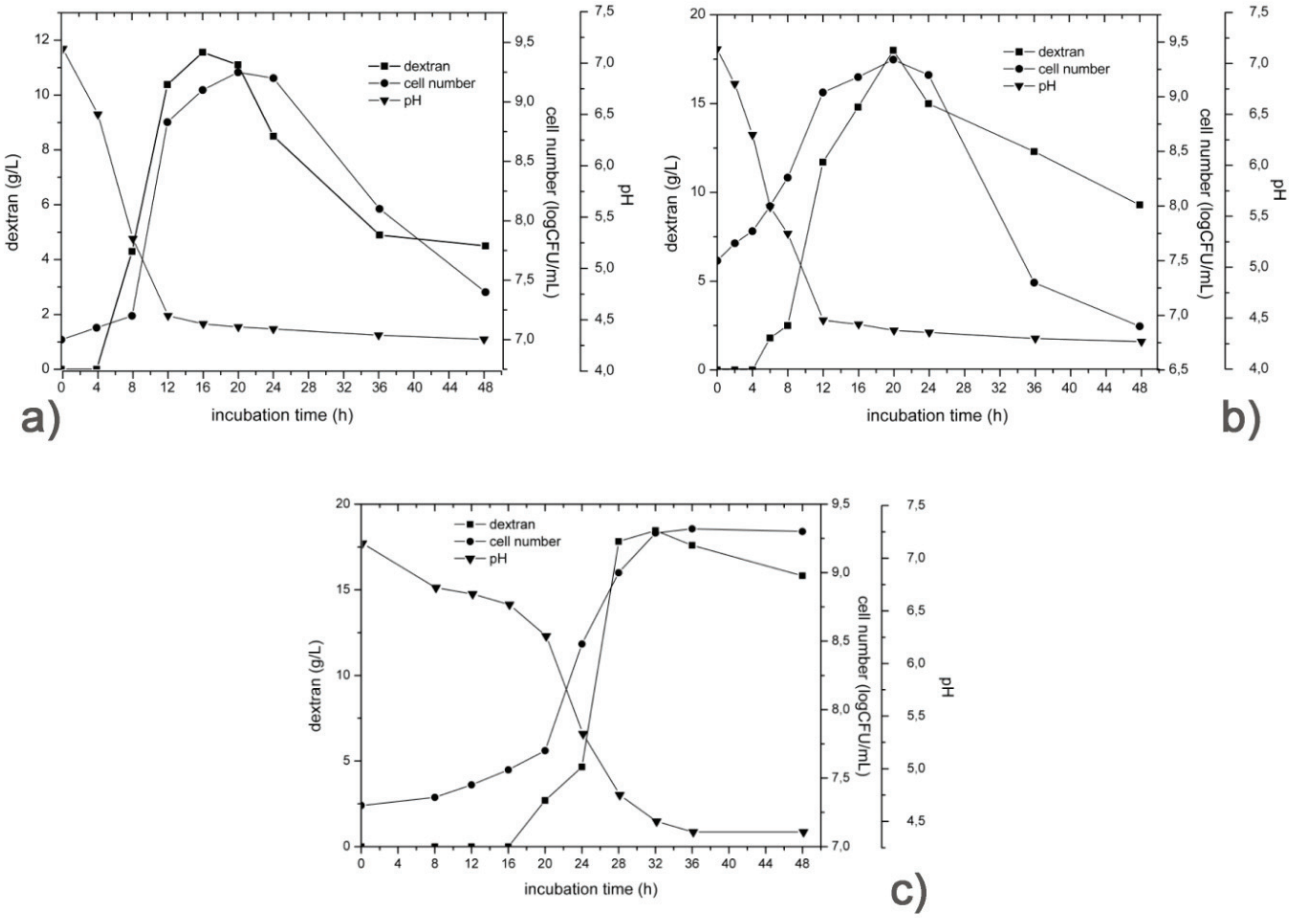

Figure 4. Effect of incubation time on dextran yield, final pH and cell growth for isolates T1 (a), T3 (b) and T5 (c) grown in mMRS broth with 5% sucrose at 23 °C (Lc. mesenteroides T1 and T3 strains) and 30°C (Lb. hilgardii T5 strain).

C–O at 1000–1200 cm^{-1} indicated the presence of the characteristic bonds of carbohydrates [24]. In this range the most intense peak for all samples are in the 1016–1020 cm^{-1} and 1030–1040 cm^{-1} which confirmed that the tested compounds are polysaccharides [25].

A characteristic absorption at 825–850 cm^{-1} indicates α-configuration of monomeric units. The absence of the signal at 900 cm^{-1} indicates the absence of β-configuration [26]. Based on the observed spectra, it was concluded that EPSs produced by all three analyzed isolates were of the same nature: homo-polysaccharides of glucose in α-configuration, and the EPS was identified as dextran.

DISCUSSION

The present study describes three new LAB strains isolated from water kefir grains that are able to produce dextran. Dextran production is a prevalent feature among LAB [27]. Dextran has numerous applications in food as well as in non-food industries [12–16], although a greater commercial use is limited by relatively small yields [28]. Most of LAB produce homopolysaccharides in quantities lower than 1g/L when growing under conditions that are not optimized for EPS production [29].

We have selected 3 among 12 LAB strains isolated from water kefir grain based on the slimy colony formation as potential dextran producers .The preliminary screening for dextran production showed that these three strains were potent dextran producers with yields ranging from 11.56 to 18.46 g/L. Dextran production yields obtained with our isolates is similar or exceeding the maximal yields of other reported dextran-producing bacteria [30–33]. In the study of Van der Meulen and colleagues, the total of 174 strains were isolated from cereal and dairy products, of which only 9 produced glucans with yields in range 0.8–17.2 g/L [30]. Majumder and coworkers reported dextran yield of 12 g/L produced by *Lc. mesenteroides* NRRL B-640 under optimized conditions [32]. This yield is similar with our strain *Lc. mesenteroides*T1, while strain *Lc. mesenteroides*T3 produced 33% more dextran from the same amount of sucrose in the medium. The strain *Lc. mesenteroides* T3 converted 36% of sucrose into dextran, which is higher than that reported by Sarwat and colleagues [31] in the study of *Lc. mesenteroides* CMG713 (32.5). Qader and coworkers optimized conditions for

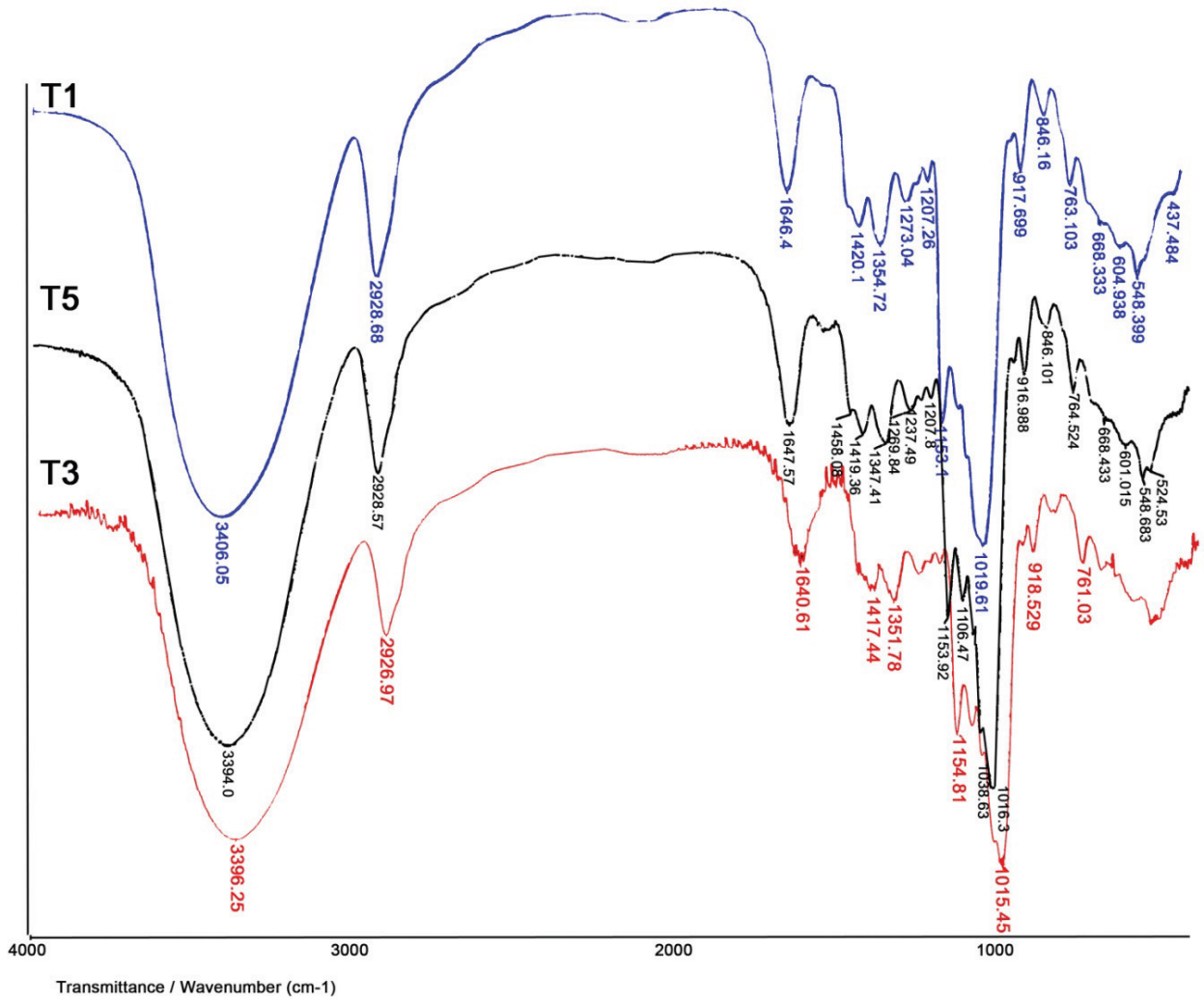

Figure 5. FT-IR spectra of the exopolysaccharides produced by the isolates Lc. mesenteroides T1, Lc. mesenteroides T3 and Lb. hilgardii T5.

dextran production by *Lc. mesenteroides* PCSIR-4 and achieved 47.8% conversion [34].

We determined the optimal temperature and incubation time for dextran production for the three analyzed strains. The optimal dextran production for *Lb. hilgardii* T5 was achieved at 30 °C, which is in agreement with previously published data [8]. *Lb. hilgardii* is responsible for dextran production and grain formation [8]. Glucose molecules in this dextran are linked by alpha 1-3 and alpha 1-6 glycosidic bonds in the main chain with additional alpha 1-3 bonds in the side chain. The presence of alpha 1-3glycosidic bonds in dextrans is known to render them insoluble in water [35].

The optimal temperature for dextran production by *Leuconostoc* strains is strain-dependent and varies from 23–30 °C [31,36,37]. Both *Leuconostoc mesenteroides* strains presented in this paper produced the highest amount of dextran at 23 °C.

Since conditions for dextran production are specific for each strain, they could be further optimized. Several factors including sucrose concentration, nitrogen source, mineral salts, initial pH medium and aeration can influence dextran production [32,33,38,39]. Further optimization of conditions that favor dextran production for our strains has a potential to achieve yields higher than ever reported in the literature, given that under tested conditions, the dextran yields were at level of exceeding those reported by others. Also, the product itself should be more detailed characterized. First, molecular mass should be determined, as well as factors affecting production of dextran desired mass, which is important for its application.

CONCLUSION

Our results show that water kefir grains are rich natural source of potent dextran-producing LAB. Our attempt to isolate dextran producing LAB from a non-commercial water kefir grains generated three strains, which yields of dextran production are exceeding those

reported in the literature, because of which these strains can be considered as candidates for commercial exploitation.

Acknowledgements

The financial support for this investigation given by Ministry of Education, Science and Technological Development of the Republic of Serbia under the project TR 31035 is gratefully acknowledged.

REFERENCES

[1] J. Reiß, Metabolic activity of Tibi grains. Zeitschrift für Lebensmittel Untersuchung und Forschung **191** (1990) 462–465.

[2] H.H. Hsieh, S.Y. Wang, T.L. Chen, Y.L. Huang, M.J. Chen, Effects of cow's and goat's milk as fermentation media on the microbial ecology of sugary kefir grains, Int. J. Food Microbiol. **157** (2012) 73–81.

[3] M. Pidoux, The microbial flora of sugary kefir grain (the gingerbeer plant): biosynthesis of the grain from *Lactobacillus hilgardii* producing a polysaccharide gel, Mircen J. **5** (1989) 223–238.

[4] A. Galli, E. Fiori, L. Franzetti, M.A. Pagani, G. Ottogalli, Composizione microbiologica e chimica deigranuli di Kefir "di frutta", Ann. Microbiol. Enzimol. **45** (1995) 85––95

[5] L. Franzetti, A.Galli, M.A. Pagani, I. De Noni, Microbiological and chemical investigations on "sugar kefir" drink, Ann. Microbiol. Enzimol. **48** (1998) 67–80.

[6] A. Gulitz, J. Stadie, M. Wenning, M.A. Ehrmann, R.F. Vogel, The microbial diversity of water kefir, Int. J. Food Microbiol. **151** (2011) 284–288.

[7] M.G. da C.P. Miguel, P.G. Cardoso, K.T.Magalhães, R.F. Schwan, Profile of microbial communities present in tibico (sugary kefir) grains from different Brazilian States, World J. Microb. Biot. **27** (2011) 1875–1884.

[8] F.W. Waldherr, V.M. Doll, D. Meißner, R.F. Vogel, Identification and characterization of a glucan-producing enzyme from *Lactobacillus hilgardii* TMW 1.828 involved in granule formation of water kefir, Food Microbiol. **27** (2010) 672–678.

[9] M.Horisberger, Structure of the dextran of the tibi grain, Carbohyd. Res. **10** (1969) 379–385.

[10] J.F. Robyt, Mechanisms in the glucansucrase synthesis of polysaccharides and oligosaccharides from sucrose, Adv. Carbohydr. Chem. Biochem. **51** (1995) 133–168.

[11] S.J.F. Vincent, E.J. Faber, J.R. Neeser., F. Stingele, J.P. Kamerling, Structure and properties of the expolysaccharide produced by *Streptococcus macedonicus* Sc 136, Glycobiology **11** (2001) 131–139.

[12] P.T. Murphy, R.L. Whistler, in: R.L. Whistler and J.N. BeMiller (Eds.), Industrial Gums. Polysaccharides and Their Derivatives, 2nd ed, Academic Press, New York, 1973, pp. 513–542.

[13] M. Auerbach, D. Witt, W. Toler,M. Fierstein, R.G. Lerner, H. Ballard, Clinical use of the total dose intravenous infusion of iron dextran, J. Lab. Clin. Med. **111** (1988) 566–570.

[14] M. Naessens, A. Cerdobbel, W. Soetaert, E. Vandamme, Leuconostoc dextransucrase and dextran: production, properties and applications, J. Chem. Technol. Biotechnol. **80** (2005) 845–860.

[15] G. Lacaze, M. Wick, S. Cappelle, Emerging fermentation technologies: Development of novel sourdoughs, Food Microbiol. **24** (2007) 155–160.

[16] R. Sen, Biotechnology in petroleum recovery: The microbial EOR, Prog. Energ. Combust. **34** (2008) 714–724.

[17] R. Shukla, S. Shukla, V. Bivolarski, I. Iliev, I. Ivanova, A. Goyal, Structural Characterization of Insoluble Dextran Produced by *Leuconostoc mesenteroides* NRRL B-1149 in the Presence of Maltose, Food Technol. Biotechnol. **49** (2011) 291–296.

[18] M. Dubois, K.A. Gilles, J.K. Hamilton, P.A. Rebers, F. Smith, Colorimetric method for determination of sugars and related substances, Anal. Chem. **28** (1956) 350–356.

[19] J. Marmur, A procedure for the isolation of deoxyribonucleic acid from microorganisms, J. Mol. Biol. **3** (1961) 208–218.

[20] R.W. Bailer, A.E. Oxford, The Nature of the Capsular Polysaccharides of the Dextran-Producing Organisms *Leuconostoc mesenteroides*, *L. dextranicum* and *Streptococcus bovis*, J. Gen. Microbiol. **20** (1959) 258–266.

[21] P. De Vos, G.M. Garrity, D. Jones, N.R. Krieg, W. Ludwig, F.A. Rainey, K.H. Schleifer, W.B. Whitman,Bergey's manual of systematic bacteriology, vol 3. Springer, Dordrecht, Heidelberg, London, New York, 2009.

[22] W. Ludwig, O. Strunk, R. Westram, H. Meier, Yadhukumar, A. Buchner, T. Lai, S. Steppi, G. Jobb, W. Förster, Brettske, S. Gerber, A.W. Ginhart, O. Gross, S. Grumann, S. Hermann, R. Jost, A. König, T. Liss, R.Lüßmann, M. May, B. Nonhoff, B. Reichell, R. Strehlow, A. Stamatakis, N. Stuckmann, A. Vilbig, M. Lenke, T. Ludwig, A. Bode, K.H. Schleifer, ARB: a software environment for sequence data, Nucleic Acids Res. **32** (2004) 1363–1371.

[23] K.J. Howe, K.P. Ishida, M.M. Clark, Use of ATR/FT-IR spectrometry to study fouling of microfiltration membranes by natural waters, Desalination **147** (2002) 251––255.

[24] P.J. Bremer, G.G. Geesey, An evaluation of biofilm development utilizing non-destructive attenuated total reflectance Fourier transform infrared spectroscopy, Biofouling **3** (1991) 89–100.

[25] S. Nataraj, R.Schomacker, M.Kraume, M.I. Mishra, A. Drews, Analyses of polysaccharide fouling mechanisms during crossflow membrane filtration, J. Membrane Sci. **308** (2008) 152–161.

[26] R.G. Zhbankov, V.M. Andrianov, M.K. Marchewka, Fourier transform IRand Raman spectroscopy and structure of carbohydrates, J. Mol. Struct. **436–437**(1997) 637–654.

[27] P. Ruas-Madiedo, C.G. de los Reyes-Gavilán, Methods for the Screening, Isolation, and Characterization of Exopolysaccharides Produced by Lactic Acid Bacteria, J. Dairy Sci. **88** (2005) 843–856.

[28] L. De Vuyst, B. Degeest, Expolysaccharides from lactic acid bacteria: technological bottlenecks and practical solutions, Macromol. Symp. **140** (1999) 31–41.

[29] M.L. Werning, S. Notararigo, M. Nácher, P. Fernández de Palencia, R.Aznar,P.López, Biosynthesis, Purification and Biotechnological Use of Exopolysaccharides Produced by Lactic Acid Bacteria. Food Additive, Prof. Yehia El-Samragy (Ed.), (2012) ISBN: 978-953-51-0067-6, InTech, (available from: http://www.intechopen.com//books/food-additive/biosynthesis-purification-and-iotechnological-use-ofexopolysaccharides-produced-by-lactic-acid-bac).

[30] R. Van der Meulen, S.Grosu-Tudor, F. Mozzi, F.Vaningelgem, M. Zamfir, G.Font de Valdez, L.De Vuyst, Screening of lactic acid bacteria isolates from dairy and cereal products for exopolysaccharide production and genes involved, Int. J. Food Microbiol. **118** (2007) 250–258.

[31] F. Sarwat, S.A.U. Qader, A. Aman, N. Ahmed, Production & Characterization of a Unique Dextran from an Indigenous *Leuconostoc mesenteroides* CMG713, Int. J. Biol. Sci. **4** (2008) 379–386.

[32] A. Majumder, S.Bhandari, R.K. Purama, S. Patel, A. Goyal, Enhanced production of a novel dextran from *Leuconostoc mesenteroides* NRRL B-640 by Response Surface Methodology, Ann. Microbiol. **59**(2) (2009) 309––315.

[33] A. Majumder, A. Singh, A. Goyal, Application of response surface methodology for glucan production from *Leuconostoc dextranicum* and its structural characterization, Carbohyd. Polym. **75** (2009) 150–156.

[34] S.A. Qader, L. Iqbal, A. Aman, E. Shireen, A. Azhar, Production of dextran by newly isolated strains of *Leuconostoc mesenteroides* PCSIR-4 and PCSIR-9, Turk. J. Biochem. **31** (2006) 21–26.

[35] M. Pidoux, G. A. De Ruiter, B. E. Brooker, I. J. Colquhoun, V. J. Morris, Microscopic and chemical studies of a gelling polysaccharide from *Lactobacillus hilgardii*, Carbohyd. Polym. **13** (1990) 351–362.

[36] E.J. Hehre, J.Y. Sugg, Serologically reactive polysaccharides producedthrough the action of bacterial enzymes: Dextran of *Leuconostoc mesenteroides* from sucrose, J. Exp. Med. **75** (1942) 339–353.

[37] A. Aman, N.N. Siddiqui, S.A.U. Qader, Characterization and potential applications of high molecular weight dextran produced by *Leuconostoc mesenteroides* AA1, Carbohyd. Polym. **87** (2012) 910–915.

[38] S.D. Sawale, S.S. Lele, Statistical Optimization of Media for Dextran Production by*Leuconostoc* sp., Isolated from Fermented Idli Batter, Food Sci. Biotechnol. **19** (2010) 471–478.

[39] P. Kanmani, R. Satishkumar, N.Yuvaraj, K.A. Paari, V. Pattukumar, V. Arul, Production and purification of a novel exopolysaccharide from lactic acid bacterium *Streptococcus phocae* PI80 and its functional characteristics activity in vitro, Bioresource Technol. **102** (2011) 4827–4833.

IZVOD

ZRNO VODENOG KEFIRA KAO IZVOR BAKTERIJA MLEČNO KISELINSKOG VRENJA POTENTNIH PRODUCENATA DEKSTRANA

Slađana Z. Davidović[1], Miona G. Miljković[1], Dušan G. Antonović[2], Mirjana D. Rajilić-Stojanović[1], Suzana I. Dimitrijević-Branković[1]

[1]*Univerzitet u Beogradu, Tehnološko–metalurški fakultet, Katedra za biohemijsko inženjerstvo i biotehnologiju, Karnegijeva 4, Beograd, Srbija*
[2]*Univerzitet u Beogradu, Tehnološko–metalurški fakultet, Katedra za organsku hemiju, Karnegijeva 4, Beograd, Srbija*

(Naučni rad)

Vodeni kefir je napitak koji nastaje fermentacionom aktivnošću bakterija mlečno-kiselinskog vrenja, kvasaca i sirćetnih bakterija. Ova kompleksna smeša mikroorganizama smeštena je unutar polisaharidnog matriksa – kefirnog zrna. Glavnu šećernu komponentu matriksa čini dekstran koji sintetišu bakterije mlečno-kiselinskog vrenja. Dekstran je homo polisaharid velike molekulske mase čija je monomerna jedinica glukoza. Zahvaljujući dobroj rastvorljivosti i stabilnosti, dekstran ima široku primenu u različitim granama industrije, kao što su medicina, farmacija, prehrambena, tekstilna i hemijska industrija. Nerastvorni dekstran može da posluži kao nosač za imobilizaciju biomolekula. Imajući u vidu veliku primenjivost dekstrana, cilj ovog rada je bio izolovati bakterije mlečno-kiselinskog vrenja iz zrna vodenog kefira koje produkuju ovaj egzopolisaharid sa visokim prinosima. U radu je prikazana izolacija i karakterizacija tri selektovana soja i optimizacija uslova za produkciju dekstrana. Na osnovu morfoloških, fizioloških i biohemijskih osobina i 16S rRNK sekvenciranja utvrđeno je da su izolati T1 i T3 sojevi vrste *Leuconostoc mesenteroides*, dok je izolat T5 identifikovan kao *Lactobacillus hilgardii*. Za produkciju dekstrana korišćena je modifikovana MRS podloga sa 5% saharoze, kao jedinim izvorom ugljenika. Maksimalni prinosi dekstrana (11,56, 18,00 i 18,46 g/l) su dobijeni nakon 16, 20 i 32 h fermentacije, za T1, T3 i T5, redom. Optimalne temperature za produkciju dekstrana su 23 °C za dva *Leuconostoc mesenteroides* soja, a za *Lactobacillus hilgardii* 30 °C. Uzorci sintetisanih polisaharida su identifikovani kao dekstrani na osnovu papirne hromatografije, dok su glavne strukturne karakteristike prečišćenih dekstrana utvrđene na osnovu FTIR spektroskopije.

Ključne reči: Dekstran • Zrno vodenog kefira • *Lc. mesenteroides* • *Lb. hilgardii*

Analitičke tehnike za određivanje i praćenje silicijuma u vodi u termoenergetskim postrojenjima

Nataša R. Ignjatović[1], Maja D. Ilić[2], Ljubinka V. Rajaković[3]

[1]*Ministarstvo unutrašnjih poslova Republike Srbije, Beograd, Srbija*
[2]*Privredno društvo „Termoelektrane i kopovi Kostolac", Kostolac, Srbija*
[3]*Univerzitet u Beogradu, Tehnološko-metalurški fakultet, Beograd, Srbija*

Izvod

U ovom radu obuhvaćena su relevantna istraživanja u oblasti specijacione analize silicijuma. Održavanje nepromenljivog sastava silicijumovih vrsta u toku pojedinačnih analitičkih faza ispitivanja (prikupljanje uzoraka, čuvanje, konzervisanje) posebno su razmatrane. Izdvojene su tehnike koje se koriste za određivanje kako ukupnog tako i pojedinih oblika silicijuma (reaktivnog i nereaktivnog). Određivanje sadržaja silicijuma u ultračistoj vodi u termoenergetskim postrojenjima je od izuzetnog značaja zbog različitog uticaja pojedinih silicijumovih vrsta (korozivnost i toksičnost) i zbog izbora postupka za efikasno uklanjanje silicijuma iz vode. Specijaciona analiza silicijuma je neophodna i u analizi procesa koji utiču na životnu sredinu.

Ključne reči: silicijum, termoenergetska postrojenja, ultračista voda, specijaciona analiza, analitičke tehnike.

Dostupno na Internetu sa adrese časopisa: http://www.ache.org.rs/HI/

PREGLEDNI RAD

UDK 546.28:621.1:544

Hem. Ind. **69** (6) 605–616 (2015)

doi: 10.2298/HEMIND140914084I

U termoelektranama voda ima značajnu ulogu. Voda je medijum koji preuzima toplotnu energiju sagorelog uglja (mazuta ili gasa) i kao para predaje energiju lopaticama turbine (sistem voda-para). Za generisanje pare u termoelektranama, koristi se demineralizovana, ultračista voda. Ultračista voda je najčistija u kategoriji procesnih industrijskih voda sa minimalnim sadržajem prirodnih jedinjenja [1]. Kvalitet procesne vode je od velikog značaja jer od njega zavisi rad termoenergetskih postrojenja. Primese u vodi štetno utiču na rad postrojenja, jer stvaraju naslage i izazivaju koroziju [2–4]. Taloženje primesa u sistemu voda-para pospešuju visoka temperatura i visok pritisak. Formirane naslage otežavaju prenos toplotne energije od produkata sagorevanja na zidove sistema, čime se smanjuje efikasnost izmenjivača toplote i protok vode [3]. Ispod sloja taloga (kamenca i mulja), dolazi do ubrzanog razvoja korozije. Korozija skraćuje životni vek komponenti postrojenja, prouzrokuje curenje i ispuštanje vode, smanjuje pogonsku bezbednost i povećava troškove održavanja.[5,6]. Korozioni procesi u termoenergetskim postrojenjima usled neadekvatnog kvaliteta vode relativno su dobro proučeni i opisani u literaturi [7–10].

Na osnovu podataka Instituta za elektroenergetska istraživanja u SAD (EPRI), godišnja šteta od korozije termoenergetskih postrojenja iznosi 3,5 milijarde dolara, od toga oko 600 miliona dolara samo od korozije turbinskih postrojenja. Prema podacima iz 1991. godine iznetim na Međunarodnoj konferenciji o vodeno–hemijskim režimima termoelektrana, u 40% termoelektrana u SAD je potrebno unaprediti hemijsku kontrolu u vodeno-parnom režimu i poboljšati kvalitet pare [11].

Mnoge vode sadrže silicijum, što nije iznenađujuće iz razloga što je silicijum drugi po rasprostranjenosti hemijski element, odmah nakon kiseonika. U većini prirodnih voda zastupljen je u obliku silikata i njegova koncentracija se kreće od 0,6–40 μg dm^{-3}. Iako silicijum-dioksid ne učestvuje u mehanizmu korozije, od velikog je značaja jer formira izuzetno tvrde, guste i termički slabo provodljive naslage u kotlovskom sistemu i turbini, što dovodi do gubitka u termodinamičkoj i mehaničkoj efikasnosti postrojenja. Prisustvo silicijuma u vodi dovodi do čestih havarija u termoenergetskim postrojenjima, pa se silicijum-dioksid smatra najnepoželjnijom komponentom vode [2–4].

Količina silicijuma predstavlja kontrolni parametar u procesnim vodama. Za kontrolu sadržaja silicijuma koriste se različite analitičke metode. U termoenergetskim postrojenjima gde se voda koristi za napajanje parnih kotlova sadržaj silicijuma mora biti manji od 20 μg dm^{-3}.

Na slici 1 prikazan je korozioni potencijal silicijuma u sistemu voda-para [2].

Hemija silicijuma

Silicijum je posle kiseonika, najzastupljeniji element u prirodi. Glavni deo mase litosfere sastavljen je od silikatnih stena i silicijum(IV)-oksida. Silicijum(IV)-oksid je najznačajnije jedinjenje silicijuma. Osnovne kristalne alotropske modifikacije ovog oksida su: kvarc, tridimit i

Prepiska: N.R. Ignjatović, Ministarstvo unutrašnjih poslova Republike Srbije, Bulevar Mihajla Pupina 2, 11000 Beograd, Srbija.
E-pošta: natassa.ignjatovic@gmail.com
Rad primljen: 14. septembar, 2014
Rad prihvaćen: 17. novembar, 2014

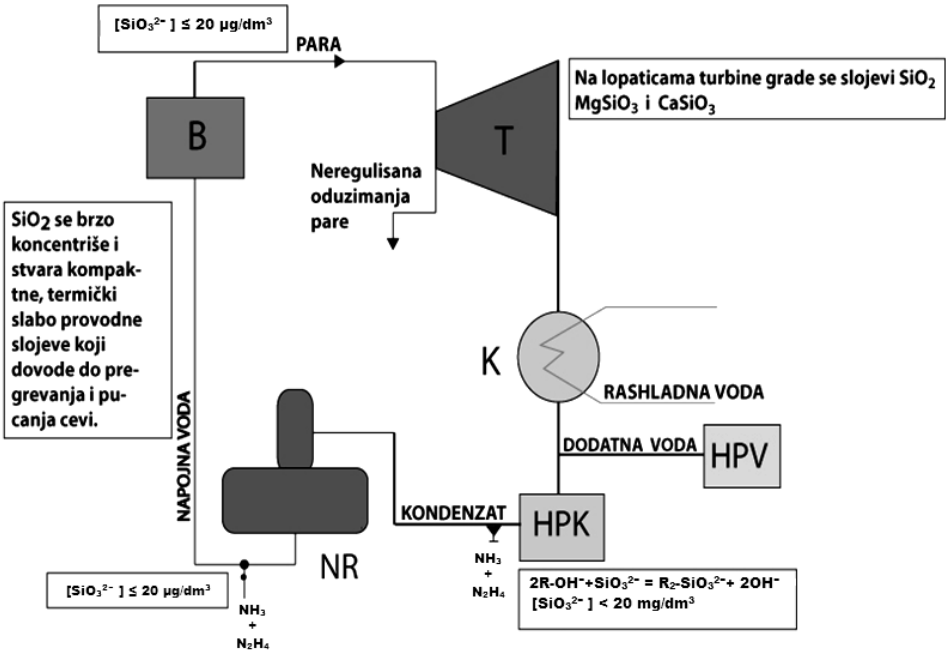

Slika 1. Korozioni potencijal silicijumovih jedinjenja u sistemu voda–para [2]; T – turbina, K – kondenzator, HPV – hemijska priprema vode, HPK – hemijska priprema kondenzata, NR – napojni rezervoar, B – kotao, bojler.
Figure 1. Corrosion potential of silicon compounds in the water steam cycle; T – turbine, K – condenser, HPV – chemical water treatment plant, HPK – chemical treatment of condensate, NR – feed water tank, B – boiler.

kristobalit. U manjoj količini u prirodi je prisutan u modifikacijama amorfne strukture-opalu i ahatu. Kristalni silicijum ima nisku rastvorljivost u vodi (ispod 6 mg dm^{-3} SiO_2), dok se rastvorljivost amorfnog silicijuma kreće u opsegu od 100–140 mg dm^{-3} SiO_2. Na slici 2 prikazana je rastvorljivost različitih modifikacija silicijum(IV)-oksida u zavisnosti od pH vrednosti [12].

Sve prirodne vode sadrže silicijum. Silicijum se u vodi javlja u jonskom i molekulskom obliku (reaktivan oblik), kao suspendovan, koloidni i polimerni (nereaktivni oblik).

Rastvorni oblici silicijuma u vodi se mogu prikazati jednačinom (1) kao ravnotežni sistem:

$$H_2SiO_3 \leftrightarrows H^+ + HSiO_3^- \leftrightarrows H^+ + SiO_3^{2-} \quad (1)$$

Monosilicijumova kiselina koja se stvara, je veoma slaba kiselina. Karakteristične vrednosti konstanti rav-

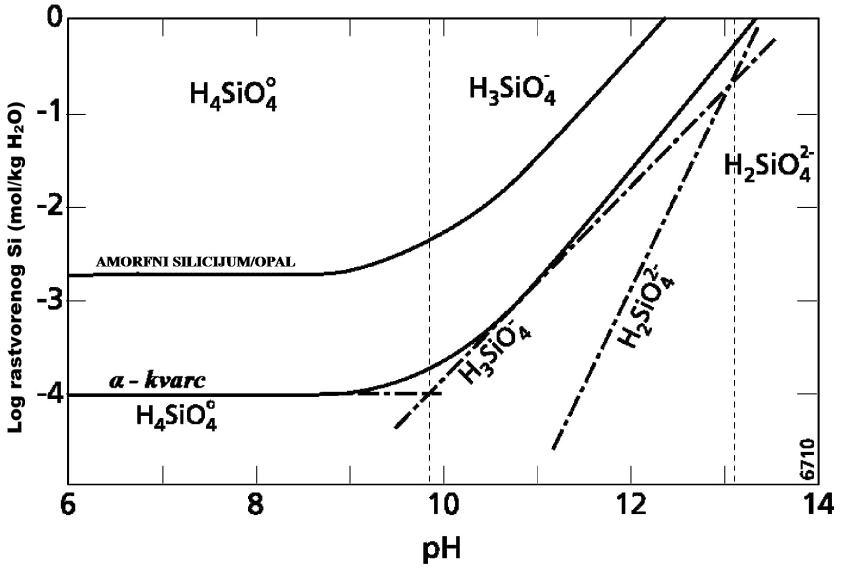

Slika 2. Rastvorljivost kvarca i amorfnog silicijuma u zavisnosti od pH vrednosti [12].
Figure 2. Solubility of quartz and amorphous silica as a function of pH value [12].

noteže, $K_1 = 1{,}4\times10^{-10}$ i $K_2 = 6{,}3\times10^{-14}$, ukazuju na nizak stepen jonizacije.

Rastvorljivost silicijuma u vodi zavisi od mnogobrojnih faktora, kao što su: temperatura, pritisak, pH vrednost i jonska jačina. Na slici 3 prikazana je rastvorljivost silicijuma u zavisnosti od pH vrednosti [13], a na slici 4 rastvorljivost silicijuma u zavisnosti od temperature [13].

Pri višim koncentracijama silicijum se nalazi u koloidnom stanju u obliku polimernih čestica veće mase [14]. Koloidno stanje nastaje i vezivanjem silicijuma sa organskim i neorganskim jedinjenjima pri čemu se formiraju kompleksna jedinjenja [13]. Polimerizacija se može predstaviti jednačinom (2):

$$[Si_nO_{2n-(nx/2)}(OH)_{nx}] + mH_4SiO_4 \rightarrow \rightarrow [Si_{n+m}O_{2n-(nx/2)+2m(2-p)}(OH)_{nx+4(m-p)}] + 2pmH_2O \quad (2)$$

gde su: n – broj silicijumovih atoma u polisilicijumovoj kiselini, x – broj OH grupa po atomu silicijuma u polimeru, koji ne prelazi broj 4, m – broj molekula monosilicijumove kiseline, p – frakcije OH grupa po molekulu monosilicijumove kiseline koje se pojavljuju u vodi u toku reakcije polimerizacije.

U tabeli 1 prikazani su različiti oblici kiselina silicijuma u zavisnosti od broja silicijumovih atoma.

Tabela 1. Različiti oblici kiselina silicijuma
Table 1. Diferent forms of silicic acid

Opšta formula	Vrednost koeficijenata	Formula kiseline	Naziv kiseline
$mSiO_2 \cdot nH_2O$	n=1	H_2SiO_3	Metasilicijumova
	n=2	H_4SiO_4	Ortosilicijumova
	n=1, m=2	$H_2Si_2O_5$	Dimetasilicijumova
	n=3, m=2	$H_2Si_2O_7$	Diortosilicijumova

Do polimerizacije dolazi kada je koncentracija rastvornog silicijuma veća od 2×10^{-3} M. Polimerizacija sledi posle oligomerizacije. Prilikom oligomerizacije $[SiO_2]_{n\leq3}$ formira se kritično jezgro sa četiri monomera.

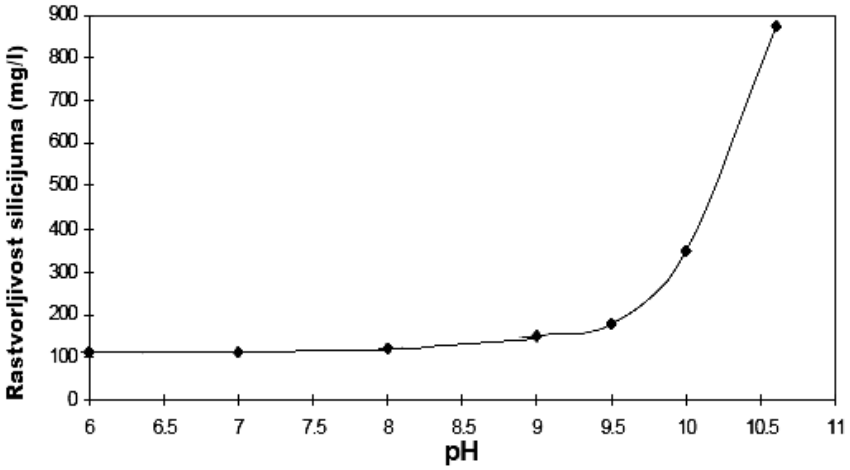

Slika 3. Rastvorljivost silicijuma u zavisnosti od pH vrednosti [13].
Figure 3. Solubility of silica silica as a function of pH value [13].

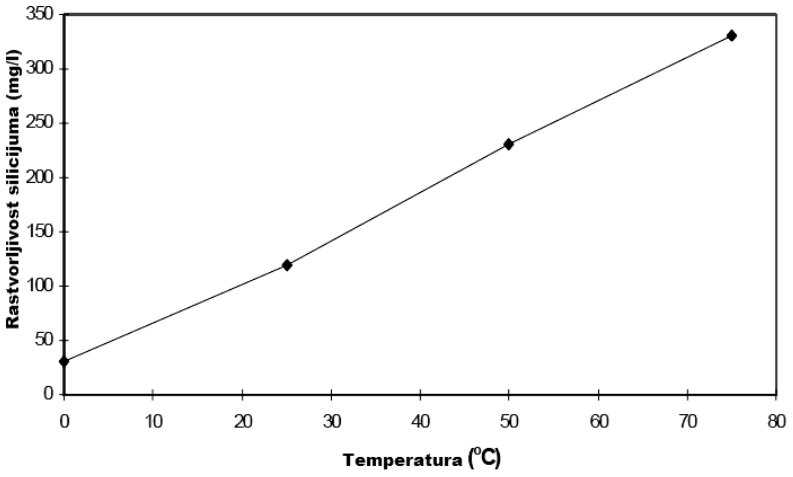

Slika 4. Rastvorljivost silicijuma u zavisnosti od temperature [13].
Figure 4. Solubility of silica silica as a function of temperature [13].

Na slici 5 predstavljen je mehanizam polimerizacije čestica silicijumove kiseline pri čemu nastaju linearne i ciklične strukture [15].

Specijaciona analiza silicijuma

Specijaciona analiza predstavlja analitičku aktivnost identifikacije i kvantifikacije jedne ili više hemijskih vrsta elemenata u uzorku. Analiza obuhvata dva koraka. U prvom koraku se određuje ukupna koncentracija elementa u uzorku, u drugom koraku se vrši separacija, identifikacija i kvantifikacija pojedinih vrsta tog elementa u ispitivanom uzorku. Specijacijom se vrši diferencijacija elementa na osnovu oksidacionog stanja, jonskih ili molekulskih oblika, protonovanih ili neprotonovanih oblika, jednostavnih ili kompleksiranih jona, monomernih ili polimernih formi.

Određivanje koncentracije pojedinih vrsta silicijuma u uzorku ultračiste vode obezbeđuje adekvatnu informaciju za razumevanje i proučavanje uticaja silicijuma na termoenergetske sisteme i zbog izbora postupka za efikasno uklanjanje silicijuma iz vode. Za analizu pojedinih oblika silicijuma razvijen je veliki broj metoda i postupaka koji uključuju hromatografske, spektrometrijske i elektrohemijske tehnike i njihove kombinacije. Preporučuju se sledeće metode:

- spektrofotometrija [16],
- AAS, atomska apsorpciona spektrometrija [17,18],
- FIA, protočno-injektirajuća analiza [19],
- MS, masena spektrometrija [20],
- GF-AAS, atomska aporpciona spektrometrija sa grafitnom kivetom [21],
- X-ray difrakcija, difrakcija rendgenskim zracima [22],
- FTIR, Furijeova transformacija infracrvene spektroskopije [23],
- IC, jonska hromatografija [24],
- IR (infra-crvena) spektrofotometrija [25],
- ICP-OES, emisiona spektrometrija [26],
- ICP-MS, ICP sa masenim detektorom [27] i
- NAA, neutron aktivaciona analiza [28].

Različite tehnike separacije koje bi mogle da se uspešno kombinuju sa osetljivim tehnikama detekcije su prikazane na slici 6.

U prirodnim vodama silicijum se nalazi u obliku različitih hemijskih jedinjenja (H_2SiO_3 i $mSiO_2 \cdot nH_2O$) i u različitim fizičkim stanjima (u obliku suspenzija, koloidnih čestica, rastvora, u obliku molekula i jona). U brojnim radovima se navodi da je silicijum u vodama prisutan kao rastvorni silicijum i nerastvorni silicijum. Pod pojmom rastvorni silicijum se podrazumevaju anjoni silicijumove kiseline i niži polimeri-oligomeri, dok se pod pojmom nerastvorni silicijum podrazumevaju viši polimeri ili čestice čiji je prečnik veći od 5 nm.

U tabeli 2 dat je pregled naučnih radova u kojima je predmet istraživanja silicijum (i vrste silicijuma) u različitim uzorcima. Navedene su analitičke metode za određivanje ukupne koncentracije silicijuma u vodi kao i metode za određivanje specija silicijuma (rastvornog i nerastvornog silicijuma). Sadržaj nerastvornog ili koloidnog silicijuma se određuje indirektno, oduzimanjem koncentracije rastvorenog silicijuma od koncentracije ukupnog silicijuma.

U poslednje dve decenije objavljen je veliki broj naučnih radova za određivanje silicijuma u različitim uzorcima. Cilj svih istraživanja je bio razvoj i poboljšanje metoda za razdvajanje i određivanje različitih oblika

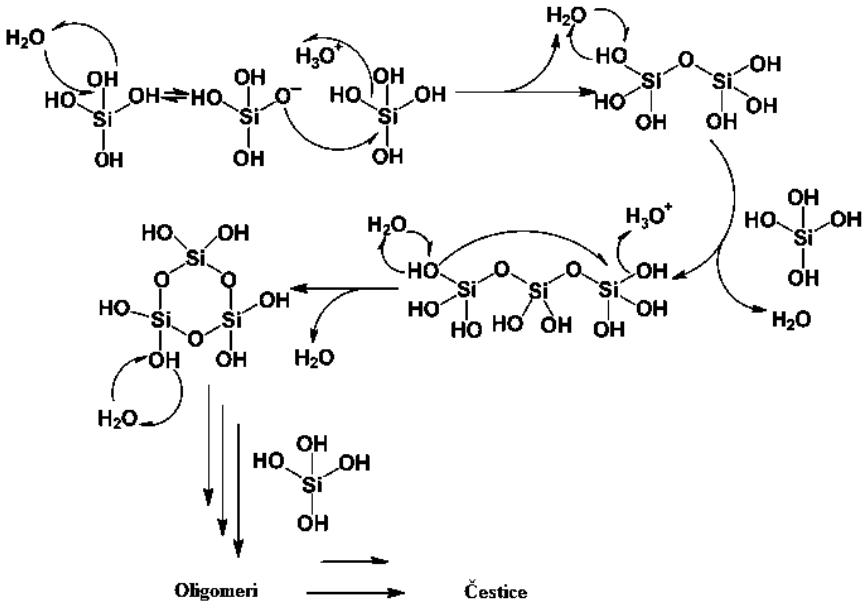

Slika 5. Mehanizam polimerizacije čestica silicijumove kiseline kojim se dobijaju linearne i ciklične strukture [15].
Figure 5. Mechanism of polymerization of silicic acid species to generate linear and cyclic structures [15].

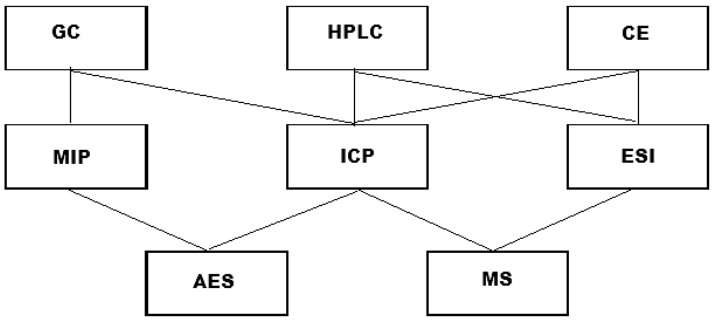

Slika 6. Tehnike koje se primenjuju za specijacionu analizu [29]; GC – gasna hromatografija; HPLC – tečna hromatografija visoke performanse; MIP – mikrotalasno-indukovana plazma; ICP – indukovano spregnuta plazma; CE – kapilarna elektroforeza; ESI – elektrosprej jonizacija; AES – atomska emisiona spektrometrija; MS – masena spektrometrija.
Figure 6. Actual techniques for speciation analysis; GC – Gas Chomatography; HPLC – High Performance Liquid Chromatography; MIP – Microwave-induced Plasma, ICP – Inductively coupled plasma; CE – Capillary Electrophoresis; ESI – Electrospray Ionization; AES – Atomic Emission Specrometry; MS – Mass Spectrometry.

Tabela 2. Pregled instrumentalnih analtičkih metoda za određivanje silicijuma u različitim uzorcima
Table 2. Review of instrumental analytical methods for the determination of silica in various matrices

Uzorak	Priprema uzorka	Analitička metoda	Granica detekcije[a]	Ref.
Urin, rastvorni Si	Razblaživanje uzorka sa H_2O, dodavanje CH_3COOH, $CaCl_2$ i NH_4OH i filtracija u cilju uklanjanja fosfata. 2N HCl, amonijum-molibdat, ekstrakcija etilacetatom. U vodenu fazu se doda limunska kiselina i 1-amon-2naftol-4sulfonska kiselina	Spektrofotometrija, 690 mμ	<60 μg dm^{-3} SiO_2	[16]
Silikatne stene, ukupni Si	Razaranje sa NaOH u retortama od nikla ili razaranje sa Na_2CO_3 u platini	AAS, 2516 Å	200 μg dm^{-3}	[17]
Geotermalne vode, ukupni Si	Filtriranje uzorka kroz vakuum filter, acidifikacija sa 3 ml 1:1 rastvorom HNO_3 (pH vrednost 1-2)	AAS	200 μg dm^{-3} SiO_2	[18]
Voda, rastvorni Si	10% HCl, razblaživanje ultra čistom dejonzovanom vodom, rastvor amonijum-molibdata i luminola	Hemiluminescencija sa protočnom analizom injektiranjem (FI–CL)	0,35 μg dm^{-3}	[19]
Uzorci sintetčkih amorfnih slikata (SAS), amorfni Si	Razaranje sa HNO_3 i HF. Rastvaranje u vodi	GF-AAS	< 0,1 mg dm^{-3}	[21]
Voda, nanočestice Si	Stöber process za dobijanje nanočestica i sušenje u cilju uklanjanja vode	WDXRF	Sadržaj približno 10%	[22]
Zemljište, sedimenti i mulj, kristalni α-Si	Mlevenje i prosejavanje, ispiranje sa etil alkoholom	IR spektrofotometrija 798 cm^{-1}	<1%	[23]
Voda, rastvorni Si	Puferovanje rastvora do pH 4, dodatak molibdatnog reagensa, zagrevanje, hlađenje, dodatak acetonitrila, filtracija	HPLC/UV-VIS detector	0,007 mg dm^{-3} SiO_2	[24]
Pirinač, sadržaj Si	Mokro razaranje uzorka u mikrotalasnom zagrevaču, rastvaranje sa amonijum-molibdatom u kiseloj sredini	UV/Vis spektrofotometrija	30 μM	[25]
Pirinač, sadržaj Si	Bez prethodne pripreme uzorka	Difrakcija X-zraka	Približno 2%	[25]
Pirinač, sadržaj Si	Bez prethodne pripreme uzorka	IR spektroskopija	0,1%	[25]
Biogeni Si u morskim stenama	Ekstrakcija, nakon tretiranja uzorka sa toplim rastvorom NaOH ili Na_2CO_3	ICP-OES	5 μg dm^{-3} SiO_2	[26]
Voda, ukupni Si	Kapilarna zonalna elektroforeza CZE (Na-hromat, elektoroosmoza sa trimetil-tetradecil-amomijum bromurom (TTAB)	ICP-MS	>1,000 ng dm^{-3}	[27]
Voda, reaktivan Si	Voda se tretira 10% rastvorom amonijum-molibdata na pH vrednosti od 1,2/1,4. Doda se 20 ml 1:1 H_2SO_4. Molibdo-silicijumova kiselina se ekstrahuje sa MIBK	NAA	0,2 μg dm^{-3}	[28]
Voda, rastvorni Si	Natrijum molibdat-askorbinska kiselina	IEC/VIS detektor 700 nm	250 μg dm^{-3}	[30]

Tabela 2. Nastavak
Table 2. Continued

Uzorak	Priprema uzorka	Analitička metoda	Granica detekcije[a]	Ref.
Čestice prašine, slobodan Si	Prosejavanje, ispiranje kiselinama i bazama u cilju uklanjanja nečistoća, uzorak se rastvara u vodi da se dobije suspenzija, a potom filtrira i filtrat rastvara u zagrejanoj fosfornoj kiselini	Difrakcija X-zraka, CuKα zračenje na 40 kV i 20mA u difrakcionoj oblasti od 5–600 (2θ)	20–25 μg	[31]
Vazduh, kristalni Si	Skupljanje uzorka u ciklonima i direktno određivanje sa filtera	FTIR-spektroskopija 620–800 cm^{-1}	0,006 μg dm^{-3}	[32]
Voda, reaktivni Si	Reakcija sa molibdatom u kiseloj sredini, redukcija sa $SnCl_2$ uz dodatak oksalne kiseline	FIA 820 nm	0,78 μg dm^{-3} SiO_2	[33]
Voda, ukupan Si	Rastvaranje u NaOH i KOH pri čemu se čestice određuju FAB-MS u alkanlnom rastvoru, dok se momomerni, dimerni i tetramerni kompleksi Si određuju kolorimetrijski preko amonijum-molibdata	FAB/MS kolorimetrija	<0,4 mmol dm^{-3}	[34]
Voda, ukupan i rastvorni Si	Taloženje sa amonijum-hloridom, rastvaranje sa amonijum-molibdatom u kiseloj sredini	FI-ET-AAS	≥280 μg dm^{-3}	[35]
Ultračista voda, rastvorni Si	Hlađenje Rodaminom B u toku procesa obrazovanja molibdo-silikata	Spektrofotometrija	34 ng dm^{-3}	[36]
Ljudska tkiva-krvni uzorci, Si	ultrasonična mešalica i dodatak 1000 μl rastvora koji sadrži 20 mg dm^{-3} Ca, 186 mg dm^{-3} EDTA and 10 ml dm^{-3} Triton TX-100 (alkilatil polietarskog alkohola)	GF-AAS	0,2 mg dm^{-3}	[37]
Procesne industrijske vode, ukupni Si	Bez prethodne pripreme uzorka. Uzorku se dodaje kalcijum sa ciljem sprečavanja obrazovanja silicijum-karbida i povećanja osetljivosti metode	F-AAS	2,5 μg dm^{-3}	[38]
Voda, ukupan silicijum	Nakon filtriranja, uzorak vode se uparava do suvog ostatka	GAA, 29Si (γ, p)	0,1 mg dm^{-3}	[39]

[a]Računato na Si. Kad je računato na SiO_2 to je posebno naznačeno

(specija) silicijuma. Poseban naučni interes predstavlja razvoj neinvazivnih metoda za razlikovanje rastvornog i nerastvornog oblika silicijuma kao i metoda za direktno određivanje koloidnog silicijuma.

Chu i saradnici [40] su razvili i istražili tri analitičke metode za određivanje silikata u ultračistim vodama. Ove metode su zasnovane na primeni ICP-AES, ICP-MS i spektrometrije sa hladnom kiselinskom digestacijom. Granica detekcije ovih tehnika su od 0,25–3 ng dm^{-3} Si. Međutim, pre analize potrebno je da se izvrši koncentrovanje rastvora uzoraka upravanjem. Yoshimura i sar. [20] su razvili metodu za spektrofotometrijsko određivanje silikata u ultračistim vodama koja se zasniva na apsorpciji kompleksnog jona molibdosilikata na sorbentu, sephadex LH-20 gel. Kombinovanim postupkom kompleksiranja i sorpcije ostvarena je granica detekcije od 0,01 ng dm^{-3}.

Formiranje obojenih kompleksa molibdosilikata sa katjonskim bojama primenjuje se za povećanje osetljivosti metode pri određivanju silicijuma u uzorcima silikata [41–43]. Motomizu i sar. [41–43] su razvili spektrofotometrijsku metodu za određivanje tragova silikata (oko 1 μg dm^{-3}), u malim zapreminama uzorka. Za rastvaranje silikata koristili su organski rastvarač. Međutim, nedostatak ove kao i svih navedenih metoda [40––43] je zanemarivanje uticaja matriksa na određivanje silikata. Sabarudin i saradnici [44] su primenili kalibracione tehnike kojima je taj nedostatak izbegnut. Li i sar. [45] su predložili novu metodu za određivanje sadržaja rastvornog silicijuma u vodi, gde se za separaciju čestica koristi tečna jonska ekskluziona hromatografija, a sadržaj eluiranih silikata određuje merenjem električne provodljivosti. Kolone su pakovane slabo kiselim katjonskim smolama, a kao eluent se koristi ultračista voda. Linearnost metode je u opsegu koncentracija silikata od 0,10–1000,0 μmol dm^{-3}, sa korelacionim koeficijentom od 0,997 (n = 6). Granica detekcije ove metode je 0,02 μmol dm^{-3} i niža je od granice detekcije metode koju su predložili Hioki i saradnici [46], koji su koristili kao detektor maseni spektrometar sa indukovano spregnutom plazmom. Ova metoda je jednostavna, omogućava direktno određivanje silikata nakon prolaska kroz kolonu i podesna je za rutinske analize.

Za određivanje silicijuma u obliku silikat-jona primenjuju se tehnike jonske hromatografije, jonske ekskluzione hromatografije i tečne hromatografije visokih performansi kod kojih se kao detektori koriste: UV-detektor, maseni spektrometar i fluorescencioni detektori. Za određivanje sadržaja silicijuma u obliku koloidnih čestica Aspanut i saradnici[47] primenili su nespektroskopske metode: foton-korelativnu spektroskopiju i turbidimetriju. Koloidne čestice se iz rastvora izdvajaju primenom eksluzione tečne hromatografije na osnovu veličine čestica. Kao mobilna faza koristi se rastvor nat-

rijum-fosfata pri pH 9. Kod foton-korelativne spektroskopije, intenzitet rasutog zračenja je direktno proporcionalan veličini koloidnih čestica silicijuma. Maksimalna vrednost intenziteta se nalazi na talasnim dužinama od 270–290 nm. Kod turbidimetrije koriste se UV detektori. Intenzitet signala raste sa porastom veličine koloidnih čestica silicijuma. Granica detekcije za foton-korelativnu spektroskopiju za koloidne čestice prečnika 78 nm je 0,06 mg dm^{-3}, dok je kod trubidimetrije granica detekcije 2 mg dm^{-3}. U radu su istraženi uticaj uslova mobilne faze i protoka na rezoluciju i pik hromatograma. Korišćenjem fosfatnog pufera u ekskluzionoj hromatografiji omogućava se izdvajanje koloidnih čestica silicijuma od ostalih čestica. Nedostatak ovih metoda je niska osetljivost ukoliko rastvor sadrži koloidne čestice silicijuma čiji je prečnik manji od 1 nm.

Burguera i sar. [35] su predložili ET-AAS za određivanje sadržaja ukupnog silicijuma u vodi, kao i za određivanje sadržaja rastvornog silicijuma. Mala zapremina uzorka se injektira u grafitnu kivetu koja zagreva na visokoj temperaturi u cilju atomizacije uzorka. U kiveti može da dođe do taloženja uzorka silicijuma sa amonijum-hloridom, talog se rastvara sa amonijum-molibdatom u kiseloj sredini (HNO_3). Kao hemijski modifikator koristi se 20 ng europijuma. Granica detekcije ove metode za ukupan silicijum je 300 μg dm^{-3}, a za rastvorni 280 μg dm^{-3}. Preciznost metode je 2–6% (n = 10) za ukupni silicijum, a za rastvorni 4–6% (n = 2).

Takaku i sar. [48] su za određivanje tragova silicijuma u ultračistim vodama primenili ICP-MS visoke rezolucije. Kod ove metode je problem signal koji potiče od plazme. Autori su u cilju prevazilaženja ovog problema vršili koncentrovanje rastvora uzorka uparavanjem. Ovom metodom se određuje sadržaj ukupnog silicijuma sa granicom detekcije ispod 1 ng dm^{-3}.

Opfergelt [49], Pramann [50] i Georg [51] primenili su ICP-MS za određivanje stabilnih izotopa silicijuma u vodi ^{28}Si, ^{29}Si i ^{30}Si. Nedostatak ove spektrometrijske tehnike je skupa oprema.

Za određivanje sadržaja silicijuma u rekama Mann i sar. [52] primenili su ^{1}H- i ^{29}Si-NMR spektroskopiju, sa ili bez kros polarizacije. Merenja se izvode na 59,6 MHz. Na slici 7 je prikazan NMR spektar silicijuma, ^{29}Si [52]. Ovo je neinvazivna metoda. Imajući u vidu da NMR spektar silicijuma sadrži multiplitete, Kim [53], Xue [54] i Yamashita [55] su primenili NMR spektroskopiju za određivanje strukture silikata što je od značaja za proučavanje procesa polimerizacije silicijuma i stvaranje koloidnih čestica.

Za indirektno određivanje rastvornog silicijuma u vodi Oltmann i sar. [28] primenili su neutron aktivacionu analizu, nakon ekstrakcije molibdensilicijumove kiseline sa metilizobutil ketonom. Uzorak se aktivira u reaktoru, a zatim se koncentracije dobijenih radioaktivnih izotopa meri na gama spektrometru visoke rezolucije. Intenzitet emitovanog gama zračenja direktno je proporcionalan količini prisutnog radionuklida u uzorku. Ovo je veoma osetljiva tehnika [56] granice detekcije od 2×10^{-4} μg dm^{-3}.

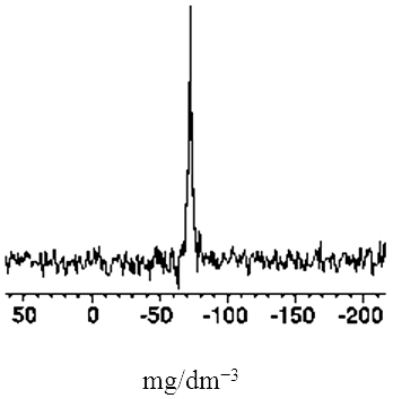

*Slika 7. ^{29}Si-NMR 800 μM silicijumove kiseline u ultračistoj vodi na sobnoj temperaturi [52]. Preuzeto uz dozvolu iz (M.D. MANN, B.F. CHMELKA, MEASUREMENT OF DILUTE 29SI SPECIES IN SOLUTION USING A LARGE VOLUME COIL AND DEFT NMR, ANAL.CHEM. **72** (2000) 5131–5135). Autorsko pravo (2014) American Chemical Society.*
*Figure 7. DEFT ^{29}Si-NMR of 800 μM silicic acid in nanopure water at room temperature [52]. (Reprinted (adapted) with permission from (M.D. MANN, B.F. CHMELKA, MEASUREMENT OF DILUTE 29SI SPECIES IN SOLUTION USING A LARGE VOLUME COIL AND DEFT NMR , ANAL.CHEM. **72** (2000) 5131–5135). Copyright (2014) American Chemical Society.*

Stabilnost silicijumovih specija: prikupljanje uzoraka, čuvanje i prezervacija

Problemi prikupljanja uzoraka kao što su gubitak analita ili kontaminacija se često javljaju kod analize elemenata koji su prisutni u tragovima, ali su oni danas dobro proučeni i kontrolisani. Prikupljanje i čuvanje uzoraka mogu se smatrati jednim od bitnih uslova za očuvanje informacije o pojedinim vrstama silicijuma tokom celog analitučkog procesa. Za postizanje ovog cilja koriste se dve strategije. Prvo, silicijumove vrste koje nas interesuju potrebno je očuvati u nepromenjenom stanju u toku svih koraka analize, bez promene u oksidacionom stanju, bez promena usled aktivnosti mikroba i bez gubitaka usled isparavanja ili adsorpcije. Drugo, silicijumove vrste mogu biti kvantitativno prevedene u derivate koji su podesni za dalju separaciju, akumulaciju i kvantifikaciju.

Najpouzdaniji metod za očuvanje prirodnih uzoraka vode je zakišeljavanje do vrednosti pH 2, hlađenje do temperature od 4 °C i deoksigenizacija. Prema Tallberg [57], zamrzavanje uzoraka površinskih voda se ne preporučuje kod spektrofotometrijskog određivanja rastvornog oblika silicijuma, jer uslovljava pad koncentracije rastvornog silicijuma za 20–40%. Ovo se objašnjava time što zamrzavanje uzoraka inicira proces kom-

pleksiranja i polimerizacije silicijuma. Ukoliko se uzorci vode nakon prikupljanja filtriraju kroz mebranski filtar veličine pora od 0,2 μm, znatno se smanjuje gubitak rastvornog oblika silicijuma u vodi u toku zamrzavanja. Silicijumove vrste su stabilne u vodi pod neutralnim uslovima nedelju dana, ukoliko se čuvaju u polipropilenskim bocama na temperaturi od 4 °C. Dodatkom hlorovodonične kiseline uzorku vode, pri čemu se pH vrednost rastvora podesi na vrednost između 2 i 3, uzorci ostaju stabilni za 3 meseca.

Filtracija uzoraka vode treba da se izvrši najkasnije do 12 h nakon prikupljanja uzoraka jer se filtriranjem uzorka uklanja najveći deo koloidnog materijala i mikroorganizama koji mogu uticati na rastvorni silicijum. Acidifikacija sprečava oksidaciju gvožđe i mangan hidroksida koji se kao talog mogu adsorbovati na silicijumu. Silicijum nije fotohemijski reaktivan.

Specijaciona analiza silicijuma u ultračistoj vodi

Određivanje sadržaja silicijuma u vodi je od izuzetnog značaja za kvalitet vode koja se koristi u termoenergetskim postrojenjima. Specijaciona analiza sadržaja silicijuma, kao najnepoželjnije primese u ultra čistoj vodi, je značajna da bi se prikazala složenost fizičkih i hemijskih oblika jednog te istog elementa u vodi. Silicijum se iz vode može ukloniti primenom jednog ili više postupaka, od klasičnih gde se mogu uvrstiti taloženje, koagulacija, flokulacija, i filtracija, preko jonske izmene, sve do najsavremenijih metoda membranske separacije, ultrafiltracije, reverzne osmoze, elektrodijalize. U termoenergetskim postrojenjima u Srbiji, za uklanjanje silicijuma koristi se jonska izmena.

Metode za on-line praćenje sadržaja rastvornog silicijuma u ultračistoj vodi (procesni analizatori)

Sadržaj silicijuma u ciklusu voda-para predstavlja kontrolni parametar, koji se mora permanentno pratiti i održavati u granicama nižim od 20 μg dm^{-3}. Silicijum se u termoenergetskim postrojenjima kontinuirano meri na *on-line* meraču-silikometru koji je postavljen na liniji za demineralizaciju vode. Ovi merači se zasnivaju na primeni kolorimetrijske metode merenja intenziteta plave boje jedinjenja silicijuma i molibdena. Merač ima peristatičku pumpu za doziranje i dotok uzorka, standarda i reagensa do optičkog detektora. Referentni sistem postavljen paralelno sa mernim sistemom, omogućava otklanjanje eventualnih grešaka usled slučajnog bojenja uzorka ili usled neodgovarajućeg prelamanja izvora svetlosti. Alarmni sistem omogućava uvid u sve nepravilnosti u radu instrumenta kao što je gubitak uzorka, gubitak reagensa, prekoračenje kompenzacionog opsega, gubitak napajanja, temperatura kućišta i alarm visoke nedozvoljene koncentracije. Odlikuje se kratkim vremenom odziva i visokom tačnošću.

Metode za laboratorijsko određivanje silicijumovih vrsta u ultračitoj vodi

Metode za određivanje ukupnog sadržaja silicijuma u ultračistoj vodi. Za određivanje ukupnog sadržaja silicijuma u uzorku ultračiste vode, bez obzira da li se silicijum nalazi u jonskom, molekulskom ili polimernom obliku koristi se ICP-MS ili GF-AAS. Kod ICP-MS, visokofrekventna indukovanospregnuta plazma se koristi za jonizaciju uzorka. Putem nebulizera direktno se raspršuje uzorak vode u argonsku plazmu na 5700 °C. U plazmi se raspršene čestice uparavaju, atomizuju i jonizuju. Generisani joni prolaze kroz maseni spektrometar gde se identifikuju i mere, na osnovu odnosa masa/ /naboj. Kod GF-AAS uzorak vode se uparava i redukuje do atoma putem termičkog razlaganja u cevi grafitne peći. Većina atoma je u osnovnom stanju i kao takvi apsorbuju karakterističnu talasnu dužinu svetlosti. Količina svetlosti koja je apsorbovana od atoma silicijuma je direktno proporcionalna količini ukupnog silicijuma u uzorku vode.

Metode za određivanje molekulskog i anjonskih oblika silicijuma u vodi

Na osnovu pH vrednosti rastvora može se izvršiti procena o preovlađujućim vrstama silicijuma u rastvoru. U tabeli 3 dati su oblici silicijumove kiseline u zavisnosti od pH vrednosti vode.

Tabela 3. Oblici silicijumove kiseline u zavisnosti od pH vrednosti vode
Table 3. Forms of silica acid depending on the pH value of water

Oblik silicijumove kiseline	pH							
	4	5	6	7	8	9	10	11
H_2SiO_3 ($SiO_2 \cdot H_2O$)	100,0	99,9	99,0	90,9	2,0	50,0	8,9	0,8
$HSiO_3^-$	–	0,1	1,0	9,1	98,0	50,0	91,0	98,2
SiO_3^{2-}	–	–	–	–	–	–	0,1	1,0

Molekulski oblici silicijuma su prisutni u jako kiseloj sredini (<7,0). Za određivanje različitih oblika silicijuma u vodi primenjen je postupak i ideja za razdvajanje molekulskih i anjonskih vrsta arsena koji takođe u vodi postoje u različitim oblicima zavisno od pH sredine [58,59]. Razdvajanje molekulskih i anjonskih vrsta silicijuma, kao i različitih vrsta arsena moguće je korišćenjem jonoizmenjivačkih smola. Anjonska jonoizmenjivačka smola zadržava anjone, a propušta molekulske oblike. Na taj način se može izvršiti jednostavno razdvajanje silicijumovih oblika u vodi koji se dalje mogu odrediti primenom ICP-MS tehnike. Ova ideja je potvrđena u radu Hou [60]. Provera postupka razdvajanja silicijumovih oblika izvršena je eluiranjem anjonskih oblika silicijuma koji su zadržani na jonoizmenjivačkoj smoli primenom mobilne faze koja se sastoji od ace-

tatnog pufera-acetonitrila i tetrabutilamonijum-bromida [60].

Za određivanje anjonskih oblika silicijuma u referentnim laboratorijama koristi se spektrofotometrijska metoda, koja se zasniva na formiranju kompleksa anjonskih oblika silicijuma sa amonijum-hepta-molibdatom ($(NH_4)_6Mo_7O_{24}$), koji nakon redukcije sa oksalnom kiselinom uz dodatak 4-metil-amino-fenol-sulfata razvija heteropolarnu plavu boju. Merenja se izvode na talasnoj dužini od 815 nm. Stepen obojenja indirektno je proporcionalan količini anjonskih oblika silicijuma u uzorku. Ovom metodom se određuje sadržaj rastvornog silicijuma u vodi. Detekcioni limit ove metode je 20 μg dm^{-3}.

Za određivanje nižih koncentracija rastvornog silicijuma u vodi koristi se modifikovana spektrofotometrijska metoda u kojoj se plavo obojen kompleks silicijuma sa molibdatom ekstrahuje sa 1-butanolom. Pored ekstrakcije, za separaciju rastvornog silicijuma koriste se i tečne separacione tehnike, kao što je HPLC i kapilarna elektroforeza. Ovim tehnikama se može povećati koncentracija silicijuma i nekoliko stotina puta. Prednost HPLC je u tome što omogućuje širok spektar separacionih mehanizama za različite mobilne i stacionarne faze. Separacione tehnike se mogu koristiti i za određivanje sadržaja različitih hemijskih stanja silicijuma u vodi.

Metode za određivanje polimernog silicijuma u ultračistoj vodi

Za određivanje koncentracije pojedinih jonskih vrsta polimernog silicijuma u vodenim rastvorima silicijuma koje su prisutne u obliku monomera [$H_3SiO_2^-$], dimera [$H_5Si_2O_7^-$] i cikličnih tetramera [$H_7Si_4O_{12}^-$], koristi se nuklearna magnetna rezonanca gde se meri integrisani intenzitet difrakcijske linije izotopa silicijuma ^{29}Si. Međutim, ova metoda je pogodna za određivanje jonskih vrsta u uzorcima koji sadrže visoke koncentracije silicijuma (iznad 0,1 mol dm^{-3}) [61,62]. U novije vreme za određivanje koncentracije pojedinih jonskih vrsta polimernog silicijuma u prirodnim vodama (monomera, dimera, trimera, linearnih i cikličnih pentamera i heksamera silicijuma) koristi se masena spektrometrija, gde se jonizacija analita vrši brzim atomima ksenona (FAB-MS). Kao matrica se koristi glicerol. Ova metoda je podesna za određivanje koncentracije pojedinih jonskih vrsta silicijuma u vodenim rastvorima u kojima je silicijum prisutan u niskim koncentracijama [63].

Metode za određivanje suspendovanog i koloidnog silicijuma u vodi

Ukoliko je u vodi (površinskoj, a ne ultračistoj) prisutan suspendovani silicijum on se može odrediti najjednostavnije iz razlike sadržaja silicijuma pre i posle propuštanja kroz peščani filtar [63]. Ukoliko je neophodno odrediti suspendovane oblike i razlikovati ih od pravog rastvora silicijuma u literaturi se preporučuje da se separacija suspendovanih čestica izvrši filtracijom kroz membranski filtar sa porama veličine 0,45 μm, razaranje sa litijum-metaboratom ili litijum-tetraboratom, i primenom ICP-AES na λ = 251,61 nm [64]. Suspendovani oblici silicijuma se ne očekuju pri izrazito niskoj koncentraciji silicijuma u ultračistoj vodi.

Za određivanje sadržaja koloidnog oblika silicijuma ne postoje direktne metode. U ovu svrhu koriste se kombinovane tehnike, najčešće ICP-MS sa kolorimetrom. Ovom kombinacijom uređaja: kolorimetra – za određivanje rastvorenog silicijuma preko molibdata, i ICP-MS može se odrediti ukupna količina silicijuma u ultra čistoj vodi. Kombinacija ove dve tehnike obezbeđuje detaljne informacije o rastvorenom, koloidnom i ukupnom silicijumu. Koloidno stanje silicijuma se ne očekuju pri izrazito niskoj koncentraciji silicijuma u ultračistoj vodi.

Koloidno stanje silicijuma se očekuje pri relativno visokim koncentracijama, u uslovima pH 13, u prisustvu organskog rastvarača (etanol) [65]. Polimerni oblici, međutim mogu uspostaviti koloidno stanje na visokim temperaturama i pritiscima [65,67].

ZAKLJUČAK

U okviru različitih temoenergetskih industrijskih postrojenja, posebna pažnja posvećuje se prečišćavanju vode do nivoa ultra čistih procesnih voda. Kvalitet vode mora da bude usklađen s propisima i standardima proizvođača opreme i u skladu sa neophodnošću unapređenja tehnoloških, ekonomskih i ekoloških efekata. Primenama odgovarajućih separacionih postupaka, osavremenjavanjem i automatizacijom pojedinih tehnoloških procesa, primenom novih tehnoloških rešenja i metoda negativni aspekti korozionih procesa mogu se minimizirati. Da bi se imao uvid u efikasnost procesa pripreme i prečišćavanja vode moraju da se primene osetljive analitičke tehnike od *on-line*, procesnih analizatora, do visoko sofisticiranih uređaja za laboratorijska određivanja. Za pouzdanu i permanentnu kontrolu sadržaja korozionih agenasa u vodi preporučuju se procesni analizatori. Za analizu i određivanje tragova korozionih agenasa u vodi primenjuju su pojedinačne ili spregnute optičke i hromatografske metode osetljivosti reda μg dm^{-3}. Za praćenje sadržaja silicijuma u vodi preporučuju se procesni analizatori, silikometri, osetljivosti veće od 1 μg dm^{-3}. Za laboratorijsko određivanje sadržaja ukupnog silicijuma se primenjuju optičke metode, preporučuje se ICP-MS metoda osetljivosti veće od 0,01 μg dm^{-3}. Pored ukupnog silicijuma izuzetno je korisno imati uvid i u sadržaj pojedinih silicijumovih vrsta od suspendovanog i koloidnog silicijuma u rečnim vodama do molekulskih, anjonskih i polimernih oblika u ultračistim vodama.

Za određivanje sadržaja suspendovanog silicijuma u sirovoj vodi preporučuje se ICP-AES. Za određivanje sadržaja koloidnog silicijuma u vodi ne postoji direktna metoda, već se koriste kombinovane tehnike (GFAAS, spektrofotometrija i ICP-spektrofotometrija) kojima se diferencijacijom dolazi do zadovoljavajućih rezultata. Sadržaj molekulskih oblika silicijuma u jako kiselim rastvorima može se odrediti ICP-MS metodom uz prethodnu pripremu uzorka vode propuštanjem vode kroz anjonsku jonoizmenjivačku kolonu koja vezuje sve jonske oblike i propušta samo molekulske oblike silicijuma. Za određivanje anjonskih oblika silicijuma koristi se spektrofotometrijska metoda (molibdensko plavi kompleks) određivanjem pomoću ICP-MS metode posle eluiranja sa jonoizmenjivačkih smola koje omogućuju razdvajanje anjonskih vrsta uz strogu kontrolu pH vodenih rastvora. Za određivanje polimernih vrsta silicijuma u vodi preporučuje se masena spektrometrija, gde se jonizacija analita vrši brzim atomima ksenona (FAB-MS).

LITERATURA

[1] V.N. Rajaković, Lj.V. Rajaković, Sprega konvencionalnih i savremenih metoda za obradu vode od ultra čistih do otpadnih, Hem.Ind. **57** (2003) 307–317.

[2] Lj.V. Rajaković, Korozijski procesi u termoenergetskim postrojenjima usled neadekvatnog kvaliteta vode, Integritet i vek konstrukcija **7** (2007) 83–88.

[3] Lj.V. Rajaković, J. Kerečki, Razvoj analitičke kontrole u sistemu voda-para u termoenergetskim postrojenjima, Hem.Ind. **7**–**8** (2003) 318–325.

[4] V.N. Rajaković-Ognjanović, D.Z. Živojinović, B.N. Grgur, Lj.V. Rajaković, Improvement of chemical control in the water-steam cycle of thermal power plants, Appl. Therm. Eng. **31** (2011) 119–128.

[5] D.Z. Živojinović, Lj.V. Rajaković, Application and validation of ion chromatography for the analysis of power plants water: analysis of corrosive anions in conditioned water-steam cycles, Desalination **275** (2011) 17–25.

[6] Lj.V. Rajaković, Lj. Gradišar, Lj. Nešić, J.Jović, Potreba za formiranjem referentne laboratorije za analizu i kontrolu vode u termoenergetskim objektima, Elektroprivreda **2** (2001) 32–35.

[7] D. Čičkarić, J. Marković, Lj. Rajaković, Određivanje tragova jona gvožđa u ultra čistim vodama metodom GF-AAS, Kvalitet voda **2** (2004) 14–16.

[8] D. Čičkarić, J. Čučković, Lj. Rajaković, Analiza tragova anjona u sistemu voda-para u termoenergerskim postrojenjima, Hem. Ind. **59** (1–2) (2005) 19–27.

[9] Lj.V. Rajaković, V. Šijački-Žeravčić, D. Čičkarić, V. Rajaković, M. Đukić, G. Bakić, Korozija u ciklusu voda-para u termoenergetskim postrojenjima, Energetika **1** (2006) 72–83.

[10] Lj.V. Rajaković, V. Šijački-Žeravčić, D. Čičkarić, V. Rajaković, K. Trivunac, S. Stevanović, A.Sadibašić, S. Stanković, Mere za praćenje korozione aktivnosti metala u ciklusu voda-para u termoenergetskim postrojenjima, Energetika **3**–**4** (2006) 23–27.

[11] S. Vidojković, Integritet i vek konstrukcija, Vol. 7, br. 2, 2007, str.105–108

[12] C.H. van der Weijden, Silica I: Silicon-Analytical, Physical and Terrestrial Geoshemistry, Department od Geosciences-Geochemistry, 2007.

[13] P. Mayers, Behavior of Silica, Water Conditioning and Purification, 2004.

[14] R.K. Iler, The chemistry of silica. John Wiley & Sons, New York, 1979.

[15] D.J. Belton, O. Deschaume, C.C. Perry, An overview of fundamentals of chemistry of silica with relevance to biosilicification and technological advances, FEBS J. **279** (2012) 1710–1720.

[16] J. Paul, Micro-Determination of Soluble Silica in Urine, Anal. Chim. Acta **23** (1960) 178.

[17] A.Katz, The direct and rapid determination of alumina and silica in silicate rocks and minerals by Atomic Absorpton Spectroscopy, Am. Miner. **53** (1968) 283–289.

[18] P.G. Lim, in Proceedings of World Geothermal Congress 2005, Antalya, Turkey, 24–29 April 2005.

[19] M. Yaqoob, A. Nabi, P.J. Worsfold, Determination of silicate in freshwaters using flow injection with luminol chemiluminescence detection, Anal. Chim. Acta **519** (2004) 137–142.

[20] K. Yoshimura, U. Hase, Flow analysis method for the determination of silicic acid in highly purified water by gel-phase absorptiometry with molybdate and Malachite Green, Analyst **116** (1991) 835.

[21] M. Resano, E. Mozas, C. Crespo, J. Perez, E. Garcia-Ruiz, M.A. Belarra, Direct analysis of silica by means of solid sampling graphite furnance atomic absorption spectrometry, Spectrochim Acta B **71**–**72** (2012) 24–30.

[22] Y.S. Choi, J. Kim, S.B. Yoon, K. Song, Y.J. Kim, Determination of water content in silica nanopowder using wavelenght-dispersive X-ray fluorescence spectrometar, Microchem. J. **99** (2011) 332–338.

[23] D.K. Verma, A Method for Determining Crystalline Silica in Bulk Samples by Fourier Transform Infrared Spectrophotometry, Ann. Occup. Hyg., British Occupational Hygiene Society, Oxford University Press, Oxford, 2002, pp. 609–615.

[24] Y. Yokoyama, T. Danno, M. Haginoya, Y. Yaso, H. Sato, Simultaneous determination of silicate and phosphate in environmental waters using pre-column derivatization ion-pair liquid chromatography, Talanta **79** (2009) 308–313.

[25] A. Samadi-Maybodi, E. Atashbozorg, Quantitative and qualitative studies of silica in different rice samples grown in north of Iran using UV–vis, XRD and IR spectroscopy techniques, Talanta **70** (2006) 756–760.

[26] C. Ohlendorf, M. Sturm, A modified method for biogenic silica determination, J Paleolimnol. **39** (2008) 137-142.

[27] A.M.C. Barciela, R. Prego, Determination of silicate simultaneously with other nutrients (nitrite,nitrate and phosphate), in river waters by capillary electrophoresis, Anal. Chim. Acta **416** (2000) 21–27.

[28] Ph. Oltmann, D.E. Ryan, The indirect determination of trace reactive silicon in waters by neutron activation analysis, J. Chem. **63** (1985) 2585.

[29] Lj.V. Rajaković, Ž.N. Todorović, V.N. Rajaković-Ognjanović, A.E. Onjia, Review, Analytical methods for arsenic speciation analysis, J. Serb.Chem.Soc. **78** (2013) 1461––1479.

[30] N. Nakatani, D.Kazaki, W.Masuda, N.Nakagoshi, K. Hasebe, M. Mori, K. Tanaka, Simultaneous spectrophotometric determination of phosphate and silicate ions in river water by using ion-exclusion chromatographic separation and post-column derivatization, Anal. Chim. Acta **619** (2008) 110–114.

[31] J. Yabuta, H. Ohta, Determination of Free Silica in Dust Particles: Effect of Particle Size for the X-Ray Diffraction and Phosphoric Acid Methods, Ind. Health **41** (2003) 249–259.

[32] Crystalline silica in respirable airborne dusts, Methode Health and Safety laboratory, 2005.

[33] US Enviroment al protection agency, Definition and Procedure for the Determination of Method Detection Limits, Appendix B to 40 CFR 136 rev.1.11. (1986).

[34] M. Tanaka, K. Takahashi, Silicate species in high pH solution molybdate, whose silica concentration is determined by colorimetry, Anal. Chim. Acta **429** (2001) 117––123.

[35] M. Burguera, J.L. Burguera,P. Carrero, C. Rondon, A flow injection-ETAAS system for the on-line determination of total and dissolved silica in waters, Talanta **58** (2002) 1157–1166.

[36] J. Isoe, K. Morita, E. Kaneko, Determination of trace silica in highly purified water based on delayed quenching of Rhodamine B through nanoparticle formation with molybdosilicate, Analyst **130** (2005) 872–877.

[37] S.J. Lugowski, D.C. Smith, H. Bonek, J. Lugowski, W. Peters, J. Semple, Analysis of silicon in human tissues with special reference to sicilicone breast implants, J. Trace Elements Med. Biol. **14** (2000) 31–42.

[38] J.A. Rawa, E.L. Henn, Determination of Trace Silica in Industrial Process Waters by Flameless Atomic Absorption Spectrometry, Anal. Chem. **51** (1979) 452–455.

[39] O.D. Malov, M.V. Gustova, A.G. Belov, T.P. Drobina, Determination of Magnesium, Aluminium and Silicon content in water samples by gamma-activation and neutron-activation analyzes using MT-25 microtron, Joint Institute for Nuclear Research, Dubina, Russia.

[40] T. Chu, M.K. Balazs, Determination of total silica at ppb levels in high-puritywater by three different analytical techniques, Ultrapure Water **11** (1994) 56.

[41] S. Motomizu, M. Oshima, T. Ikegami, Flotation/Extraction and Spectrophotometric Determination of Silicate with Molybdate and Cationic Dyes, Anal. Sci. **5** (1989) 767–769.

[42] S. Motomizu, M. Oshima,K. Araki, Sensitivity Enhancement in Spectrophotometric Determination of Silicate by Flotation-Excnange-Extraction Method Using an Ion Associate, Analyst **115** (1990) 1627–1630.

[43] J.P. Susanto, M. Oshima, S. Motomizu, Adsorption-Concentration of Ion Associate Formed Between Molybdosiliate and Malachite Green on a Miniature Filter: Its Application to Trace and Ultratrace Determination of Silicon, Analyst **120** (1995) 2605–2611.

[44] A.Sabarudin, M. Oshima, S. Motomizu, Slope comparasion method (SCM) for determination of trace amounts of silicate in ultrapurifed water, Anal. Chim. Acta **532** (2005) 27–35.

[45] H.B. Li, F. Chen, Determination of silicate in water by ion exclusion chromatography with conductivity detection, J. Chromatogr. A, **874** (2000) 143–147.

[46] A.Hioki, J.W.H. Lam, J.W. McLaren, On-Line Determination of Dissolved Silica in Seawater by Ion Exclusion Chromatography in Combination with Inductively Coupled Plasma Mass Spectrometry, Anal. Chem. **69** (1997) 21–24.

[47] Z. Aspanut, T. Yamada, L.W. Lim, Light-Scattering and turbidimetric detection of silica colloids in size-exclusion chromatography, Anal. Bional. Chem **391** (2008) 353––359.

[48] Y. Takaku, K. Masuda, T. Takahashi, Determination of Trace Silicom in Ultra-high-purity Water by Inductively Coupled Plasma Mass Spectrometry, J. Anal. At. Spectrom. **9** (1994) 1385–1387.

[49] S. Opfergelt, P. Delmelle, Silicon isotopes and continental weathering processes: Assessing controls on Si transfer to the ocean, C.R.Geosci. **344** (2012) 723-738.

[50] A.Pramann, O. Rienitz, D. Schiel, B. Guttler, S. Valkiers, Novel concept for the mass spectrometric determination of absolute isotopis abundances with improved measurement uncertainty: Part 3-Molar mass of silicon highly enriched in ^{28}Si, Int. J. Mass Spectrom. **305** (2011) 56-68.

[51] R.B. Georg, B.C. Reynolds, M. Frank, A.N. Halliday, Mechanisms controlling the silicon isotopic compositions of river waters, Earth Planet. Sci. Lett. **249** (2006) 290–306.

[52] M.D. Mann, B.F. Chmelka, Measurement of Dilute ^{29}Si Species in Solution Using a Large Volume Coil and DEFT NMR , Anal.Chem. **72** (2000) 5131–5135.

[53] H.N. Kim, S.K. Lee, Atomic structure and dehydration mechanism of amorphous silica: Insights from ^{29}Si ^{1}H solid-state MAS NMR study of SiO_2 nanoparticles, Geochim. Cosmochim. Acta **120** (2013) 39–64.

[54] X.Y. Xue, Water speciation in hydrous silicate and aluminosilicate glasses: direct evidence ^{29}Si-^{1}H and ^{27}Al-^{1}H double-resonance NMR, Am. Mineral. **94** (2009) 395–398.

[55] S. Yamashita, H. Behrens, B.C. Schmidt, R. Dupree, Water speciation in sodium silicate glasses based on NIR and NMR spectroscopy, Chem. Geol. **256** (2008) 231––241.

[56] A.Onjia, Analitičke tehnike za određivanje i praćenje hemijskih supstanci od uticaja na koroziju, Integritet i vek konstrukcija **7**(2) (2007) 79–82.

[57] P. Tallberg, H. Hartikainen, T. Kairesalo, Why is soluble silicon in interstitial and lake water samples immobilized by freezing?, Wat. Res. **31** (1997) 130–134.

[58] N. Ben Issa, V.N. Rajaković-Ognjanović, B.M. Jovanović, Lj.V. Rajaković, Determination of inorganic arsenic

species in natural waters-Benefits of separation and preconcentracion of on ion exchange and hybrid resins, Anal. Chim. Acta **673** (2010) 185–193.

[59] N. Ben Issa, V.N. Rajaković-Ognjanović, A.D. Marinković, Lj.V. Rajaković, Separation and determination of arsenic species in water by selective exchange and hybrid resins, Anal. Chim. Acta **706** (2011) 191–198.

[60] S. Hou, M. Ding, J. Zhu, Simultaneous determination of silicon and phosphorus in soil and plants by reversed-phase ion-pair chromatography, Talanta **75** (2008) 178––182.

[61] R.K. Harris, C.T.G. Knight, Silicon-29 nuclear magnetic resonance studies of aqueous silicate solutions. Part 5. First-order patterns in potassium silicate solutions enriched with silicon-29, J. Chem. Soc., Faraday Trans. **79** (1983) 1525–1538.

[62] R.K. Harris, C.T.G. Knight, Silicon-29 nuclear magnetic resonance studies of aqueous silicate solutions. Part 6. Second-order patterns in potassium silicate solutions enriched with silicon- 29. J. Chem. Soc., Faraday Trans. **79** (1983) 1539–1561.

[63] M. Tanaka, K. Takahasi, Ionised silica in estuary of river as supply to seawater: Identifikacion and ionization efficiency of silica species by FAB MS, Estuarine Coastal Shelf Sci. **1–7** (2013) 121–122.

[64] F. Ödman, Th. Ruth, Ch. Pontèr, Validation of a field filtration technique for characterization of suspended particulate matter from freshwater. Part I. Major elements, Appl. Geochem. **14** (1999) 301–307.

[65] S.J. Park, Y.J. Kim, S.J. Park, Size-Dependent Shape Evolution of Silica Nanoparticles into Hollow Structures, Langmuir **24** (2008) 12134–12137.

[66] M.G. Browman, R.B. Robinson, G.D. Reed, Silica polymerizations and other factors in iron control by sodium silicate and sodium hypochlorite addition, Environ. Sci. Technol. **25** (1989) 566–572.

[67] J.C. Rushing, L.S. McNeill, M. Edwards, Some effects of aqueous silica on the corrosion of iron, Wat. Res. **37** (2003) 1080–1090.

SUMMARY

ANALYTICAL TECHNIQUES FOR DETERMINATION AND CONTROL OF SILICA CONTENT IN THE WATER IN THERMAL POWER PLANTS

Nataša R. Ignjatović[1], Maja D. Ilić[2], Ljubinka V. Rajaković[3]

[1]*Ministry of Internal Affairs of the Republic of Serbia, Belgrade*
[2]*Serbia Business Company Thermal Power Plants and Mines Kostolac, Kostolac, Serbia*
[3]*University of Belgrade, Faculty of Technology and Metallurgy, Belgrade, Serbia*

(Review paper)

Ultrapure water with minimum contents of impurities is used for the preparation of steam in thermal power plants. More recently, it has been found that the corrosion process is also influenced by sodium ions, chloride ions and all forms of silicon in water. At higher temperatures and under high pressure the less soluble compounds of silicon are extracted, which form deposits on the walls of the boiler, the piping system and the turbine blades. Silicon is found in water in the form of different types (species) which are characterized by specific physical and chemical properties. Distinctions can be made between highly reactive species of ionic (silicate anions) and molecular forms (silicic acid) and relatively inert types (suspended, colloidal and polymerized silicon). The determination of various forms of silicon in water is a complex analytical task. This paper covers relevant research in the field of silicon specification analysis. Maintaining the unchanged, original composition of silicon species during various stages of analysis (sample collection, storage and conservation) has been given special attention. A large number of methods and procedures have been developed for the analysis of species of silicon, including chromatographic, spectroscopic and electrochemical techniques and combinations thereof. The techniques used for determining both the total amount and individual forms of silicon have been singled out. There is also an overview of the coupled techniques used most frequently in practice by using the methodology which involves preliminary separation of species and then individual specification. The paper offers an overview of analytical properties, advantages and disadvantages of the most representative analytical methods developed specifically for the analysis of silicon species in ultrapure water. The most important studies focusing on the silicon species in water have been highlighted and presented in detail. The determination of silicon content in water is of great importance due to various effects of silicon species (corrodibility and toxicity) and the selection of methods for the efficient removal of silicon from water.

Keywords: Silica • Thermal power plants • Ultapure water • Speciation analysis • Analytical techniques

$CaSO_4$ and cationic polyelectrolyte as possible pectin precipitants in sugar beet juice clarification

Tatjana Kuljanin[1], Biljana Lončar[1], Lato Pezo[2], Milica Nićetin[1], Violeta Knežević[1], Rada Jevtić-Mučibabić[3]

[1]*University of Novi Sad, Faculty of Technology, Novi Sad, Serbia*
[2]*Institute of General and Physical Chemistry, Belgrade, Serbia*
[3]*University of Novi Sad, Institute for Food Technology, Novi Sad, Serbia*

Abstract

Three pectin preparations were isolated from fresh sugar beet pulp during the 150 min of extraction, at pH values of 1, 3.5 and 8.5. $CaSO_4$ precipitant was added to 100 cm^3 of 0.1 wt.% solution of pectin. Studies were performed with 9 different concentrations of $CaSO_4$ solution (50–450 mg dm^{-3}) with the addition of a cationic polyelectrolyte (cationic PAM) in concentrations of 3 and 5 mg dm^{-3}. The efficiency of pectin precipitation was monitored by measuring the zeta potential of pectin preparations. Optimal amounts of precipitant $CaSO_4$, without the use of a cationic polyelectrolyte, were as follows: 490–678 mg $CaSO_4$/g pectin. After the use of a cationic polyelectrolyte, the optimal amounts of $CaSO_4$ were smaller (353–512 mg/g pectin). These quantities are significantly lower than the average amount of CaO used in the conventional clarification process of sugar beet juice (about 9 g/g pectin of sugar beet juice).

Keywords: clarification, pectin, sugar beet juice, $CaSO_4$, cationic polyelectrolyte, zeta potential.

Available online at the Journal website: http://www.ache.org.rs/HI/

SCIENTIFIC PAPER

UDC 664.126:544.6:66

Hem. Ind. **69** (6) 617–625 (2015)

doi: 10.2298/HEMIND141015085K

Removal of impurities from sugar beet juice by clarification is an essential part of the process of raw sugar manufacture. Application of CaO, in its $Ca(OH)_2$ form in sugar beet juice clarification is very well known. However, huge quantities of lime are used in everyday sugar production. This might have negative influence on the area that surrounds sugar factory. Calcium is known for its good absorption characteristics that can cause undesired alkalinisation process in the soil [1].

Precipitation of pectins can be performed by process of discharging, *i.e.*, carboxylic acid groups of acids from pectins can take a part in the complexation of divalent and trivalent cations from various compounds [2–4]. It is known that the colloidal particles in the solution surrounded by an electric double layer that is composed of a stationary (Stern's) and diffuse layer. The potential at the interface between these layers is easily measurable size and it is known as zeta potential (ζ). By keeping zeta potential close to zero, pectin colloidal particles will discharge and the conditions for effective precipitation of particles will be achieved [5,6]. According to the selectivity order of the binding affinity of various divalent cations by citrus and sugar-beet pectins, it is evident that Cu^{2+} are more efficient than Ca^{2+} due to marked surface complexation ability [7,8]. On the other hand, it is known that Ca^{2+} with the smaller hydrated radius have a large dehydration effect. Therefore, hydrophylic macromolecules (such as pectin) hydration considerably decreases in the presence of Ca^{2+} which is an important prerequisite for coagulation besides charge neutralisation [9]. In the presence of Ca^{2+}, electrostatic interactions are performed between the negatively charged side chains of polysaccharide, leading to formation of "egg-box" structure. This binding takes place preferably between the side chains of the same macromolecule forming the intramolecular complexes [10].

Investigation performed in paper [18] suggests that salts: $CaCl_2$, $CuSO_4$ and $AlCl_3$&$NaHCO_3$ are more efficient in pectin precipitation than commonly used CaO. Also, in previous paper (Kuljanin and others, in press) was proved that Ca^{2+} bounded with SO_4^{2-} has greater affinity to complexation than Ca^{2+} bonded with $(OH)^{1-}$.

The total capacity of pectin polysaccharide to complex metal cations was directly related to the degree of methyl esterification, degree of polymerisation and glycosil residue composition of pectins [11]. The cation binding capacity of pectin macromolecules (CBC) can be calculated on the basis of simplified equation [12]. It is accepted that only free carboxyl group of the galacturonic acid take part in the binding of cations:

$$CBC = \frac{Gal.A\left(1-\frac{DE}{100}\right)}{176}\left[\frac{\text{mmol}}{g_{SM}}\right] \quad (1)$$

where *Gal.A* corresponds to the content of pure galactouronic acid, *DE* denotes degree of methyl esterific-

Correspondence: B. Lončar, University of Novi Sad, Faculty of Technology, Bulevar cara Lazara 1, 21000 Novi Sad, Serbia.
E-mail: biljanacurcicc@mail.com
Paper received: 15 October, 2014
Paper accepted: 8 December, 2014

ation, value 176 denotes molar masse of dehydrated galactouronic acid [13,14].

Another mechanism that causes the coagulation and precipitation of the macromolecules is interparticle bridging. Interparticle bridging occurs using high molecular weight polyelectrolytes where colloids are adsorbed into the polymers branches or share ions directly to form ionic bridges [19–21,24]. The mechanism of cationic polyelectrolyte action is more complex: At the beginning of the process attractive electrostatic forces (mechanism of charge neutralization) are active and when their action stops, destabilization occurs by mechanism of interparticle bridging. The mechanism of this process is related to the density of the charges on the polyelectrolytes vis-à-vis the density of charges on the pectin macromolecule surfaces [22]. Earlier studies in application of polyelectrolytes, cationic or anionic, were related to purification of waste water [22,21]. Also, cationic and anionic polyelectrolytes have been claimed to enhance the flocculation of sugar cane juice. The best results in clarification of sugar cane juice were obtained by adding cationic polyelectrolytes with low molar mass in quantities of 40–200 mg dm^{-3} in combination with anionic flocculant with high molar mass, concentration of 3 mg dm^{-3} [19]. It has been also studied the use of cationic polyelectrolytes and polyacrylamide flocculants in sugar beet juice clarification according to classical method (application of CaO). Industrial trials confirmed the technological and economic justification of this method in the phase prior to defecation [23,24]. Investigation performed in paper [18] suggests that three salts: $CaCl_2$, $CuSO_4$ and $AlCl_3$ and $NaHCO_3$ are more efficient in pectin precipitation than commonly used Cano. Cationic polyelectrolytes in combination with $Al_2(SO_4)_3$ and $CuSO_4$, were studied in the paper [25]. By measuring the zeta potential it has been proven that the efficiency of precipitation of pectin and protein particles in the presence of polyelectrolyte increases.

Although Al^{3+} due to its high charge have greater bonding strength to natural organic matter than Ca^{2+} (the $H^+/Me^{2+,3+}$ molar exchange ratios ranging of 2.1––2.7 and 0.2–0.5, for Al^{3+} and Ca^{2+}, respectively) [26], the reason for $CaSO_4$ selection was primarily acceptable solubility in water and not expansive for eventual industrial application.

Beet juice has a concentration of undesirable colloids as most of the waste and contaminated water (about 1 wt.%). Previous practice in the modern plants for the improved water treatment showed that zeta potential control enhances the removal of colloids [27]. According to this, zeta potential measurements should be effective for the control of discharging pectin particles [28,17,19].

The aim of this study was to investigate the effect of $CaSO_4$ and cationic polyelectrolyte concentration, as well as the pectin type on sugar beet juice clarification. The reason for $CaSO_4$ selection was primarily acceptable solubility in water and not expensive for eventual industrial application. Since cationic polyelectrolytes additionally neutralize the charge of pectin particles, applying them would decrease the amount of $CaSO_4$. That would further reduce the cost of cleaning sugar beet juice while protecting the environment.

Simple regression models, using second order polynomial and Response Surface Methodology (RSM) have been proposed for calculation of zeta potential capabilities as function of proposed process parameters ($CaSO_4$ concentration, polyelectrolyte concentration and the pectin type). Analysis of variance (ANOVA) has been applied to show relations between applied assays.

MATERIALS, METHODS AND PLAN OF EXPERIMENTS

Materials

Three pectins were isolated from pressed sugar-beet slices (*Beta vulgaris L*. ssp. vulgaris var. Latissimi Dell) from Vojvodina – region situated at the Panonian basin (factory Žabalj), Serbia. Then, three model solutions were prepared, concentration of which was 1 g dm^{-3}. The metal salt $CaSO_4$, in crystal hydrate form ($CaSO_4 \times 2H_2O$), was used for preparation of the solutions with de-ionized water (Zorka Pharma, Šabac, Serbia; purity of salt was 99.0%). For the adjustment of pH values, aqueous solutions of HCl and NaOH were used.

Magnafloc LT24 is a high purity (99%) cationic polyacrylamide (PAM) purchased from Henan, Shandong China (Mainland). Cationic PAM is made by a vinyl monomer and cationic acrylamide copolymer $[–CH_2–CH(CONH_2)]_n$. It is one kind of high molecular weight of linear polymer (5×10^6–15×10^6 million g mol^{-1}), solid content: ≥ 90% and ion degree: 30–80%. It is described as a white, low dusting powder containing less than 0.05% free acrylamide.

Methods

Isolation of pectins

Pectins were isolated by the extraction, under the acidic conditions (pH 1 and 3.5) and under the alkaline conditions (pH 8.5), according to the standardized laboratory scale procedure [29,30] presented in Fig. 1. Each extraction was carried out three times. Because of the differences among the extraction conditions, three pectin samples were of different composition and degree of esterification.

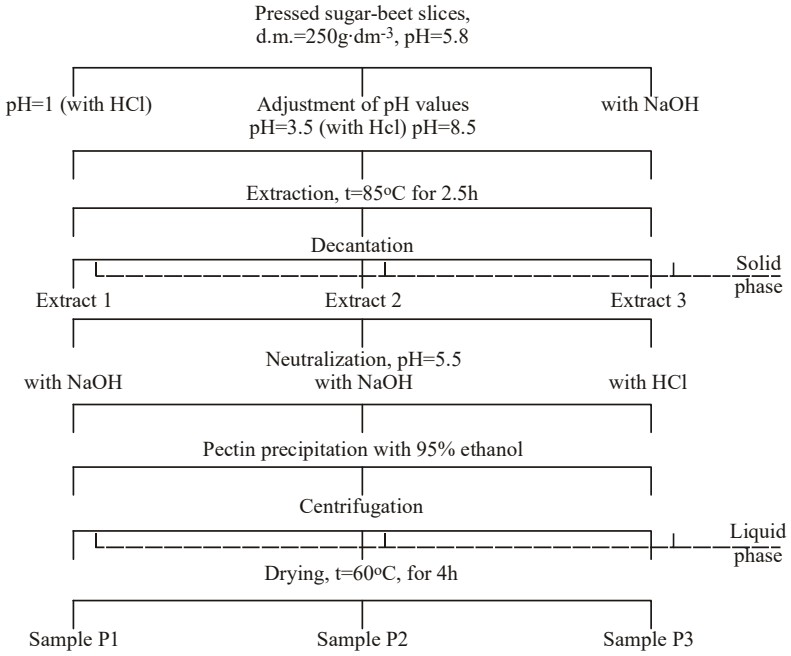

Figure 1. Laboratory scale extraction procedure [18].

Determination of content of galacturonic acid

For the quantitative determination of the purity of pectin preparations using the content of galacturonic acid, the titration method was applied. The principle of this method was the determination of the volumetric equivalent of total carboxyl groups of galacturonic acids. The equivalent of free carboxyl groups was determined by potentiometric titration of solution of pectin preparations with 0.01 M NaOH. The content of galacturonic acid, *Gal.La*, *i.e*., purity of pectin preparations, was calculated using the equation [31]:

$$Gal.A = \frac{100 m_g}{g} \left[\frac{g_{gal.A}}{100\ g_{D.M.}} \right] \quad (2)$$

Weight of pure galacturonic acid, mg, expressed by the equivalent of free (X) and the equivalents of methyl-esterified carboxyl groups (Y), is given by Eq. (3) where: 176 and 190 – the molecular weights of anhydrous free galacturonic or methyl-esterified galacturonic acid (g / mol):

$$m_g = 176X + 190Y \text{ [g]} \quad (3)$$

Determining the degree of esterification

Ester-linked carboxyl groups were determined by adding 0.1 M NaOH to a solution of pectin mixture while stirring. After aging and addition of HCl, the potentiometric titration with 0.01 M NaOH solution was carried out. From the expenditure of a base, the content of associated ester groups was calculated. The degree of esterification (*DE*) of pectin sample, was calculated using equation [31]:

$$DE = \frac{100Y}{X+Y} \ [\%] \quad (4)$$

Zeta potential

Charge of particles in a colloidal solution was expressed by the zeta potential value determined by applying Zeta-meter ZM-77 and well-known equation of Helmoltz–Smoluchowski:

$$\zeta = (4\pi\eta / D_t) EM \quad (5)$$

where ζ denotes zeta potential, η corresponds to the solution viscosity, D_t signifies its dielectric constant, while *EM* represents electrophoretic mobility. From the measured *EM* value of 20 particles, an average value was used to derive the zeta potential in the tested solutions using a diagram based on the Helmoltz––Smoluchowski equation. Experiments were conducted at 6-fold magnitude on a stereoscopic microscope and voltage adjusted at 150 V. Just before zeta potential measurements, solution temperatures were measured. Zeta potential was read from the diagram and multiplied by a correction factor for a given temperature.

Plan of experiments

Experiments were performed in accordance with the plan presented in Table 1. Nine flasks were filled with the model solutions of pectin (0.1mass%). After the adjustment of pH value, in 1–9 flasks, pectin solution was treated: *i*) with a $CaSO_4$ solution and *ii*) with $CaSO_4$ solution with added cationic polyelectrolyte (Magnafloc LT24) concentrations of 3 and 5 mg dm^{-3}.

Table 1. Plan of experiments with pectin solutions P1, P2 and P3; precipitants: flask, each filled with 50 cm^3 of pectin solution (0.1 mass%), at pH 7

$CaSO_4$ and cationic polyelectrolyte (0, 3, 5 mg dm^{-3})	1	2	3	4	5	6	7	8	9
Concentration of $CaSO_4$, mg dm^{-3}	50	100	150	200	250	300	350	400	450
Volume of $CaSO_4$ solution, cm^3	0.625	1.250	1.875	2.500	3.125	3.750	4.375	5.000	5.625

The zeta potential values of colloidal particles were measured after the induced precipitation. The process of agglomeration and precipitation lasted for 10 h, so as to enable precipitants to react with pectin as complete as possible. This experimental plan was performed three times, once for each particular pectin solution.

RESULTS

The results of the measurements are presented in Table 2 and Figure 2.

Table 2. Zeta potential, experimental data, mV

$CaSO_4$ concentration mg dm^{-3}	Pectin type								
	P1			P2			P3		
	Floculant concentration, mg dm^{-3}								
	0	3	5	0	3	5	0	3	5
50	–21	–19	–19	–22	–19	–20	–18	–15	–14
100	–20	–17	–16	–18	–13	–15	–17	–11	–11
150	–19	–14	–13	–17	–10	–10	–15	–9	–9
200	–17	–9	–8	–16	–8	–7	–13	–5	–4
250	–14	–6	–5	–13	–4	–4	–12	–1	–1
300	–11	–3	–1	–10	–1	–1	–9	4	3
350	–7	3	3	–7	2	3	–1	6	6
400	–3	6	5	–1	5	4	4	7	8
450	2	7	6	4	6	6	5	7	8

Statistical analyses

Simple regression models, using second order polynomial and response surface methodology (RSM) have been proposed for calculation of zeta potential capabilities as function of proposed process parameters ($CaSO_4$ concentration, polyelectrolyte concentration and the pectin type).

The experimental data used for the study of experimental results were obtained using a 9×3 experimental design, with 27 runs, for three types of pectin, according to RSM. It was used to design tests for sugar beet juice clarification, considering two factors: $CaSO_4$ and cationic polyelectrolyte (used as flocculant) concentration, and the type of used pectin (P1, P2 and P3).

The following second order polynomial (SOP) model was fitted to the data [32,33]. The model of the following form was developed to relate one response (Y) and three process variables (X):

$$Y = \beta_0 + \sum_{i=1}^{3} \beta_i X_i + \sum_{i=1}^{3} \beta_{ii} X_i^2 + \sum_{i=1}^{3} \sum_{j=i+1}^{3} \beta_{ij} X_i X_j \qquad (6)$$

where β_0, β_i, β_{ii}, β_{ij}, are constant regression coefficients; Y - zeta potential; X_1 – $CaSO_4$ concentration; X_2 – flocculant concentration; X_3 – pectin type, numbers 1, 2 and 3 represent types of tested preparations P1, P2 and P3 (Figure 2).

Descriptive statistical analyses for all the obtained results were expressed as the mean ± standard deviation (*SD*). The evaluation of one-way ANOVA analyses of the obtained results was performed using StatSoft Statistica 10.0® software.

Pectin isolation and characterization

Isolation of pectins from fresh sugar beet was performed with the aim to obtain pectins similar to those appeared in sugar-beet processing. Also, acidic and alkali conditions were applied due to broadening characteristics of investigated pectins. As it is well known, beet pectins contain galacturonic acid, rhamnose, arabinose and galactose as the major sugar constituents. Typical for beet pectins is also presence of both acetyl and ferulic acid, linked arabinose residues in the arabinan chains and galactose residues in (1-4)-linked galactans [29,34]. The presence of ferulic acid contributes to cross-linking of particular components thus increasing molar mass of pectins. By acidic extraction a degradation of arabinan side chains takes place as well as a loss of feruloyl groups, which causes a significant decrease of molar mass of pectins [35]. Under alkali conditions, similar processes occur. By alkali treatment the ester bonds, such as linkages between ferulic acid and arabinan or galactan, can be partially or completely cleaved [36], resulting in severe decrease of molar mass. Probably because of that, our alkali extracted pectin (P3) has molar mass approximately 64 500 g mol^{-1} (pH 8.5, t = 85 °C, τ = 2.5 h), which is significantly smaller than the value of 118000 g mol^{-1}, obtained for both pectins P1 and P2, extracted by acidic process (pH 1, t = 85 °C, τ = 2.5 h and pH 3.5, t = 85 °C, τ = 2.5 h, respectively). The molar mass was determined by rather approximate viscosity method, but the results are in acceptable agreement with the results for alkali conditions (75 100 g mol^{-1}, 2% NaOH, t = 45 °C, τ = 3 h), and results for acidic conditions (119000 g mol^{-1}, pH 1, t = 45 °C, τ = 1.5 h and 122000 g mol^{-1}, pH 3, t = 45 °C, τ = 1.5 h) [35,36]. Due to differences in the conditions

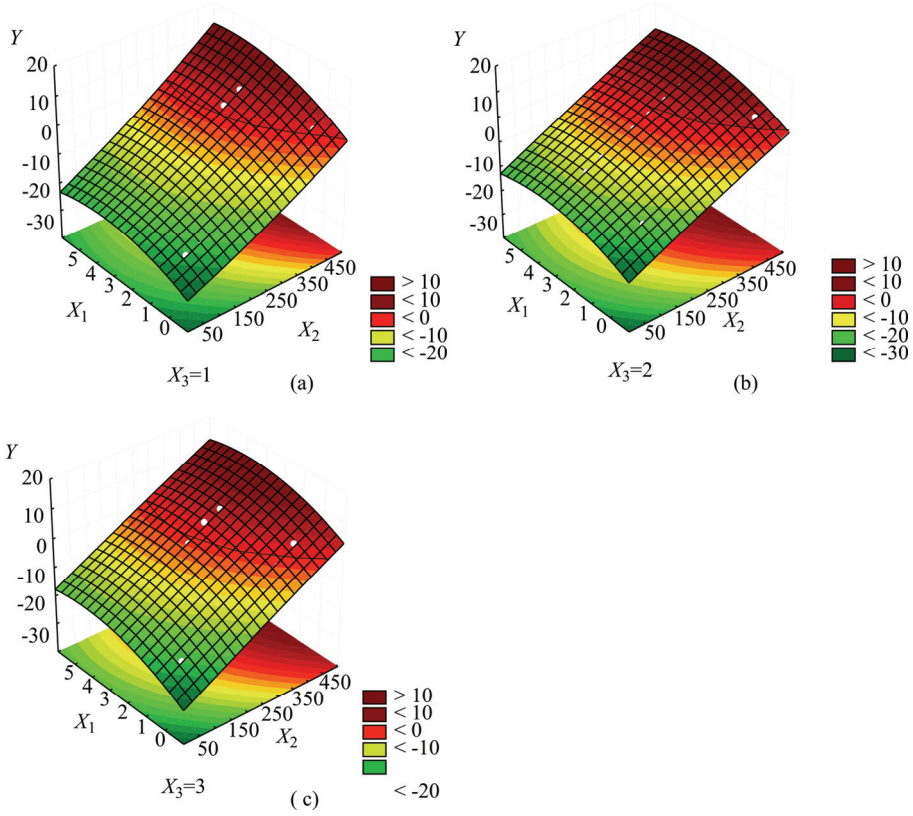

Figure 2. The effect of the precipitant concentration, flocculant concentration and the type of pectin on the charge of zeta potential: a) pectin type P1, b) pectin type P2 and c) pectin type P3. Y-zeta potential (mV); X_1 – $CaSO_4$ concentration (mg/dm^3), X_2 – flocculant concentration (mg/dm^3), X_3 – pectin type.

of extraction, the obtained pectin preparations had a different composition and degree of esterifiction (Table 3).

Table 3. Basic physicochemical composition and the cation binding capacity of pectin preparation

Pectin solution	P1	P2	P3
Solid content, SC /(g/100 g)	81.55	82.25	80.35
Equivalent of free COOH groups, $X\times10^5$	16.83	10.60	24.58
Equivalent of esterified COOH groups, $Y\times10^5$	19.74	27.55	16.05
Content of galacturonic acid, *Gal.A* / %	63.45	66.31	72.24
Degree of esterification, *DE*	53.98	72.21	39.50
Mean molar mass M_{Wsr} / g mol^{-1}	118000	118000	64 500
Cation binding capacity CBC_t / mmol g^{-1}	0.1659	0.1048	0.2480

The content of galacturonic acid in the tested preparations is in accordance with the mean content of pectin found in raw sugar beet juices from diffuser reported in literature [17,18]. As set out in Eq. (1), the degree of esterification of pectin P1, P2 and P3 (53.98, 72.21 and 39.50, respectively) is inversely proportional to the cation binding capacity (0.1659, 0.1048 and 0.2480 mmol/g, respectively). The cation binding capacity is proportional to the equivalent of free –COOH groups (16.83, 10.60 and 24.58 respectively for P1, P2 and P3) which are responsible for the surface charge of pectin particles [12,17].

RSM analysis

Analysis of variance was performed for comparison of zeta potential for different process parameters. The measured values of zeta potential, under different processing conditions, are presented in Table 2, and statistically significant differences for observed data were found in almost all samples, using Tukey HSD test.

Investigated samples are characterized by relatively low zeta potential, especially in case of increased flocculant concentration. According to ANOVA analysis (Table 4), response variable *Y* is mostly affected by $CaSO_4$ concentration, statistically significant at $p < 0.001$ level. The flocculant concentration is also influential, while pectin type has been the least important variable for zeta potential calculation. Linear terms have been found most influential for mathematical model developing (Eq. (6)), and according to ANOVA, these terms have been found statistically significant at $p < 0.001$ level, 95 % confidence limit. The quadratic term in SOP model for $CaSO_4$ concentration has been

found statistically insignificant, while the quadratic terms for flocculant concentration and pectin type have been found statistically significant for zeta potential calculation, but not very influential. The influence of all interchange (nonlinear) terms has been found statistically insignificant.

The average error between the predicted values and experimental values (calculated by Eq. (6)) was below 10%. Values of average error below 10 % indicate an adequate fit for practical purposes. To verify the significance of the models, analysis of variance (ANOVA) was conducted and the results indicate that all models were significant with minor lack of fit, suggesting that they adequately represented the relationship between response and factors.

*Table 4. ANOVA calculation for zeta potential; * – significant at p < 0.001 level, ** – significant at p < 0.01 level, 95% confidence limit, error terms were found statistically insignificant*

Variable	*dF*	Zeta potential (Sum of squares)	*F* test	*p*
X_1	1	5274.32*	1830.01	<0.001
X_1^2	1	0.18	0.06	0.80
X_2	1	600.00*	208.18	<0.001
X_2^2	1	109.38*	37.95	<0.001
X_3	1	195.13*	67.70	<0.001
X_3^2	1	18.67**	6.48	0.01
$X_1 \times X_2$	1	4.10	1.42	0.24
$X_1 \times X_3$	1	4.01	1.39	0.24
$X_2 \times X_3$	1	0.00	0.00	0.99
Error	71	204.63		
r^2		0.969		

Table 5 shows the regression coefficients for the (SOP) model of zeta potential calculation, used by Eq. (6). The three-dimensional graph has been plotted for experiment data visualization (white coloured points) and for the purpose of observation the fitting of regression models to experimental data, Figure 2.

Table 5 is also used in calculation the optimum values of $CaSO_4$ and flocculant concentration, for each of the pectins in order to obtain zero zeta potential. It seems that zeta potential reaches zero most promptly when using pectin P3 (this is due to relatively high β_{33} regression coefficient). Other two parameters, $CaSO_4$ and flocculant concentration, also contribute to final value of zeta potential. Zero zeta potential is reached with higher $CaSO_4$ concentration (300–400 mg dm^{-3}, depending on pectin used). All these observation coincide very well to obtained experimental results. Zero zeta potential curves have been drawn on 3D surfaces for each used pectin representing sugar beet clarification process, Figure 2.

*Table 5. Regression coefficients for zeta potential calculation; * – significant at p < 0.001 level, ** – significant at p < 0.01 level, 95% confidence limit, error terms were found statistically insignificant*

Coefficient	Regr. coeff.	*SD*	*t* test	*p*
β_0	–27.060*	1.992	–13.586	<0.001
β_1	0.063*	0.008	8.151	<0.001
β_2	3.186*	0.443	7.192	<0.001
β_{22}	–0.414*	0.067	–6.160	<0.001
β_{33}	1.019**	0.400	2.545	0.013

Precipitation and cation-binding characteristics

Charge inversion of zeta potential was observed within the whole series of tested coagulants concentrations (Table 2 and Figure 2). This indicates that in addition to the simple charge neutralization mechanism and ion exchange, a mechanism of specific adsorption occurs.

The beneficial effect of SO_4^{2-} is well known from the literature on the coagulation of colloidal particles [27]. However, by comparing the binding efficiency of the $CaSO_4$ and $CaCl_2$ with pectins under the same experimental conditions [18], it can be seen that the Ca^{2+} bounded with SO_4^{2-} have no better affinity to complexation than Ca^{2+} bounded with Cl^-. In this case, the influence of anion size present in solution (SO_4^{2-}, Cl^-) cannot be neglected, which requires additional testing. The influence of anion size is greater at higher concentrations of ions whose valence is ≥ 2 and for systems with large electric charge of the colloidal particles [37].

In the experiment, the used concentrations of the polyelectrolyte were in range from 3 to 5 mg dm^{-3}, since they have proved to be the most favourable in the experiments with $Al_2(SO_4)_3$ and $CuSO_4$. However, cationic polyelectrolytes applied with the precipitant $Al_2(SO_4)_3$ and $CuSO_4$ showed lower efficiency in the deposition of pectin and protein particles (the amount of Al^{3+} and Cu^{2+} necessary to bring to zero zeta potential values decreased by 15 mg dm^{-3}) [25]. With the application of a cationic polyelectrolyte of the same type, the amount of $CaSO_4$ is necessary to bring to zero zeta potential values decreased to about 100 mg dm^{-3} (Table 6). This means that the cationic polyelectrolyte can function as both coagulant (through charge neutralization) and flocculant (through interparticle bridging) of pectin solutions. The results indicate that such a complexation–flocculation process is of potential interest for the removal of pectins during sugar beet juice clarification.

Cationic polyelectrolyte (cationic PAM) concentration of 5 mg dm^{-3} shows slightly higher removal efficiency of pectin from the tested model-solutions, suggesting that the cationic polyelectrolyte with large molar mass (over 100000 g mol^{-1}) targets a pectin macromolecules with different molar mass.

The pectin preparation P3 showed better cation-binding characteristics in relation to the pectin P1 and P2 (from Table 3: $CBC_{(P3)}$ = 2.37$CBC_{(P2)}$ and $CBC_{(P3)}$ = = 1.49$CBC_{(P1)}$). This is understandable, since the pectin P3, besides at least the value of mean molar mass (64500 g mol^{-1}), has the highest content of galacturonic acid (72.24%) and the lowest degree of esterification (39.50).

Compared with conventional process where is approximately used 9 g CaO per g of pectin, the amount of $CaSO_4$ (in the form of pure salt or salt with cationic electrolyte) was significantly lower, ranging in the interval of 353–678 mg per g pectin (Table 6).

Acknowledgement

The Ministry of Education, Science and Technological Development of the Republic of Serbia financially supported this work (Project TR -31055).

REFERENCES

[1] H. Haapala, N. Goltsova, V. Pitulko, M. Lodenius, The effects of simultaneous large acid and alkaline airborne pollutants on forest soil, Environ. Pollut. **94** (1996) 159––168.

[2] S.K. Wiedemer, A. Cassely, M. Hong, M.V. Novotny, M.L. Riekkola, Electrophoretic studies of polygalacturonate oligomers and their interactions with metal ions, Electrophoresis **21** (2000) 3212–3219.

[3] M.A.V. Axelos, C. Garnier, C.M.G.C. Renard, J.F. Thibault, Interaction of pectins with multivalent cations: phase diagrams and structural aspects, in: Pectins and Pectinase, J. Visser, A.G.J. Voragen, Eds., Elsevier Science, Amsterdam, 1996.

[4] A. Pinotti, N. Zaritzky, Effect of aluminium sulfate and cationic polyelectrolytes on the destabilization of emulsified wastes, Waste Manag. **21** (2001) 535–542.

[5] G.J.M. Koper, An Introduction to Interfacial Engineering, VSSD, Delft, 2007.

[6] C. Schneider, M. Hanisch, B. Wedel, A. Jusufi, M. Ballauff, Experimental study of electrostatically stabilized colloidal particles: Colloidal stability and charge reversal, J. Colloid. Interf. Sci. **358** (2011) 62–67.

[7] V.M. Dronnet, C.M.G.C. Renard, M.A.V. Axelos, J.F. Thibault, Characterisation and selectivity of divalent metal ions binding by citrus and sugar-beet pectins, Carbohyd. Polym. **30** (1996) 253–263.

[8] C. Garnier, M.A.V. Axelos, J.F. Thibault, Selectivity and cooperativity in the binding of calcium ions by pectins, Carbohyd. Res. **256** (1994) 71.

[9] F. Gaucheron, Y. L. Graët, E. Boyaval, M. Piot, Binding of cations to casein molecules: Imortance of physico-chemical conditions, Milchwissenschaft **52** (1997) 322–327.

[10] D. Bergmann, G. Furth, C. Mayer, Binding of bivalent cations by xanthan in aqueous solution, Int. J. Biol. Macromol. **43** (2008) 245–251.

[11] P. Pellerin, M.A. O'Neill, The interaction of the pectic polysaccharide Rhamnogalacturonan II with heavy metals and lanthanides in wines and fruit juices, Analysis Magazine **26** (1998) M32–M36.

Table 6. $CaSO_4$ and cationic polyelectrolyte concentration for zero zeta potential of pectin solutions obtaining Zero zeta potential (0 mV)

Precipitant	P1		P2		P3	
	mg dm^{-3}	mg g_p^{-1}	mg dm^{-3}	mg g_p^{-1}	mg dm^{-3}	mg g_p^{-1}
$CaSO_4$ + 0 mg dm^{-3} cationic polyelectrolyte	430	678	410	618	355	490
$CaSO_4$ + 3 mg dm^{-3} cationic polyelectrolyte	320	512	320	482	260	360
$CaSO_4$ + 5 mg dm^{-3} cationic polyelectrolyte	310	504	315	475	255	353

CONCLUSION

The assumption that a small amount of a cationic polyelectrolyte will have an influence on the improvement of coagulation characteristics of Ca^{2+} in $CaSO_4$ as precipitant extracting pectin, has proved to be true. Cationic polyelectrolyte achieves additional charge neutralization. This mechanism is combined with mechanism of interparticle bonding. The optimal amount of cationic polyelectrolytes was found to be (cationic PAM) 3 mg dm^{-3}. Addition of increased amounts of cationic polyelectrolyte did not give an improvement, suggesting that the cationic bridging polyelectrolyte targets pectin macromolecules with different molar mass.

The quality of precipitation of pectin is affected by precipitant concentration ($CaSO_4$) the most, which is confirmed by ANOVA calculation, (RSM) and standard score evaluation.

With an adequate dosing of $CaSO_4$ and cation polyelectrolyte along with zeta potential control, significant economic effect can be achieved. It has been found that the consumption of this coagulant is about 20 times lower in comparison with the consumption of a conventional coagulant CaO. In this way, the contamination of soil would be reduced to a minimum.

However, reliable comparison between the proposed compounds and traditional coagulant CaO, requires additional testing under industrial conditions of sugar beet juice processing.

[12] Z. Reddad, C. Gerente, Y. Andres, M.C. Ralet, J.F. Thibault, P. Le Cloriec, Ni (II) and Cu (II) binding properties of native and modified sugar beet pulp, Carbohyd. Polym. **49** (2002) 23–31.

[13] A.D. Blackwood, M.F. Chaplin, Disaccharide, oligosaccharide and polysaccharide analysis, Encyclopedia of Analytical Chemistry, R.A. Meyers, Ed., Wiley, Chichester, 2000, pp. 741–765.

[14] B.M. Yapo, Pectin quantity, composition and physicochemical behavior as influenced by the purification process, Food Res. Int. **42** (2009) 1197–1202.

[15] T.B. Kinraide, U. A Yermiyahu, Scale of metal ion binding strengths correlating with ionic charge, Pauling electronegativity, toxicity and other physiological effects, J. Inorganic Biochem. **101** (2007) 1201–1213.

[16] N.A. Wall, G.R. Choppin, Humic acids coagulation: influence of divalent cations, Appl. Geochem. **18** (2003) 1573–1582.

[17] T. Kuljanin, L. Jevrić, B. Ćurčić, M. Nićetin V. Filipović J. Grbić, Aluminium and calcium ions binding to pectin in sugar beet juice: Model of electrical double layer, Hem. Ind. **68**(1) (2014) 89–97.

[18] Lj. Lević, M. Tekić, M. Djurić, T. Kuljanin, $CaCl_2$, $CuSO_4$ and $AlCl_3$ & $NaHCO_3$ as possible pectin precipitants in sugar juice clarification. Int. J. Food Sci. Tech. **42** (2007) 609–614.

[19] W.O.S. Doherty, C. M. Fellows, S. Gorjian, E. Senogles, W. H. Cheung, Flocculation and sedimentation of cane sugar juice particles with cationic homo- and copolymers. J. Appl. Polym. Sci. **90** (2003) 316–325.

[20] N. Hilal, M. Al-Abri, A. Moran, H. Al-Hinai, Effect of heavy metals and polyelectrolytes in humic substance coagulation under saline conditions, Desalination **220** (2008) 85–95.

[21] S. Pattabi, K. Ramasami, K. Selvam, K. Swaminathan, Influence of polyelectrolytes on sewage water treatment using inorganic coagulants, Indian J. Environ. Prot. **20** (2000) 499–507.

[22] B.M. Baraniak, E. Walerianczyk, Flocculation. Encyclopedia of Food Sciences and Nutrition, 2nd ed., 2003, pp. 2531–2535.

[23] D. Sargent, E. Philip, M.T.G. Cubero, Lime reduction in juice purification, Zuckerindustrie, **123** (1998) 442–448.

[24] J.L. Carlson, U. Samaraweera, Improvement in first carbonation sludge settling by selection of a better flocculant addition point and the addition of starch as a second flocculant., in Proceedings of 35th General Meeting of American Society of Sugar Beet Technologists, February 25–28, 2009 Wyndham Orlando Resort, Orlando, FL, ND 58075–9698.

[25] T. Kuljanin, G. Koprivica, L. Jevrić, R. Jevtić-Mučibabić, B. Filipčev, J. Grbić, Binding Al^{3+}, Cu^{2+} ions and polyelectrolytes with macromolecules in sugar beet juice, PTEP **16** (2012) 71–74.

[26] D.G. Kinniburgh, W.H. van Riemsdijk, L.K. Koopal, M. Borkovec, M.F. Benedetti, M.J. Avena, Ion binding to natural organic matter: competition, heterogeneity, stoichiometry and thermodynamic consistency, Colloids Surfaces,. A **151** (1999) 147–166.

[27] J. Duan, J. Gregory, Coagulation by hydrolysing metal salts. Adv. Colloid Interface Sci. **102** (2003) 475–502.

[28] Lj. Lević, J. Gyura, M. Djurić, T. Kuljanin, Optimization of pH value and aluminium sulphate quantity in the chemical treatment of molasses, Eur. Food Res. Technol. **202** (2005) 70–73.

[29] K. Fares, C.M.G. Renard C. Q. R'Zina, J.F. Thibault, Extraction and composition of pectins and hemicelluloses of cell walls of sugar beet roots grown in Morocco, Int. J. Food Sci.Technol. **36** (2001) 35–46.

[30] M. Marry, M.C. McCann, F. Koplak, A.R. White, N.J. Stacey, K. Roberts, Extraction of pectic polysaccharides from sugar-beet cell walls. J. Sci. Food Agr. **80** (2000) 17–28.

[31] AOAC, Methods of Analysis of Official Analytical Chemists, Washington DC, 2000.

[32] P.S. Madamba, The Response Surface Methodology: An Application to Optimize Dehydration Operations of Selected Agricultural Crops, Lebensm.-Wiss. Technol. **35** (2002) 584–592.

[33] T. Brlek, L. Pezo, N. Voća, T. Krička, Đ. Vukmirović, R. Čolović, M. Bodroža-Solarov, Chemometric approach for assessing the quality of olive cake pellets. Fuel Process Technol. **16** (2013) 250–256.

[34] I.E. Baciu, H.J. Jördening, Kinetics of galacturonic acid release from sugar beet pulp. Enzyme. Microb. Tech. **34** (2004) 505–512.

[35] S.V. Levigne, M.C. Ralet, J.F. Thibault, Characterisation of pectins extracted from fresh sugar beet under different conditions using an experimental design. Carbohyd. Polym. **49** (2002) 145–153.

[36] R.C. Sun, S. Hughes, Fractional isolation and physicochemical characterization of alkali-soluble polysaccharides from sugar beet pulp. Carbohyd. Polym. **38** (1999) 273–281.

[37] A.M. Molina, M.Q. Perez, F.G. Gonzales, R.H. Alvarez, Primitive models and electrophoresis: an experimental study, Colloids Surfaces, A **222** (2003) 155–164.

IZVOD

$CaSO_4$ I KATJONSKI POLIELEKTROLITI KAO MOGUĆI PRECIPITANTI PEKTINA PRI PREČIŠĆAVANJU SOKA ŠEĆERNE REPE

Tatjana Kuljanin[1], Biljana Lončar [1], Lato Pezo[2], Milica Nićetin[1], Violeta Knežević[1], Rada Jevtić-Mučibabić[3]

[1]*Tehnološki fakultet, Univerzitet u Novom Sadu, Srbija*
[2]*Institut za opštu i fizičku hemiju, Univerzitet u Beogradu, Srbija*
[3]*Naučni Institut za prehrambene tehnologije, Univerzitet u Novom Sadu, Srbija*

(Naučni rad)

U toku industrijske obrade šećerne repe, jedna od najvažnijih faza je čišćenje soka šećerne repe. U tu svrhu, najčešće se koristi CaO u obliku $Ca(OH)_2$. Pošto kalcijumovi joni iz ovih jedinjenja imaju relativno mali afinitet vezivanja sa pektinima soka šećerne repe, potrebne su vrlo velike količine kreča (oko 15 g CaO/100 g soka). Zbog toga je razmatrana mogućnost izdvajanja pektina procesom razelektrisanja čestica dodavanjem jedinjenja sa dvo- i trovalentnim katjonima kao i katjonskog polielektrolita. U ovom radu, izneta su istraživanja i date su teorijske osnove nove metode čišćenja soka šećerne repe koja se bazira na primeni $CaSO_4$ i katjonskog polielektrolita. U toku trajanja ekstrakcije od 150 min, na pH vrednostima od 1, 3.5 i 8.5, iz rezanaca sveže šećerne repe izolovana su tri pektinska preparata. Precipitant $CaSO_4$ u vidu vodenog rastvora, dodavan je u 100 cm^3 0.1 % (mas) rastvora pektina. Ispitivanja su vršena sa 9 različitih koncentracija rastvora $CaSO_4$ (u intervalu 50–450 g/dm^3) bez dodavanja katjonskog polielektrolita i uz dodatak katjonskog polielektrolita koncentracije 3 i 5 mg/dm^3 (cationic PAM). Efikasnost taloženja pektina praćena je merenjem zeta potencijala modelrastvora pektinskih preparata. Izmerene vrednosti zeta potencijala za različite procesne parametre upoređivane su statistički, primenom RSM analize. Optimalne količine precipitanta $CaSO_4$, bez primene katjonskog polielektrolita, iznosile su: 490–678 mg $CaSO_4$/g pektina. Nakon primene katjonskog polielektrolita, optimalne količine $CaSO_4$ su bile manje (u intervalu 353–512 mg/g) što znači da je katjonski polielektrolit uticao na poboljšanje koagulacionih karakteristika jona Ca^{2+} iz $CaSO_4$. U ovom slučaju, došlo je dodatne neutralizacije naelektrisanja – mehanizam neutralizacije naelektrisanja je udružen sa mehanizmom međučestičnog povezivanja. Utvrđena je optimalna doza katjonskog polielektrolita (cationic PAM) od 3 mg/dm^3 dok veća doza (5 mg/dm^3) nije značajno uticala na povećanje taloženja pektina. Ove količine su znatno manje od prosečne količine CaO upotrebljenog u klasičnom postupku čišćenja soka šećerne repe (oko 9 g/g pektina soka šećerne repe). Delimičnom ili potpunom zamenom klasičnog koagulanta sa $CaSO_4$ uz primenu katjonskog polielektrolita, smanjili bi se troškovi uklanjanja pektina iz soka šećerne repe uz očuvanje životne sredine.

Ključne reči: Čišćenje • Pektini • Sok šećerne repe • $CaSO_4$ • Katjonski polielektrolit • Zeta potencijal

Primena gljiva koje razgrađuju lignocelulozu za proizvodnju bioetanola iz obnovljive biomase

Jelena M. Jović[1], Jelena D. Pejin[2], Sunčica D. Kocić-Tanackov[2], Ljiljana V. Mojović[1]

[1]*Tehnološko–metalurški fakultet, Univerzitet u Beogradu, Beograd, Srbija*
[2]*Tehnološki fakultet, Univerzitet u Novom Sadu, Novi Sad, Srbija*

Izvod

Predtretman predstavlja neophodan korak u procesu konverzije lignocelulozne biomase do etanola. On unapređuje enzimsku hidrolizu promenama u strukturi lignoceluloze, ali je često utrošak energije za predretman veliki i/ili se primenjuju skupe i toksične hemikalije, što proces čini ekonomski i ekološki nepogodnim. Primena lignocelulolitičkih gljiva (iz klasa Ascomycetes, Deuteromycetes i Basidiomycetes) je atraktivna metoda za predtretman, ekološki prihvatljiva i ne zahteva ulaganje energije. U ovom radu su predstavljeni mehanizmi razgradnje lignoceluloze pomoću gljiva. One proizvode širok spektar enzima i hemijskih supstanci kojima uspešno razgrađuju lignocelulozu, ali i aromatične polimere slične strukture ligninu. U ovom radu je prikazana mogućnost njihove primene u tehnologiji proizvodnje bioetanola, a navedene su i prednosti i nedostaci biološkog predtretmana.

Ključne reči: biološki predtretman, fungalni enzimi, bioetanol, fermentacija na čvrstom supstratu, lignocelulozna biomasa.

Dostupno na Internetu sa adrese časopisa: http://www.ache.org.rs/HI/

PREGLEDNI RAD

UDK 662.754:66:58

Hem. Ind. **69** (6) 627–641 (2015)

doi: 10.2298/HEMIND140916086J

Napredak u nauci i medicini, razvoj industrije i unapređenje poljoprivredne proizvodnje omogućili su kvalitetniji i duži život ljudi, ali su, eksplozija ljudske populacije i nesavesno ponašanje većine, stvorili brojne probleme: uvećane su potrebe za hranom, energijom i prostorom; izmenjeni ili uništeni brojni ekosistemi; uvećane količine akumuliranog otpada, a sa njima i zdravstveni i bezbednosni rizici. Zbog intenzivne upotrebe fosilnih sirovina (za proizvodnju energije, brojnih neophodnih hemikalija, proizvoda poput plastike), danas se susrećemo sa dva značajna problema [1]:

1. predviđa se nestanak prirodnih rezervi fosilnih sirovina u narednim godinama;
2. uočen je značajan negativan uticaj na životnu sredinu povezan sa njihovom upotrebom.

Radi prevazilaženja navedenih problema, danas se sve više teži: održivom razvoju (koji podrazumeva reciklažu otpadnog materijala i korišćenje obnovljivih resursa – vode, vazduha i biomase), alternativnim izvorima energije i čistijoj, ekološki prihvatljivoj proizvodnji.

Iz biomase se potrebne hemikalije dobijaju fermentacijom šećernog supstrata ili hemijskom sintezom produkata fermentacije, zbog čega se, svaki materijal koji u sebi sadrži šećere, može koristiti u biotehnološkoj proizvodnji. Prema tipu sirovog materijala sirovine na bazi biomase se dele na šećerne (šećerna repa, šećerna trska, sirak, voće i dr.), skrobne (kukuruz, pšenica, pirinač i dr.) i lignocelulozne [2,3]. Prema poreklu sirovog materijala i procesu transformacije dele se na [1]: sirovine prve generacije (poljoprivredne kulture), druge generacije (lignocelulozni i drugi otpad) i treće generacije (fermentativne i fotosintetičke bakterije i alge) – tabela 1.

Lignoceluloznu biomasu čine suvi ostaci biljaka. Veoma je važan obnovljivi izvor energije i jedini je obnovljivi izvor ugljenika. Sastoji se od lignina (aromatičnog polimera) i polisaharida (hemiceluloze i celuloze). Hemijske karakteristike strukturnih komponenata čine je veoma vrednim biotehnološkim supstratom, ali njena primena zahteva uklanjanje lignina i oslobađanje fermentabilnih šećera iz polisaharida, zbog čega su savremena istraživanja usmerena ka pronalaženju efektivne metode kojom se može dobiti visok prinos šećera.

Biološki predtretman podrazumeva konverziju biomase lignocelulolitičkim organizmima; bezbedan je, ekološki prihvatljiv i ne zahteva puno energije za uklanjanje lignina, bez obzira na njegovu obimnu razgradnju. Do 1976. godine je sakupljeno više od 14000 gljiva koje razgrađuju celulozu i druga nerastvorljiva vlakna [4]. Saprofitne gljive klase Agaricomycetes su još krajem karbona razvile sposobnost degradacije lignina [5].

Tekuća istraživanja su usmerena i na primenu fungalnih ligninolitičkih mehanizama u procesu bioremedijacije (transformacije ili razgradnje opasnih supstanci do bezbednih ili manje opasnih). Zahvaljujući nespecifičnom enzimskom sistemu, sačinjenom od lakaza i lignin-, mangan- i verzatil-peroksidaza, gljive su u stanju da razgrađuju složene aromatične polimere, slične strukture kao lignin – pesticide, poliaromatične ugljovodonike (PAH), polihlorovane bifenile (PCB), boje [6].

Prepiska: Lj. Mojović, Tehnološko–metalurški fakultet, Univerzitet u Beogradu, Karnegijeva 4, 11000 Beograd, Srbija.
E-pošta: lmojovic@tmf.bg.ac.rs
Rad primljen: 16. septembar, 2014
Rad prihvaćen: 28. novembar, 2014

Tabela 1. Podela i karakteristike sirovina biomase prema poreklu sirovog materijala i procesu transformacije
Table 1. Classification and characteristics of biomass feedstocks according to origin of raw materials and transformation process

Vrsta sirovine	Poreklo sirovine	Karakteristike
Sirovine prve generacije	Koriste se u ishrani, poreklom su iz poljoprivredne proizvodnje: skrobni, šećerni i uljani usevi (uljarice)	Visok sadržaj šećera ili ulja; visoka cena zbog kompeticije sa hranom
Sirovine druge generacije	Nejestive sirovine: lignocelulozna biomasa i materijal zaostao nakon različitih procesa u poljoprivredi, prehrambenoj industriji i šumarstvu kao i usevi namenjeni proizvodnji energije	Ekonomski povoljnije sirovine; konverzija znatno kompleksnija zbog otpornosti celulozne biomase prema razgradnji.
Sirovine treće generacije	Širok spektar fermentativnih i fotosintetičkih bakterija i alge, koje se za sada proučavaju kao biokatalizatori	Visok sadržaj ulja, ugljenih hidrata ili proteina u njima, prepoznate kao izvanredne sirovine

U ovom radu su opisani mehanizmi razgradnje lignoceluloznog supstrata pomoću gljiva i, kroz različite proizvodne faze**,** od predtretmana do fermentacije, prikazana je mogućnost njihove primene u tehnologiji proizvodnje bioetanola. Cilj je bio, pre svega, da se predstavi jeftina metoda predtretmana, koja ne zahteva ulaganje energije niti primenu skupih hemikalija. Kroz pregled radova, dosadašnjih istraživanja biološkog predtretmana, ukazano je na prednosti i nedostatke ove metode.

ZNAČAJ BIOETANOLA

Bioetanol predstavlja alternativu fosilnom gorivu. Njegova važnost je, poslednjih godina, porasla zbog potrebe da se smanji zavisnost od sve iscrpljenijih fosilnih resursa, kao i emisija gasova koji uvećavaju efekat staklene bašte. Proizvodnja iz obnovljivih sirovina čini etanol CO_2-neutralnim: ugljen-dioksid oslobođen njegovim sagorevanjem je apsorbovan u toku fotosinteze i iskorišćen za rast biljke. Etanol omogućava čistije sagorevanje i bolje performanse motora, što doprinosi smanjenju emisije polutanata čak i kada se samo pomeša sa benzinom [3,7]. Biorazgradiv je i efikasniji nego konvencionalna goriva; karakteriše ga veći oktanski broj u odnosu na konvencionalna goriva; njegovim sagorevanjem oslobađa se značajna količina toplote i praktično je bez sumpora [8]. Razmatra se i njegova primena u proizvodnji biodizela umesto metanola: u odnosu na metanol nije toksičan i na taj način bi se dobio kompletno biljni biodizel. Proizvodnja bioetanola omogućava zemljama – koje ne poseduju fosilne – oslanjanje na sopstvene resurse i smanjenu zavisnost od uvoza energenata. Trenutno se dobija iz skrobnih i šećernih sirovina koje se koriste i u ishrani, pa bi primena jeftinih sirovina (poput lignoceluloznog otpada) mogla da obezbedi nižu cenu, a zalihe hrane ne bi bile ugrožene. Procenjuje se da se iz poljoprivrednog otpada i neiskorišćenih kultura može proizvesti oko 491 milijardi litara bioetanola godišnje [9]. Proizvodnja goriva bioetanola u svetu je od 2001. do 2011. godine porasla sa 31 na 88,7 milijardi litara [10]. Očekuje se da će do 2020. proizvodnja dostići 125 milijardi litara [11]. Najveći proizvođači u svetu su Brazil i Sjedinjene Američke Države (62% svetske prozvodnje) [9].

HEMIJSKE I FIZIČKE KARAKTERISTIKE LIGNOCELULOZNE BIOMASE

Tri glavne strukturne komponente lignoceluloze su polimeri celuloza, hemiceluloza i lignin (slika 1). Osim njih, mogu se naći i neke nestrukturne komponente poput vode, proteina, minerala, nestrukturnih saharida i nekih drugih, koje se mogu izdvojiti ekstrakcijom.

Sastav lignoceluloze u velikoj meri zavisi od izvora biomase [12–14]: postoje značajne razlike u udelu strukturnih komponenti – kao i u hemijskom sastavu hemiceluloze i lignina – u zavisnosti od toga da li je biomasa poreklom od mekog, tvrdog drveta ili zeljastih biljaka (videti tabelu 2).

Celuloza (slika 1) je prirodni polimer, polisaharid hemijske formule $(C_6H_{10}O_5)_n$. Predstavlja gradivnu komponentu primarnog ćelijskog zida viših biljaka, nekih algi i oomiceta; neke bakterije sekretuju celulozu prilikom formiranja biofilma. Celuloza se odlikuje visokim stepenom polimerizacije (od nekoliko stotina, pa čak do 17000 jedinica); u prirodi se najčešće sreće 800 do 10000 jedinica [12]. Osnovna gradivna jedinica celuloze je celobioza (dimer glukoze). Primarno celuloza je linearni homopolimer sastavljen od glukoznih ostataka D-konfiguracije međusobno povezanih β-(1→4)-glikozidnim vezama (slika 1, B1). Uspostavljanjem vodoničnih veza, nekoliko celuloznih lanaca srasta gradeći mikrofibrile koji se ujedinjuju i formiraju vlakna (slika 1, M, F i V). Rezultat brojnih inter- i intrapolimernih vodoničnih veza je kristalno uređenje celuloze (sekundarna struktura, slika 1, B2). Osim kristalnih, prirodna celuloza sadrži i amorfne tj. parakristalne regione [15].

Hemiceluloza je termin kojim se predstavlja familija polisaharida kao što su arabinoksilani, glukomanani, galaktani, ksiloglukani, ksilani, manani i β-(1→3, 1→4)--glukani, koji se mogu naći u ćelijskom zidu biljaka i čiji sastav i organizacija zavise od porekla i metode ekstrahovanja. Za razliku od celuloze, hemiceluloza (slika 1, C)

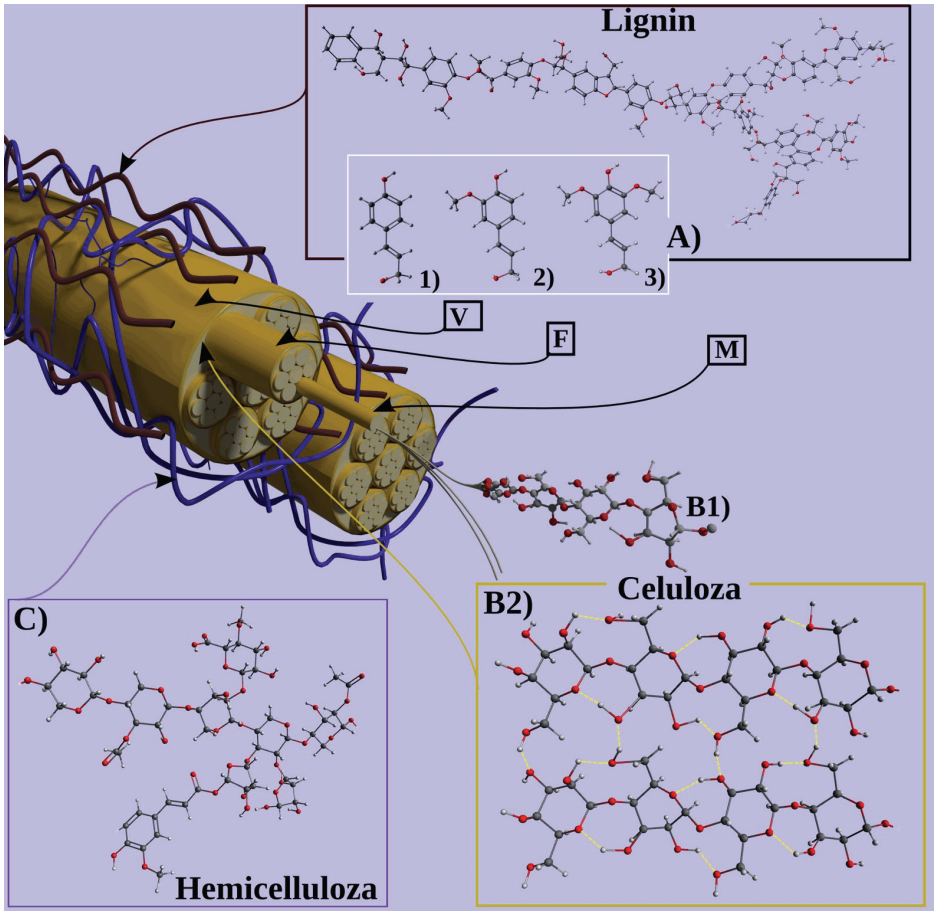

Slika 1. Struktura lignocelulozne biomase; A) deo polimera lignina, 1) p-kumaril, 2) koniferil i 3) sinapil alkohol; B1) linearni polimer celuloze; B2) kristalna struktura celuloze; C) deo polimera hemiceluloze; M) mikrofibril; F) fibril; V) celulozno vlakno.
Figure 1. Lignocellulosic biomass structure: A) part of lignin polymer, 1) p-coumaryl, 2) coniferyl and 3) sinapyl alcohol; B1) linear cellulose, B2) crystalline structure of cellulose; C) part of hemicellulose polymer; M) microfibril; F) fibril; V) cellulose fiber.

Tabela 2. Udeo osnovnih komponenti lignoceluloze u zavisnosti od porekla biomase
Table 2. Proportion of basic components of lignocellulose depending on source of biomass

Lignocelulozni materijal	Sadržaj celuloze, %	Sadržaj hemiceluloze, %	Sadržaj lignina, %	Referenca
Stablo tvrdog drveta	40–55	24–40	18–25	[12]
Stablo mekog drveta	45–50	25–35	25–35	[12]
Ljuska oraha	25–30	25–30	30–40	[12]
Kukuruzni oklasak	33–45	31–35	6–15	[12,13]
Trave	25–43	24–50	10–30	[12,14]
Stabljike kukuruza	35	16,8	7	[13]
Pšenična slama	30–38	24–50	8–15	[12–14]
Lišće	15–20	80–85	0	[12]
Ražana slama	31–38	25–31	0–19	[13,14]

nema kristalno uređenje, veoma je razgranate strukture i poseduje acetil grupe vezane za polimerni lanac. Razgranati polisaharidni lanci sačinjeni su uglavnom od aldopentoznih jedinica (ksiloza i arabinoza) i od nekih aldoheksoza (glukoza, manoza i galaktoza). Osim visokog stepena polimerizacije, polimer hemiceluloze obično ima supstituente na glavnom lancu ili granama [16]. Glavni tip intrapolimernih veza hemiceluloze čine estarske veze, a prisutna je i značajna količina karboksilnih grupa [12]. U literaturi se sreću različiti podaci o stepenu polimerizacije, ali jedna opšta slika je da ne prelazi 200 jedinica, dok je granica minimuma oko 50 [2,12,17]. Najvažnija funkcija hemiceluloze je doprinos jačanju ćelijskog zida, što se postiže njenom interakcijom sa celulozom i ligninom. Na slici 1 (C) prikazan je

deo molekula ksilana, najčešćeg polimera iz familije hemiceluloza.

Lignin je najkompleksniji biopolimer u prirodi i jedini konstituent biomase baziran na aromatičnim jedinicama (slika 1, A). On čini 15–25% suve mase drvenastih biljaka i 40% energije sadržane u lignoceluloznoj biomasi [18]; obezbeđuje mehaničku čvrstoću biljkama, povezivanjem sa polisaharidima omogućava vaskularnom tkivu biljaka efikasan transport vode i nutrijenata, štiti biljku od degradacije sprečavanjem penetracije lignocelulolitičkih enzima kroz ćelijski zid. Struktura lignina još uvek nije u potpunosti razjašnjena, ali je utvrđeno da su primarni prekursori njegove sinteze (tj. reakcije sparivanja radikala) tri monolignola: *p*-kumaril, koniferil i sinapil alkohol (slika 1, A pod 1), 2) i 3), redom) [19], koji nastaju od fenilalanina (Phe) u opštem fenilpropanoidnom i specifičnom monolignolnom putu [20]. Oni se inkorporiraju u lignin u formi fenilpropanoida: *p*-hidroksifenil (H), guajacil (G) i siringil (S) [19]. Pošto nastaje polidisperzni polimer – u kom se ne može uočiti pravilno ponavljanje većih jedinica – razlika u strukturi lignina različitog porekla se predstavlja razlikom u brojnosti fenilpropan jedinica i distribuciji veza unutar jedinica. Glavne intrapolimerne veze lignina su etarske veze (70%) i ugljenik–ugljenik veze (30%) [21]. Svi lignini u manjim količinama sadrže i nekompletne ili modifikovane monolignole, pa se mogu uočiti i drugačiji mnomeri [19,22].

PREDTRETMAN LIGNOCELULOZNE BIOMASE

Lignoceluloznu bimasu karakteriše velika otpornost prema razgradnji enzimima ili mikroorganizmima. Različite su pretpostavke uzroka ove otpornosti. U literaturi se najčešće navode: struktura i količina lignina; acetilovana hemiceluloza; lignin-ugljenohidratni kompleks (eng. *lignin carbohydrate complexes*, LCC); kristaličnost celuloze i stepen polimerizacije; zapremina pora; specifična površina celuloze [23,24]. Nerazgranata hemiceluloza (ksiloglukani, homoksilani i manani) formira vodonične veze sa površinom celuloznih fibrila, dok su bočni lanci (uronska kiselina i arabinoza) kovalentno vezani sa drugim hemicelulozama ili ligninom [23]. Na ovaj način se formiraju za enzime nepropustne mreže – lignin–ugljenohidratni kompleksi.

Konverzija lignoceluloze do željenih produkata je višestepeni proces (slika 2) koji obuhvata: predtretman (fizički, hemijski, fizičkohemijski i/ili biološki), hidrolizu polimera do metabolišućih molekula, primenu ovih molekula za mikrobni rast i fermentaciju do željenih produkata, separaciju i prečišćavanje produkata. Metode predtretmana se mogu kombinovati ili primeniti samostalno.

Da bi jedan predtretman bio efektivan treba da zadovolji određene kriterijume: efikasnost u širokom spektru vrsta i količina lignoceluloznog materijala; mogućnost dobijanja najvećeg dela lignoceluloznih komponenti u upotrebljivoj formi u različitim frakcijama; treba minimizirati potrebu za pripremom koja prethodi predtretmanu (npr. redukcija veličine); da ne proizvodi uopšte ili proizvede što manje količine inhibitora narednih procesa – hidrolize i fermentacije; male potrebe za energijom ili da se uložena energija upotrebi u druge svrhe; da bude ekonomski isplativ.

Biološki predtretman

Biološki predtretman se izvodi organizmima sposobnim da proizvode enzime i druge hemijske supstance kojima se može ukloniti lignin i osloboditi šećeri (pentoze i heksoze) iz kompleksnog lignoceluloznog supstrata. Ne zahteva primenu skupih hemikalija, niti utrošak energije – u kombinaciji sa drugim metodama omogućava veći prinos, smanjuje potrebe za energijom, ublažava oštre uslove metoda sa kojim se kombinuje [25,26] – i ekološki je bezbedan. Pošto pomenuti organizmi ne mogu da koriste ugljenik iz lignina, već iz oslobođenih šećera, biološki predtretman može dovesti do gubitka dela ugljenih hidrata. Iako bi represija hidrolitičkih enzima mogla da uspori ovaj proces, dodatno bi se produžilo vreme trajanja predtretmana čija dužina već predstavlja problem. Rešenje može biti korišćenje brzorastućih organizama koji proizvode veće količine enzima ili primena neke druge metode predtretmana pre biološke. Studija na pirinčanim ljuskama je pokazala da je, nakon primene vodonik-peroksida, vreme inkubacije *Pleurotus ostreatus* skraćeno sa 60 na 18 dana [27].

Organizmi razgrađivači lignoceluloze

Razgradnja lignoceluloze u prirodi je raspodeljena među gljivama i bakterijama. Bakterije su uglavnom ograničene na biomasu sa manjom količinom lignina,

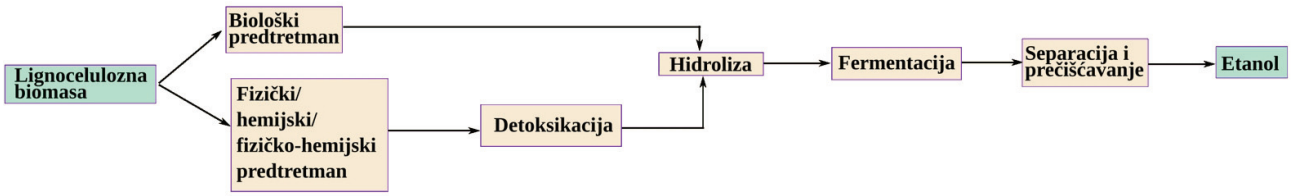

Slika 2. Uprošćena šema proizvodnje bioetanola iz lignocellulozne biomase.
Figure 2. Simple flow chart of bioethanol production from lignocellulosic biomass.

jer slabo proizvode ligninaze (neke aktinomicete [28]). Kao bolje adaptirani organizmi na vodeno okruženje nego gljive, pretežno razgrađuju biljke vodenih staništa. Nalaze se i u crevnom sistemu herbivora. Celulolitičke bakterije obuhvataju vrste rodova *Clostridium, Ruminococcus, Caldicellulosiruptor, Butyrivibrio, Acetivibrio, Cellulomonas, Erwinia, Thermobifida, Fibrobacter, Cytophaga* i *Sporocytophaga* [29].

Na osnovu iskorišćenosti materijala i karakteristika trulog drveta, razlikuju se tri tipa lignocelulolitičkih gljiva: gljive izazivači belog, braon i mekog truljenja; dok je sposobnost iskorišćenja celuloze rasprostranjena u čitavom carstvu Fungi od protista, poput Chytridiomycetes, do naprednih Basidiomycetes. Belo i braon truljenje izazivaju bazidiomicete; meko truleljenje je posledica delovanja askomiceta i deuteromiceta [30].

Gljive izazivači belog truljenja su sposobne da razgrađuju sve frakcije drveta. Najefikasniji su razgrađivači lignina u prirodi, zbog čega imaju veoma važnu ulogu u reciklaži ugljenika iz lignifikovanog tkiva. Nakon razgradnje drvo ostaje u vidu belih vlakana. Pretežno rastu na tvrdom drvetu (poput breze i jasike), ali se mogu naći i na mekom, npr. boru (*Heterobasidion annosum*, *Phellinus pini* i *Phlebia radiata*) [30]. Sposobne su za selektivnu (*Ceriporiopsis subvermispora*, *Dichomitus squalens*, *Phlebia radiata* i dr.) [31] i neselektivnu razgradnju lignina (*Phanerochaete chrysosporium, Trametes versicolor* i *Fomes fomentarius*) [30]. Selektivnom razgradnjom uklanjaju lignin i hemicelulozu dok celuloza uglavnom ostaje intaktna [31]; neselektivnom uklanjaju podjednako sve komponente lignoceluloze [28,30,31].

Gljive izazivači braon truljenja razgrađuju hemicelulozu i celulozu, dok lignin u izvesnoj meri modifikuju. Braon trulež je drvo tamne (braon) boje (što ukazuje na prisustvo modifikovanog lignina), smanjeno i razbijeno na fragmente oblika cigle ili kocke koji se lako mrve dajući braon prah. Za razliku od gljiva izazivača belog truljenja – koje hidrolizuju polisaharide samo do one količine hidrolizata koje mogu da iskoriste za sopstveni metabolizam – gljive izazivači braon truljenja depolimerizuju celulozu i hemicelulozu brže nego što gljiva može da iskoristi hidrolizate, pa dolazi do akumulacije neiskorišćenih šećera [28,32]. Lignin, modifikovan ovim gljivama, je reaktivniji nego prirodni zbog većeg sadržaja fenolnih hidroksilnih i karboksilnih grupa [33]. Među gljivama izazivačima braon truljenja najizučavanija je *Gloeophyllum trabeum*.

Meko truljenje izazivaju gljive klasa Ascomycetes i Deuteromycetes (*Fungi imperfecti*) – drvo postaje mekano, braon boje. Postoje dva tipa meke truleži [34]: tip I se odlikuje bikoničnim ili cilindričnim šupljinama u sekundarnom zidu, tip II je erozivni tip degradacije. Ispitivanja vrste *Daldinia concentrica* su pokazala da ove gljive prevashodno oksiduju i mineralizuju siringil jedinice lignina dok je guajacil veoma otporan na njihovo dejstvo, zbog čega su u degradaciji mekog drveta, koje sadrži znatno više G jedinica, veoma neefikasne [28].

Osim aerobne razgradnje, koja se vrši slobodnim enzimima, postoji i, značajno drugačija, anaerobna razgradnja u kojoj učestvuju enzimi multienzimskih kompleksa – celulozoma (slika 3). Celulozomi su prvi put identifikovani i opisani kod termofilne, anaerobne, celulolitičke bakterije *Clostridium thermocellum*. Biohemijska istraživanja celulozoma su pokazala da se najveći deo celulolitickog procesa odvija u ekstracelularnim celulozomima koji su organizovani na površini ćelija u formi policelulozomalnih organela [35]. Podjedinice celulozoma su sastavljene od brojnih funkcionalnih domena koji interaguju međusobom i sa celuloznim supstratom. Jedna od ovih podjedinica je veliki glikoprotein skafoldin koji ima ulogu nosača [29]. On selektivno vezuje različite podjedinice celulaza i ksilanaza u kohezivni kompleks (slika 3), kombinujući njihove „ko-

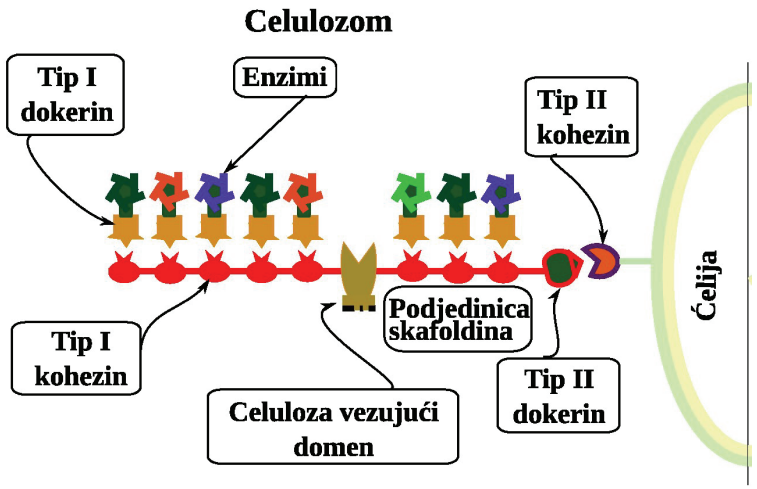

Slika 3. Struktura celulozoma.
Figure 3. Structure of cellulosome.

hezin“ domene sa karakterističnim „dokerin“ domenima [35], prisutnim na svakoj od podjedinica. Skafoldin nekih celulozoma poseduje i mesta za vezivanje ugljenih hidrata. Celulozomalne sisteme produkuju i anaerobne bakterije *Acetivibrio cellulolyticus*, *Bacteroides cellulosolvens*, *Ruminococcus albus*, *Ruminococcus flavefaciens* i anaerobne gljive rodova *Neocallimastix*, *Piromyces* i *Orpinomyces*.

FUNGALNI ENZIMI I NJIHOVI MEHANIZMI RAZGRADNJE LIGNOCELULOZE

Gljive proizvode širok spektar enzima i hemijskih supstanci koji, na različite načine iskombinovani kod različitih vrsta, zajedno razgrađuju lignocelulozu biomasu. Mehanizmi razgradnje se mogu podeliti na oksidativne i hidrolitičke.

Oksidativni mehanizmi

Akcijom fungalnih redoks enzima (glioksal oksidaze, piranoza-2-oksidaze i aril-alkohol oksidaze) nastaje vodonik peroksid (H_2O_2), koji reaguje sa redoks-aktivnim gvožđem (prisutnim u drvetu u dovoljnim količinama) i, kroz Fentonovu reakciju (1), proizvodi hidroksilni radikal – $^{\bullet}OH$. $^{\bullet}OH$ je veoma moćan oksidujući agens, sposoban da katalizuje visoko nespecifične reakcije i raskida kovalentne veze lignina i celuloze [36].

$$Fe^{2+} + H_2O_2 \rightarrow Fe^{3+} + {}^{\bullet}OH + OH^{-}$$

$$Fe^{3+} + H_2O_2 \rightarrow Fe^{2+} + O_2^{\cdot -} + 2H^{+} \quad (1)$$

Gljive (kao i mnoge biljke, insekti i bakterija *Azospirillum lipoferum*) proizvode multibakarne enzime – lakaze. Fungalne lakaze katalizuju formiranje fenoksil radikala, čija nespecifična reakcija vodi C_α-hidroksil oksidaciji do ketona, raskidanju veze između alkil i aril grupa, demetoksilaciji i raskidanju C_α–C_β veze u ligninu, kao i do reakcije polimerizacije [30,37]. Mehanizam razgradnje obuhvata prenos jednog elektrona sa malog molekula supstrata (tzv. medijatora) na molekul kiseonika, nakon čega oksidovani medijator difunduje u gusto pakovanu lignocelulozu i inicira reakciju slobodnih radikala koja vodi depolimerizaciji [5]. U prisustvu medijatora malog molekula, poput hidroksibenzotriazola, moguća je i oksidacija nefenolnih komponenti lignina [30].

Drugu grupu fungalnih ligninolitičkih enzima čine hem peroksidaze: lignin peroksidaze (LiP), mangan peroksidaze (MnP) i verzatil (hibridne) peroksidaze (VP). U supstratu je obično prisutno više izoenzima LiP, MnP, VP. LiP katalizuju reakcije cepanje β-O-4 etarskih veza i C_α–C_β veza u ligninu [38], oksidaciju aromatičnih C_α alkohola, hidroksilaciju, formiranje hinona i raskidanje aromatičnog prstena. Registrovane su kod 40% proučavanih gljiva [39]. Zahvaljujući invarijantnim ostacima triptofana (trp171) prisutnim u izoenzimu LiP-A, mogu oksidovati i nefenolne aromatične komponente lignina [40]. LiP su poznate kao jaki oksidansi zbog većeg deficita elektrona u gvožđu u porfirinskom prstenu u odnosu na druge peroksidaze. MnP oksiduju Mn^{2+} u visoko reaktivan Mn^{3+} (medijator u procesu oksidacije organskog supstrata, reakcija (2) [30]), koji je stabilizovan helatorima fungalnog porekla, poput oksalne kiseline [41]:

$$Mn^{3+} + RH \rightarrow Mn^{2+} + R + H^{+} \quad (2)$$

MnP ne poseduju invarijantne ostatke triptofana, pa u odsustvu intermedijera, poput tiola, ne mogu oksidovati nefenolne komponente lignina [42]. Verzatil peroksidaze ispoljavaju i LiP i MnP aktivnost. One poseduju Mn-vezujuće mesto i kada vežu Mn [39] sposobne su da oksiduju Mn^{2+} do Mn^{3+}. Poput lignin peroksidaza i VP poseduju ostatke triptofana, trp164, analoge onim u LiP, koji im omgućavaju oksidaciju nefenolnih aromatičnih komponenti lignina [30].

Katalitički ciklus peroksidaza obuhvata 3 odvojena koraka, reakcija (3):

$$\text{Enzim[Fe(III)]} + H_2O_2 \rightarrow \text{Komponenta-I[Fe(IV)=O}^{+}\text{]} + H_2O$$

$$\text{Komponenta-I} + AH \rightarrow \text{Komponenta-II[Fe(IV)=O]} + A^{\bullet +} \quad (3)$$

$$\text{Komponenta-II} + AH \rightarrow \text{Enzim} + A^{\bullet +}$$

Ciklus počinje raskidanjem O–O veze u molekulu H_2O_2 i uklanjanjem dva elektrona iz enzima; oslobađa se voda i formira intermedijerno jedinjenje O=Fe(IV)–porfirin π-radikalski katjon (tj. komponenta-I[Fe(IV)=O^{+}]) [43]. U narednom koraku, redukcijom porfirinskog radikala komponente-I, nastaje drugi intermedijer (komponenta-II[Fe(IV)=O]) čijom redukcijom se (u trećem koraku) enzim vraća u prirodno stanje; istovremeno se (sa redukcijom komponenti I i II) oksiduje supstrat i oslobađaju dva supstratna radikala ($A^{\bullet +}$) [44], po jedan u svakom koraku.

U oksidacione procese su uključene i celobioza dehidrogenaze (CDH), enzimi koje sintetišu i gljive koje razgrađuju i gljive koje ne razgrađuju lignin. CDH sadrže dve prostetičke grupe: hem i flavin adenin dinukleotid (FAD). Neke poseduju samo FAD prostetičku grupu, zbog čega su dugo vremena posmatrane kao poseban enzim celobioza:hinon oksidoreduktaza (eng. *cellobiose quinone oxidoreductase* – CBQ) [45]. Oksiduju oligomerne šećere do laktona koristeći širok spektar akceptora elektrona poput hinona, fenoksiradikala, Fe^{3+} i Cu^{2+}. Mogu direktno modifikovati lignin raskidanjem β-etarskih veza, demetoksilacijom aromatičnih komponenti, uvođenjem hidroksilnih grupa u nefenolne komponente kroz produkciju hidroksil radikala [46]; ili indirektno, kroz interakciju sa manganom: oksidovanjem celobioze do 4-O-b-D-glukopiranozil-D-glukonske kise-

line (celobionske kiseline) koja je efikasan helator mangana (Mn(III)) [47]; prevođenjem nerastvornog MnO_2 u depoe rastvornog Mn, u formi Mn(II) i Mn(III), čime je olakšano formiranje MnP i obezbeđen dodatni Mn(II) za MnP katalizu; redukcijom toksičnih hinona do odgovarajućih fenola koji služe kao supstrat za MnP [47,48].

Hidrolitički mehanizmi

Potrebnu energiju lignocelulolitičke gljive obezbeđuju iz molekula šećera oslobođenih hidrolizom polisaharida (celuloze i hemiceluloze) odgovarajućim enzimima.

Razgradnju celuloze katalizuju celulaze. Celulaze poseduju katalitički modul i modul za vezivanje za ugljene hidrate (eng. *carbohydrate-binding module* – CBM). Prema načinu delovanja dele se u tri klase: endo-(1,4)-β-glukanaze (endocelulaze), celobiohidrolaze (egzocelulaze) i β-glukozidaze [4,29,49]. Egzocelulaze razgrađuju kristaliničnu celulozu uklanjajući celobiozne jedinice sa krajeva celuloznih lanaca; endocelulaze razgrađuju amorfnu celulozu hidrolizom unutrašnjih glikozidnih veza. Postoji značajan sinergizam celobiohidrolaza i endocelulaza, a njihovo zajedničko prisustvo i kooperativnost određuju visoko efikasan enzimski sistem za industrisjku primenu [49,50]. Nakon delovanja endo- i egzocelulaza, β-glukozidaze oslobađaju molekule glukoze iz celobioze i celodekstrina; poseduju aktivna mesta u obliku džepa, koja im omogućavaju da deluju na neredukujuće glukozne jedinice [49,51].

Odvajanje celuloze od hemiceluloze, kao i razgradnju hemiceluloze, vrše hemicelulaze. Hemicelulaze deluju sinergistički sa drugim hemicelulazama, ali i sa celulazama [49]. Prema tipu veze koju hidrolizuju hemicelulaze se dele na: glikozidne hidrolaze (hidrolizuju glikozidne veze) i ugljenohidratne esteraze (hidrolizuju estarske veze); prema načinu na koji razgrađuju hemicelulozu dele se na: enzime koji vrše depolimerizaciju i enzime koji uklanjaju grane i bočne lance (eng. *debranching*). Depolimerizacija osnovnog lanca vrši se endo- i egzohidrolizom [52,53]; endohidroliza počinje negde oko sredine lanca i teče nasumično; egzohidroliza kreće sa krajeva lanaca. Odvajanje grana i bočnih lanaca od osnovnog vrše tzv. „pomoćni“ enzimi: neki mogu da napadnu samo kratke oligomere lanca, dok drugi kidaju grane i bočne lance ne dodirujući osnovni lanac [53]. Za potpunu hidrolizu hemiceluloze neophodno je usklađeno delovanje sve tri grupe enzima [49]. U tabeli 3 navedene su šire zastupljene hemicelulaze, supstrati na koje deluju i proizvodi razgradnje [29,49,54].

Procesni uslovi biološkog predtretmana

Biološki predtretman se može izvoditi fermentacijom na čvrstom supstratu (SSF) ili submerznom fermentacijom (SmF). Za razliku od SmF, kultivacija na čvrstom supstratu podrazumeva rast organizama i formiranje produkata u uslovima relativno male vlažnosti (60–70%, koliko je potrebno organizmima za rast i metaboličke procese) [13]. Druge prednosti SSF nad SmF su: veći prinos i produktivnost; bolje karakteristike dobijenih proizvoda; i niža cena procesa zbog mogućnosti primene agroindustrijskog i poljoprivrednog otpada kao supstrata, smanjenog mešanja, niže cene sterilizacije, primene manjih reaktora (koriste se reaktor sa pakovanim slojem, sa fluidizovanim slojem i horizontalni bubanj) [13].

Da bi gljive, izazivači belog i braon truljenja, mogle da se razviju na lignoceluloznom supstratu poljoprivrednog porekla, neophodna je dekontaminacija supstrata. U laboratorijskim uslovima se dekontaminacija postiže autoklaviranjem pre zasejavanja, što za industriju predstavlja skup postupak; pa, da bi industrijska upotreba biomase iz poljoprivrede ipak bila moguća, predložena je dekontaminacija jeftinim hemikalijama poput natrijum-bisulfita, natrijum-metabisulfita i natrijum-ditionita, kojima se postižu jednako dobri rezultati [55]. Gljive se mogu razviti i rasti i na supstratu koji je podvrgnut samo površinskoj sterilizaciji. Nakon što se formira na površini, gljiva se lako može izboriti sa ostalim organizmima u supstratu [55]. Međutim, tokom razgradnje lignina stvaraju se sve povoljniji uslovi za razviće celulolitičkih organizama (kojih u unutrašnjosti

Tabela 3. Neke fungalne hemicelulaze, njihovi supstrati i produkti razgradnje
Table 3. Some fungal hemicellulase, their decomposition products and substrates

Supstrat	Enzim	Proizvod	Reference
Ksilan	Endo-β-ksilanaza	Oligosaharidi	[49,54]
Ksiloglukan/ksilan/oligosaharidi oslobođeni endo-β-ksilanazom	β-Ksilozidaza	Ksiloza	[49]
Ksilan/druge hemiceluloze	Acetilksilanska esteraza	Acetil grupa	[29,49]
Ksilan	Feruloilna esteraza	Ferulinska kiselina	[29,49]
Bočni lanci arabinoze na ksilanu/ksilan/ksiloglukan	α-Arabinofuranozidaza	α-Arabinoza	[29,49]
Galaktomanan/galaktoglukomanan/ksilan	α-Galaktozidaza	D-Galaktoza	[29,49]
Veza između ksilana i glukuronske kiseline	α-Glukuronidaza	D-Glukuronska kiselina	[29,49]
β-(1→4)-D-manozil polimer/(galakto)(gluko)manani	Mananaze	Manooligosaharidi	[49]
Manooligosaharidi	β-Manozidaze	Manoza	[49]

supstrata uvek ima) i koji mogu dovesti do većeg gubitka celuloze, zbog čega je dubinska dekontaminacija neophodna [56].

Pravilno pripremljena i primenjena adekvatna veličina inokuluma je još jedan veoma bitan faktor. Inokulacija gljiva se može vršiti dodavanjem suspenzije spora u supstrat do postizanja odgovarajuće inicijalne koncentracije, obično reda 10^5–10^7 spora/ml [57–59]. Za inokulaciju se mogu koristiti i konidije, micelijumi gajeni u tečnom medijumu ili na agaru, supstrat od cerealija za rast na kom su razvijeni micelijumi gljiva (eng. *spawn grown*) i prekolonizacija lignoceluloze gljivom [56]. Kultivacija micelijumima gajenim u tečnom medijumu omogućava bržu i lakšu inokulaciju nego u slučaju primene agarnih diskova; obično se koriste agarni diskovi prečnika 8–10 mm [60,61]. U eksperimentu sa prekolonizovanim iverom, kada je primenjivana gljiva *P. chrysosporium*, primećeno je da udeo inokuluma 2–5% daje dobre performanse i omogućava uštedu energije pri mehaničkom usitnjavanju, međutim, sa uvećanjem udela inokuluma do 20%, ušteda energije ne raste [62].

Ligninolitički sistem operiše pod sekundarnim metabolizmom. Dodavanjem inducera poput Mn^{2+}, H_2O_2 i aromatičnih komponenti, može se stimulisati sekrecija ligninolitičkih enzima i razgradnja biomase; dok se dodavanjem nutrijenata stimuliše uvećanje fungalne biomase i ubrzava kolonizacija u dublje slojeve lignoceluloznog supstrata [62]. Međutim, dovoljne količine nutrijenata nisu uslov i za produkciju ligninolitičkih enzima. Istraživanja su pokazala da se ligninolitički sistem *P. chrysosporium* aktivira u uslovima nedovoljne količine azota, što je okidač za otpočinjanje sekundarnog metabolizma kod najvećeg broja gljiva koje izazivaju belo truljenje; u ređim slučajevima okidač može biti nedovoljno ugljenika ili sumpora [39].

Još jedan bitan faktor predstavlja veličina čestica supstrata. Velike čestice mogu da ometaju prodor gljiva i difuziju vazduha, vode i metaboličkih intermedijera u dublje slojeve biomase. Sa smanjenjem veličine čestica povećava se dodirna površina, smanjuje zapremina, čime je olakšano prodiranje u dublje slojeve. Međutim, prevelikom redukcijom veličine smanjuje se međučestični prostor i time onemogućava nesmetana cirkulacija vazduha kroz interčestične kanale. Treba istaći i da svako veće usitnjavanje biomase zahteva više energije, pa je neophodno odrediti najveću optimalnu veličinu čestica kako bi se smanjili troškovi ulaganja energije. Na osnovu dosadašnjih eksperimenata (koje su sproveli Nazarpour i sar. [63], Membrilo i sar. [64], Wan i Li [65] i dr.) može se zaključiti da se najveće uklanjanje lignina postiže na česticama prečnika 5–10 mm; znatno manje lignina se uklanja kada su čestice supstrata prečnika manjeg od 1 mm ili većeg od 15 mm – za dobijanje malih čestica (<1 mm) troši i više energije.

Vlažnost je veoma važan parametar za proces fermentacije na čvrstom supstratu. Inicijalna vlažnost utiče na rast i razvoj gljiva, kao i na sekundarni metabolizam. Nekim optimumom se smatra 70–85% vlage [62]. U slučaju premalo vlage onemogućen je rast i razvoj gljiva, dok previše vlage može negativno uticati na cirkulaciju gasova i moguća je kontaminacija supstrata bakterijama. Dobri rezultati razgradnje lignina su dobijeni pri vlažnosti od 70% [62].

Bazidiomicete koje izazivaju belo truljenje su mezofili, koje visoku razgradnju lignina postižu između 25––30 °C [65]; askomicete dobro rastu na oko 39 °C [62]. Metabolizam ligninolitičkih gljiva generiše toplotu i stvara temperaturni gradijent. Da temperatura ne bi porasla do visine koja inhibira rast i metabolizam, ili ubija gljive, tokom predtretmana je potrebno uklanjati višak toplote iz sistema.

Optimalne pH vrednosti rasta većine gljiva koje izazivaju belo truljenje su između 4 i 5. Mnoge od njih mogu tokom predtretmana acidifikovati supstrat do vrednosti koja inhibira rast gljiva, pa je potrebno pratiti i korigovati uslove kisolosti sredine [56].

Degradacija lignina je gotovo u popunosti oksidativni proces, zbog čega je aeracija još jedan veoma bitan parametar. Povećanjem nivoa kiseonika može se znatno unaprediti proces razgradnje lignina gljivama. Eksperimentalno je utvrđeno da brzina formiranja $^{14}CO_2$ u uslovima povećanog nivoa kiseonika značajno raste (u eksperimentu sa *P. chrysosporium* brzina formiranja $^{14}CO_2$ je bila tri puta veća u uslovima čistog kiseonika (100% O_2) u odnosu na atmosferu sa 21% O_2 [39]). Kada se predtretman izvodi u erlenmajeru u statičkom procesu, pasivna difuzija vazduha je dovoljna, međutim ako se proces izvodi sa pakovanim slojem neophodno je primeniti prinudnu cirkulaciju vazduha [62]. Da bi se obezbedilo izvođenje fungalnog predtretmana aeracija mora biti kontrolisana, jer visoka koncentracija kiseonika ne unapređuje selektivnost delignifikacije, iako unapređuje brzinu [56,62].

Najveći nedostatak biološkog predtretmana predstavlja dugo vreme trajanja procesa, uglavnom nekoliko nedjelja do nekoliko meseci. Uprkos tome što je u pitanju jeftina metoda, ima zanemarljive zahteve za energijom, ekološki je pogodna, zbog dugog vremena još uvek nije primenljiva u industriji. *P. chrysosporium* je brzorastuća gljiva i može za svega nekoliko dana da značajno razgradi lignin, ali je neselektivni razlagač. Nasuprot njoj, *P. ostreatus*, druga široko proučavana gljiva, može za nekoliko nedjelja ostvariti značajnu razgradnju lignina [62]. U zavisnsti od vrste gljive i supstrata zavisi i vreme trajanja procesa; za dostizanje maksimuma razgradnje tvrdog drveta je najčešće potrebno 3–8 nedelja, a slame 3–4 nedelje [56].

METODE HIDROLIZE

Razgradnja polisaharida do fermentabilnih šećera vrši se kiselinama (razblaženom ili koncentrovanom sumpornom ili hlorovodoničnom kiselinom) ili enzimima (fungalnim i bakterijskim celulazama i hemicelulazama). Proces razblaženim kiselinama može biti jednostepeni ili dvostepeni (slika 4). U oba slučaja dolazi do dehidratacije jednog dela oslobođenih šećera, zbog čega nastaju inhibitori fermentacije: hidroksimetilfurfurali (HMF, od heksoza) i furfurali (od pentoza). Hidroliza koncentrovanim kiselinama je efikasnija; razgradnja polisaharida je potpuna i brza i skoro da nema formiranja HMF i furfurala [2]. Međutim, iz bezbednosnih razloga i da bi se snizila cena procesa, na kraju je neophodno kiselinu ukloniti i neutralisati, za šta se koristi kalcijum-hidroksid; problem predstavlja formiranje hidratisanog gipsa ($CaSO_4 \cdot 2H_2O$) jer je zagađivač životne sredine.

Enzimskom hidrolizom se postiže visok prinos redukujućih šećera i visoka selektivnost; niža je cena procesa, procesni uslovi za naredni korak (fermentacije) su umereni; međutim, cena samih enzima je još uvek visoka, što onemogućava da bioetanol iz lignoceluloze bude konkurentan fosilnom gorivu ili bioetanolu dobijenom iz skrobnih sirovina [2]. Enzimska hidroliza (slika 4) može teći paralelno sa fermentacijom (simultana saharifikacija i fermentacija, SimSF) [66] – procesi fermentacije i hidrolize teku u suboptimalnim uslovima, smanjena je inhibicija krajnjim proizvodima hidrolize; ili može biti odvojen proces od fermentacije (en. separate hydrolysis and fermentation, SHF) – moguće je podesiti optimalne uslove za procese fermentacije i hidrolize, ali inhibicija supstratom je izraženija i veći su troškovi proizvodnje nego kod SimSF.

INHIBITORI FERMENTACIJE I DETOKSIKACIJA

Iako tokom biološkog predtretmana ne nastaju inhibitori hidrolize i fermentacije, u eksperimentu sa neprečišćenim enzimima Wang i sar. su pokazali da prisustvo lakaze, posebno aktivne lakaze, utiče represivno na aktivnost celulaza [67], pa je poželjno ukloniti ovaj enzim pre početka hidrolize. Za razliku od biološkog

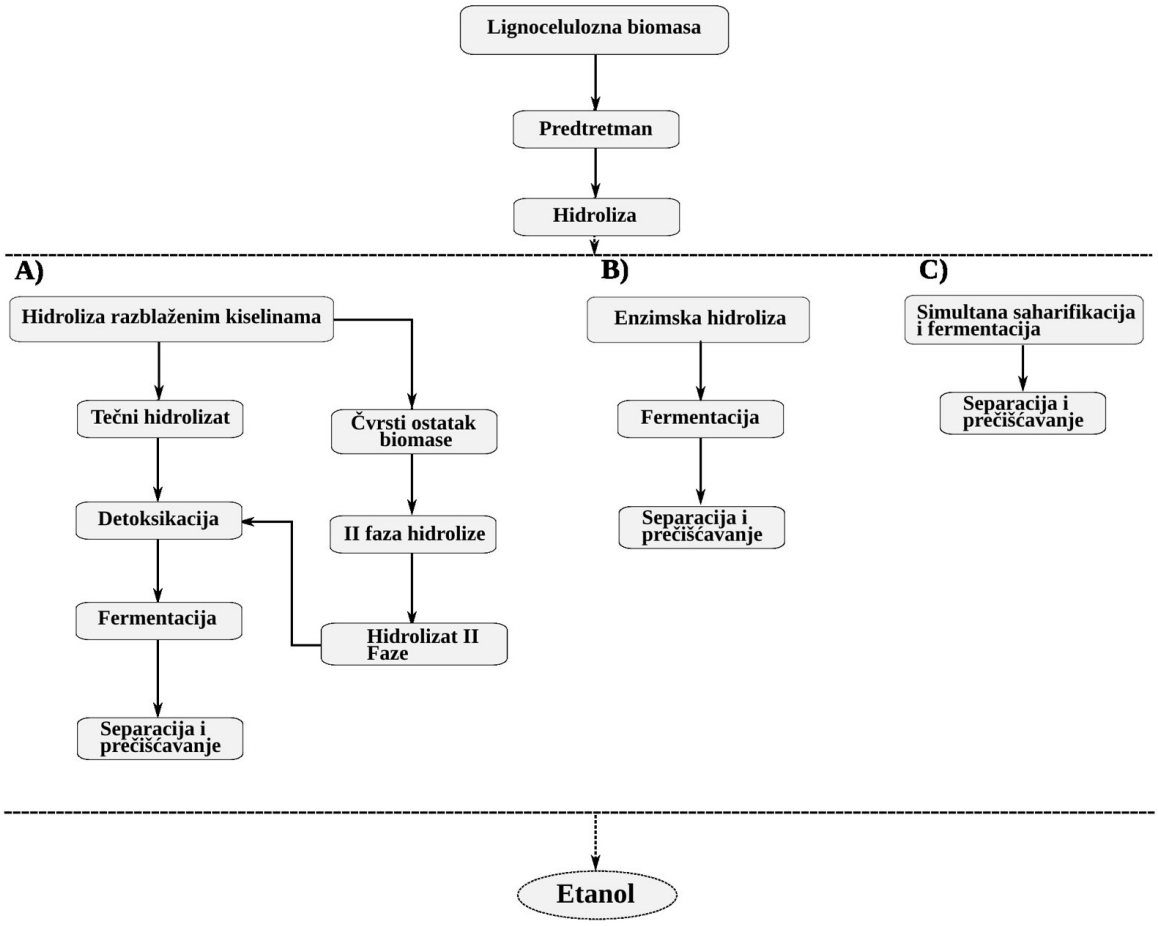

Slika 4. Metode hidrolize: A) dvostepeni postupak razblaženim kiselinama, B) enzimska hidroliza – odvojena hidroliza i fermentacija, C) enzimska hidroliza – simultana saharifikacija i fermentacija.
Figure 4. Hydrolysis methods: A) two-stage dilute-acid hydrolysis process; B) enzymatic hydrolysis – separate hydrolysis and fermentation; C) enzymatic hydrolysis – simultaneous saccharification and fermentation.

predtretmana tokom fizičkih, fizičko–hemijskih i hemijskih metoda, kao i u procesu hidrolize kiselinama, često nastaju inhibitori, koje čine: slabe kiseline, derivati furana i fenolne komponente. Inhibitorni efekat mogu imati i primenjene hemikalije, ekstrakti uključujući terpene, alkohole i aromatične komponente (tanine), metali oslobođeni iz opreme koja se koristi i aditivi kao što su nikl, gvožđe, bakar i hrom.

Inhibitori imaju toksičan efekat na proizvodne mikroorganizme i na taj način smanjuju prinos i produktivnost. Stepen toksičnosti zavisi od fiziološkog stanja ćelije, rastvorenog kiseonika i pH medijuma [12]. Detoksikacija se vrši hemijskim (bazama [68], najčešće $Ca(OH)_2$), fizičkim (evaporacijom u rotacionom evaporatoru, ekstrakcijom, jonskom izmenom, aktivnim ugljem) i biološkim metodama (enzimima lakazama i peroksidazama, gljivama *Trametes versicolor, Trichoderma reesei* ili različitim bakterijama [69]).

Fermentacija hidrolizata

Fermentacija je metabolički proces konverzije šećera do kiselina, gasova i/ili alkohola. U lignoceluloznom hidrolizatu su prisutne dve grupe šećera: heksoze (glukoza, manoza i galaktoza) i pentoze (ksiloza i arabinoza), ali organizmi, koji se pretežno koriste u industriji etanola, uglavnom ne mogu efikasno fermentisati pentoze (videti tabelu 4) [70–72].

Metabolizam glukoze se odvija Embden-Majerhofovim (EM, slika 5) (pr. u kvascu *Saccharomyces cerevisiae*) ili Entner–Doudorofovim (ED) putem (slika 5, u bakterijama poput *Zymomonas sp*.). ED putem se oslobađa upola manje ATP po molu glukoze nego u slučaju EM puta, zbog čega se biomasa proizvodnog mikroorganizma ne uvećava mnogo, pa više šećera može da se konvertuje do željenog proizvoda. U industriji etanola se prioritetno koristi kvasac *S. cerevisiae*

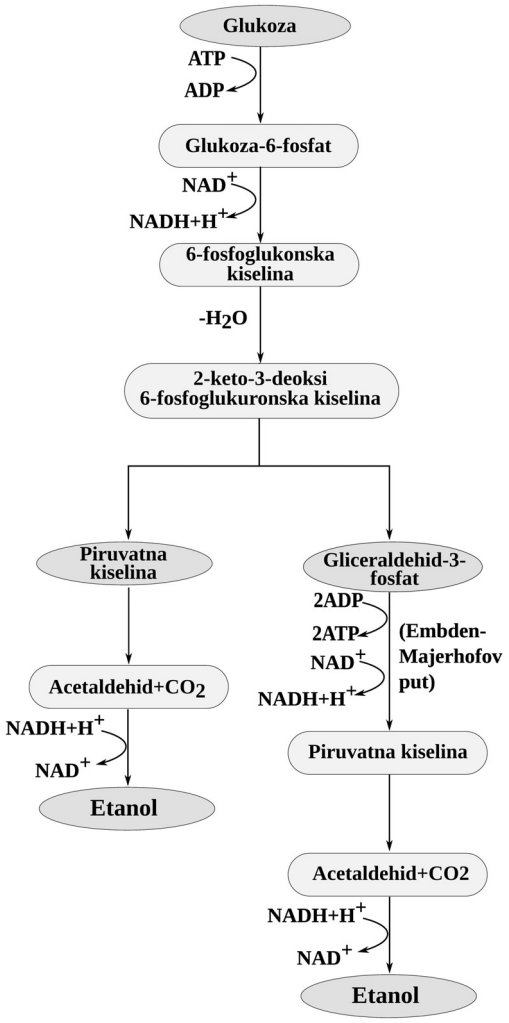

Slika 5. Metabolički putevi fermentacije glukoze: Entner–Doudorofov (ED) i Embden Majerhofov (EM).
Figure 5. The metabolic pathways for glucose fermentation: Entner–Doudoroff (ED) and Embden Meyerhof (EM) pathways.

Tabela 4. Organizmi producenti etanola i supstrat koji mogu fermentisati
Table 4. Organisms producers of ethanol and substrate they can ferment

Organizam	Supstrat
Gljive	
Saccharomyces cerevisiae	Glukoza, fruktoza, galaktoza, maltoza, maltotrioza, ksiluloza
S. carlsbergensis	Glukoza, fruktoza, galaktoza, maltoza, maltotrioza, ksiluloza
Kluyveromyces fragilis	Glukoza, galaktoza, laktoza
Candida tropicalis	Glukoza, ksiloza, ksiluloza
Bakterije	
Zymomonas mobilis	Glukoza, fruktoza, saharoza, inženjerovana da koristi ksilozu
Clostridium thermocellum	Glukoza, celobioza, celuloza
C. acetobutylicum	Konverzija ksiloze do acetona i butanola, u manjim količinama do etanola
Escherichia coli	Ksiloza
Klebsiella oxytoca	Ksiloza, celobioza, glukoza
Lactobacillus plantarum	Brže iskorišćenje celobioze nego glukoze
L. casei	Laktoza
L. xylosus	Celobioza ukoliko su dodati nutrijenti, glukoza, ksiloza i arabinoza

[73,74]: bezbedan (GRAS), tolerantan prema inhibitorima fermentacije, ali ne može fermentisati aldopentoze do etanola.

Kanalisanje pentoznih šećera do centralnog metabolizma u bakterijama se vrši izomeraznim putem; u kvascima i filamentoznim gljivama metaboličkim putem reduktaza/dehidrogenaza [75]. Malo organizama je sposobno prirodno da fermentiše pentoze (neke vrsta rodova *Pichia* i *Candida*, kao i filamentozna gljiva *Fusarium oxysporum* [75]), ali je brzina konverzije ovim organizmima mala. Predloženi put katabolizma ksiloze dat je na slici 6. Metaboličkim inženjerstvom uvedeni su putevi ksiloza izomeraze i arabinoza izomeraze u *S. cerevisiae* i, na taj način, stvoreni sojevi kojima se postižu visoki prinosi. Metode genetičkog i metaboličkog inženjerstva primenjene su i na drugim proizvodnim mikroorganizmima; osim unapređenju fermentacije, teži se i povećanju otpornosti organizama prema inhibitorima fermentacije [76].

Neke bakterije poput *Clostridium thermocellum* i filamentozne gljive *Monilia sp.*, *Neurospora sp.*, *Zygosaccharomyces rouxii*, *Aspergillus sp.*, *Trichoderma viride* [72], mogu direktno transformisati celulozu do etanola, ali je mali prinos etanola, dugo vreme konverzije i nastaju sporedni produkti poput sirćetne i mlečne kiseline.

U novije vreme razmatra se primena samo jednog organizma sposobnog za četiri biološke konverzije: produkciju glikolitičkih enzima (celulaze i hemicelulaze), hidrolizu predtretirane biomase, fermentaciju heksoza i fermentaciju pentoza. Ova metoda je poznata pod nazivom konsolidovani bioproces (CBP) – ili direktna mikrobna konverzija (DMC). Kako još uvek nije pronađen niti stvoren idealan organizam, često se primenjuje bakterija *Clostridium thermocellum,* koja je sposobna da hidrolizuje celulozu i fermentiše glukozu, zajedno sa *C. thermosaccharolyticum* koja može fermentisati pentoze [77,78]. Novije studije su fokusirane na kombinovanju proizvodnje celulaza i sojeva mikroorganizama koji daju visoke prinose etanola poput *Escherichia coli*, *Klebsiella oxytoca* i *Zymomonas mobilis*.

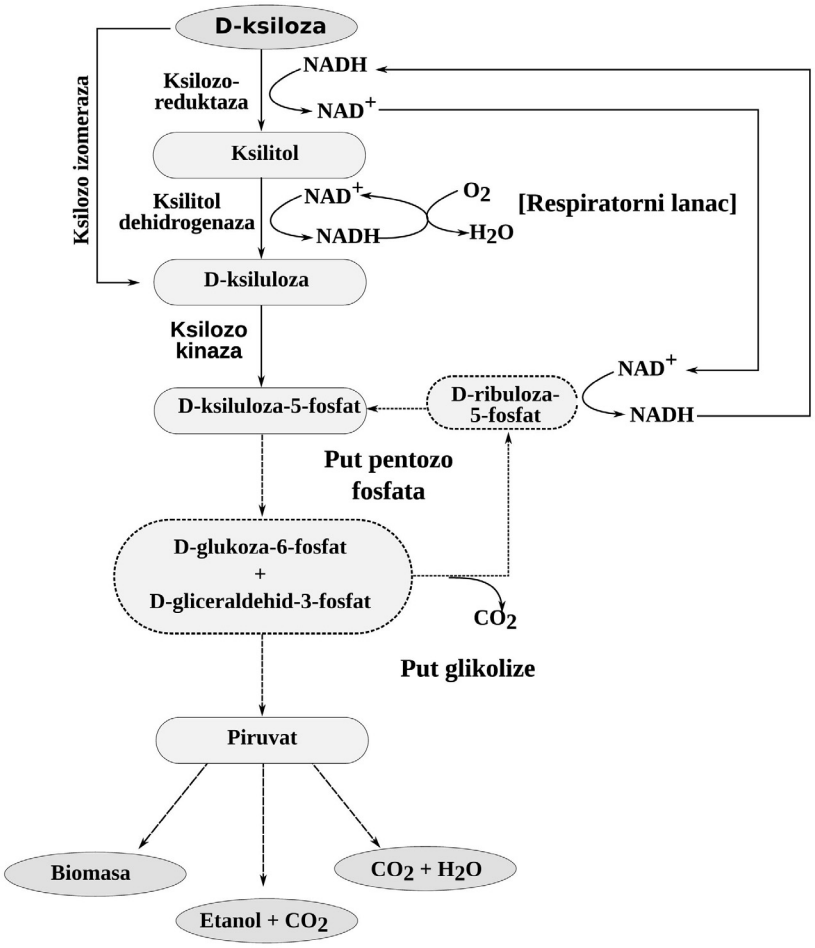

Slika 6. Metabolički putevi fermentacije ksiloze.
Figure 6. The metabolic pathways for xylose fermentation.

ZAKLJUČAK

Potreba za zamenom fosilnog alternativnim gorivima je usmerila mnoga istraživanja ka razvoju tehnologije proizvodnje etanola na jeftinim sirovinama, poput lignocelulozno otpada. Zbog kompleksnosti strukture i velike otpornosti lignocelulozne biomase prema dejstvu enzima i mikroorganizama, razvijene su različite metode predtretmana (fizičke, hemijske, fizičko–hemijske, biološke), koje većinom zahtevaju skupe i toksične hemikalije, ulaganje energije ili specijalno konstruisanu opremu. Biološkim predtretmanom bi se mogla obezbediti jeftina, ekološki bezbedna tehnologija, koja ne zahteva dodatno ulaganje energije ni toksičnih hemikalija. Postojeći probelem – dugo vreme inkubacije – sa kojima se susreće biloški predtretman, bi se mogao rešiti primenom brzorastućih gljiva koje mogu proizvesti veće količine ligninolitičkih enzima, ili kombinovanjem biološke i neke druge metode predtretmana; dok primena selektivnih razgrađivača lignina omogućava da se celuloza sačuva. Još jedna pozitivna strana primene biološkog predtretmana su sporedni proizvodi: od fungalne biomase se mogu dobiti hitin i hitozan, koji se koriste za proizvodnju superapsorbenata; upotreba jestive gljive, poput bukovače (*P. ostreatus*), se može koristiti u ishrani; a prečišćavanjem enzimskih ekstrakata, nastalim tokom predtretmana, dobijaju se industrijski enzimi koji se mogu koristiti u procesima bioizbeljivanja, bioremedijacije...

Trenutna istraživanja fungalnih ligninolitičkih mehanizama su usmerena na mogućnost primene gljiva i njihovih enzima u biološkom predtretmanu, biopulpiranju i bioremedijaciji (zbog sposobnosti da razgrađuju aromatična jedinjenja po strukturi slična komponentama lignina).

LITERATURA

[1] K. Srirangan L. Akawi, M. Moo-Young C.P. Chou, Towards sustainable production of clean energy carriers from biomass resources, Appl. Energy **100** (2012) 172––186.

[2] V. Semenčenko, L. Mojović, S. Petrović, O. Ocić, Novi trendovi u proizvodnji bioetanola, Hem. Ind. **65** (2011) 103–114.

[3] Lj. Mojović i grupa autora, Bioetanol kao gorivo: stanje i perspektive, Monografija, Tehnološki fakultet, Leskovac, 2007.

[4] I.S. Thakur Thakur, Industrial Biotechnology: Problems and Remedies, I.K. International Pvt Ltd., 2006.

[5] T. Canam, J. Town, K. Iroba, L. Tabil, T. Dumonceaux, in: A. Chandel, S. S. da Silva (Eds.), Sustainable Degradation of Lignocellulosic Biomass – Techniques, Applications and Commercialization, InTech, 2013. pp.181–206.

[6] P. Siripong, B. Oraphin, T. Sanro, P. Duanporn, Screening of Fungi from Natural Sources in Thailand for Degradation of Polychlorinated Hydrocarbons, Am.-Eurasian J. Agric. Environ. Sci. **5** (2009) 466–472.

[7] BNDES, CGEE (Orgs.), Sugarcane-based bioethanol: energy for sustainable development. 1st ed., BNDES, Rio de Janeiro, 2008.

[8] Bioethanol - a very special compound, http:// //www.cropenergies.com/en/Bioethanol/

[9] N. Sarkar, S.K. Ghosh, S. Bannerjee, K. Aikat, Bioethanol production from agricultural wastes: An overview, Renew. Energ. **37** (2012) 19–27.

[10] Lj. Mojović, D. Pejin, M. Rakin, J. Pejin, S. Nikolić, Al. Djukić-Vuković, How to improve the economy of bioethanol production in Serbia, Renewable Sustainable Energy Rev. **16** (2012) 6040–6047.

[11] L. Mojović, S. Nikolić, D. Pejin, J. Pejin, A. Djukić-Vuković, S. Kocić-Tanackov, V. Semenčenko, in: A. Méndez-Vilas, (Eds.), Materials and processes for energy: communicating current research and technological developments, Formatex Research Center, 2013, pp. 380–392.

[12] P.F.H. Harmsen, W.J.J. Huijgen, L.M. Bermudez Lopez, R.R.C. Bakker, Literature review of physical and chemical pretreatment process for lignocellulosic biomass. Wageningen UR, Food Biobased Res. (ECN-E-10-013), 2010.

[13] S.I. Mussatto, L.F. Ballesteros, S. Martins, J.A. Teixeira, in: K.-Y. Show, X. Guo (Eds.), Industrial Waste, 2012, pp. 121–140.

[14] D.K. Lee, V.N. Owens, A. Boe, P. Jeranyama, Composition of Herbaceous Biomass Feedstocks, South Dakota State University, 2007.

[15] T.T. Teeri, Crystalline cellulose degradation: new insight into the function of cellobiohydrolases, Trends Biotechnol. 1**5** (1997) 160–167.

[16] S.E. Jacobsen, C.E. Wyman, Cellulose and Hemicellulose Hydrolysis Models for Application to Current and Novel Pretreatment Processes, Appl. Biochem. Biotechnol. **84**––**86** (2000) 81–96.

[17] Z. Fang, Pretreatment techniques for biofuels and biorefineries, Springer-Verlag, Berlin, 2013.

[18] Pure lignin environmental technology, http:// //purelignin.com/lignin.

[19] J.P. Marković, J.B. Radović, R.T. Štrbanović, D.S. Bajić, M.M. Vrvić, Changes in the infrared attenuated total reflectance (ATR) spectra of lignins from alfalfa stem with growth and development, J. Serb. Chem. Soc. **74** (2009) 885–892.

[20] R. Vanholme, B. Demedts, K. Morreel, J. Ralph, W. Boerjan, Lignin Biosynthesis and Structure, Plant Physiol. **153** (2010) 895–905.

[21] V.K. Gupta, M.G. Tuohy, Biofuel technologies: recent developments, Springer, Berlin, 2013.

[22] J. Ralph, C. Lapierre, J.M. Marita, H. Kim, F. Lu, R.D. Hatfield, S. Ralph, C. Chapple, R. Franke, M.R. Hemm, J. Van Doorsselaere, R.R. Sederoff, D.M. O'Malley, J.T. Scott, J.J. MacKay, N. Yahiaoui, A.M. Boudet, M. Pean, G. Pilate, L. Jouanin, W. Boerjan, Elucidation of new structures in lignins of CAD- and COMT-deficient plants by NMR, Phytochemistry **57** (2001) 993–1003.

[23] S.P.S. Chundawat, G.T. Beckham, M. Himmel, B.E. Dale, Deconstruction of Lignocellulosic Biomass to Fuels and

Chemicals, Annu. Rev. Chem. Biomol. Eng. **2** (2011) 121––145.

[24] V.S. Chang, M.T. Holtzapple, Fundamental factors affecting biomass enzymatic reactivity, Appl. Biochem. Biotechnol. **84–86** (2000) 5–37.

[25] H. Itoh, M. Wada, Y. Honda, M. Kuwahara, T. Watanabe, Bioorganosolve pretreatments for simultaneous saccharification and fermentation of beech wood by ethanolysis and white rot fungi, J. Biotechnol. **103** (2003) 273–280.

[26] V. Balan, L. da Costa Sousa, S.P. Chundawat, R. Vismeh, A.D. Jones, B.E. Dale, Mushroom spent straw: a potential substrate for an ethanol-based biorefinery, J. Ind. Microbiol. Biotechnol. **35** (2008) 293–301.

[27] J. Yu, J. Zhang, J. He, Z. Liu, Z. Yu, Combinations of mild physical or chemical pretreatment with biological pretreatment for enzymatic hydrolysis of rice hull, Bioresour. Technol. **100** (2009) 903–908.

[28] A. Hatakka, in: A. Steinbüchel (Ed.), Biopolymers Online, Wiley-VCH Verlag GmbH & Co. KgaA, 2005, pp. 129–145.

[29] W.R. de Souza, in: A. Chandel, S.S. da Silva (Eds.), Sustainable Degradation of Lignocellulosic Biomass – Techniques, Applications and Commercialization, InTech, Rijeka, 2013, pp. 207–247.

[30] I. Isroi, R. Millati, S. Syamsiah, C. Niklasson, M.N. Cahyanto, K. Lundquist, M.J. Taherzadeh, Biological pretreatment of lignocelluloses with white-rot fungi and its applications: a review, BioResources **6** (2011) 5224––5259.

[31] A.B. Gore, Environmental research at the leading edge, Nova Science Publishers, New York, 2006.

[32] M. Monrroy, I. Ortega, M. Ramírez, J. Baeza, J. Freer, Structural change in wood by brown rot fungi and effect on enzymatic hydrolysis, Enzyme Microb. Technol. **49** (2011) 472–477.

[33] L. Jin, T.P. Schultz, D.D. Nicholas, Structural Characterization of Brown-Rotted Lignin, Holzforschung **44** (1990) 133–138.

[34] R.A. Blanchette, B.W. Held, J.A. Jurgens, D.L. McNew, T.C. Harrington, S.M. Duncan, R.L. Farrell, Wood-Destroying Soft Rot Fungi in the Historic Expedition Huts of Antarctica, Appl. Environ. Microbiol. **70** (2004) 1328––1335.

[35] E.A. Bayer, L.J. Shimon, Y. Shoham, R. Lamed, Cellulosomes-structure and ultrastructure, J. Struct. Biol. **124** (1998) 221–234.

[36] A.C. Ritschkoff, Decay mechanisms of brown-rot fungi. Espoo 1996, Technical Research Centre of Finland, VTT Publications 268, 1996.

[37] H.D. Youn, Y.C. Hah, S.O. Kang, Role of laccase in lignin degradation by white-rot fungi, FEMS Microbiol. Lett. **132** (1995) 183–188.

[38] T. Lundell T.R. Wever, R. Floris, P. Harvey, A. Hatakka, G. Brunow, H. Schoemaker, Lignin peroxidase L3 from *Phlebia radiata*. Pre-steady-state and steady-state studies with veratryl alcohol and a non-phenolic lignin model compound 1-(3,4-dimethoxyphenyl)-2-(2-methoxyphenoxy)propane-1,3-diol, Eur. J. Biochem. **211** (1993) 391–402.

[39] K-E.L. Eriksson, H. Bermek, in: M. Schaechter (Ed.), Encyclopedia of microbiology, 3rd ed., Elsevier, cop. 2009.

[40] W. Blodig, A.T. Smith, K. Winterhalter, K. Piontek, Evidence from spin-trapping for a transient radical on tryptophan residue 171 of lignin peroxidase, Arch. Biochem. Biophys. **370** (1999) 86–92.

[41] M. Hofrichter, Review: lignin conversion by manganese peroxidase (MnP), Enzyme Microb. Technol. **30** (2002) 454–466.

[42] M.G. Paice, I.D. Reid, R. Bourbonnais, F.S. Archibald, L. Jurasek, Manganese Peroxidase, Produced by Trametes versicolor during Pulp Bleaching, Demethylates and Delignifies Kraft Pulp, Appl. Environ. Microbiol. **59** (1993) 260–265.

[43] D.W.S. Wong, Structure and Action Mechanism of Ligninolytic Enzymes, Appl. Biochem. Biotechnol. **157** (2009) 174–209.

[44] R.S. Koduri, M. Tien, Oxidation of guaiacol by lignin peroxidase. Role of veratryl alcohol,J. Biol. Chem. **270** (1995) 22254–22258.

[45] S.D. Mansfield, E. De. Jong, J.N. Saddler, Cellobiose dehydrogenase, an active agent in cellulose depolymerization, Appl. Environ. Microbiol. **63** (1997) 3804–3809.

[46] G. Henriksson, L. Zhang, J. Li, P. Ljungquist, T. Reitberger, G. Pettersson, G. Johansson, Is cellobiose dehydrogenase from Phanerochaete chrysosporium a lignin degrading enzyme?, Biochim. Biophys. Acta, Protein Struct. Mol. Enzymol. **1480** (2000) 83–91.

[47] G. Henriksson, G. Johansson, G. Pettersson, A critical review of cellobiose dehydrogenases, J. Biotechnol. **78** (2000) 93–113.

[48] B.P. Roy, T. Dumonceaux, A.A. Koukoulas, F.S. Archibald, Purification and Characterization of Cellobiose Dehydrogenases from the White Rot Fungus *Trametes versicolor,* Appl. Environ. Microbiol. **62** (1996) 4417–4427.

[49] M.D. Sweeney, F. Xu, Biomass Converting Enzymes as Industrial Biocatalysts for Fuels and Chemicals: Recent Developments, Catalysts **2** (2012) 244–263.

[50] L.T.A.S. Semêdo, R.C. Gomes, E.P.S. Bon, R.M.A. Soares, L.F. Linhares, R.R.R. Coelho, Endocellulase and Exocellulase Activities of Two Streptomyces Strains Isolated from a Forest Soil, Twenty-First Symposium on Biotechnology for Fuels and Chemicals, Appl. Biochem. Biotechnol. **84–86** (2000) 267–276.

[51] J. Kaur, B. Chadha, B. Kumar, G. Kaur, H. Saini, Purification and characterization of β-glucosidase from Melanocarpus sp. MTCC 3922, Electron. J. Biotechnol. **10** (2007) 260–270.

[52] R. Varnaitė, V. Raudonienė, Destruction of hemicellulose in rye straw by micromycetes, Ekologija **54** (2008) 169–172.

[53] J.M. Vivanco, F. Bal, Secretions and Exudates in Biological Systems, Springer, Berlin, 2012.

[54] A. Krisana, S. Rutchadaporn, G. Jarupan, E. Lily, T. Sutipa, K. Kanyawim, Endo-1,4-β-xylanase B from *Aspergillus* cf. niger BCC14405 Isolated in Thailand: Purification, Characterization and Gene Isolation, J. Biochem. Mol. Biol. **38** (2005) 17–23.

[55] G.M. Scott, M. Akhtar, M.J. Lentz, in: R.A. Young, M. Akhtar (Eds.), Environmentally friendly technologies for the pulp and paper industry, Wiley, New York, 1997.

[56] J. Lee, Biological conversion of lignocellulosic biomass to ethanol, J. Biotechnol. **56** (1997) 1–24.

[57] J.S. Bak, J.K. Ko, I.G. Choi, Y.C. Park, J.H. Seo, K.H. Kim, Fungal pretreatment of lignocellulose by *Phanerochaete chrysosporium* to produce ethanol from rice straw, Biotechnol. Bioeng. **104** (2009) 471–482.

[58] K. Selvam, K.P. Saritha, K. Swaminathan, M. Manikandan, K. Rasappan, P. Chinnasamy, Pretreatment of wood chips and pulps with *Fomes lividus* and *Trametes versicolor* to reduce chemical consumption in paper industries, Asian J. Microbiol. Biotechnol. Environ. Sci. **8** (2006) 771–776.

[59] U.G. Phutela, K. Kaur, M. Gangwar, N.K. Khullar, Effect of Pleurotus florida on paddy straw digestibility and biogas production, International Journal of Life Sciences **6** (2012) 14–19.

[60] X. Feng, M. del Pilar Castillo, A. Schnürer, Fungal pretreatment of straw for enhanced biogas yield, SGC Rapport, 2013.

[61] Y.A.-G. Mahmoud, Biodegradation of water hyacinth by growing *Pleurotus ostreatus* and *P. sajor-caju* and trial for using in production of mushroom spawn, Acta Aliment. **5** (2006) 63–72.

[62] C. Wan, Y. Li, Fungal pretreatment of lignocellulosic biomass, Biotechnol. Adv. **30** (2012) 1447–1457.

[63] F. Nazarpour, D.K. Abdullah, N. Abdullah, N. Motedayen, R. Zamiri, Biological Pretreatment of Rubberwood with Ceriporiopsis subvermispora for Enzymatic Hydrolysis and Bioethanol Production, BioMed Res. Int. (2013) 268349.

[64] I. Membrillo, C. Sánchez, M. Meneses, E. Favela, O. Loera, Effect of substrate particle size and additional nitrogen source on production of lignocellulolytic enzymes by Pleurotus ostreatus strains, Bioresour. Technol. **99** (2008) 7842–7847.

[65] C. Wan, Y. Li, Microbial pretreatment of corn stover with Ceriporiopsis subvermispora for enzymatic hydrolysis and ethanol production, Bioresour. Technol. **101** (2010) 6398–403.

[66] D.J. Pejin, Lj.V. Mojović, J.D. Pejin, O.S. Grujić, S.L. Markov, S.B. Nikolić, M.N. Marković, Increase in bioethanol production yield from triticale by simultaneous saccharification and fermentation with application of ultrasound, J. Chem. Technol. Biotechol. **87** (2012) 170––176.

[67] F.Q. Wang, H. Xie, W. Chen, E.T. Wang, F.G. Du, A.D. Song, Biological pretreatment of corn stover with ligninolytic enzyme for high efficient enzymatic hydrolysis, Bioresour. Technol. **144** (2013) 572–578.

[68] B. Alriksson, A. Sjöde, N.O. Nilvebrant, L.J. Jönsson, Optimal conditions for alkaline detoxification of dilute-acid lignocellulose hydrolysates, Appl. Biochem. Biotechnol. **13** (2006) 599–611.

[69] E. Palmqvist, B. Hahn-Hägerdal, Fermentation of lingocellulosic hydrolysates. I: inhibition and detoxification, Bioresour. Technol. **74** (2000) 17–24.

[70] S.O. Serna-Saldívar, C. Chuck-Hernández, E. Pérez-Carrillo, E. Heredia-Olea, in: M.A.P. Lima, A.P.P. Natalense, Bioethanol, InTech, 2012, pp. 51–74.

[71] V. Senthilkumar, P. Gunasekaran, Bioethanol production from cellulosic substrates: Engineered bacteria and process integration challenges, J. Sci. Ind. Res. **64** (2005) 845–853.

[72] Y. Lin, S. Tanaka, Ethanol fermentation from biomass resources: current state and prospects, Appl. Microbiol. Biotechnol. **69** (2006) 627–642.

[73] S. Nikolić, Lj. Mojović, D. Pejin, M. Rakin, M. Vukašinović, Production of bioethanol from corn meal hydrolyzates by free and immobilized cells of *Saccharomyces cerevisiae* var. *Ellipsoideus*, Biomass Bioenergy **34** (2010) 1449–1456.

[74] S.B. Nikolić, Lj.V. Mojović, M.B. Rakin, D.J. Pejin, V.A. Nedović, Effect of different fermentation parameters on bioethanol production from corn meal hydrolyzates by free and immobilized cells of Saccharomyces cerevisiae var. ellipsoideus , J. Chem. Technol. Biotechnol. **84** (2009) 497–503.

[75] L. Viikari, J. Vehmaanperä, A. Koivula, Lignocellulosic ethanol: From science to industry, Biomass Bioenergy **46** (2012) 13–24.

[76] K. Fujitomi, T. Sanda, T. Hasunuma, A. Kondo, Deletion of the PHO13 gene in Saccharomyces cerevisiae improves ethanol production from lignocellulosic hydrolysate in the presence of acetic and formic acids, and furfural, Bioresour. Technol. **111** (2012) 161–166.

[77] C.E. Wyman, Ethanol from lignocellulosic biomass: technology, economics, and opportunities, Bioresour. Technol. **50** (1994) 3–16.

[78] D.G. Olson, J.E. McBride, A.J. Shaw, L.R. Lynd, Recent progress in consolidated bioprocessing, Curr. Opin. Biotechnol. **23** (2011) 1–10.

SUMMARY

APPLICATION OF LIGNOCELLULOLYTIC FUNGI FOR BIOETHANOL PRODUCTION FROM RENEWABLE BIOMASS

Jelena M. Jović[1], Jelena Pejin[2], Sunčica Kocić-Tanackov[2], Ljiljana Mojović[1]

[1]*Faculty of Technology and Metallurgy, University of Belgrade, Belgrade, Serbia*
[2]*Faculty of Technology, University of Novi Sad, Novi Sad, Serbia*

(Review paper)

Pretreatment is a necessary step in the process of conversion of lignocellulosic biomass to ethanol; by changing the structure of lignocellulose, enhances enzymatic hydrolysis, but often it consumes large amounts of energy and/or needs an application of expensive and toxic chemicals, which makes the process economically and ecologically unfavourable. Application of lignocellulolytic fungi (from the class Ascomycetes, Basidiomycetes and Deuteromycetes) is an attractive method for pre-treatment, environmentally friendly and does not require the investment of energy. Fungi produce a wide range of enzymes and chemicals, which, combined in a variety of ways, together successfully degrade lignocellulose, as well as aromatic polymers that share features with lignin. On the basis of material utilization and features of a rotten wood, they are divided in three types of wood-decay fungi: white rot, brown rot and soft rot fungi. White rot fungi are the most efficient lignin degraders in nature and, therefore, have a very important role in carbon recycling from lignified wood. This paper describes fungal mechanisms of lignocellulose degradation. They involve oxidative and hydrolytic mechanisms. Lignin peroxidase, manganese peroxidase, laccase, cellobiose dehydrogenase and enzymes able to catalyze formation of hydroxyl radicals ($^{\bullet}$OH) such as glyoxal oxidase, pyranose-2-oxidase and aryl-alcohol oxidase are responsible for oxidative processes, while cellulases and hemicellulases are involved in hydrolytic processes. Throughout the production stages, from pre-treatment to fermentation, the possibility of their application in the technology of bioethanol production is presented. Based on previous research, the advantages and disadvantages of biological pre-treatment are pointed out.

Keywords: Biological pretreatment • Fungal enzymes • Bioethanol • Solid state fermentation • Lignocellulosic biomass

Chemometric approach to evaluate heavy metals' content in *Daucus carota* from different localities in Serbia

Violeta D. Mitic[1], Vesna P. Stankov-Jovanovic[1], Snezana B. Tosic[1], Aleksandra N. Pavlovic[1], Jelena S. Cvetkovic[1], Marija V. Dimitrijevic[1], Snezana D. Nikolic-Mandic[2]

[1]*University of Niš, Faculty of Science and Mathematics, Department of Chemistry, Višegradska 33, Niš, Serbia*
[2]*University of Belgrade, Faculty of Chemistry, Studentski trg 12–16, Belgrade, Serbia*

Abstract

The aim of this study was to evaluate heavy metal content in carrots (*Daucus carota*) from the different localities in Serbia and to assess by the cluster analysis (CA) and principal components analysis (PCA) the heavy metal contamination of carrots from these areas. Carrots were collected at 13 locations in five districts. Chemometric methods (CA and PCA) were applied to classify localities according to heavy metal content in carrots. CA separated localities into two statistical significant clusters. PCA permitted the reduction of 12 variables to four principal components explaining 79.94% of the total variance. The first most important principal component was strongly associated with the value of Cu, Sb, Pb and Tl. This study revealed that CA and PCA appear as useful tools for differentiation of localities in different districts using the profile of heavy metal in carrot samples.

Keywords: *carrot, heavy metal, ICP-OES, cluster analysis, principal component analysis*.

Available online at the Journal website: http://www.ache.org.rs/HI/

SCIENTIFIC PAPER

UDC 633.43(497.11):54:519.237.8

Hem. Ind. **69** (6) 643–650 (2015)

doi: 10.2298/HEMIND140705070M

Carrots (*Daucus carota*) are one of the most popular vegetables in Serbia and their consumption has been increasing in recent decades. Carrots belong to the *Apiaceae* family, which also includes celery, coriander and parsley. Carrots vary widely in color and shape, depending on the cultivar types. Their color originates from anthocyanin and carotenoid pigments, which contribute to health benefits [1]. Among 38 other fruits and vegetables, carrots have been ranked 10th in terms of their nutritional value and 7th for their contribution to human health [2]. Carrot is a rich source of carotene (pro-vitamin A), vitamin B1, vitamin B2, vitamin B3, vitamin B6, vitamin C, vitamin E, vitamin K and minerals (potassium, cobalt, iron, magnesium, copper, iodine and phosphorus).

Plants demonstrate ability to absorb minerals from soil and accumulate them in roots and aerial organs. Plants growing in metal contaminated environment would accumulate toxic metal ions and efficiently compartmentalize these into various plant parts [3].

Accumulation of heavy metals is very important, due to their effect on human health. Heavy metals, such as lead, zinc, cadmium, mercury and chromium, refer to metals and metalloids having densities greater than 5 g cm^{-3} [4]. Metalloids, such as arsenic, often fall into the heavy metal category due to similarities in chemical and environmental properties [5]. They are naturally present in environment and aren't biodegradable, so in higher amount can be very dangerous. Food contaminated with heavy metals is major contributor to human exposure [6]. Heavy metals imitate the action of essential elements in the body, interfering with the metabolic process to cause illness. Poisoning caused by lead, cadmium and arsenic are the most investigated, due to their usage and toxicity. Cadmium compounds are used in re-chargeable nickel–cadmium batteries, while lead poisoning in recent years is associated with lead emissions from petrol. Epidemiological studies showed that metals could cause acute toxic, mutagenic, teratogenic and carcinogenic damage to red blood cells, liver and kidneys [7].

Concentrations of the metals in different vegetables depend on soil composition, water, nutrient balance, as well as metal permissibility, selectivity and absorption ability of the species [8]. Heavy metals soil pollution is widespread during last few decades. Heavy metals are naturally present in soil, but anthropogenic activities contribute to their concentration in soil. Contribution of anthropogenic pollution is associated with social and economic development. Serbia is a modest producer of mineral commodities, although the soil is rich in minerals. The Bor district is rich in copper and gold deposits, especially in Bor and Kosovska Mitrovica district is rich in lead and zinc (Figure 1).

Elements content in plants provides a lot of information about the pollution of the environment. In order to determine the contamination of certain areas of Southern and South–Eastern Serbia the analysis of heavy metals content in carrot was performed. Carrot was collected at 13 locations in five districts: Pirot,

Correspondence: V. Mitic, University of Niš, Faculty of Science and Mathematics, Department of Chemistry, Višegradska 33, Niš, Serbia.
E-mail: violetamitic@yahoo.com
Paper received: 5 July, 2014
Paper accepted: 24 September, 2014

Toplica, Bor, Kosovska Mitrovica and Rasina district. Twelve elements were analyzed by inductively coupled plasma optical emission spectrometry (ICP-OES): As, Cd, Cr, Cu, Fe, Mn, Mo, Ni, Pb, Sn, Sb and Tl. These elements are listed as heavy metals and some of them are harmful to human health. Cluster analysis (CA) and principal component analysis (PCA) were performed to group localities based on metal content in carrot.

Figure 1. *Map of districts of Serbia.*

EXPERIMENTAL

Carrot samples

Carrot samples were collected in 13 locations in five districts (Figure 1) in Serbia: Pirot and Dolac (Pirot district), Mala Plana, Bučince and Kupinovo (Toplica district), Bor, Krivelj, Slatina I and Slatina II (Bor district), Velika Vrbnica and Bivolje (Rasina district), Zubin Potok and Lipljan (Kosovska Mitrovica district), Table 1.

Carrot samples were collected in September 2010, at full maturity, and kept frozen until analysis.

Chemicals and instruments

Nitric acid (65%), hydrochloric acid and hydrogen peroxide (30%), analytical grade, were purchased from Merck® (Darmstadt, Germany). Multi-element standard solutions (20.00±0.10 mg L^{-1}) used for ICP analysis were purchased from Ultra Scientific (North Kingstown, RI, USA).

The measurements were carried with an ICP OES iCAP 6000, Thermo Scientific. Table 2 shows the analytical parameters for ICP-OES. These conditions were used for all measurements.

Table 2. ICP-OES instrumental parameters

Flush pump rate	100 rpm
Analysis pump rate	50 rpm
Nebulizer gas	0.7 L min^{-1}
Coolant gas flow	12 L min^{-1}
Auxiliary gas flow	0.5 L min^{-1}
Plasma view	Axial
Flush time	30 s

Sample preparation

Plant material was washed, peeled, finely ground and dried before analysis. Samples were dried in an oven at 105 °C to constant weight and then stored in desiccators. 1 g of sample was measured, mixed with concentrated HNO_3 and left in the dark for 12 h. After that, H_2O_2 (30%) and water were added. Digestion procedure was applied to obtained mixtures in order to reduce the volume and improve decomposition. Another portion of H_2O_2 was added and evaporation continued. After cooling concentrated HCl was added, and mixture was left overnight. The resulting suspension was filtered and the rest is rinsed with hot HCl and then heated deionized water. Filtrate was collected in volumetric flask and diluted [9].

Statistical analysis

Multivariate analysis included principal component analysis (PCA) and cluster analyses (CA) were performed using a statistical package running on a computer (Statistica 8.0, StatSoft, Tulsa, OK, USA). A probability level of $p < 0.05$ was considered statistically significant [10]. Correlation between metal content was established using regression analysis at a 95% significance level ($p \leq 0.05$).

RESULTS

Heavy metals' content

The heavy metal contents determined in this study are presented in Table 3. Heavy metal content varied

Table 1. Geographic coordinates of sampling sites

District	Pirot		Toplica			Bor			Rasina		Kosovska Mitrovica	
Locality	Pirot	Dolac	Mala Plana	Bučince	Kupinovo	Bor	Krivelj	Slatina	Velika Vrbnica	Bivolje	Zubin Potok	Lipljan
Latitude	43° 09′ 07"	43° 19′ 05"	43° 15′ 06″	43° 9′ 49″	42° 59′ 11″	44° 04′ 25"	44° 07′ 28"	44° 02′ 14"	43° 29′ 15"	43° 35′ 16"	42° 54′ 52"	42° 31′ 18"
Longitude	22° 35′ 06"	22° 11′ 31"	21° 28′ 23"	21° 35′ 9″	21°20′ 49″	22° 05′ 26"	22° 05′ 28"	22° 09′ 25"	20° 58′ 02"	21° 20′ 47"	20° 41′ 23"	21° 07′ 33"

significantly between localities. Concentrations of heavy metals varied between 343.99 μg g^{-1} for Fe in carrots from Slatina 2 to 0.005 μg g^{-1} for Cd in carrots from Mala Plana.

Statistical analysis

In cluster analysis (CA), the dataset was treated by the Ward's method of linkage with Euclidean distance as measure of similarity. The dendrogram in Figure 2 shows the results of applying cluster analysis, in order to group metals.

CA was applied to a dataset of 12 variables (As, Cd, Cr, Cu, Fe, Mn, Mo, Ni, Pb, Sn, Sb and Tl) and 13 localities. Localities are divided into two main groups, each with sub-groups (Figure 3).

PCA was applied in order to reduce the number of original variables. The PC1 explains about 39.92% of initial variance, Figures 4 and 5.

DISCUSSION

Toxic heavy metals entering the ecosystem may lead to bioaccumulation, particularly by eating fruits and vegetables [11]. Some of metals analyzed (Cu, Cr, Fe and Mn) are necessary for human body, but in higher amounts they can be very harmful. Most abundant element is iron, and its content varied between 8.091 μg g^{-1} in Pirot (Pirot district) to 343.989 μg g^{-1} at Slatina 2 (Bor district). The highest average content of this element was observed in the Bor district (186.181 μg g^{-1}), while the lowest was in Rasina district (50.802 μg/g). Iron content was approximately the same in both localities in Rasina district. Our results for Fe content in carrots was similar to those recorded by Ali and Al-Qahtani [12], who analyzed different vegetables and reported high concentrations of Fe (77.9–256.5 μg g^{-1}) in Saudi Arabia.

Table 3. Heavy metals' content in carrot (c_{sr} / μg g^{-1})

District	Locality	As	Cd	Cr	Cu	Fe	Mn	Mo	Ni	Pb	Sb	Sn	Tl
Pirot	Pirot	0.464	0.035	3.553	0.079	8.092	2.923	0.722	5.208	1.208	0.162	1.764	7.391
	Dolac	0.545	0.226	0.036	1.800	142.360	11.508	1.465	9.487	0.273	1.321	0.159	1.316
Toplica	Mala Plana	0.055	0.005	0.162	0.118	57.779	8.249	0.708	9.801	0.824	0.516	0.897	8.975
	Bučince	0.666	0.060	0.090	0.010	205.886	9.239	0.746	8.694	0.746	0.711	0.816	8.368
	Kupinov	0.511	0.043	3.446	0.247	33.295	7.744	0.758	11.391	0.835	0.098	1.295	9.789
Bor	Bor	2.042	0.231	0.553	2.743	51.692	4.389	0.638	7.101	0.273	0.960	0.746	5.850
	Krivelj	2.108	0.316	3.074	6.294	163.074	14.924	0.820	9.938	0.356	1.849	1.098	7.449
	Slatina I	1.007	0.034	3.007	6.936	185.971	14.041	0.977	11.591	0.293	0.934	0.484	8.894
	Slatina II	1.372	0.035	3.036	12.085	343.989	15.298	0.897	6.728	0.181	2.523	1.777	2.989
Rasina	Velika Vrbnica	0.060	0.022	0.445	0.947	52.276	5.529	7.730	5.224	0.331	0.079	0.953	7.253
	Bivolje	0.307	0.035	0.377	1.195	49.330	6.149	0.673	4.946	0.362	0.082	0.852	7.125
Kosovska Mitrovica	Zubin Potok	0.452	0.080	0.720	0.211	32.074	3.926	0.589	11.649	0.593	0.208	0.770	7.218
	Lipljan	0.720	0.048	5.444	3.963	163.199	11.496	1.369	9.054	0.712	0.761	0.937	10.231

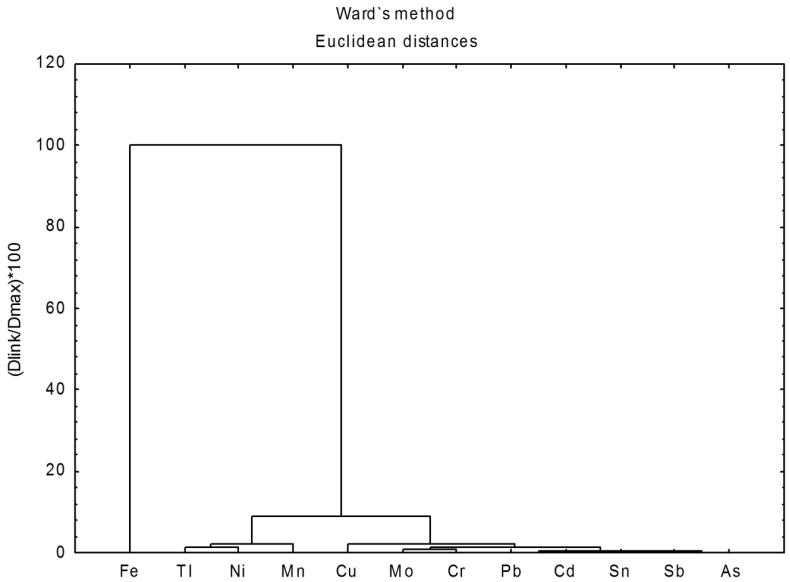

Figure 2. Dendrogram showing clustering of heavy metals based on chemical analysis of their concentrations.

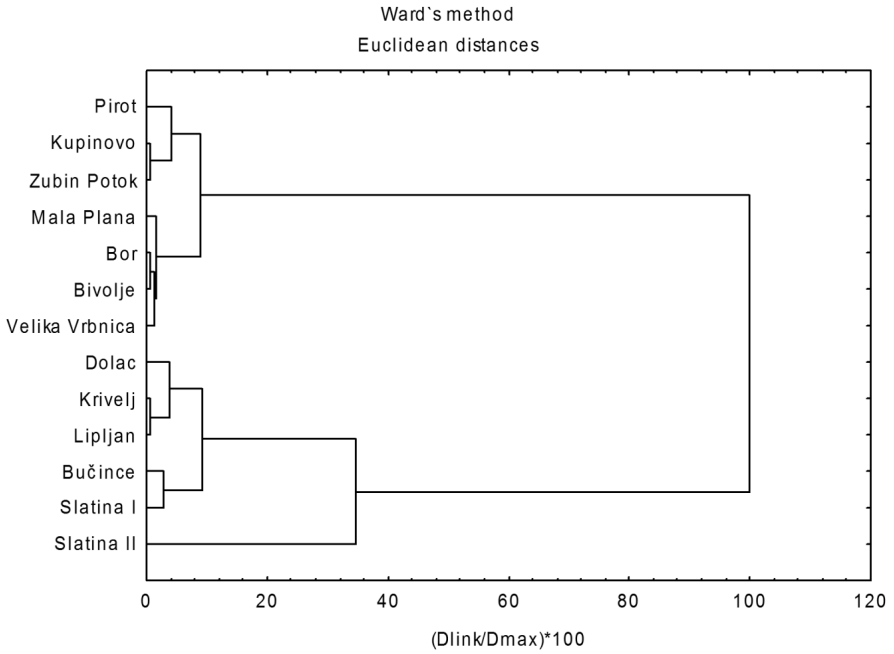

Figure 3. Dendrogram showing clustering of sampling sites based on chemical analysis of heavy metal content in carrots.

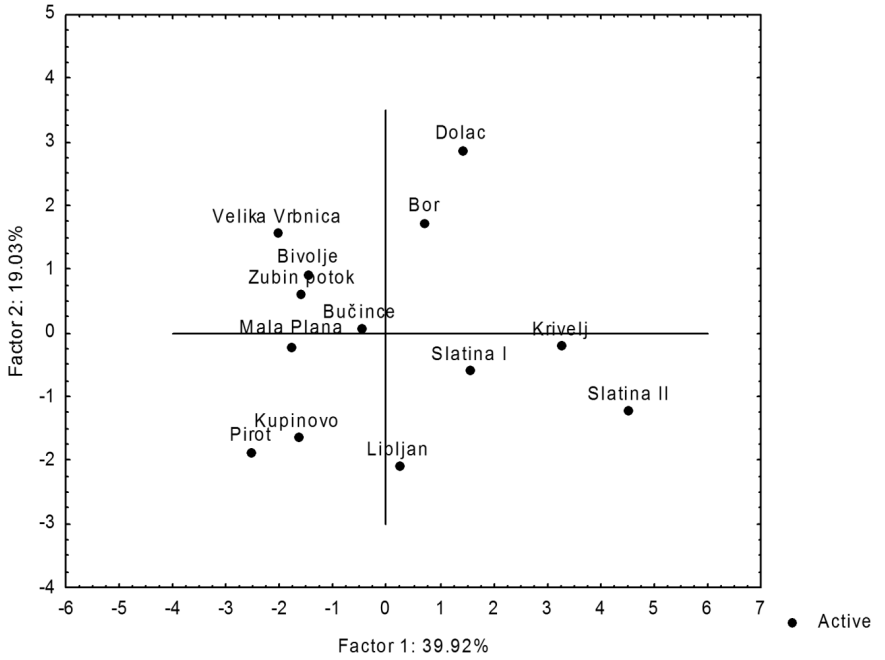

Figure 4. Representation of sampling sites as function of the PC1 vs. PC2.

Cu is necessary for body pigmentation in addition to Fe, the maintenance of a healthy central nervous system, prevention of anemia, and is interrelated with the function of Zn and Fe in the body [13].

As expected, the highest amount of cooper was found in carrots from Bor district (average content 7.014 μg g^{-1}). Bor mine has reserves of cooper, and average amount of cooper in Serbia is the highest in this region [14]. Heavy metals are of great significance in ecotoxicology due to their toxicity at low levels and tendency to accumulate in human organs [15]. Lead, arsenic and cadmium are listed as carcinogenic [16,17]. Inorganic arsenic is the most toxic fraction of this metalloid, and uptake limit is 15 mg of inorganic arsenic per kg body weight per week for arsenic intake by humans. Arsenic tends to accumulate in the vegetable root [18], so it is expected that its value is higher in carrots and root vegetables, than in other vegetables. Arsenic content was the highest in Bor (2.042 μg g^{-1}), and lowest in Mala Plana (0.055 μg g^{-1}). Samples from

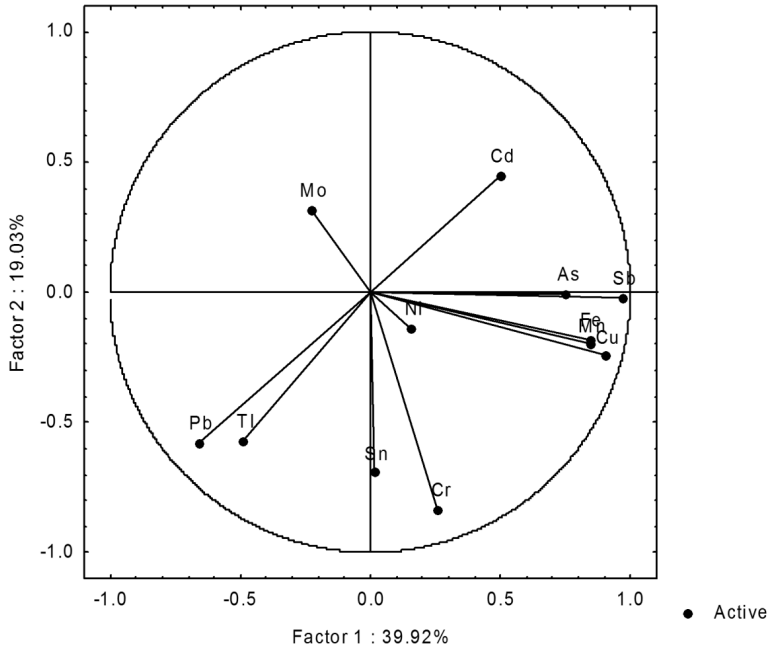

Figure 5. Representation of the variables as function of the PC1 vs PC2.

Bor district differ significantly in arsenic content compared to other districts. Average arsenic content was 1.632 μg g^{-1} in Bor district, while the lowest content of this element was recorded in samples from Rasina district (average content was 0.184 μg g^{-1}). Compared to other analyzed metals, cadmium content was the lowest in carrot samples. Acute Cd toxicity is rare, but chronic exposure can increase accumulation of this metal in certain organs. The main organ for long-term cadmium accumulation is the kidney [19]. The highest amount of cadmium was found in carrots from Krivelj (0.316 μg g^{-1}). Mining and smelting operations can increase Cd level in environment, so it is expected that Bor district has the highest level of this element. Cadmium occurs naturally in soils rich in zinc, carbonates and clay, but anthropogenic pollution is major source of Cd in plant and soil. This pollutant, used in many industrial processes, can also be found beside roads, as well in cultivable soil, due to the usage of some fertilizers and fungicides. Cd content in other regions was significantly lower, and the lowest content of this element was 0.005 μg g^{-1} found in carrots from Mala Plana (Toplica district). Lead is highly toxic to human and animals. Most of the accumulated Pb is sequestered in the bone and teeth [20]. Pb can reduce cognitive development and intellectual performance in children and damage kidneys and reproductive system [21]. Highest amount of lead is found in carrots from Pirot (1.208 μg g^{-1}). Higher concentration of Pb in carrots from this locality may be attributed to proximity to the highway, because main source of lead in environment are vehicle exhaust emissions. It is interesting that samples from Pirot had five times higher lead concentration than samples from Dolac, although they are in the same district. The lowest lead content was detected in samples from Bor district, only 0.276 μg g^{-1}. Musliu and Shallari [22] investigated Pb, Zn and Cd content in carrots from Kosovska Mitrovica, and average Pb content was 0.612 μg g^{-1}, which is in agreement with our study.

PCA and CA are the most common multivariate statistical methods used in environmental and foodstuff studies [23,24]. Cluster analysis (CA) is a multivariate technique, with the purpose of classifying the objects of the system into categories or clusters based on their similarities [25]. Results obtained by cluster analysis are typically illustrated by a dendrogram. Cluster analysis was done by Ward's method using Euclidean distances as a measure of similarity. Ward's methods minimize the sum of squares of any two (hypothetical) clusters that can be formed at each step. Euclidean distance is most common way to measure distance between objects:

$$\text{Distance}(x,y) = \left\{ \sum_i (x_i - y_i)^2 \right\}^{1/2} \quad (1)$$

The linkage distance is reported as D_{link}/D_{max}, which represents the quotient between the linkage distances for a particular case divided by the maximal linkage distance. All variables from this study were standardized before PCA and CA were applied.

According to CA, metals are group in two statistically significant clusters at $100(D_{link}/D_{max}) < 50$. Cluster 1 contains Tl, Ni, Mn, Cu, Mo, Cr, Sn, Pb, Cd, Sb and As, while cluster 2 contains only Fe. As expected, results

described in the previous sections are confirmed. Fe content is the highest in all samples that were analyzed, and that's why it is separated cluster. Euclidean distance between Fe content and all the others metals analyzed is above 10, which is in agreement with results obtained by analyzing carrot samples. Minimum Euclidean distance is recorded between Pb and Cd and As and Sb (0.00). Pb and Cd are not essential microelements and their content in plants are influenced by their content in soil, the pH of the soil and the presence of other microelements [26]. Cluster analysis was also applied in order to group localities based on heavy metal content in carrots. Cluster 1 is composed of Pirot, Kupinovo, Zubin Potok, Mala Plana, Bor, Velika Vrbnica and Bivolje and cluster 2 is composed of Dolac, Lipljan, Krivelj, Bučince, Slatina 1 and Slatina 2. It can be seen that carrots from the same district don't have similar heavy metal content. Pirot and Dolac belong to Pirot district by administrative division, but carrots from these localities do not have similar metal content and that's why they belong to different clusters. Carrots from Kupinovo and Zubin Potok demonstrated the most similar heavy metal content, even though they don't belong to the same district. Euclidean distance was the highest between Slatina 2 and Pirot (7.24), which is in agreement with metal content in carrots from these localities. As and Fe content in carrots from Slatina 2 were much higher than in carrots from Pirot, and that can be explanation for so big Euclidean distance.

PCA as the multivariate analytical tool reduces a set of original variables and extracts a small number of latent factors (principal components and PCs) for analyzing relationships between the observed variables and samples [27]. The first principal component (PC) describes the maximum possible variation that can be projected onto one dimension; the second PC captures the second most and so on [28]. The first two PC describe 58.95% of the total variance, being 39.92% explained by PC1 and 19.03% by PC2 (Table 4). Figure 4 shows the scores plot for the studied samples. Samples from Pirot, Kupinovo, Mala Plana, Bučince, Zubin Potok, Bivolje and Velika Vrbnica are located at the negative side of PC1, which corresponds to their grouping by CA analysis. The only difference in grouping between PCA and CA is Bučince. This distribution is a confirmation that the vegetables from different localities in the same district contain varying amounts of heavy metals. On the other hand, Cu and Sb have the highest positive loadings on PC1; descriptors Pb and Tl have the highest negative loadings. The rest of the descriptors have less importance due to their minor contribution to PC1. These results are in good agreement with the fact that samples accumulated at the right side of the plot exhibit high contents of Cu and Sb, whereas samples situated at the left side are characterized by low contents for these variables. Samples located at the left side of the plot demonstrated higher content of Pb and Tl. Therefore, after applying PCA methods, the two most discriminating features appear to be Pb and Sb.

Table 4. Principal Component Analysis of heavy metal content in carrots – Eigenvalues

Eigenvalue	Total variance %	Cumulative eigenvalue	Cumulative %
4.79	39.92	4.79	39.92
2.28	19.03	7.07	58.95
1.74	14.47	8.81	73.42
1.27	10.60	10.08	84.02
0.81	6.79	10.90	90.81

CONCLUSION

The concentration of selected heavy metals in carrots was used to differentiate between carrots grown in different localities in Serbia. The content of selected elements is a reflection of the soil type and, importantly, the environmental growing conditions. The geographic origin of carrots can be determined by their chemical profile. It can be seen that carrots from the same district do not have similar heavy metal content. Application of CA and PCA for analyzing these complex data provides optimization of analytical procedures by selecting for analysis only 4 variables (Cu, Sb, Pb and Tl) and differentiation among contaminated areas.

Acknowledgements

The research was supported by Ministry of Education, Science and Technological Development (MESTD) of the Republic of Serbia [172051]. Marija Dimitrijevic is grateful to MESTD for providing scholarships for researchers.

REFERENCES

[1] S.A. Arscott, S.A. Tanumihardjo, Carrots of many colors provide basic nutrition and bioavailable phytochemicals acting as a functional food, Compr. Rev. Food Sci. Food Saf. **9** (2010) 223–239.

[2] A.H. Ensminger, M.E. Ensminger, J.E. Konlande, J.R.K. Robson, The concise encyclopedia of foods and nutrition, CRC Press, Boca Raton, FL, 1995.

[3] M.N.V. Prasad, H.M.O. Freitas, Feasible biotechnological and bioremediation strategies for serpentine soils and mine spoils, Electron. J. Biotechnol. **2** (1999) 36–50.

[4] M. Oves, M.S. Khan, in: A. Zaidi, P.A. Wani, M.S. Khan (Eds.), Toxicity of Heavy Metals to Legumes and Bioremediation, Springer, New York, 2012.

[5] H.M. Chen, C.R. Zheng, C. Tu, Y.G. Zhu, Heavy metal pollution in soils in China: status and countermeasures, Ambio **28** (1999) 130–134.

[6] N. Loutfy, M. Fuerhacker, P. Tundo, S. Raccanelli, A.G. Dien, M.T. Ahmed, Dietary intake of dioxins and dioxin-like PCBs, due to the consumption of dairy products, fish/seafood and meat from Ismailia city, Egypt, Egypt. Sci. Total Environ. **370** (2006) 1–8.

[7] S. Nakatsuka, H. Tanaka, M. Namba, Mutagenic effects of ferric nitilotriacetate Fe-NTA on V79 Chinese hamster cells and its inhibitory effects on cell-cell communication, Carcinogenesis **11** (1990) 257–260.

[8] J.U. Ahmad, M.A. Goni, Heavy metal contamination in water, soil, and vegetables of the industrial areas in Dhaka, Bangladesh, Environ. Monit. Assess **166** (2010) 347–357.

[9] United States Environmental Protection Agency, Method 3050B: Acid Digestion of Sediments, Sludges and Soils, 1996.

[10] J.N. Miller, J.C. Miller, Statistics and Chemometric for analytical chemistry, Pearson Education Limited, Harlow, 2005.

[11] S.R. Kashif, M. Akram, M. Yaseen, S. Ali, Studies on heavy metals status and their uptake by vegetables in adjoining areas of Hudiara drain in Lahore, Soil Environ. **28** (2009) 7–12.

[12] H.H.A. Mohamed, M.A.Q. Khairia, Assessment of some heavy metals in vegetables, cereals and fruits in Saudi Arabian markets, Egypt. J. Aquat. Res. **38** (2012) 31–37.

[13] I.O. Akinyele, O. Osibanjo, Levels of trace elements hospital diet, Food Chem. **8** (1982) 247–251.

[14] Agency for Environmental Protection, Ministry of Energy, Development and the Environment, Report on the status of the land in the Republic of Serbia, 2009.

[15] N. Viqar, R. Ahmed, Decomposition of vegetables for determination of Zn, Cd, Pb and Cu by stripping voltammetry, Microchim. Acta **106** (1992) 137–141.

[16] International Agency for Research on Cancer (IARC), Cadmium and cadmium compounds, in: Beryllium, cadmium, mercury and exposure in the glass manufacturing industry. IARC Monographs on the evaluation of carcinogenic risks to humans, 58, 119, ARC Scientific Publications, Lyon, 1993.

[17] International Agency for Research on Cancer (IARC), Lead and lead compounds. Lead and inorganic lead compounds (Group 2b), Organolead compouds (Group 3), IARC monographs, 23, Lyon, 1987.

[18] A. Carbonell-Barrachina, F. Burlo-Carbonell, J. Mataix-Beneyto, Effect of sodium arsenite on arsenic accumulation and distribution in leaves and fruit of *Vitis vinifera*, J. Plant Nutr. **20** (1997) 379–387.

[19] C. Orlowski, J.K. Piotrowski, Biological levels of cadmium and zinc in the small intestine of non-occupationally exposed human subjects, Hum. Exp. Toxicol. **22** (2003) 57–63.

[20] G.C. Todd, Environ. Vegetables grown in mine wastes, Toxicol. Chem. **19** (1996) 600–607.

[21] F. Qin, W. Chen, Lead and copper levels in tea samples marketed in Beijing, Bull. Environ. Contam. Toxicol. **78** (2010) 28–31.

[22] A. Musliu, S. Shallari, Soil pollution in Mitrovica town surroundings and absorption of heavy metals by carrot plant, Albanian J. Agric. Sci. **12** (2013) 705–706.

[23] L. Tomsone, Z. Krumab, I. Alsina, The application of hierarchical cluster analysis for clasifying horseradish genotypes (*Armoracia rusticana* L.) roots, Chem. Technol. **4** (2012) 52–56.

[24] C. Mendiguchia, C. Moreno, R.M.D. Galindo, M. Garcia-Vargas, Using chemometric tools to assess anthropogenic effects in river water. A case study: Guadalquivir River (Spain), Anal. Chim. Acta **515** (2004) 143–149.

[25] A.J. Richard, W.W. Dean, Applied multivariate statistical analysis, Prentice-Hall, London, 2002.

[26] J.C. Akan, F.I.A. Abdulrahman, V.O. Ogugbuaja, J.T. Ayodele, Heavy metals and anion levels in some samples of vegetable grown within the vicinity of challawa industrial area, Am. J. Applied Sci. **6** (2009) 534–542.

[27] B. Škrbić, N. Durišić–Mladenović, Chemometric interpretation of heavy metal patterns in soils worldwide Chemosphere **80** (2010) 1360–1369.

[28] K.A. Anderson, B.A. Magnuson, M.L. Tschirgi, B. Smit, Determining the Geographic Origin of Potatoes with Trace Metal Analysis Using Statistical and Neural Network Classifiers, J. Agric. Food Chem. **47** (1999) 1568––1579.

IZVOD

HEMOMETRIJSKI PRISTUP U PROCENI SADRŽAJA TEŠKIH METALA U ŠARGAREPI (*Daucus carota*) SA RAZLIČITIH LOKALITETA U SRBIJI

Violeta D. Mitic[1], Vesna P. Stankov-Jovanovic[1], Snezana B. Tosic[1],Aleksandra N. Pavlovic[1], Jelena S. Cvetkovic[1], Marija V. Dimitrijevic[1], Snezana D. Nikolic-Mandic[2]

[1]*Univerzitet u Nišu, Prirodno–matematički fakultet, Departman za hemiju, Višegradska 33, Niš, Srbija*
[2]*Univerzitet u Beogradu, Hemijski fakultet, Studentski trg 12–16, Beograd, Srbija*

(Naučni rad)

Povrće spada u grupu namirnica koje je od velikog značaja za čovekovu ishranu. Ukoliko se gaji na zagađenom zemljištu, postoji mogućnost akumulacije štetnih materija, koje mogu da ugroze ljudsko zdravlje. Teški metali imaju uticaj kako na biljku koja ih apsorbuje, tako i na čoveka. Sadržaj teških metala u biljnom tkivu ukazuje na zagađenost životne sredine. U ovom radu analiziran je sadržaj 12 teških metala u šargarepi (*Daucus carota*). Uzorci su prikupljani na 13 lokaliteta, u okviru 5 okruga jugositočne Srbije: Pirotski, Toplički, Borski, Kosovsko-mitrovački i Rasinski. Sadržaj teških metala određen je metodom indukovano kuplovane plazme sa optičkom emisionom detekcijom. Sadržaj teških metala značajno se razlikovao između lokaliteta, što ukazuje na to da su neki lokaliteti više zagađeni. Tako je sadržaj bakra najveći u Borskom okrugu, što je i očekivano, obzirom na blizinu rudnika bakra. Borski okrug se karakteriše i najvećim sadržajem arsena, antimona, kadmijuma, gvožđa, hroma, mangana. Kosvsko mitrovači i Rasinski okrug imaju najveći sadržaj telura. Olova najviše ima u uzorcima iz Pirotskog okruga, pošto su lokaliteti sa kojih je vršeno uzorkovanje bili u neposrednoj blizini magistralnog puta. Hemometrijski pristup primenjen je kako bi se elementi i lokaliteti klasifikovali na osnovu koncentracije metala u uzorcima šargarepe. Klasterskom analizom izvšena je podela lokaliteta u dva klastera. Metoda glavnih komponenti (PCA) korišćena je kako bi se analizirani uzorci klasifikovali u grupe, na osnovu sadržaja teških metala. PCA analizom ekstrahovana su četiri faktora, koja zajedno objašnjavaju 79.94% ukupne varijanse. Prvi faktor (PC1) objašnjava Cu, Sb, Pb i Tl, sa 39.92% udela u ukupnoj varijansi. Klaster analiza i analiza glavnih komponenti mogu se uspešno koristiti u cilju sagledavanja zagađenja životne sredine teškim metalima.

Ključne reči: Šargarepa • Teški metali • ICP-OES • Klaster analiza • Analiza glavne komponente

Studija o nalazu aflatoksina u hrani za životinje i sirovom mleku u Srbiji tokom 2013. godine

Danka M. Spirić, Srđan M. Stefanović, Tatjana M. Radičević, Jasna M. Đinović Stojanović, Vesna V. Janković, Branko M. Velebit, Saša D. Janković

Institut za higijenu i tehnologiju mesa, Kaćasnkog 13, Beograd, Srbija

Izvod

Vremenski i klimatski uslovi koji su bili atipični za umereno kontinentalno proleće i leto 2012. godine smatraju se jednim od razloga kontaminacije useva mikotoksinima u Srbiji. Upotreba hrane za životinje poreklom iz žetve 2012. god. za posledicu je imala pojavu aflatoksina M_1 (AFM_1) u mleku krava. Kvantitativni ELISA testovi korišćeni su za analizu uzoraka hraniva, odnosno mleka. Konfirmacija pozitivnih rezultata dobijenh imunoenzimskim testom obavljena je pomoću UPLC-MS/MS metoda. Od 281 uzorka potpunih smeša za ishranu krava muzara, 67 uzoraka (24%) je sadržalo aflatoksin B_1 (AFB_1) u koncentraciji većoj od vrednosti MDK (maksimalno dozvoljena količina) od 0,005 mg/kg [4]. Uzorci kukuruza su, takođe, ispitani na prisustvo AFB_1 i utvrđena je kontaminacija 22% uzoraka iznad vrednosti maksimalno dozvoljene količine (0,03 mg/kg). Uzorci druge vrste hraniva, kao što su suncokretova sačma, seno, kukuruzna silaža i repini rezanci bili su negativni na prisustvo aflatoksina B_1. Sadržaj AFM_1 u 934 „*skrining*" pozitivna uzorka je bio u opsegu 0,005–1,25 µg/kg. Najviši stepen kontaminacije zabeležen je tokom marta 2013, kada je 65% ispitanih uzoraka mleka sadržalo više od 0,05 µg/kg, a 13% više od 0,5 µg/kg aflatoksina M_1.

Ključne reči: aflatoksin B_1, aflatoksin M_1, hrana za životinje, mleko, ELISA, UPLC-MS/MS.

Dostupno na Internetu sa adrese časopisa: http://www.ache.org.rs/HI/

NAUČNI RAD

UDK 613.287:615.9(497.11)"2013"

Hem. Ind. **69** (6) 651–656 (2015)

doi: 10.2298/HEMIND140619087S

Mikotoksini su sekundarni metaboliti toksikogenih plesni, značajni zbog toksičnih efekata koje ispoljavaju kada dospeju u organizam ljudi ili životinja.

Od poznatih mikotoksina, najveću toksičnost ispoljava AFB_1 koji, prema kriterijumima Ekonomske komisije Ujedinjenih nacija za Evropu (*United Nations Economic Commission for Europe*) [1], spada u supstance sa akutnim toksičnim delovanjem prve kategorije, u slučaju oralne i perkutane ekspozicije. U supstance prve kategorije, prema ovoj klasifikaciji spadaju jedinjenja čiji je LD_{50} do 5 mg/kg TM u slučaju oralne ekspozicije i do 50 mg/kg TM u slučaju perkutane ekspozicije (Tabela 1). Usled kumulativnog delovanja u organima, AFB_1 je označen kao kancerogena supstanca za ljude i svrstan u grupu 1A, prema Internacionalnoj agenciji za istraživanje o raku (IARC, 2002) [2]. Prema postojećim zakonskim regulativama koje se odnose na mikotoksine u žitaricama u našoj zemlji, najniža *MDK* je određena za aflatoksin B_1 i iznosi 0,005 mg/kg za žita namenjena ljudskoj ishrani [3] i 0,03 mg/kg za hranu namenjenu ishrani životinja) [4].

Kontaminacija mikotoksinima nastaje u različitim fazama rasta biljke, sazrevanja ploda, ili neodgovarajućeg skladištenja nakon žetve. Iako su tropski klimatski uslovi najpovoljniji za pojavu aflatoksina u žitaricama i orašastim plodovima, promene klimatskih uslova u vidu sve dužih perioda sa visokim dnevnim minimalnim temperaturama, dovode do povećanja rizika za pojavu mikotoksina i u umerenom pojasu [5]. Visoke prosečne temperature i dug sušni period izazivaju toplotni stres kod biljaka, pri čemu dolazi do kontaminacije biljke plesnima roda *Aspergillus,* naročito u periodu cvetanja kukuruza i tamnjenja kukuruzne svile [6,7].

Tabela 1. Kategorizacija supstanci prema akutnoj toksičnosti i procenjene granične vrednosti za akutnu toksičnost. Akutna toksičnost se izražava kao LD_{50}. (deo tabele, izvor: GHS [1])
Table 1. Acute toxicity hazard categories and acute toxicity estimate (ATE) values defining the respective categories. Acute toxicity is expressed as LD_{50}. (part of the table, source: GHS [1])

Put unošenja	Kategorija				
	1	2	3	4	5
Oralni (mg/kg T. M.)	5	50	300	2000	5000
Perkutani (mg/kg T. M.)	50	200	1000	2000	5000

Prepiska: D. Spirić, Institut za higijenu i tehnologiju mesa, Kaćanskog 13, 11000 Beograd, Srbija.
E-pošta: dankaspiric@inmesbgd.com
Rad primljen: 19. jun, 2014
Rad prihvaćen: 15. decembar, 2014

Pored rotacije useva [8], kao načina smanjenja rizika od kontaminacije plesnima i mikotoksinima u polju, od izuzetne važnosti za prevenciju pojave mikotoksina su i uslovi skladištenja, nakon žetve. Sortiranje i sušenje semena su važni parametri za sprečavanje naknadne kontaminacije žitarica mikotoksinima [9,10].

U toku 2012. godine, na osnovu izveštaja RHMZ, u Srbiji je zabeležena suša, koja je naročito loše uticala na poljoprivredne kulture tokom juna meseca [11]. Visoke vrednosti minimalne dnevne temperature i visoke vrednosti prosečnih temperatura povoljno su uticale na kontaminaciju klipova kukuruza mikotoksikogenim plesnima *Aspergillus flavus* u polju.

Početkom 2013. godine, usled upotrebe kontaminiranog kukuruza, zabeležena je pojava povećanog sadržaja AFB_1 u hrani za životinje, što je za posledicu imalo povećan sadržaj AFM_1 u mleku mlečnih krava. Praćenje kontaminacije uzoraka sa farmi, u periodu od februara do aprila 2013. godine, imalo je za cilj da se utvrdi stepen kontaminacije hrane za životinje i mleka krava aflatoksinima. Na ovaj način su obezbeđeni podaci subjektima u poslovanju potrebni za procenu rizika i bezbednost hrane [12]. Takođe, uvid u stepen kontaminacije hrane za životinje i mleka važan je parametar za procenu ekonomskog gubitka mlečne industrije i farmi [13].

MATERIJAL I METODE

U toku 2013. godine, u periodu od februara do aprila, uzorkovano je 396 različitih uzoraka hrane za životinje, namenjene ishrani mlečnih krava, i to: 281 uzorak potpunih smeša za ishranu mlečnih krava, 55 uzoraka kukuruza, odnosno kukuruzne prekrupe, i po 12 uzoraka silaže, sojine sačme, deteline, sena i suncokretove sačme, i ispitano na prisustvo i sadržaj aflatoksina B_1. Ukupno 2.045 uzorka sirovog kravljeg mleka ispitano je na prisustvo i sadržaj aflatoksina M_1. Uzorci su bili deo pojačane kontrole farmi mlečnih krava i otkupnih stanica.

Za obe ELISA metode korišćen je spektrofotometar Multiskan Ascent, ThermoFisher Scientific (Waltham, MA, SAD). Priprema uzoraka hrane za životinje obavljena je u skladu sa dokumentovanom metodom prema uputstvu proizvođača (Tecna, Trst, Italija). Korišćen je metanol p.a. čistoće (Sigma, St. Louis, SAD). Uzorci hrane za životinje ispitani su ELISA metodom sa limitom detekcije od 0,001 mg/kg, za AFB_1. Kao interna kontrola korišćeni su: slepa proba (blanko uzorak), i četiri obogaćene slepe probe u koncentracijama od 0,00; 0,010; 0,030 i 0,050 mg/kg AFB_1.

Metoda za određivanje sadržaja aflatoksina B_1 je direktni kompetitivni ELISA test. Tokom predinkubacije, ekstrakti uzoraka se mešaju sa peroksidazom rena (*horse radish peroxidase* – HRP), enzimom, koji je konjugovan sa aflatoksinom i zajedno se dodaju u mikrotitarske bunarčiće, obložene anti-aflatoksin antitelima, za koje se kompetitivno vezuju slobodni i kojugovani aflatoksini [14]. Nakon ispiranja nevezanog sadržaja i inkubacije fiksne količine hromogenog supstrata tetrametilbenzidina (TMB), koji je donor vodonika u reakciji redukcije vodonik peroksida do vode pomoću HRP enzima, dolazi do formiranja proizvoda plave boje. Reakcija se zaustavlja dodavanjem 0,1 M sumporne kiseline, koja inaktiviše HRP enzim, a proizvod postaje žuto obojen. Intenzitet boje se očitava na talasnoj dužini od 450 nm.

Za određivanje AFB_1, tečnom hromatografijom ultra performansi sa masenom spektroskopijom (UPLC/MS-MS), deset grama samlevenog i homogenizovanog zrna kukuruza je odmereno na tehničkoj vagi i preliveno sa 40 mL smeše acetonitril–voda–sirćetna kiselina (79:20:1, *V*/*V*/*V*). Čaše su, zatim, postavljene na orbitalni šejker, a ekstrakcija se odvijala na 150 o/min, tokom jednog časa na sobnoj temperaturi. Uz svaki set uzoraka pripremani su i kontrolni uzorci (jedna slepa proba i tri slepe probe obogaćene AFB_1 u koncentracijama od 0,005; 0,010 i 0,020 mg/kg). Nakon ekstrakcije i taloženja kukuruza na dno čaše, automatskom pipetom je odmereno 500 μL supernatanta kome je dodato 500 μL smeše acetonitril–voda–sirćetna kiselina. Jedan mililitar dobijenog rastvora je profiltriran kroz najlonski špric-filter prečnika pora 0,2 μm direktno u vialu za autosampler. Jonizacija AFB_1 do molekulskog jona se izvodila korišćenjem elektrosprej sistema u pozitivnom modu (ES+). Temperatura jonskog izvora je bila 115 °C a desolvacionog gasa 350 °C. Kapilarni napon je iznosio 4000 V, a napon na konusu 35 V. Kao kolizioni gas korišćen je Ar_2. Detekcija AFB_1 se izvodila u MRM načinu rada spektrometra, praćenjem masa molekulskog jona (313,1 Da) i tri tranziciona produkta (285,2, 270,1 i 241,1 Da). Kvantifikacioni tranzicioni produkt je bio fragment molekulske mase 285,2 Da.

ELISA metoda za određivanje sadržaja aflatoksina M_1 predstavlja sendvič tip ELISA testa. Mikrotitarski bunarčići su impregnirani sa anti-aflatoksin M_1 antitelima i tokom prve inkubacije aflatoksin M_1 iz uzoraka se vezuje za antitela. Nakon ispiranja nevezanog materijala, u bunarčiće se dodaje tačno određena količina HRP enzimom konjugovanog aflatoksina M1. Konjugat se vezuje za slobodna mesta na impregniranim antitelima. Nakon ispiranja viška materijala, u bunarčiće se dodaje TMB supstrat, koji reaguje sa enzimom i nastaje obojeni proizvod. Nakon dodavanja 0,1 M H_2SO_4 i zaustavljanja reakcije, boja se očitava na spektrofotometru, na talasnoj dužini od 450 nm. Za internu kontrolu korišćeni su slepa proba (blanko uzorak), i tri obogaćene slepe probe u koncentracijama od 0,010; 0,020; 0,050 i 0,075 μg/kg AFM_1.

Svi uzorci mleka u kojima su ELISA testom dokazane vrednosti AFM_1 0,050 μg/kg kao i odgovarajući uzorci

kukuruza u kojima je dokazano više od 30 μg/kg AFB_1, ispitani su i UPLC/MS-MS metodom.

Za potrebe UPLC/MS-MS mleko je, pre ekstrakcije AFM_1, podvrgnuto procesu obezmašćivanja. Deset mililitara mleka je preneto u polipropilenske kivete za centrifugu od 50 mL. Kivete su, zatim, prebačene u zamrzivač na –18 °C na 10 min da bi se mleko ohladilo na 1–4 °C. Nakon centrifugiranja, 5 mL obezmašćenog mleka sa dna kivete je preneto u čistu polipropilensku kivetu za centrifugu. Mleku je dodato 100 μL 18% vodenog rastvora sumporne kiseline da bi se postigla pH vrednost od 2±0,5. Zatim je dodato 16 mL acetonitrila i 10 mL *n*-heksana. Dobijena smeša je homogenizovana na vibracionoj mešalici trajanju od 30 s. Aflatoksin M_1 je zatim ekstrahovan na orbitalnom šejkeru 10 min na 150 o/min, nakon čega su kivete postavljene u centrifugu i uzorci centrifugirani 15 min na 4000 o/min. Staklenom pipetom je odbačen gornji sloj *n*-heksana. Acetonitrilski sloj je dekantovan u staklene balone za uparavanje. Acetonitril je uparen na vakuum uparivaču na 60 °C, do suva. Suvi ostatak je rekonstituisan u 2 mL acetonitrila i prenet, nakon filtriranja kroz špric filter veličine pora 0,22 μm, direktno u vialu za autosampler.

UPLC-MS/MS instrument se sastoji od Waters Acquity UPLC sistema (Waters, Milford, MA, SAD) sa kvaternarnom pumpom, autosamplerom, grejačem kolone i tripl kvadripol masenim spektrometrom „TQD" (Waters Micromass, Manchester, Velika Britanija). Hromatografija je izvedena na Merck (Darmstadt, Nemačka) Purospher Star RP-18, reverzno-faznoj koloni (50 mm×2,1 mm), veličina čestica 2 μm. Mobilna faza se sastojala od 0,1 % sirćetne kiseline u vodi i metanola u odnosu 40:60, *V*/*V*. Protok je bio izokratni i iznosio je 0,25 mL/min. Separacija na hromatografskoj koloni se odvijala na 30±1 °C. Temperatura uzoraka u autosempleru je održavana na 20±1 °C.

Kalibracija se izvodila u pet tačaka, uključujući i nulu. Limit detekcije metode je 0,5 μg/kg za AFB_1 i 0,02 μg/kg za AFM_1. Aflatoksin M_1 je detektovan praćenjem masa molekulskog jona (329 Da) i dva tranziciona produkta (273 i 259,1 Da). Kvantifikacioni tranzicioni produkt je bio fragment molekulske mase 259,1 Da. Akvizicija i obrada podataka obavljena je MassLynx 4.1 softverom proizvođača Waters.

Rezultati dobijeni ELISA metodom su interpretirani korišćenjem "spreadsheet" programa autorizovanog od strane proizvođača kitova. Modelom regresione analize utvrđena je veza između rezultata dobijenih ELISA i UPLC/MS-MS metodom.

REZULTATI I DISKUSIJA

Od ukupno 281 uzorka potpune krmne smeše za ishranu mlečnih krava više od 0,005 mg/kg aflatoksina B_1 utvrđeno je u 67 uzoraka.

Od 55 ispitanih uzoraka kukuruza i kukuruzne prekrupe, 11 uzoraka je imalo vrednost AFB_1 iznad propisane MDK od 0,03 mg/kg [4], a 19 uzoraka je imalo više od 0,02 mg/kg aflatoksina B_1, što je vrednost MDK koja je određena evropskim propisima [15]. Ovakva zastupljenost aflatoksina B_1 u kukuruzu u skladu je sa sličnim nalazima drugih autora za mikotoksine u kukuruzu iz žetve iz 2012. godine [16]. Stepen kontaminacije kukuruza, na osnovu različitih kriterijuma i propisanih MDK, prikazan je na slici 1.

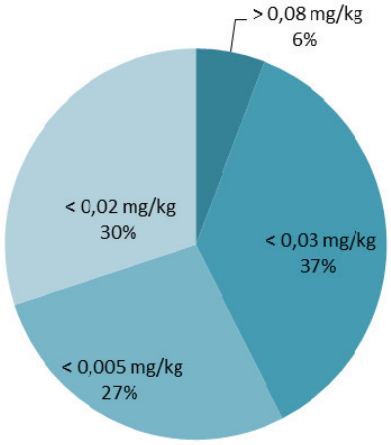

Slika 1. Rezultati ispitivanja uzoraka kukuruza na prisustvo aflatoksina B1 (mg/kg) u periodu februar–april 2013, prema kriterijumima različitih pravilnika.
Figure 1. Data for the presence of aflatoxin B1 (mg /kg) in the maize samples during February–April 2013, according to the criteria of different regulations.

U preostalih 60 uzoraka kukuruzne silaže, sojine pogače, deteline, sena i suncokretove sačme nije utvrđeno prisustvo aflatoksina B_1. Na osnovu toga može se zaključiti da se kontaminacija odnosila samo na kukuruz i kukuruznu prekrupu, koji su osnovni sastojci potpune smeše za ishranu krava.

Od 2.045 ispitanih uzoraka sirovog mleka, u 934 ispitana uzorka utvrđeno je prisusutvo AFM_1 iznad limita kvantifikacije metode (0,005 μg/kg). U zavisnosti od primenjenih kriterijuma za vrednosti MDK od 0,05 [17] i 0,25 μg/kg [18], na slici 2 prikazana je distribucija pozitivnih uzoraka.

Rezultati ispitivanja uzoraka sirovog mleka sa teritorije Srbije drugih autora pokazali su sličnu procentualnu zastupljenost AFM_1 [19], a rezultati ispitivanja prisustva aflatoksina u mleku koje iznose autori iz okolnih zemalja [20] ukazuju da je problem kontaminacije žitarica u 2012. godini i posledično, sirovog mleka bio problem regionalnog karaktera.

Kada se uzme u obzir odnos između rezultata ispitivanja stepena kontaminacije aflatoksinima hraniva i mleka dobija se slaba korelaciona veza [21]. Objašnjenje za ovu pojavu leži u činjenici da je AFB_1 u kukuruzu raspoređen veoma heterogeno što je dobro doku-

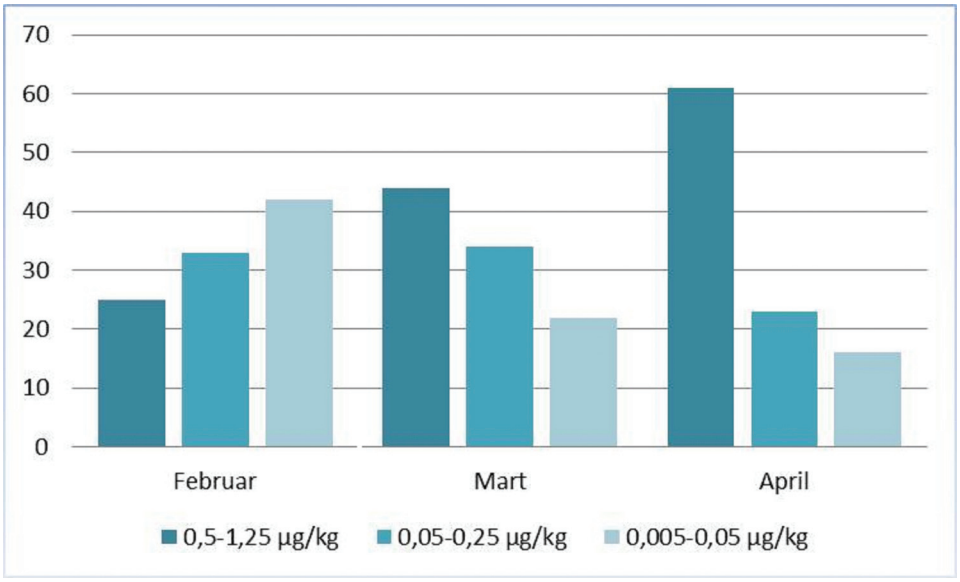

Slika. 2. Procentualna zastupljenost tri nivoa rezidua aflatoksina M_1 u uzorcima sirovog mleka u periodu februar–april 2013.
Figure 2. Percentage of three levels of aflatoxin M_1 presence in raw milk samples during the period February–April 2013.

mentovano u dostupnoj naučnoj literaturi [22]. Sa druge strane, AFM_1 je u mleku pravilno distribuiran. Stoga je način uzorkovanja kukuruza od velike važnosti za dobijanje reprezentativnog uzorka [23].

Poređenjem rezultata dobijenih ELISA i UPLC/MS--MS metodom utvrđen je stepen korelacije R^2 = 0,75, za aflatoksin M_1 i R^2 = 0,99, za aflatoksin B_1, što je prikazano na slikama 3 i 4. Sa grafikona se može videti veći stepen korelacije metoda za AFB_1 u odnosu na AFM_1. Objašnjenje za ovu pojavu leži u činjenici da su nivoi AFM_1 za dva reda veličine manji od merenih nivoa AFB_1, te je i relativna standardna devijacija rezultata AFM_1 veća, međutim, može se reći da obe analitičke tehnike pokazuju visok stepen korelacije.

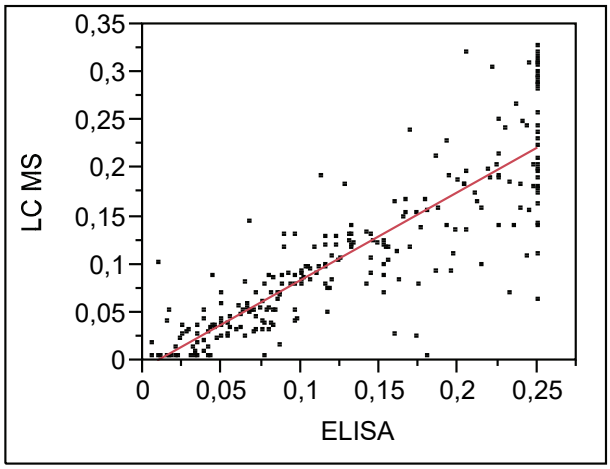

Slika 3. Regresiona prava korelacije između ELISA i UPLC-MS/MS metode za određivanje AFM_1 u mleku.
Figure 3. Regression correlation curve between ELISA and UPLC-MS/MS method for determination of AFM_1 content in milk.

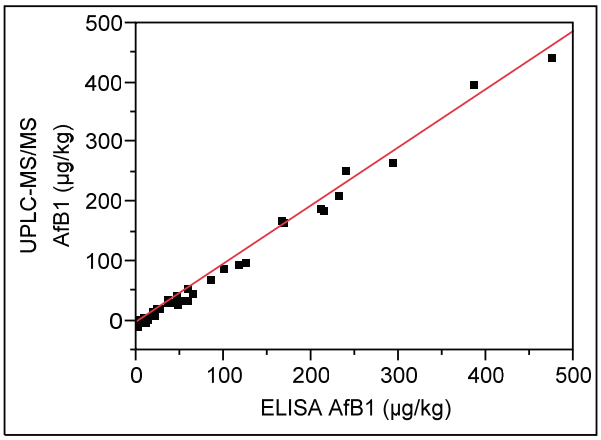

Slika 4. Regresiona prava korelacije između ELISA i UPLC--MS/MS metode za određivanje AFB_1 u kukuruzu.
Figure 4. Regression correlation curve between ELISA and UPLC-MS/MS method for determination of AFB_1 content in corn.

ZAKLJUČAK

U ukupno 281 uzorku potpunih krmnih smeša i 55 uzoraka kukuruza utvrđen je određeni stepen kontaminacije aflatoksinima koji ukazuje da 24%, odnosno 20% ispitanih uzoraka ne ispunjava zahteve Pravilnika o kvalitetu hrane za životinje. Tokom tromesečnog perioda ispitivanja uzoraka sirovog mleka utvrđeno je da je najveći stepen kontaminacije bio u martu 2013. godine, kada je 65% uzoraka bilo kontaminirano aflatoksinom M_1 iznad propisane MDK vrednosti u Evropi, a 13% uzoraka je imalo sadržaj aflatoksina M_1 deset i više puta veću od 0,5 µg/kg [3].

Zahvalnica

Deo prikazanih rezultata proistekao je iz rada na realizaciji projekta III46009, koji, u okviru istraživanja u oblasti integralnih i interdisciplinarnih istraživanja, finansira Ministarstvo prosvete, nauke i tehnološkog razvoja Republike Srbije.

LITERATURA

[1] Globally Harmonized System of Classification and Labeling of Chemicals (GHS), 2013, 5th rev. ed., http://www.unece.org/fileadmin/DAM/trans/danger/publi/ghs/ghs_rev05/English/ST-SG-AC10-30-Rev5e.pdf.

[2] ARC Monographs on the evaluation of carcinogenic risk to humans, Vol. 82, Some traditional herbal medicines, some mycotoxins, naphthalene and styrene, International Agency for Research on Cancer (IARC), Lyon, France, 2002.

[3] Pravilnik 1: Pravilnik o maksimalno dozvoljenim količinama ostataka sredstava za zaštitubilja u hrani i hrani za životinje i o hrani i hrani za životinje za koju se utvrđuju maksimalno dozvoljene količine ostataka sredstava za zaštitu bilja (Sl. glasnik RS br. 25/10 i Sl. glasnik RS br. 28/11)

[4] Pravilnik 2: Pravilnik o kvalitetu hrane za životinje (Sl. Glasnik RS br. 4/10, 113/12 i 27/14).

[5] R. Russell, M. Paterson, N. Lima, How will climate change affect mycotoxins in food? Food Res. Int. **43** (2010) 1902–1914.

[6] S.F. Marsh, G.A. Payne, Preharvest infections of Corn silks and kernels by Aspergillus flavus, Phytopathology **74** (1984) 1284–1289.

[7] S.D. Kocić-Tanackov, G.R.Dimić, Gljive i mikotoksini – kontaminenti hrane, Hem. Ind. **67** (2013) 639–653.

[8] R. Jaime-Garcia, P.J. Cotty, Crop rotation and soil temperature influence the community structure of *Aspergillus flavus* in soil, Soil Biol. Biochem. **42** (2010) 1842––1847.

[9] P.J. Cotty, R. Jaime-Garcia, Influences of climate on aflatoxin producing fungi and aflatoxin contamination, Int. J. Food Microbiol. **119** (2007) 109–115.

[10] N.M.M. Birck, I. Lorini, V.M. Scussel, Fungus and mycotoxins in wheat grain at post harvest, 9th International Working Conference on Stored Product Protection, Brazil, 2006, PS2-12 – 6281, pp. 195–205.

[11] Klimatološka analiza 2012. godine na teritoriji republike Srbije, Republički hidrometeorološki zavod Srbije, 2012. http://www.hidmet.gov.rs/podaci/meteorologija/latin/2012.pdf.

[12] V. Janković, M. Škrinjar, J. Vukojević, D. Karan, M. Radmili, Mikotoksini – potencijalna opasnost za žive organizme, Tehnologija mesa **47** (2006) 97–103.

[13] D. Milićević, Mycotoxins in food chain, old problems new solutions, Tehnologija mesa **50** (2009) 99–111.

[14] P. Li, Q. Zhang, W. Zhang, Immunoassays for aflatoxin, TrAC **28** (2009) 1115–1126.

[15] Pravilnik 3: Commission Directive 2003/100/EC. O.J, L **285** (2009) 33–37.

[16] J. Kos, J. Mastilović, E. Janić Hajnal, B. Šarić, Natural occurrence of aflatoxins in maize harvested in Serbia during 2009–2012, Food Control **34** (2013) 31–34.

[17] Pravilnik 4: Commission Regulation (EC) No. 1881/2006 of 19 December 2006 setting maximum levels for certain contaminants in foodstuffs.

[18] Pravilnik 5: Pravilnik o maksimalno dozvoljenim količinama ostataka sredstava za zaštitu bilja u hrani i hrani za životinje i o hrani i hrani za životinje za koju se utvrđuju maksimalno dozvoljene količine ostataka sredstava za zaštitu bilja (Sl. glasnik RS, br, 29/14, 37/14, 39/14 i 72/14)

[19] J. Kos, J. Lević, O. Đuragić, B. Kokić, I. Miladinović, Occurrence and estimation of aflatoxin M_1 exposure in milk in Serbia, Food Control **38** (2014) 41–46.

[20] N. Bilandžić, Đ. Božić, M.Đokić, M. Sedak, B. Solomun Kolanović, I. Varenina, S. Tanković, Ž. Cvetnić, Seasonal effect on aflatoxin M_1 contamination in raw and UHT milk from Croatia, Food Control **40** (2014) 260–264.

[21] D. Spiric, J. Djinovic-Stojanovic, V. Jankovic, B. Velebit, T.Radicevic, S. Stefanovic, S.Jankovic , Study of aflatoxins incidence in cow feed and milk in Serbia Book of Abstracts: 6th International Symposium on Recent Advances in Food Analysis, November 5–8, 2013, Prague, Czech Republic, p. 338.

[22] P.B. Hamilton, Fallacies in our understanding of mycotoxins. J. Food Protect. **41** (1978) 404–408.

[23] M. Škrinjar, A. Vengušt, S. Kocić-Tanackov, Mikotoksini u hrani-uzorkovanje, detekcija, zakonski propisi, Tehnologija mesa **45** (2004) 163–169.

SUMMARY

STUDY OF AFLATOXINS INCIDENCE IN COW FEED AND MILK IN SERBIA DURING 2013

Danka M. Spirić, Jasna M. Đinović, Vesna V. Janković, Branko M. Velebit, Tatjana M. Radičević, Srđan M. Stefanović, Saša D. Janković

Institute of meat hygiene and technology, Kaćanskog 13, 11000 Belgrade, Serbia

(Scientific paper)

Atypical weather and climate conditions during the spring and summer 2012 were assumed to be the main reason for the aflatoxins contamination of corn crops in Serbia. High humidity in spring, and summer temperatures above the average contributed to the increased possibility of mycotoxins occurrence in cereals in the fields. As a consequence, at the beginning of 2013 the contaminated corn used for dairy cows diet had negative impact on the safety of cow milk. The routine laboratory control data revealed an increased content of aflatoxin M_1 in milk samples. Large number of raw milk and various feedstuff samples were collected from February to April 2013 and were analyzed for the presence of aflatoxin M_1 (AFM_1) and aflatoxin B_1 respectively. The collected samples were a part of enhanced self-control plans of the large dairy farms. Quantitative competitive and sandwich types of ELISA tests were used for the screening analysis of the feed and milk samples. Confirmation of the positive results obtained by ELISA tests was performed by UPLC-MS/MS method. Out of 281 samples of complete mixtures for dairy cows, 67 samples (24%) contained aflatoxin B_1 quantities higher than the MRL of 0.005 mg/kg [4]. Corn samples were also tested for the presence of aflatoxin B_1 revealing contamination of 22% above the MRL (0.03 mg/kg). Aflatoxin M_1 content in the 934 positive milk samples ranged from 0.005–1.25 μg/kg. The corresponding feed samples of sunflower meal, hay silage, corn silage and sugar beet pulp were screening negative, with the content of aflatoxin B_1 less than 2 μg/kg. The main sources of aflatoxins were corn samples, wholemeal and feed mixtures derived from contaminated corn. The contamination peak was during March 2013, when 65% of milk samples contained amounts of aflatoxin M_1 higher than 0.05 μg/kg, and 13% of milk samples contained amounts higher than 0.5 μg/kg.

Keywords: Aflatoxins • Feed • Milk • ELISA • UPLC-MS/MS

Comparison of ultraviolet radiation/hydrogen peroxide, Fenton and photo-Fenton processes for the decolorization of reactive dyes

Miljana D. Radović, Jelena Z. Mitrović, Miloš M. Kostić, Danijela V. Bojić, Milica M. Petrović, Slobodan M. Najdanović, Aleksandar Lj. Bojić

Department of Chemistry, Faculty of Science and Mathematics, University of Niš, Niš, Serbia

Abstract

The effectiveness of UV/H_2O_2 process, Fenton and photo-Fenton process on decolorization of commercially important textile dyes Reactive Orange 4 (RO4) and Reactive Blue 19 (RB19) was evaluated. The effect of operational condition such as initial pH, initial H_2O_2 concentration, initial Fe^{2+} concentration and initial dye concentration on decolorization of RO4 and RB19 was studied. The photo-Fenton process is found to be more efficient than UV/H_2O_2 and Fenton process for decolorization of simulated dye bath effluent and solutions of the dyes in water alone under optimum conditions. In simulated dye bath the removal efficiency was slightly lower than for the solutions of the dyes in water alone for both dyes types. The results revealed that the tested advanced oxidation processes were very effective for decolorization of RO4 and RB19 in aqueous solution.

Keywords: dyes, Fenton process, oxidations, photo-Fenton process, UV/H_2O_2 process.

Available online at the Journal website: http://www.ache.org.rs/HI/

SCIENTIFIC PAPER

UDC 667.2:66.094.3:54:66

Hem. Ind. **69** (6) 657–665 (2015)

doi: 10.2298/HEMIND140905088R

Synthetic dyes are widely used in the textile and dyestuff industries for textile dyeing, paper printing, food, cosmetics, pharmaceutical and colour photography [1]. Nearly 10000 different dyes and pigments are used industrially and 0.7 million tons of synthetic dyes are produced each year all over the world [1,2]. The textile industry consumes considerable amounts of water during the dyeing and finishing operations. Wastewaters from the textile industry are discharged into the environment and can be highly contaminated due to extensive use of dyes [3]. It was reported that the loss of the dyes during processes can be from 1 to 15% [4]. Dyes are very resistant to biological degradation [5,6] and thus strongly influence on aquatic ecosystem [7].

Textile dyes are divided as acid, reactive, metal complex, disperse, vat, mordant, direct, basic and sulfur dyes, as to their way of application [8]. Azo dyes make the largest group of colorants with the respect to both the number and production volume. These compounds contain one or more azo groups (–N=N–) mostly linked to benzene or naphthalene rings [9]. Some azo dyes via metabolic cleavage of azo linkage can produce potentially carcinogenic aromatic amines [10]. Therefore, more attention should be paid to the azo dyes release in the environment. Anthraquinone reactive dyes are the second most commonly used group of dyes. Because of their structure which is highly stabilized by resonance, these dyes are very resistant to chemical oxidation. Thus, there is a need to remove dyes from wastewaters before discharging them to receiving waters. Chemical and physical processes such as chemical precipitation, coagulation, electrocoagulation, elimination by adsorption on activated carbon and reverse osmosis are used for the dye removal from textile effluents [11]. Nevertheless these (traditional methods) processes merely transfer the contamination from one phase (wastewater) to another (solid waste-sludge) and as a result make secondary waste and the problem remains still unsolved [12,13].

Alternatively, advanced oxidation processes (AOPs), such as homogeneous and heterogeneous photocatalysis, are promising technologies which aim at the decolorization and mineralization of the largest number of dyes or their transformation into biodegradable and harmless products [14–16]. AOPs refer to a set of different methods leading to the generation of highly oxidative species such as hydroxyl radicals ($^{\bullet}OH$) which are capable of oxidizing the pollutants to such an extent that the treated wastewater may be reintroduced into receiving streams. The use of homogeneous degradation or photodegradation systems such as Fe^{n+}/H_2O_2 (Fenton), H_2O_2/UV and Fe^{n+}/H_2O_2/UV (photo-Fenton) have attracted much attention due to their high efficiency in the oxidation of different pollutants including dyes [17,18]. Some advantages of use AOPs in comparison to other systems are no sludge formation, no salt formation, considerably safe and easy operation, short reaction time, reduction of COD [19]. Reaction of hydroxyl radicals with organic contaminant inc-

Correspondence: M. Radović, Department of Chemistry, Faculty of Science and Mathematics, Višegradska 33, Niš, Serbia.
E-mail: mimaradovic@gmail.com
Paper received: 5 September, 2014
Paper accepted: 15 December, 2014

ludes three different mechanisms: hydrogen abstraction, electrophilic addition and electron transfer [20].

For practical use of these processes in wastewater treatment, there is a need to determine the optimal conditions of experimental parameters (pH, initial concentration of dye, H_2O_2 and Fe^{2+}) for efficient removal. In the present study, we have investigated the decolorization of azo dye Reactive Orange 4 (RO4) and anthraquinone dye Reactive Blue 19 (RB19) by three different AOPs.

EXPERIMENTAL

Reagents

The commercial samples of textile dyes, Reactive Orange 4 (RO4) and Reactive Blue 19 (RB19), were obtained from Farbotex (Italy) and used without further purification. H_2O_2 (30%), acetic acid, $FeSO_4{\cdot}7H_2O$, HCl and NaOH were of reagent grade and purchased from Merck (Germany). Kutregal PN (commercial product) was purchased from Chromos (Croatia). The pH of solutions was adjusted pH-metrically, without buffering. All other used reagents were of analytical grade. All solutions were prepared with deionized water.

Apparatus

UV–Vis spectra were recorded on UV–vis spectrophotometer UV-1650 PC (Shimadzu, Japan). UV irradiation experiments were carried out using batch UV photoreactor (originally manufactured) [21].

Photodecolorization procedures

The photoreactor was operated with an initial working volume of 100 cm^3. Solutions were prepared by dissolving the required quantity of the dye, H_2O_2 and $FeSO_4{\cdot}7H_2O$ (for Fenton and photo-Fenton processes where $FeSO_4{\cdot}7H_2O$ was used as a source of Fe^{2+}) in deionized water. During the irradiation, the solution was magnetically stirred in a constant rate (200 rpm) and the temperature was maintained at 25.0±0.5 °C by thermostating. The pH of solutions was adjusted using NaOH or HCl (0.1, 0.01 mol dm^{-3}) with pH-meter (Senslon5, HACH, USA). At regular time intervals samples were taken and absorbance was measured using UV–vis spectrophotometer, to determine degree of decolorization of the dye.

RESULTS AND DISCUSSION

UV/H_2O_2 process

Initial results demonstrate that neither H_2O_2 nor UV alone was able to noticeably decolorize these two reactive dyes in period of 24 h (result not shown). Combination of UV and H_2O_2 is necessary for production of hydroxyl radicals by photolysis of the hydrogen peroxide [22,23]. This radical is a non-selective and very powerful oxidiser with an oxidation potential of 2.8 V and can initiate the decolorization reactions by reacting with the dye molecules [24,25]. The changes in UV–Vis spectrum of RO4 and RB19 during UV/H_2O_2 process are presented in Fig. 1.

Figure 2 shows semi-logarithmic graphs of the concentration of reactive dyes versus illumination time. The apparent rate constants (k) for photodecolorization of RO4 and RB19 in the presence of hydrogen peroxide are obtained from above graphs. The inset of Figure 2 shows the change of removal efficiency *versus* time.

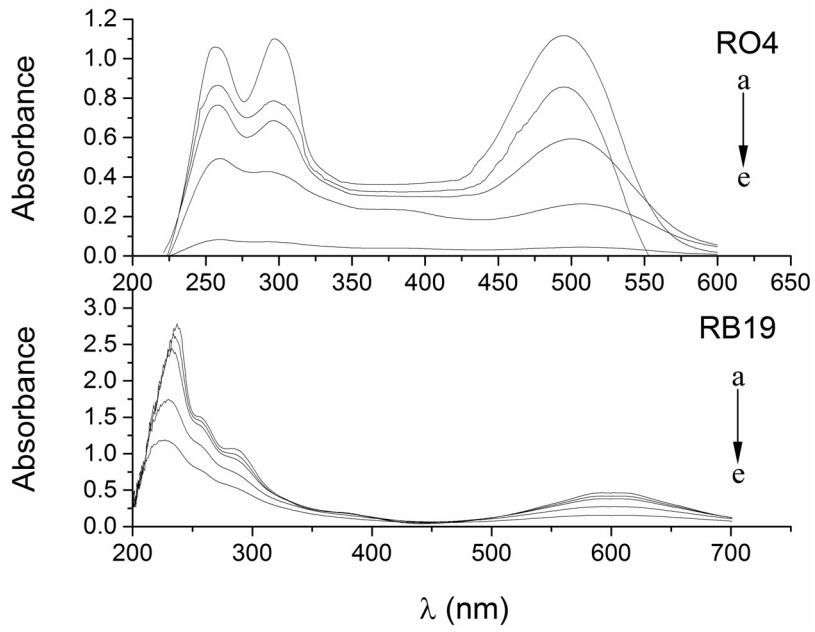

Fig. 1. The changes in UV–Vis spectrum of RO4 and RB19 in UV/H_2O_2 process after: a) 0, b) 2, c) 4, d) 10 and e) 20 min.

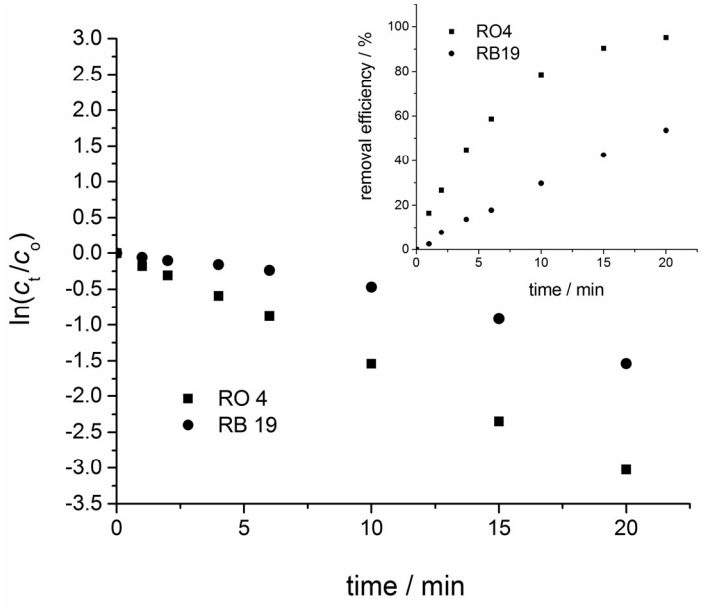

Fig. 2. Effect of UV/H_2O_2 process on decolorization of RO4 and RB19. [dye]$_0$ = 50 mg dm^{-3}, [H_2O_2]$_0$ = 25 mmol dm^{-3}, initial pH 7, UV radiation intensity 730 μW cm^{-2}, temperature 25.0±0.5 °C. Inset shows the relation between removal efficiency and illumination time.

This is a typical pseudo-first-order reaction with respect to dye concentration [21,23,26–28]. The kinetic constant can be linked to dye concentration by the following equation:

$$\ln(c_t/c_0) = -kt \quad (1)$$

where c_t is the concentration of dye after irradiation time t, c_0 is dye concentration at t = 0 and k (min^{-1}) is apparent pseudo-first rate constant. A linear fit was done for the first 15 min of the treatment. In all experimental results, the values of square of relative correlation coefficients (R^2) were higher than 0.98 which confirmed proposed kinetic model.

Effect of H_2O_2

Hydrogen peroxide concentration is an important parameter for the decolorization of the color in the UV/H_2O_2 process. Due to a low molar absorption coefficient of H_2O_2 at 254 nm [29], an excess of H_2O_2 is theoretically needed to produce enough hydroxyl radicals.

However in our previous work [21] in addition to other reports [30,31], we observed that the concentration of H_2O_2 may either enhance or inhibit the photoreaction rate depending on concentration. Therefore, an optimum concentration of H_2O_2 in the reaction course must be reached. The effect of the initial concentration of H_2O_2 (10, 20, 30, 40, 60, 80 and 100 mmol dm^{-3}) on the photodecolorization efficiency of the system was investigated using fixed concentrations of dyes (50 mg dm^{-3}) at pH 7.0 and 25.0±0.5 °C. The applied UV light intensity was 730 μW cm^{-2}, because of too fast decolorization at maximal value (1950 μW cm^{-2}), which made the investigation of this operational parameter difficult. The apparent rate constants versus different initial concentrations of H_2O_2 have been summarized in Fig. 3.

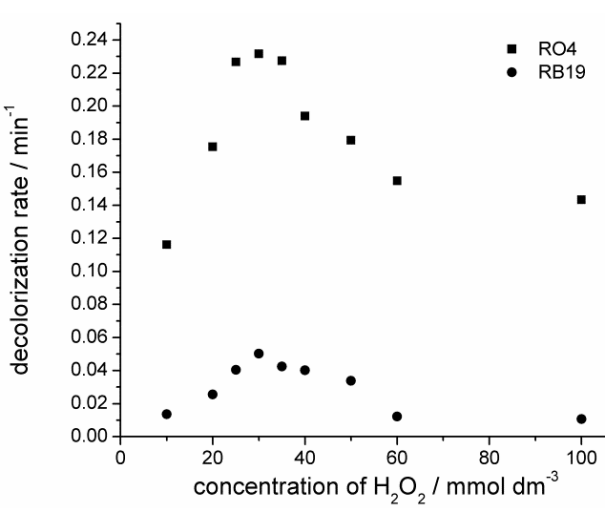

Fig. 3. Effect of initial peroxide concentration on the rate of decolorization of RO4 and RB19 by UV/H_2O_2 process. [dye]$_0$ = = 50 mg dm^{-3}, initial pH 7, UV radiation intensity 730 μW cm^{-2}, temperature 25.0 ± 0.5 °C.

Figure 3 shows that the addition of H_2O_2 from 10 to 30 mmol dm^{-3} increases the apparent constant rate from 0.116 to 0.232 min^{-1} for RO4 and from 0.015 to 0.053 min^{-1} for RB19. Further increase of H_2O_2 concentration above 30 mmol dm^{-3} decreases the apparent constant rate from 0.232 to 0.143 min^{-1} for RO4 and from 0.053 to 0.017 min^{-1} for RB19. This occurrence

can be explained by two opposing effects with increasing H_2O_2 concentration:

1) At low concentration of H_2O_2, relatively low concentration of $^{\bullet}OH$ was formed for dye oxidation, which results in low decolorization rate. Nevertheless, by increasing peroxide concentration, more $^{\bullet}OH$ were generated upon its photodissociation [32].

2) The $^{\bullet}OH$ free radicals produced upon photolysis of H_2O_2 can react with dye molecules, but also with an excess of H_2O_2. Excess of hydrogen peroxide and high $^{\bullet}OH$ concentration result in competitive reactions, producing an inhibitory effect on the decolorization. $^{\bullet}OH$ radicals are prone to react or to recombine [33].

When the initial peroxide concentration is very high, the generated $^{\bullet}OH$ mostly react by excess of peroxide and produce hydroperoxyl radical, $HO_2^{\bullet}$, which are less reactive than $^{\bullet}OH$, and the rate of dye removal decreased. Generated $^{\bullet}OH$ can also react with $HO_2^{\bullet}$ and produce water and dioxigen or dimerize to H_2O_2 and the concentration of $^{\bullet}OH$ available for dye decolorization also decreased [34]. A very important parameter for the optimization of the method is the determination of adequate amount of H_2O_2, to avoid reagent surplus which can slow down the decolorization. The results of Fig. 3 point out the negative effect of a defect or excess of concentration of H_2O_2 on the decolorization rate. We can observe an optimum value at about 30 mmol dm^{-3} for the hydrogen peroxide concentration.

Effect of pH

Since the waste water from the textile industry can be of different pH values, we have studied the effect of pH on the decolorization rate. The solutions of the dyes were adjusted to the desired pH by addition of HCl or NaOH. The different concentrations of acid or base have been chosen in order to add the minimum quantity of these species to avoid the volume change of the reaction mixture.

To investigate the effect of initial pH, the solutions of RO4 and RB19 were irradiated at various initial pH (2,3,5,7,9, 10 and 11), during 20 min of treatment time, using 50 mg dm^{-3} dye solutions, 25 mmol dm^{-3} H_2O_2 and radiation intensity 730 μW cm^{-2}. The decolorization rate constants of dyes as a function of the reaction pH are shown in Fig. 4.

The decolorization rate of RO4 increases from 0.062 to 0.152 min^{-1} with increasing pH from 2 to 7. After this value we have observed a decrease of the decolorization rate to 0.067 min^{-1} as the pH increases to 11. In case of other dye RB19, a steady increase in rate constants with increasing pH was observed. This is perhaps a consequence of different structures of these two dyes.

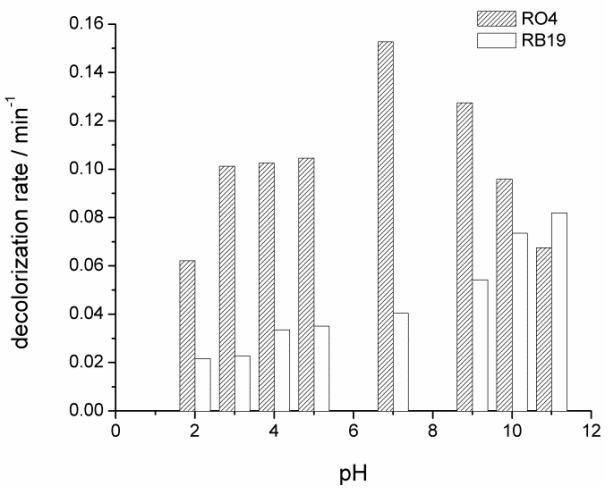

Fig. 4. Effect of pH on the rate of decolorization of RO4 and RB19 by UV/H_2O_2 process. $[dye]_0$ = 50 mg dm^{-3}, $[H_2O_2]_0$ = 25 mmol dm^{-3}, UV radiation intensity 730 μW cm^{-2}, temperature 25.0±0.5 °C.

Effect of initial dye concentration

The pollutant concentration is one of the important parameters in UV/H_2O_2 process. The effect of the initial RO4 concentration on the efficiency of dye decolorization was investigated at a concentration range from 10 up to 100 mg dm^{-3}, using fixed concentrations of H_2O_2 (25 mmol dm^{-3}) at pH 7.0, 25.0±0.5 °C and UV light intensity 730 μW cm^{-2} during 20 min of treatment time. The results are shown in Fig. 5.

It is evident that removal efficiency (*RE*) decreased with the increase of initial dyes concentrations from 10 to 100 mg dm^{-3}. This can be explained by considering that both aromatic dyes and H_2O_2 absorb UV radiation in the range emitted by the lamp. However, the molar absorption coefficient of dyes at 254 nm is higher than that of H_2O_2, so that an increase in dyes concentration induces a rise of the internal optical density and the solution becomes more and more impermeable to UV radiation. Then, H_2O_2 can only be irradiated by a smaller portion of UV light to form lower free radicals and the removal efficiency decreases.

Fenton and photo-Fenton process

As described above, the photodecolorization of reactive dyes was mainly initiated by the production of $^{\bullet}OH$ resulting from the direct photolysis of H_2O_2. Degradation experiments using Fenton and photo-Fenton processes were studied to investigate the effect of increased production of $^{\bullet}OH$.

In these processes $^{\bullet}OH$ radicals are produced by catalytic decomposition of H_2O_2 in the reaction with Fe^{2+} (Eq. (2)) and UV light (for photo-Fenton process) [35]. The mechanism of the Fenton's process can be summarized by the following steps:

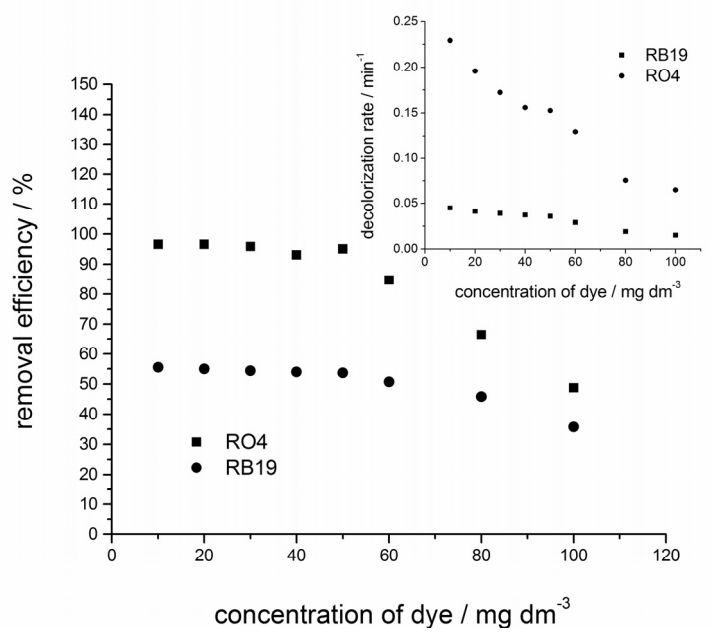

Fig. 5. Effect of initial dye concentration on the removal efficiency of RO4 and RB19 by UV/H_2O_2 process. $[H_2O_2]_0$ = 25 mmol dm^{-3}, initial pH 7, UV radiation intensity 730 μW cm^{-2}, temperature 25.0±0.5 °C. Inset shows the relation between decolorization rate and initial dye concentration.

1) Mixture of H_2O_2 and Fe^{2+} in acidic solution generates the $^{\bullet}$OH (Eq. (2)) [36,37], which will subsequently attack the organic compounds present in the solution:

$$Fe^{2+} + H_2O_2 \rightarrow Fe^{3+} + HO^- + HO^{\bullet} \quad (2)$$

2) As Fe^{2+} acts as a catalyst, it has to be regenerated, which happened through the following scheme:

$$Fe^{3+} + H_2O_2 \Leftrightarrow Fe - OOH_2^{\ +} + H^+ \quad (3)$$

$$Fe - OOH_2^{\ +} \rightarrow Fe^{2+} + HO_2^{\bullet} \quad (4)$$

The photo-Fenton process is nearly similar to the Fenton one, but includes also radiation. Additional reactions occur in the presence of light that produce $^{\bullet}$OH [32] or increase the production rate of $^{\bullet}$OH [38]. The obtained Fe^{3+} or its complexes behave as the light absorbing species that produces another radical, and the initial Fe^{2+} is regenerated as seen in Eqs. (5) and (6) [38,39]:

$$Fe^{3+} + H_2O_2 + h\nu \rightarrow Fe^{2+} + H^+ + HO^{\bullet} \quad (5)$$

$$\left[Fe^{3+} + Ln\right] + h\nu \rightarrow \left[Fe^{2+} + Ln^{-1}\right] L^{\bullet} \quad (6)$$

The conclusion is that in this process, the regeneration of Fe^{2+} by photo-reduction of Fe^{3+} (Eqs. (5) and (6)) is accelerated and photo-reduction is an additional source of highly oxidative $^{\bullet}$OH (Eq. 5), as compared with the Fenton's process. This is the reason of higher efficiency of photo-Fenton than Fenton process.

Effect of Fe^{2+} on Fenton and photo-Fenton process

For Fenton and photo-Fenton processes, the concentration of Fe^{2+} is one of the important parameters. To investigate the effect of Fe^{2+} on the decolorization of RO4 and RB19, a series of experiments were conducted by varying Fe^{2+} concentration from 0.05 to 1 mmol dm^{-3}, at fixed pH, initial concentration of H_2O_2 and dyes.

The RO4 and RB19 initial decolorization rate for various concentrations of Fe^{2+} was presented in Fig. 6.

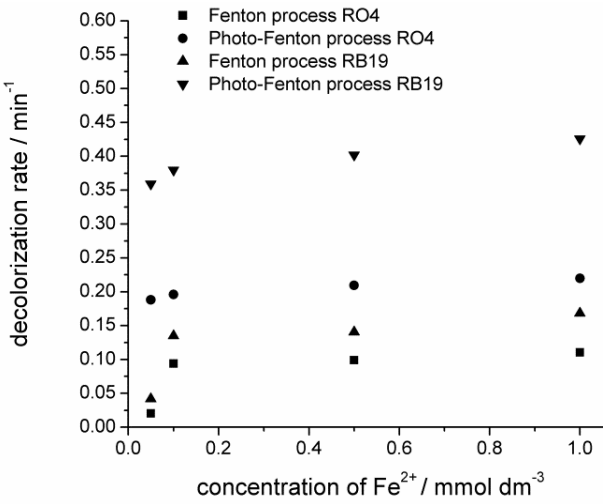

Fig. 6. Effect of initial Fe^{2+} concentration on the rate of decolorization of RO4 and RB19. $[dye]_0$ = 50 mg dm^{-3}, $[H_2O_2]_0$ = 25 mmol dm^{-3}, UV radiation intensity 730 μW cm^{-2}, temperature 25.0±0.5 °C.

From the Fig. 6. it can be seen that there is slight difference in the efficiency of Fenton and photo-Fenton processes at concentrations of Fe^{2+} from 0.1 to 1 mmol dm^{-3}. Therefore for further experiments as an optimal concentration of Fe^{2+} was used 0.1 mmol dm^{-3} in order to lessen risk of the ions excess and eventual forming of an iron sludge. The results showed that in Fenton process addition of Fe^{2+} from 0.05 to 1 mmol dm^{-3} increases decolorization rate from 0.020 to 0.110 min^{-1} for RO4 and from 0.042 min^{-1} to 0.168 for RB19. In photo-Fenton process the increase is from 0.188 to 0.220 min^{-1} for RO4 and from 0.359 to 0.425 min^{-1} for RB19 for the same addition of Fe^{2+}. Hence, photo-Fenton process is more efficient than Fenton process. Decolorization of dyes is mainly due to hydroxyl radical generated by chemical and photochemical reactions of each process. The reason of this increase is more produced $^{\bullet}OH$ with the increase in the concentration of Fe^{2+}.

Effect of H_2O_2

Initial concentration of H_2O_2 plays an important role in the Fenton and photo-Fenton processes. The effect of addition of H_2O_2 from 5 to 50 mmol dm^{-3}, at fixed pH, initial concentration of Fe^{2+} and dye, on the decolorization of RO4 and RB19 by both processes is shown in Fig. 7.

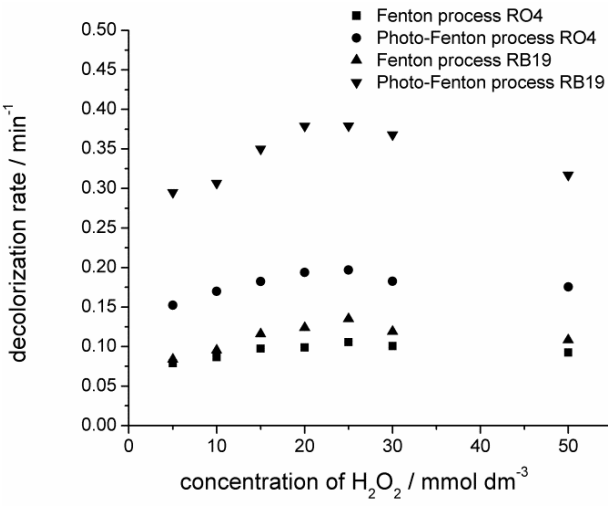

Fig. 7. Effect of initial peroxide concentration on the rate of decolorization of RO4 and RB19 by Fenton and photo-Fenton processes. $[dye]_0$ = 50 mg dm^{-3}, $[Fe^{2+}]_0$ = 0.1 mmol dm^{-3}, UV radiation intensity 730 μW cm^{-2}, temperature 25.0±0.5 °C.

In Fenton and photo-Fenton processes, the addition of H_2O_2 from 5 to 25 mmol dm^{-3} increases the decolorization rate. Further increase from 25 to 50 mmol dm^{-3} causes the decrease of decolorization rate for both processes.

The increase in the decolorization by the addition of H_2O_2 is due to increase in the $^{\bullet}OH$ concentration [32]. But at high dosage of H_2O_2 the decrease in decolorization is due to the $^{\bullet}OH$ radical scavenging effect of H_2O_2 and recombination of $^{\bullet}OH$ [34,40]. Hence, 25 mmol dm^{-3} of H_2O_2 appear as optimal dosages for Fenton and photo-Fenton processes.

Effect of initial dye concentration

Influence of concentration of the RO4 and RB19 dye on its decolorization was examined in this study, varying dye concentration from 10 to 100 mg dm^{-3}, at fixed pH, initial concentration of H_2O_2 and Fe^{2+}. The effect of initial dye concentration in these processes is shown in Fig. 8.

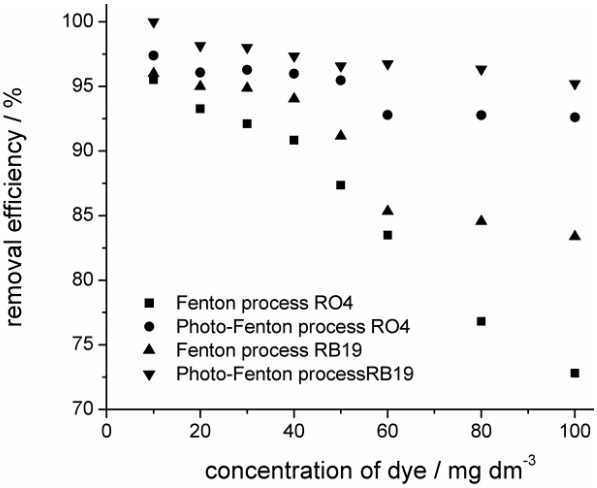

Fig. 8. Effect of initial dye concentration on the removal efficiency of RO4 and RB19 by Fenton and photo-Fenton processes. $[H_2O_2]_0$ = 25 mmol dm^{-3}, $[Fe^{2+}]_0$ = 0.1 mmol dm^{-3}, UV radiation intensity 730 μW cm^{-2}, temperature 25.0±0.5 °C.

The figures clearly reveal that the increase in dye concentration from 10 to 100 mg dm^{-3} decreases the removal efficiency for Fenton and for photo-Fenton process in 20 min. The results are shown in Fig. 8. $^{\bullet}OH$ is mainly responsible for dye decolorization and its concentration remains constant for all dye concentrations. The increase in dye concentration increases the number of dye molecules and not the $^{\bullet}OH$ radical concentration and so the removal efficiency decreases. Photochemical processes extremely depend on solution absorption. in solutions with high absorption, *e.g.*, dye solution, the penetration of light can be very limited. In photo-Fenton process there is a strong light absorption of the dye solution at high concentration which causes lowering concentration of $^{\bullet}OH$ radicals and decrease of removal efficiency.

Comparison of UV/H_2O_2, Fenton and photo-Fenton processes

Comparison of efficiencies of UV/H_2O_2, Fenton and photo-Fenton processes on decolorization of RO4 and RB19 was presented in Fig. 9. For comparison of these

processes we studied decolorization on optimum conditions for all processes.

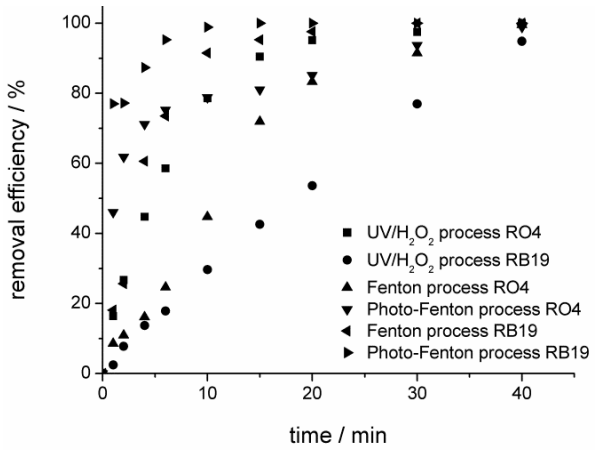

Fig. 9. Comparison of removal efficiency of RO4 and RB19 by UV/H_2O_2, Fenton and photo-Fenton processes.

Among the processes tested here for RO4 and RB19 dyes decolorization, the ranking of efficiency of color removal was as follows: photo-Fenton process > UV/H_2O_2 > Fenton reagent for RO4 and photo-Fenton process > Fenton reagent > UV/H_2O_2 for RB19. The photo-Fenton process achieved decolorization in 15 min for RO4 and 10 min for RB19, UV/H_2O_2 process in about 20 min for RO4 and 40 min for RB19 and Fenton process in about 30 min for RO4 and RB19.

From these results, it can be concluded that the photo-Fenton process is highly efficient at degrading RO4 and RB19 dyes. Purification of water and wastewater using the Fenton and photo-Fenton processes tend to be less expensive to build and operate than most other AOPs. But on the other hand, the operations of Fenton-type processes usually require strict pH control as they are most efficient at pH 2.8 [41]. Iron sludge usually forms, after the process is completed and neutralization is carried out, which requires appropriate disposal [14]. In the case of UV/H_2O_2 the final products of dyes degradation are carbon dioxide, water and inert salts. Therefore this process is a promising environmental engineering technique.

Decolorization of dyes in simulated dyebath effluent

According to previous research [42], wastewater composition from textile industries can greatly influence the photochemical oxidation process. Certain ions found at high concentrations in textile wastewater can affect the process.

In order to relate the present study to the real situation which comes out from the commercial dyeing of cotton, a simulated spent dye bath was formulated and its response to photodecolorization was tested. The reactive dyebath effluent was simulated by dissolving proper amounts of two commercial reactive dyestuff formulations and dye assisting chemicals in hot (T = 70 °C) deionized water. Acetic acid for neutralization and Kutregal PN as surfactant were used as assisting chemicals. Surfactants are used for the purpose of improving dispersing properties. They are also used to achieve a better contact between dyestuff formulations and fabric and improve dye diffusion through the fabric pores. The exact composition of the simulated reactive dyebath is given in Table 1. For preparing a model effluent, simulated dyebath effluent was diluted to get a new solution with 50.0 mg dm^{-3} of dyes. The highest percentage of the removal of RO4 and RB19 by photo-Fenton process was achieved after 15 min irradiation. Based on the results previously shown for the solutions of the dyes in water alone and the results for the simulated dyebath effluent shown in Table 2, it can be concluded that the decolorization efficiency is higher for solutions of the dyes in water alone than for the dyes in a simulated dyebath effluent for both dyes types.

Table 1. Composition of the simulated reactive dyebath

Reactive dyebath component	Concentration in the dyebath, g dm^{-3}
Reactive Orange 4 (azo type)	2.5
Reactive Blue 19 (anthraquinone type)	2.5
“Kutregal PN” (dispersing properties)	0.5
Acetic acid (neutralization)	0.79

CONCLUSION

In this study, we assessed the possibility of different AOPs for RO4 and RB19 decolorization. UV/H_2O_2 process was obviously affected by the initial pH and the amount of hydrogen peroxide. Desired amount of peroxide was 30 mmol dm^{-3}, with RO4 and RB19 concentrations of 50 mg dm^{-3} for UV/H_2O_2, Fenton and photo-Fenton processes, while optimum UV light intensity for

Table 2. Removal efficiency of RO4 and RB19 in simulated dyebath effluent after 15 min. $[dye]_0$ = 50 mg dm^{-3}

Process	Removal efficiency (RO4), %		Removal efficiency (RB19), %	
	The solutions of the dyes in water alone	The simulated dyebath effluent	The solutions of the dyes in water alone	The simulated dyebath effluent
UV/H_2O_2	90.45	46.49	42.57	32.57
Fenton	71.94	35.59	81.06	72.31
Photo-Fenton	95.29	91.63	98.25	87.72

UV/H_2O_2 and photo-Fenton processes was 730 μW cm^{-2}. The best working condition was found for an initial Fe^{2+} concentration of 0.1 mmol dm^{-3} for Fenton and photo-Fenton processes. The removal efficiency of these three processes is in the following order: photo-Fenton process > UV/H_2O_2 > Fenton reagent for RO4 and photo-Fenton process > Fenton reagent > UV/H_2O_2 for RB19. The decolorization efficiency is higher for solutions of the dyes in water alone than for dyes in a simulated dyebath effluent.

Acknowledgement

Authors would like to acknowledge for financial support to the Ministry of Education, Science and Technological Development of the Republic of Serbia (Grant No. TR34008).

REFERENCES

[1] S. Padmavathy, S. Sandhya, K. Swaminathan, Y.V. Subrahmanyam, T. Chakrabarti, S.N. Kaul, Aerobic decolorization of reactive azo dyes in presence of various cosubstrates, Chem. Biochem. Eng. Q. **17** (2003) 147–151.

[2] H. Zhang, L. Duan, Y. Zhang, F. Wu, The use of ultrasound to enhance the decolorization of the C.I. Acid Orange 7 by zero-valent iron, Dyes Pigm. **65** (2005) 39–43.

[3] C. Galindo, P. Jacques, A. Kalt, Photochemical and photocatalytic degradation of an indigolid dye: a casecstudy of acid blue 74 (AB74), J. Photochem. Photobiol., A **141** (2001) 47–56.

[4] T. Sauer, G.C. Neto, H.J. Jose, R.F.P. M. Moreira, Kinetics of photocatalytic degradation of reactive dyes in a TiO_2 slurry reactor, J. Photochem. Photobiol., A **149** (2002) 147–154.

[5] W.S. Kuo, P.H. Ho, Solar photocatalytic decoloriyation of methylene blue in water, Chemosphere **45** (2001) 77–83.

[6] Z. Sun, Y. Chen, Q. Ke, Y. Yang, J. Yang, Photocatalytic degradation of cationic azo dye by TiO_2/bentonite nanocomposite, J. Photochem. Photobiol. A **149** (2002) 169–174.

[7] L.G. Devi, S.G. Kumar, K.M. Reddy, C. Munikrishappa, Photo degradation of Methyl Orange an azo dye by Advance Fenton Process using zero valent metallic iron: Infuence of varius reaction parameters and its degradation mechanism, J. Hazard. Mater. **164** (2009) 459–467.

[8] S. Parsons, Advansed oxidation processes for water and wastewater treatment, IWA, London, 2004.

[9] H. Zollinger, Color Chemistry: Syntheses, Properties and Applications of Organic Dyes and Pigments, Wiley, Germany, 2003.

[10] M.H. Habibi, A. Hassanzadeh, S. Mahdavi, The effect of operational parameters on the photocatalytic degradation of three textile azo dyes in aqueous TiO_2 suspensions, J. Photochem. Photobiol., A **172** (2005) 89–96.

[11] N. Daneshvar, H. Ashassi-Sorkhabi, A. Tizpar, Decolorization of orange II by electrocoagulation method, Sep. Purif. Technol. **31** (2003) 153–162.

[12] K. Tanaka, K. Padermpole, T. Hisanage, Photocatalytic degradation of commercial azo dyes, Water Res. **34** (2000) 327–333.

[13] C. Hachem, F. Boequillon, O. Zahraa, M. Bouchy, Decolorization of textile industry wastewater by the photocatalytic degradation process, Dyes Pigm. **49** (2001) 117–125.

[14] R. Andreozzi, V. Caprio, A. Insola, R. Marotta, Advanced oxidation processes (AOP) for water purification and recovery, Catal. Today **53** (1999) 51–59.

[15] W.M. Ralph, Photooxidative degradation of coloured organics in water using supported catalysts. TiO_2 on sand, Water Res. **25** (1991) 1169–1176.

[16] W.Z. Tang, H. An, UV/TiO_2 photocatalytic oxidation of commercial dyes in aqueous solutions, Chemosphere **31** (1995) 4157–4170.

[17] C.L. Hsueh, Y.H. Huang, C.C. Wang, C.Y. Chen, Degradation of azo dyes using low Fe concentration of Fenton and Fenton-like system, Chemosphere **58** (2005) 1409–1414.

[18] N. Daneshvar, A.R. Khataee, Removal of azo dye C.I. Acid Red 14 from contaminated water using Fenton, UV/H_2O_2, UV/H_2O_2/Fe(II), UV/H_2O_2/Fe(III) and UV/H_2O_2/Fe(III)/oxalate processes: a comparative study, J. Environ. Sci. Health, A **41** (2006) 315–328.

[19] M. Le Marechal, Y.M. Slokar, T. Taufer, Decolorisation of chlortriazine reactive azo dyes with UV/H_2O_2, Dyes Pigm. **33** (1997) 281–298.

[20] O. Legrini, E. Oliveros, A.M. Braun, Photochemical Processes for Water Treatment, Chem. Rev. **93** (1993) 671–698.

[21] J. Mitrović, M. Radović, D. Bojić, T. Anđelković, M. Purenović, A. Bojić, Decolorization of textile azo dye Reactive Orange 16 with UV/H_2O_2 process, J. Serb. Chem. Soc. **77** (2012) 465–481.

[22] C.G. Namboodri, W.K. Walsh, Ultraviolet light/hydrogen peroxide system for decolourizing spent reactive dyebath waste water, Am. Dyest Rep. **85** (1996) 15–25.

[23] J.R. Guimaraes, M.G. Maniero, R.N. De Araujo, A comparative study on the degradation of RB-19 dye in aqueous medium by advanced oxidation processes, J. Environ. Manage. **110** (2012) 33–39.

[24] M. Muruganandham, M. Swaminathan, Photochemical oxidation of reactive azo dye with UV-H_2O_2 process, Dyes Pigm. **62** (2004) 269–275.

[25] A.R. Khataee, V. Vatanpour, A.R. A. Ghadim, Decolorization of C.I. Acid Blue 9 solution by UV/Nano-TiO_2, Fenton, Fenton-like, electro-Fenton and electrocoagulation processes: A comparative study, J. Hazard. Mater. **161** (2009) 1225–1233.

[26] P.K. Malik, S.K. Sanyal, Kinetics of decolourisation of azo dyes in wastewater by UV/H_2O_2 process, Sep. Purif. Technol. **36** (2004) 167–175.

[27] A. Aleboyeh, Y. Moussa, H. Aleboyeh, The effect of operational parameters on UV/H_2O_2 decolourisation of Acid Blue 74, Dyes Pigm. **66** (2005) 192–134.

[28] B. Xu, N. Gao, H. Cheng, S. Xia, M. Rui, D. Zhao, Oxidative degradation of dimethyl-phthalate (DMP) by UV/H_2O_2 process, J. Hazard. Mater. **162** (2009) 954–959.

[29] K. Li, D.R. Hokanson, J.C. Crittenden, R.R. Trussell, D. Minakata, Evaluating UV/H2O2 processes for methyl tert-butyl ether and tertiary butyl alcohol removal: Effect of pretreatment options and light sources, Water Res. **42** (2008) 5045–5053.

[30] H. Ghodbane, O. Hamdaoui, Decolorization of antraquinonic dye,C.I. Acid Blue 25, in aqueous solution by direct UV irradiation, UV/H_2O_2 and UV/Fe(II) processes, Chem. Eng. J. **160** (2010) 226–231.

[31] D. Jiraroj, F. Unob, A. Hagege, Degradation of Pb–EDTA complex by a H_2O_2/UV process, Water Res. **40** (2006) 107–112.

[32] F.H. Al Hamedi, M.A. Rauf, S.S. Ashraf, Degradation studies of Rhodamine B in the presence of UV/H_2O_2, Desalination **239** (2009) 159–166.

[33] J.H. Baxendale, J.A. Wilson, The photolysis of hydrogen peroxide at high intensities, Trans. Farad. Soc. **53** (1957) 344–356.

[34] G.V. Buxton, C.L. Greenstock, W.P. Helman, A.B. Ross, Critical review of rate constants of hydrated electrons, hydrogen atoms and hydroxyl radicals (AOH/AO^-) in aqueous solution, J. Phys. Chem. Ref. Data **17** (1988) 513–886.

[35] E. Chamarro, E. Marco, S. Esplugas, Use of Fenton reagent to improve organic chemical biodegradability, Water Res. **35** (2001) 1047–1051.

[36] C. Walling, Fenton's reagent revisited. Accounts of Chemical Research, Acc. Chem. Res. **8** (1975) 125–131.

[37] W. Li, V. Nanaboina, Q. Zhou, G.V. Korshin, Effect of Fenton treatment on the properties of effluent organic matter and their relationships with the degradation of pharmaceuticals and personal care products, Water Res. **46** (2012) 403–412.

[38] H. Fallmann, T. Krutzler, R. Bauer, S. Malato, J. Blanco, Applicability of the Photo-Fenton method for treating water containing pesticides, Catal. Today **54** (1999) 309––319.

[39] C.R. Silva, M.G. Maniero, S. Rath, J.R. Guimaraes, Degradation of flumequine by Fenton and photo-Fenton processes: Evaluation of residual antimicrobial activity, Sci. Total Environ. **445–446** (2013) 337–346.

[40] K. Schested, O.L. Rasmussen, H. Fricke, Rate constants of $^{\bullet}OH$ with $HO_2^{\bullet}$, $O_2^{\bullet-}$ and $H_2O_2^{+}$ from hydrogen peroxide formation in pulse-irradiated oxygenated water, J. Phys. Chem. **72** (1968) 626–631.

[41] C. Fan, L. Tsui, M.C. Liao, Parathion degradation and its intermediate formation by Fenton process in neutral environment, Chemosphere **82** (2011) 229–236.

[42] I. Arslan, I.A. Balcioglu, T. Tuhkanen, D. Bahnemann, H_2O_2/UV-C and Fe^{2+}/ H_2O_2/UV-C versus TiO2/UV-A treatment for reactive dye wastewater, J. Environ. Eng. **126** (2000) 903–911.

IZVOD

POREĐENJE ULTRALJUBIČASTO ZRAČENJE/VODONIK- PEROKSID, FENTON I FOTO-FENTON PROCESA ZA DEKOLORIZACIJU REAKTIVNIH BOJA

Miljana D. Radović, Jelena Z.Mitrović, Miloš M. Kostić, Danijela V. Bojić, Milica M. Petrović, Slobodan M. Najdanović, Aleksandar Lj. Bojić

Departman za hemiju, Prirodno–matematički fakultet, Univerzitet u Nišu, Srbija

(Naučni rad)

U ovom radu ispitivana je efikasnost dekolorizacije komercijalno važnih tekstilnih boja Reactive Orange 4 (RO4) i Reactive Blue 19 (RB19) procesima UV/H_2O_2, Fenton i foto-Fenton. Tretmani fotodekolorizacije su vršeni u UV reaktoru, originalne izrade, sa živinim lampama niskog pritiska čiji je maksimum energije zračenja na talasnoj dužini 254 nm. Ispitivan je uticaj parametara procesa kao što su inicijalni pH, inicijalna koncentracija H_2O_2, inicijalna koncentracija Fe^{2+} i inicijalna koncentracija boja, na efikasnost dekolorizacije boja RO4 i RB19. Rezultati su pokazali da je potpuna dekolorozacija UV/H_2O_2 procesom postignuta za manje od 20 min za tekstilnu boju RO4, odnosno za manje od 40 min za tekstilnu boju RB19. Fenton procesom potpuno uklanjanje boje bilo je postignuto u vremenskom periodu od 30 min. Najefikasnija metoda za dekolorizaciju ove dve boje bio je foto--Fenton proces gde je efikasnost dekolorizacije od 95% postignuta za 15 min. Daljim istraživanjem utvrđeno je da je foto-Fenton proces bio efikasniji od UV/ /H_2O_2 i Fenton procesa za dekolorizaciju boja u simuliranim otpadnim vodama kada za bojenje, pri optimalnim uslovima procesa. U simuliranim kadama za bojenje efikasnost uklanjanja je nešto niža u odnosu na efikasnost uklanjanja u vodenim rastvorima boja. Rezultati su pokazali da se ispitivani unapređeni oksidacioni procesi mogu primeniti kao efikasni tretmani za uklanjanje boja RO4 i RB19 iz otpadnih i prirodnih voda.

Ključne reči: Boje • Fenton proces • Oksidacija • Foto-Fenton proces • UV/H_2O_2 proces

Plant waste materials from restaurants as the adsorbents for dyes

Marija D. Pavlović, Ivan R. Nikolić, Milica D. Milutinović, Suzana I. Dimitrijević-Branković, Slavica S. Šiler-Marinković, Dušan G. Antonović

Faculty of Technology and Metallurgy, University of Belgrade, Department of Biochemical Engineering and Biotechnology, Belgrade, Serbia

Abstract

This paper has demonstrated the valorization of inexpensive and readily available restaurant waste containing most consumed food and beverage residues as adsorbents for methylene blue dye. Coffee, tea, lettuce and citrus waste have been utilized without any pre-treatment, thus the adsorption capacities and dye removal efficiency were determined. Coffee waste showed the highest adsorbent capacity, followed by tea, lettuce and citrus waste. The dye removal was more effective as dye concentration increases from 5 up to 60 mg/L. The favorable results obtained for lettuce waste have been especially encouraged, as this material has not been commonly employed for sorption purposes. Equilibrium data fitted very well in a Freundlich isotherm model, whereas pseudo-second-order kinetic model describes the process behavior. Restaurant waste performed rapid dye removal at no cost, so it can be adopted and widely used in industries for contaminated water treatment.

Keywords: adsorption, dye, restaurant waste, isotherms, kinetics.

Available online at the Journal website: http://www.ache.org.rs/HI/

SCIENTIFIC PAPER

UDC 66.081.3:667.2:628.4

Hem. Ind. **69** (6) 667–677 (2015)

doi: 10.2298/HEMIND140917089P

The discharge of dyes in the environment is a matter of concern for both toxicological and aesthetic reasons. Many industries use dyes in order to color their products. As a result, they generate a considerable amount of colored wastewater. Most of the dyes are toxic, mutagenic and carcinogenic [1]. Furthermore, wastewater containing dyes is very difficult to be treated, since the dyes are recalcitrant organic molecules, resistant to aerobic digestion, and stable to light, heat and oxidizing agents [2]. Many techniques have been investigated for such purposes [3–14], but adsorption is considered to be relatively superior to others, because of low cost, simplicity of design and ability to treat dyes in more concentrated form [15]. Besides activated carbons, these are well known commercial adsorbents, some waste materials may also offer an inexpensive and renewable additional alternative for such processes. Waste materials have little or no economic value and often present a disposal problem [16].

According to the authors' knowledge, no attempt has been made to use restaurant food waste for removal of dyes from contaminated waters. Restaurants daily generate large quantities of food residues. Thus, coffee and tea waste, followed by lettuce and mix of citrus fruit waste have been utilized for sorption purposes. This waste is inexpensive and does not require an additional pre-treatment step before its application. In addition, an efficient management of such waste is very desirable. Methylene blue (MB) dye was selected as a model compound in adsorption experiments. It is a basic dye with the structure of heterocyclic aromatic chemical compound [17] that has been widely applied, including coloring paper, temporary hair colorations, dyeing cottons, wools, and coating for paper stock [18]. In water streams, it can cause some harmful effects on human health [18].

The aim of this study was to evaluate the adsorption capacity of restaurant waste, without any pre-treatment, for methylene blue dye removal from its aqueous solutions. The work has been designed to represent a comparative review of coffee, tea, lettuce and citrus residues capabilities for MB uptake efficiency. The second objective was to investigate the sorption equilibrium behaviors using several most commonly used isotherm models. Finally, kinetic studies have been conducted in order to determine the rate of MB adsorption and analyze the mechanism of the process for each of the tested adsorbents.

MATERIAL AND METHODS

Materials

Coffee residues, as well as tea, lettuce and citrus residues were obtained from „Hotel-Restaurant Hyatt", Belgrade, Serbia. All materials, one by one, separately, were rinsed well with distilled water to remove any dirt, and then were dried in an oven at 110 °C for 24 h. Dry materials were crushed and powdered. The pow-

Correspondence: M.D. Pavlović, Faculty of Technology and Metallurgy, University of Belgrade, Department of Biochemical Engineering and Biotechnology, Karnegijeva 4, 11000 Belgrade, Serbia.

E-mail: marija.pavlovic@tmf.bg.ac.rs

Paper received: 17 September, 2014

Paper accepted: 23 December, 2014

dered materials (except for coffee residues) were sieved to obtain a particle size < 0.5 mm. Obtained samples were stored in sealed vials and used for further experimental work.

Preparation of dye stock solution

Methylene blue (MB) dye was obtained from Acros Organics, New Jersey, USA. A stock solution of 100 mg/L of the dye was prepared by dissolving 0.1 g in 1 L of distilled water. The working concentrations of the dye in aqueous solutions were varied from 5 to 60 mg/L by diluting the MB stock solution with distilled water. Fresh dilutions of desired dye concentrations were prepared at the beginning of each experiment, without any adjustment of pH values.

Dye adsorption experiments

100 mL of MB solutions with different initial concentrations of 5–60 mg/L were placed in a series of 250 mL Erlenmeyer flask. 0.70 g of the adsorbent was added into each flask and placed in translatory shaker (IKA – KS 4000i control, Staufen, Germany) at room temperature (27 °C), at 120 rpm, for the time period of 180 min. After a certain time, samples were collected, filtered and analyzed by UV/Vis spectrophotometer (Ultrospec 3300 pro, Amersham Biosciences, USA) at 668 nm for residual dye concentration. This experimental procedure has been repeated for each adsorbent individual. The MB removal in the aqueous solution was computed by monitoring the dye removal percentage (Eq. (1)) and adsorption capacity (Eq. (2)):

$$\text{MB removal (\%)} = 100\left(\frac{c_\text{i} - c_\text{e}}{c_\text{e}}\right) \tag{1}$$

$$q = \frac{(c_\text{i} - c_\text{e})V}{m_\text{ads}} \tag{2}$$

where c_i and c_e are the initial and equilibrium MB concentrations (mg/L), respectively, q is the adsorption capacity (mg/g), m_{ads} is adsorbent dose (g) and V is solution volume (L) [19]. All the experiments were performed in triplicate and their mean values have been reported here.

Adsorption isotherms

Equilibrium experiments were conducted by contacting of 100 mL of different initial dye concentrations (5, 10, 20, 40, 50 and 60 mg/L) with 0.70 g of the adsorbent in six different capped 250 mL Erlenmeyer flasks. The contact was made using a translatory shaker at a constant agitation speed of 120 rpm, at room temperature of 27 °C. The agitation has been made for 180 min. Samples were collected, filtered and analyzed spectrophotometrically at 668 nm.

The most widely used isotherm models, named Langmuir, Freundlich, Temkin–Pyzhev and Dubinin–Radushkevich, have been employed for adsorption isotherm modeling of the experimental data.

The Langmuir model assumes that the adsorbent surface contains energetically homogenous cites, where the monolayer surface coverage is formed with no interactions between the molecules adsorbed [20]. The model can be presented in the linear form of modified Langmuir-2 Equation:

$$\frac{1}{q_\text{e}} = \left(\frac{1}{K_\text{L} q_\text{m}}\right)\frac{1}{c_\text{e}} + \frac{1}{q_\text{m}} \tag{3}$$

where q_e (mg/g) is the amount of dye adsorbed per unit weight of adsorbent, q_m (mg/g) indicates the monolayer sorption capacity of adsorbent and the Langmuir constant K_L (L/mg) is a direct measure of the intensity of adsorption [20].

The Freundlich isotherm model considers multilayer and heterogeneous surface adsorption [21]. The linear form of the model is given by the following equation:

$$\log q_\text{e} = \log K_\text{F} + \frac{1}{n}\log c_\text{e} \tag{4}$$

where K_F (mg/g)(L/g)^n and n are Freundlich constants related to adsorption capacity and adsorption intensity, respectively [21].

The Temkin–Pyzhev isotherm also describes the behavior of an adsorption system on a heterogeneous surface [22,23]. It includes the assumption that the heat of adsorption of all the molecules in the layer decreases linearly with increasing surface coverage. The model equation is represented as follows:

$$q_\text{e} = \frac{RT}{b_\text{T}}\ln c_\text{e} + \frac{RT}{b_\text{T}}\ln A \tag{5}$$

where R is the gas constant (8.314 J/(mol K)), T is the absolute temperature (K), and A and b_T are the isotherm constant (mL/mg) and Temkin–Pyzhev constant (J/mol), respectively [22].

The Dubinin–Radushkevich isotherm is partly analogous to the Langmuir isotherm and it is relatively more commonly applied to distinguish between the physical and chemical adsorption [22]. It considers that the adsorption takes place on a single type of uniform pores, but it does not suppose a homogeneous surface or constant adsorption potential [22]. The model equation is described as follows:

$$\ln q_\text{e} = -\beta\varepsilon^2 + \ln q_\text{m} \tag{6}$$

where β is a constant related to the mean free energy of adsorption per mol of an adsorbate (mol^2/J^2) while ε is the Polanyi potential, equal to $RT\ln(1 + 1/c_e)$ [22].

Kinetic studies

Adsorption kinetic experiments were conducted under the same conditions as previously described adsorption isotherms procedure. Samples were taken at predetermined time intervals, filtered and analyzed spectrophotometrically.

The controlling mechanism of the adsorption process was investigated by fitting pseudo-first- and second-order kinetic models to the experimental data.

The pseudo-first-order model considers a reversible equilibrium of adsorbates between a liquid and a solid phase [24]. The linearized first-order kinetic model is given as:

$$\log\left(q_e - q_t\right) = \log q_e - \frac{k_1}{2.303}t \tag{7}$$

where q_e and q_t are the amount of dye adsorbed on adsorbent (mg/g) at equilibrium and at time t (min), respectively, and k_1 (1/min) is the rate constant of pseudo-first-order kinetics [21].

The pseudo-second order kinetics assumed that the rate-limiting step might be the chemical adsorption, in which concentrations of both adsorbate and adsorbent were involved [22]. The linearized second-order kinetic model is given as:

$$\frac{t}{q_t} = \frac{1}{k_2 q_e^2} + \frac{1}{q_e}t \tag{8}$$

where q_e and q_t have the same meaning as mentioned previously and k_2 (g/(mg min)) is the rate constant for the pseudo-second-order kinetics [21].

Adsorption mechanism

An intraparticle diffusion model was defined by using the following equation [21]:

$$q_t = k_{pi}t^{1/2} + c_i \tag{9}$$

where k_{pi} (mg/(g min$^{1/2}$)) is the rate parameter of stage i, and is obtained from the slope of the straight line of q_t *versus* $t^{1/2}$. C_i is the plot intercept and represents the boundary layer effect [21].

Statistical analysis

Results are shown as the mean ± standard deviation (*SD*). One-way analysis of variance (ANOVA) was applied for each parameter. Tukey test was used as a test a posteriori with a level of significance of 95%. All statistical analyses were performed using the Origin Pro 8 software package.

RESULTS AND DISCUSSION

Effect of contact time on dye removal

Increasing the duration of contact time causes an increased amount of dye uptake (Figure 1). The adsorption of MB onto coffee and tea waste was rapid during the initial stage of the contact period. It occurred within the first 30 min and then gradually slowed down while it reached equilibrium. In terms of effectiveness and efficiency of adsorption process, completion of the process within a short time is extremely important for industrial applications [25]. Similar results have been obtained by Nasuha *et al.* (2010) [17] for the initial adsorption stage of MB onto rejected tea within the first 40 min. The fast adsorption at the initial stage may be due to the fact that a large number of surface sites are available for adsorption. After a lapse of time, the remaining surface sites are difficult to be occupied, probably because of the repulsion between the solute molecules of the solid and bulk phases make it took long time to reach equilibrium [21]. In addition, the later process regime may also be followed by slower adsorption inside the pores of adsorbents [1].The same observations have been previously reported by Dutta *et al.* (2011) these have investigated the MB removal using citrus fruit peel [26].

MB uptake onto citrus waste, as well as lettuce waste, was in a constant increase during the examined contact time, except in a case of two lowest concentrations of 5 and 10 mg/L, where the dye uptake was almost insignificant. These materials require extended contact time for the establishment of process equilibrium. Nevertheless, results obtained in this study have been improved, in terms of faster reaching the equilibrium, compared to literature reports. For example, Ahmad and Rahman (2011) [21] have noted that contact time of 5 h was required for reaching the equilibrium in the process of RBO3R dye adsorption onto coffee husks (with the initial dye concentrations of 25––50 mg/L), while the other study by Oliveira *et al*. (2008) [27] indicated that 12 h of the contact time assured attainment of equilibrium onto coffee husks for all initial MB concentrations evaluated up to 400 mg/L. In addition, adsorption equilibrium has been reached within 5 h for methylene blue adsorption onto tea waste, wherein the dye concentrations were in a range of 20–50 mg/L [28].

Effect of concentration on dye removal

The amount of MB adsorbed per unit of mass of adsorbent increased with the increase in initial concentration, bearing in minds all of tested adsorbents. Raising the dye concentration from 5 to 60 mg/L allows the adsorbents to increase their sorption capacities. The phenomenon has also been reported previously in the literature [17,28–32]. The initial dye concentration provides an important driving force to overcome the mass transfer resistance of the dye between the aqueous and solid phases [21]. At higher initial dye concentrations, the number of molecules competing for the available sites on the surface of activated carbon was

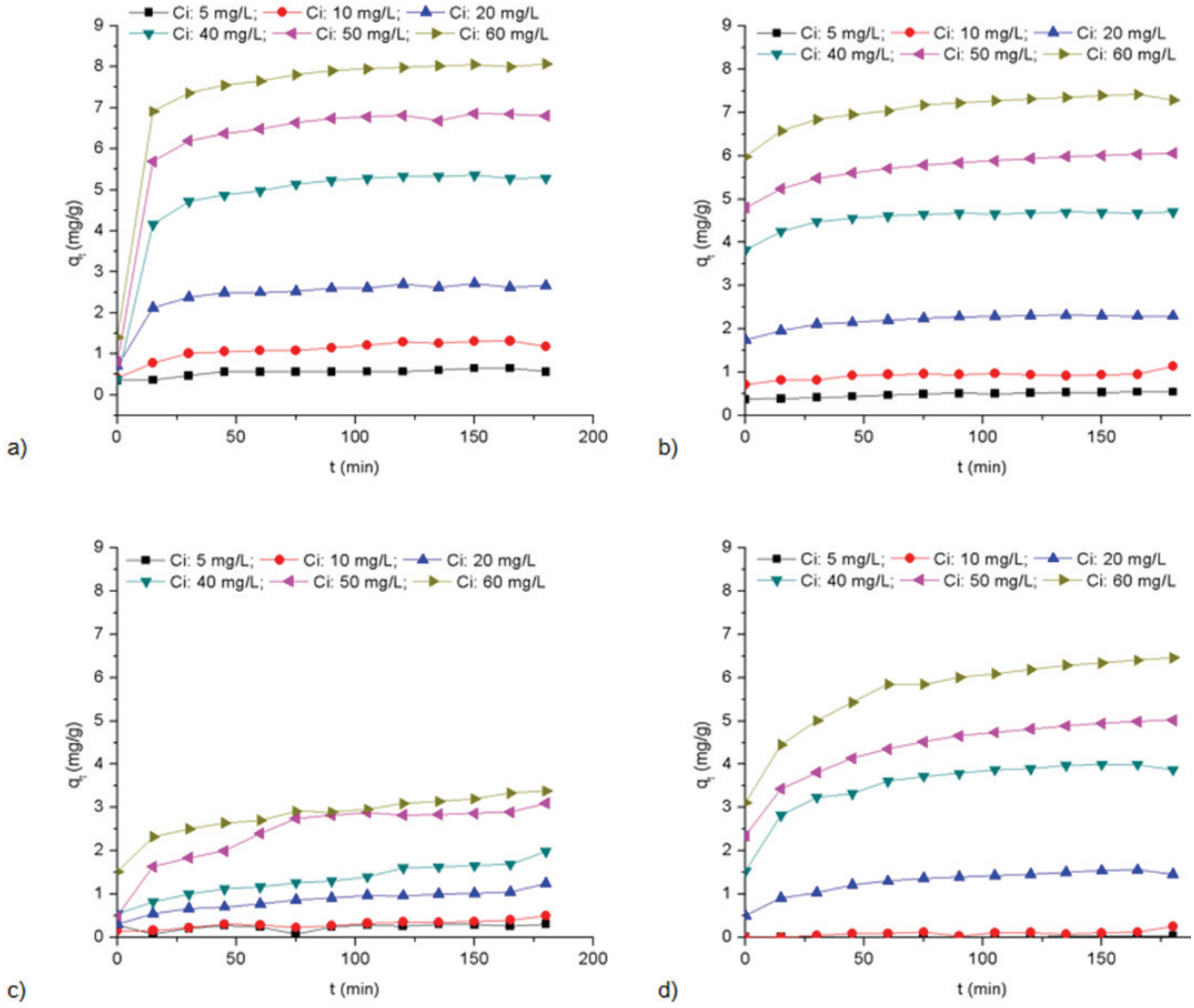

Figure 1. Effect of contact time on methylene blue dye adsorption onto: coffee waste (a), tea waste (b), citrus waste (c) and lettuce waste (d), at various initial dye concentrations (adsorbent mass: 7g/L, 120 rpm, 27 °C).

high, hence resulting in higher adsorption capacity. In fact, the ratio of the initial number of dye molecules to the available surface area is lower at a lower initial concentration compared to higher initial concentration [21]. Some researchers have observed the fast adsorption of dye at lower concentrations, as an indication that dyes adsorption occurs mainly on the surface of the adsorbent [27]. As the dye concentration increases, the adsorption process will probably occur in two stages: the first one at the adsorbent surface (faster) and the second one (slower) in the adsorbent pores [27]. It appears that in our investigation the dye concentration had not affected the adsorption speed.

Coffee waste expressed maximum adsorption capacity (8.07 mg/g), followed by tea waste (7.42 mg/g), lettuce waste (6.46 mg/g) and citrus waste (3.38 mg/g), respectively. It was observed that the adsorption capacities depend upon the sources of the raw materials used. Bearing in mind that many raw materials have been modified by various physical and chemical treatments (these include the use of more or less expensive and adverse chemicals) in order to affect and improve the adsorption capacity, this study aims with the exemption of usage of any chemical agents and immediate utilization of raw restaurant waste. In addition, their cost approaches zero. The adsorption capacity of these unconventional adsorbents was due to their nature composition, and the variations in the content of polymers such as polysaccharides, lignin, hemicelluloses and cellulose, proteins, fats and a variety of other elements [33].

It is not uncommon that coffee and tea residues have been already applied as adsorbents for many types of adsorbates, and the obtained results were more or less improved, compared with the literature reports. Their main role in this investigation basically consisted as a reference point for assessing the effectiveness of other types of tested adsorbents. The research reports about the dye adsorption onto lettuce waste have been weak. It was an interesting that such rare type of adsorbent showed very good sorption capabilities, even better than those obtained for citrus

waste. In this respect, it may be suggested that dye sorption studies should take into further consideration lettuce waste as potential effective and available low cost adsorbent.

Coffee and tea waste performed better adsorption affinity in MB dye, compared to some heavy metals, evidenced by the following literature reports. Oliveira *et al.* (2008) [34] noted that adsorption capacities of untreated coffee husks were in a range from 5.57 up to 7.50 mg/g for copper, zinc, cadmium and chrome removal from its aqueous solutions. Also, Ahluwalia and Goyal (2005) [35] reported adsorption capacity of waste tea leaves for nickel removal of 5 mg/g. In addition, results presented in this paper were higher than those found for other nonspecific types of bio materials for MB adsorption capacity. For example, Ncibi *et al*. (2007) [36] reported adsorption capacities of 0.44 up to 4.64 mg/g of *Posidonia oceanica* (L.) fibers for MB uptake, as dye concentration raises from 10 to 50 mg/L, respectively. Another study by Hana *et al*. (2006) [32] noted chaff capacity for MB uptake of 3.60 mg/g after 60 min of contact.

It should be noted that higher adsorption capacities have been previously reported for MB uptake by tea waste [17], as well as orange peel [37]. Those materials were also utilized without any pretreatment, but some additional effects have been included in the investigation, like varying the pH of the dye solution and temperature, as well. Temperature effects have been exempted in this study, in terms of overall cost reduction, while preliminary experimental results showed that pH variations of initial dye solutions did not significantly affect the process efficiency (data not shown). Thus, pH remained unmodified during the entire period of the process duration. Some literature reports also testify about irrelevant pH effects in dye adsorption experiments [32].

The dye removal percentages of all tested adsorbents have been presented in Table 1.

Maximum obtained dye removal percentage was attained with coffee waste, followed by tea waste, lettuce waste and citrus waste, respectively. A comparative review of the effect of time on the percentages of MB removal of all tested adsorbents is graphically presented on Figure 2.

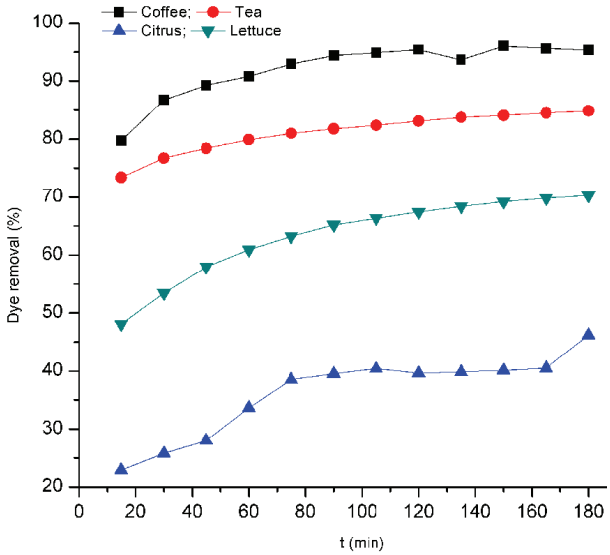

Figure 2. Effect of time on methylene blue dye removal on coffee, tea, lettuce and citrus waste (c_i: 50 mg/L, adsorbent mass: 7g/L, 120 rpm, 27 ℃).

It was calculated that coffee waste removed almost 90% of initial dye concentration within 30 min from the start of the experiment, at the initial MB concentration of 60 mg/L. For the specified period of time, tea waste removed 80%, lettuce waste 60 % and citrus waste 30 % of the initial dye concentration. The results presented in this paper have been improved compared to previously reported. Oliveira *et al.* (2008) [27] noted that the amount of MB adsorbed onto coffee husks ranged from 70 to 85% after 2 h and from 90 to 96% after 12 h of contact, while Hana *et al*. (2006) [32] reported MB removal efficiency by chaff of 95% up to 60 min. Some researchers have observed the decline of MB removal percentage as the initial dye concentration increased [1,15,29]. Nevertheless, reported concentrations were much higher than those presented in this paper. The researchers explained that the increased number of dye molecules leads to saturation of adsorbent surface, and thus most of the dye adsorption took place slowly inside the pores [1]. The mentioned phenomena have not been observed within the range of concentrations tested in this paper. Thus, it might be said that dye molecules have been predominantly adsorbed on the outer surface.

Table 1. Maximum dye removal percentages for different methylene blue dye initial concentrations on coffee, tea, lettuce and citrus waste (adsorbent mass: 7 g/L, 120 rpm, 27 ℃)

Adsorbent	c_i / mg L^{-1}					
	5	10	20	40	50	60
Coffee waste	91.41±0.37	92.20±0.34	94.44±0.38	93.86±0.09	96.03±0.13	94.16±0.13
Tea waste	76.61±0.54	79.41± 0.36	81.14±0.55	82.43±0.61	84.83±0.54	86.57±0.51
Lettuce waste	32.98±0.90	38.52±0.69	54.52±0.55	70.11±1.02	70.52±0.68	75.68± 1.16
Citrus waste	43.29±0.68	35.29±0.58	43.56±0.88	45.70±0.98	46.52±0.65	49.35±0.77

Equilibrium adsorption Isotherms

The adsorption equilibrium provides fundamental physiochemical data for evaluating the applicability of the sorption process as a unit operation [18]. The suitability of isotherm models has been mostly compared by judging the correlation coefficients, R^2. Isotherm model parameters are presented in Table 2. Only the Langmuir isotherm parameters were omitted due to wrong experimental data fitting. The Langmuir model calculations resulted in obtaining of negative parameter values, indicating to it's completely incompatibility to fit the actual sorption system. This fact might be the first note referring that adsorbents surfaces were not homogenous nor we can exclude assumptions that the interactions exist between adsorbed molecules.

The Freundlich isotherm model exhibited better experimental fit than both the Temkin–Pyzhev and Dubinin–Radushkevich, respectively, for all of tested adsorbents. This assumption primary indicates that the sorption process was based on sorption on a heterogeneous surface or surface supporting sites of varied affinities [21]. By comparing K_F values, it was confirmed that the highest sorption capacity possesses coffee waste, followed by tea, lettuce and citrus waste. Regarding to n values it was generally established that values of $n > 1$ illustrate that adsorbate is favorably adsorbed on the adsorbent whereas $n < 1$ demonstrate the adsorption process is chemical in nature [20,21]. n values obtained for all types of adsorbents were less than 1, demonstrated the adsorption process might be chemical in nature.

These results were somewhat expected. As raw materials were used, without any pre-treatment, it was unlikely that their surface contains homogenous cites, as the Langmuir model suggests. Literature reports about pre-treated coffee residues, these are used as dye adsorbents showed good agreement with Langmuir isotherm [21]. The same was observed for tea waste [30], as well as orange peel [31].

Kinetic study

Adsorption kinetics describes the rate of adsorbate uptake governing the contact time of adsorption reaction [18,38]. The results showed that the sorption process followed a pseudo-second-order mechanism for all tested adsorbents, based on the high correlation coefficient values (Table 3). Further, compared with experimental results ($q_{e,exp}$), the values of $q_{e,cal}$ for the pseudo-second-order model were much more reasonable than those for the pseudo-first-order model. Most of the $q_{e,cal}$ values of the pseudo-first-order model deviated significantly from the experimental values. The best fit showed tea and coffee waste, followed by lettuce and citrus waste. Also, pseudo-second order model was developed on the principle that the rate limiting step may be chemisorption promoted by either valency forces, through sharing of electrons between biosorbent and sorbate, or covalent forces, through the exchange of electrons between the parties involved [27].

The pseudo-second-order kinetic plot for the adsorption of MB dye onto coffee, tea, lettuce and citrus waste is presented in Figure 3. The specified model follows the process with an overall tested range of concentrations.

Previous researchers have also reported the pseudo--second-order mechanism of MB adsorption onto coffee husks [27], spent tea [17,29], orange peel [31], and other adsorbents, such as rice husks [18]. In addition, this kinetic model was common for some other adsorbed dyes and heavy metals onto coffee and tea waste [1,21,30,39].

Table 2. Isotherm constants for methylene blue dye adsorptions on coffee, tea, lettuce and citrus waste (adsorbent mass: 7 g/L, 120 rpm, 27 °C)

Isotherm model	Coffee waste	Tea waste	Lettuce waste	Citrus waste
Freundlich				
R_F^2	0.9942	0.9923	0.9778	0.9671
n	0.6031	0.7815	0.6956	0.8775
K_f / (mg/g) (L/mg)$^{1/n}$	0.9698	0.4236	0.0903	0.0707
Temkin–Pyzhev				
R_T^2	0.9292	0.8659	0.8116	0.8359
b_T / J mol^{-1}	522.38	768.86	940.36	2432.3
A	1.2210	0.7562	0.3173	0.3173
Dubinin–Radushkevich				
R_D^2	0.9397	0.8581	0.6732	0.6233
β / mol^2 J^{-2}	6.5920	1.1711×10^{-6}	3.7696×10^{-6}	3.6628×10^{-6}
q_m / mg g^{-1}	8.0422	5.3682	3.4446	1.8651

Table 3. Kinetic constants for methylene blue adsorption on coffee, tea, lettuce and citrus waste, at 50 mg/L of dye concentration (adsorbent mass: 7 g/L, 120 rpm, 27 °C)

Adsorbent	Pseudo-first order kinetic model			Pseudo-second order kinetic model			$(q_e)_{exp}$ [b] mg/g
	$(q_e)_{cal}$ [a] mg/g	k_1 1/min	R^2	$(q_e)_{cal}$ mg/g	k_2 g/(mg min)	R^2	
Coffee waste	2.0850	1.6863	0.4668	6.7654	5.7952	0.9978	6.6876
Tea waste	1.2530	1.2578	0.9712	6.0861	3.4971	0.9994	6.0601
Lettuce waste	2.6975	1.4142	0.9706	5.1440	1.4762	0.9963	5.0201
Citrus waste	1.3717	0.9253	0.6995	3.1260	1.4474	0.9848	3.2994

[a]Calculated adsorption capacity; [b]experimental adsorption capacity

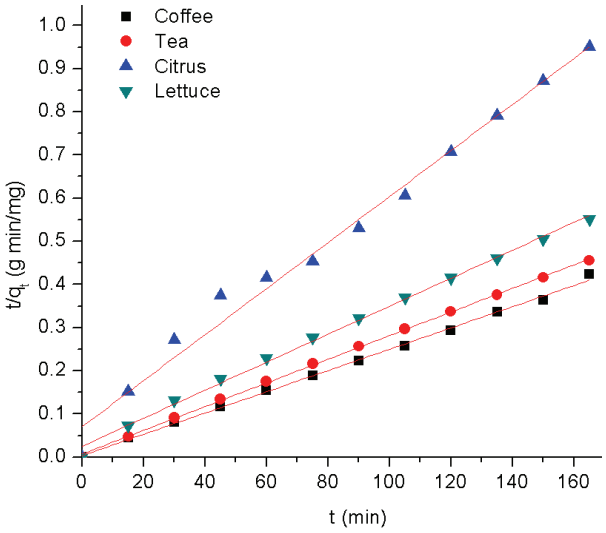

Figure 3. Pseudo-second-order kinetic plot for the adsorption of methylene blue dye on coffee, tea, lettuce and citrus waste (c_i:50 mg/L, adsorbent mass: 7 g/L,120 rpm,27 °C).

Adsorption mechanism

An intraparticle diffusion model was employed in order to further clarify the adsorption mechanism and determine rate controlling steps [25,40]. In accordance with the applied model, the plot of q_t *versus* $t^{1/2}$ should be linear if the intraparticle diffusion occurs. Further, if the plot passes through the origin, the rate limiting process is only due to the intraparticle diffusion [21].

The results of experimental data fitting within intraparticle diffusion model are presented in Figure 4 and corresponding parameters are obtained in Table 4. It was found that the sorption process exhibit multilinearity and tends to be followed by two stages (Fig. 4). The same multilinearity pattern has also been reported previously by various researchers, thus indicating that the process involves more than one kinetic stage [18,21,25,40]. The first initial linear stage may be referred to an instantaneous adsorption and is probably due to an electrostatic attraction between the dye molecules and the external surface of the adsorbent [21,40]. The second stage is a gradual adsorption stage, ascribed to the intraparticle diffusion [21,40]. It may be also regarded as the solute diffusion from larger pores to the micropores causing a slow adsorption rate [14,40].

Vadivelan and Kumar (2005) [18] had noted that the adsorption of methylene blue dye onto the low cost rice husk based adsorbent followed similar two-portion intraparticle diffusion pattern, as well as adsorption of acid violet onto orange peel [41]. Another type of adsorbates, such as phenols, demonstrated that adsorption onto tea waste also occurred in the same manner as previously described [20].

From the Figure 4, it was clear that intraparticle diffusion was not the fully operative mechanism, since slopes of the plots do not pass through the origin and this observation might be applied to all of tested adsorbents. However, the process does not occur identically at all examined concentrations. The linear plots for lower concentrations (5 and 10 mg/L) tend to pass very close to the origin. With further increase of initial dye concentrations, the intercept values increase, too, indicating to the greater contribution of surface sorption in the process [21]. This deviation from the origin may be due to the difference in the rate of mass transfer in the initial and final stages of adsorption [42]. Almost all the intercepts reported here were positive, indicating that relatively rapid adsorption occurs within a short period of time. Also, the k_{pi} values increase as the dye initial concentrations increase. It might be concluded that intraparticle diffusion tends to be rate controlling step for lower dye concentrations, while for higher concentrations the other mechanism, such as film diffusion, is considered to be involved.

CONCLUSIONS

Inexpensive and readily available restaurant waste, including coffee, tea, lettuce and citrus residues, have been tested for methylene blue efficiency removal andtheir adsorption capacities were determined. Coffee waste showed highest adsorption capacity, and therefore the highest dye removal efficiency. Thereupon, there are tea as well as lettuce and citrus waste, respectively, with considerate adsorption capabilities. The dye removal was more effective as dye concen-

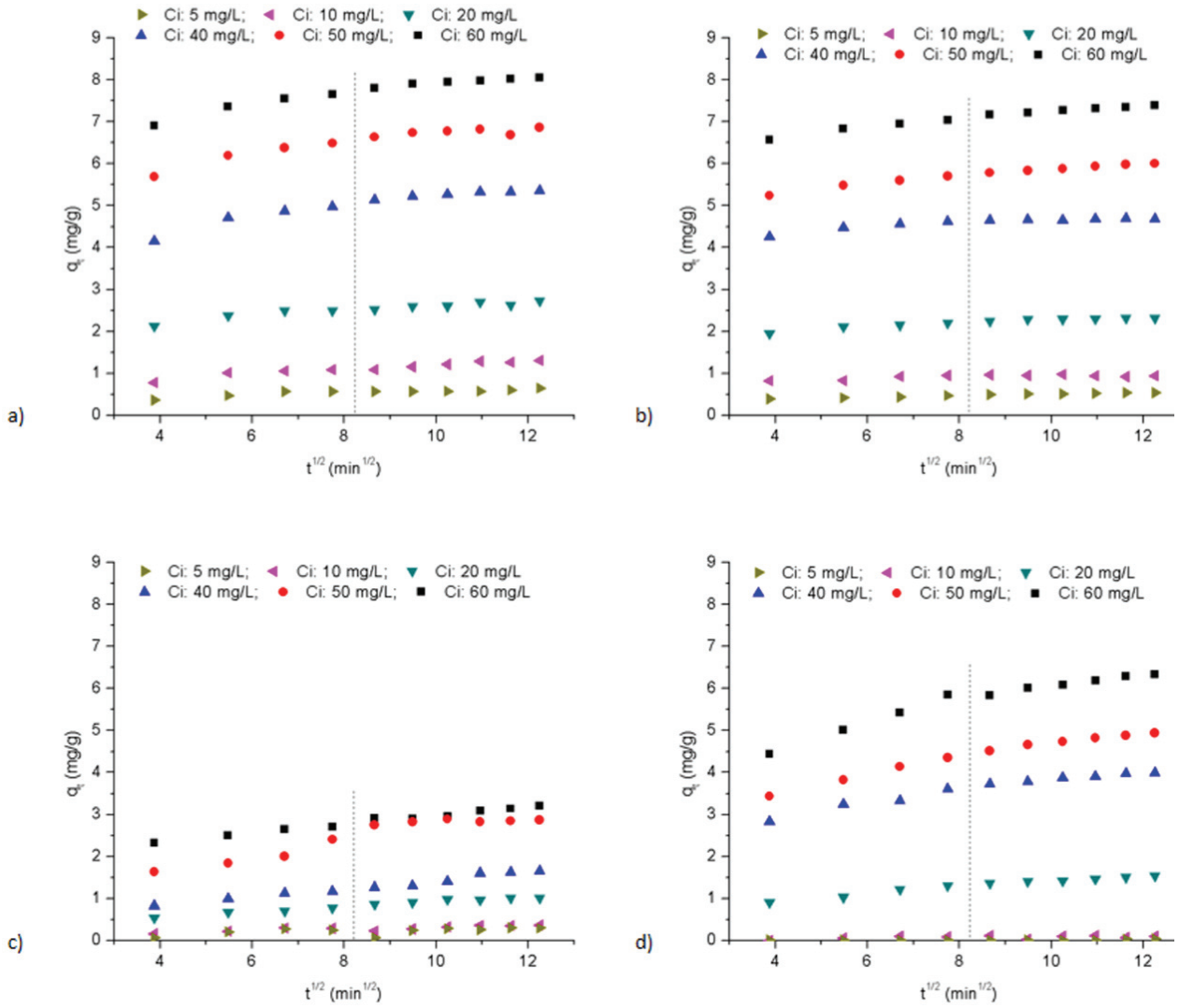

Figure 4. Intraparticle diffusion model plots for the adsorption of methylene blue dye onto coffee waste (a), tea waste (b), lettuce waste (c) and citrus waste (d) (adsorbent mass: 7 g/L, 120 rpm, 27 ℃).

Table 4. Intraparticle diffusion model constants and correlation coefficients for adsorption of methylene blue dye on coffee, tea, lettuce and citrus waste (adsorbent mass: 7 g/L, 120 rpm, 27 ℃)

Adsorbent	Parameter	Concentration, mg/L					
		5	10	20	40	50	60
Coffee waste	k_{pi} / mg g^{-1} min$^{-1/2}$	0.1954	0.4327	0.4652	1.0146	0.9467	0.9892
	c_i / mg g^{-1}	0.3297	0.6389	2.0039	3.9003	5.4639	6.6097
	R^2	0.7529	0.9225	0.8667	0.8861	0.8476	0.9205
Tea waste	k_{pi} / mg g^{-1} min$^{-1/2}$	0.1434	0.1120	0.3150	0.3445	0.6777	0.7285
	c_i / mg g^{-1}	0.3211	0.7943	1.8642	4.2085	4.9843	6.2946
	R^2	0.9706	0.4812	0.8989	0.7738	0.9672	0.9659
Lettuce waste	k_{pi} / mg g^{-1} min$^{-1/2}$	0.0207	0.0641	0.5724	1.0500	1.3821	1.6701
	c_i / mg g^{-1}	0.0079	0.0054	0.6718	2.4457	2.8769	3.8716
	R^2	0.3680	0.2880	0.9556	0.9407	0.9657	0.9226
Citrus waste	k_{pi} / mg g^{-1} min$^{-1/2}$	0.1522	0.1697	0.4516	0.7804	1.2882	0.8032
	c_i / mg g^{-1}	0.0556	0.0958	0.3345	0.4222	1.0410	1.9362
	R^2	0.3232	0.7516	0.9747	0.9700	0.8705	0.9839

tration increases from 5 up to 60 mg/L. Sorption isotherm results asserted that the sorption process was based on interactions on a heterogeneous surface as all of adsorbents followed Freundlich model. Kinetic analysis revealed that pseudo-second-order model was the primary process mechanism, but also there was the tendency that intraparticle diffusion model follows the process at very low dye concentrations.

Restaurant waste performs well in removing the MB at no cost, so it can be adopted and widely used in industries for contaminated water treatment as a concept of waste-to-wealth. Further process investigation may include the form of integrated and comprehensive restaurant waste for treatment of industrial effluents, containing not only dyes, but also other pollutants, like heavy metals, etc.

Acknowledgements

The financial support for this investigation given by Ministry of Education, Science and Technological Development of the Republic of Serbia under the project TR 31035 is gratefully acknowledged. The authors would also like to thank the Hotel - Restaurant "Hyatt", Belgrade, Serbia, for providing materials for investigation.

REFERENCES

[1] B.H. Hameed, M.I. El-Khaiary, Removal of basic dye from aqueous medium using a novel agricultural waste material: Pumpkin seed hull, J. Hazard. Mater. **155** (2008) 601–609.

[2] G.Z. Kyzas, N.K. Lazaridis, A.C. Mitropoulos, Removal of dyes from aqueous solutions with untreated coffee residues as potential low-cost adsorbents: Equilibrium, reuse and thermodynamic approach, Chem. Eng. J. **189**––**190** (2012) 148–159.

[3] M.R. Sohrabi, M. Ghavami, Photocatalytic degradation of Direct Red 23 dye using UV/TiO_2: effect of operational parameters, J. Hazard. Mater. **153** (2008) 1235–1239.

[4] M. Abbasi, N.R. Asl, Sonochemical degradation of Basic Blue 41 dye assisted by nanoTiO_2 and H_2O_2, J. Hazard. Mater. **153** (2008) 942–947.

[5] N. Zaghbani, A. Hafiane, M. Dhahbi, Removal of Safranin T from wastewater using micellar enhanced ultrafiltration, Desalination **222** (2008) 348–356.

[6] J.S. Wu, C.H. Liu, K. H. Chu, S.Y. Suen, Removal of cationic dye methyl violet 2B from water by cation exchange membranes, J. Membrane Sci. **309** (2008) 239–245.

[7] L. Fan, Y. Zhou, W. Yang, G. Chen, F. Yang, Electrochemical degradation of aqueous solution of Amaranth azo dye on ACF under potentiostatic model, Dyes Pigments **76** (2008) 440–446.

[8] M.X. Zhu, L. Lee, H.H. Wang, Z. Wang, Removal of an anionic dye by adsorption/ precipitation processes using alkaline white mud, J. Hazard. Mater. **149** (2007) 735––741.

[9] G. Sudarjanto, B. Keller-Lehmann, J. Keller, Optimization of integrated chemical–biological degradation of a reactive azo dye using response surface methodology, J. Hazard. Mater. **138** (2006) 160–168.

[10] V. Sarria, M. Deront, P. Peringer, C. Pulgarin, Degradation of a biorecalcitrant dye precursor present in industrial wastewaters by a new integrated iron (III) photo-assisted-biological treatment, Appl. Catal., B **40** (2003) 231–246.

[11] J. Garcıa-Montano, L. Perez-Estrada, I. Oller, M.I. Maldonado, F. Torrades, J. Peral, Pilot plant scale reactive dyes degradation by solar photo-Fenton and biological processes, J. Photoch. Photobio., A **195** (2008) 205–214.

[12] B. Lodha, S. Chaudhari, Optimization of Fenton-biological treatment scheme for the treatment of aqueous dye solutions, J. Hazard. Mater. **148** (2007) 459–466.

[13] B.H. Hameed, F.B.M. Daud, Adsorption studies of basic dye on activated carbon derived from agricultural waste: Heveabrasiliensis seed coat, Chem. Eng. J. **139** (2008) 48–55.

[14] F.C. Wu, R.L. Tseng, High adsorption capacity NaOH-activated carbon for dye removal from aqueous solution, J. Hazard. Mater. **152** (2008) 1256–1267.

[15] N.M. Mahmoodi, B. Hayati, M. Arami, C. Lan, Adsorption of textile dyes on Pine Cone from colored wastewater: Kinetic, equilibrium and thermodynamic studies, Desalination **268** (2011) 117–125.

[16] M. Rafatullah, O. Sulaiman, R. Hashim, A. Ahmad, Adsorption of methylene blue on low-cost adsorbents: A review, J. Hazard. Mater. **177** (2010) 70–80.

[17] N. Nasuha, B.H. Hameed, A.T.M. Din, Rejected tea as a potential low-cost adsorbent for the removal of methylene blue, J. Hazard. Mater. **175** (2010) 126–132.

[18] V. Vadivelan, K.V. Kumar, Equilibrium, kinetics, mechanism, and process design for the sorption of methylene blue onto rice husk, J. Colloid. Interf. Sci. **286** (2005) 90––100.

[19] M. Kousha, E. Daneshvar, H. Dopeikar, D. Taghavi, A. Bhatnagar, Box–Behnken design optimization of Acid Black 1 dye biosorption by different brown macroalgae, Chem. Eng. J. **179** (2012) 158–168.

[20] K.V. Kumar, S. Sivanesan, Prediction of optimum sorption isotherm: Comparison of linear and non-linear method, J. Hazard. Mater., B **126** (2005) 198–201.

[21] M.A. Ahmad, N.K. Rahman, Equilibrium, kinetics and thermodynamic of Remazol Brilliant Orange 3R dye adsorption on coffee husk-based activated carbon, Chem. Eng. J. **170** (2011) 154–161.

[22] Y. Liu, Q. Bai, S. Lou, D. Di, J. Li, M. Guo, Adsorption characteristics of (−)-epigallocatechingallate and caffeine in the extract of waste tea on macroporous adsorption resins functionalized with chloromethyl, amino, and phenylamino groups, J. Agr. Food Chem. **60** (2012) 1555−1566.

[23] J. Kammerer, R. Carle, D.R. Kammerer, Adsorption and Ion Exchange: Basic Principles and Their Application in Food Processing, J. Agr. Food Chem. **59** (2011) 22–42.

[24] M.L. Soto, A. Moure, H. Domínguez, J.C. Parajó, Recovery, concentration and purification of phenolic com-

pounds by adsorption: A review, J. Food Eng. **105** (2011) 1–27.

[25] [A. Gundogdu, C. Duran, H.B. Senturk, M. Soylak, D. Ozdes, H. Serencam, M. Imamoglu, Adsorption of Phenol from Aqueous Solution on a Low-Cost Activated Carbon Produced from Tea Industry Waste: Equilibrium, Kinetic, and Thermodynamic Study, J. Chem. Eng. Data **57** (2012) 2733–2743.

[26] [S. Dutta, A. Bhattacharyya, A. Ganguly, S. Gupta, S. Basu, Application of Response Surface Methodology for preparation of low-cost adsorbent from citrus fruit peel and for removal of Methylene Blue, Desalination **275** (2011) 26–36.

[27] L.S. Oliveira, A.S. Franca, T.M. Alves, S.D.F. Rocha, Evaluation of untreated coffee husks as potential biosorbents for treatment of dye contaminated waters, J. Hazard. Mater. **155** (2008) 507–512.

[28] A. Bhatnagar, M. Sillanpaa, Utilization of agro-industrial and municipal waste materials as potential adsorbents for water treatment - A review, Chem. Eng. J. **157** (2010) 277–296.

[29] B.H. Hameed, Spent tea leaves: a new non-conventional and low-cost adsorbent for removal of basic dye from aqueous solutions, J. Hazard. Mater. **161** (2009) 753––759.

[30] M. Auta, B.H. Hameed, Preparation of waste tea activated carbon using potassium acetate as an activating agent for adsorption of Acid Blue 25 dy. Chem. Eng. J. **171** (2011) 502–509.

[31] K.Y. Foo, B.H. Hameed, Preparation, characterization and evaluation of adsorptive properties of orange peel based activated carbon via microwave induced K_2CO_3 activation, Bioresource Technol. **104** (2012) 679–686.

[32] R. Hana, Y. Wang, P. Hana, J. Shi, J. Yang, Y. Lu, Removal of methylene blue from aqueous solution by chaff in batch mode, J. Hazard. Mater., B **137** (2006) 550–557.

[33] E. Contreras, L. Sepulveda, C. Palma, Valorization of Agroindustrial Wastes as Biosorbent for the Removal of Textile Dyes from Aqueous Solutions, Int. J. Chem. Eng. (2012), Article ID 679352, doi:10.1155/2012/679352.

[34] W.E. Oliveira, A.S. Franca, L.S. Oliveira, S.D. Rocha, Untreated coffee husks as biosorbents for the removal of heavy metals from aqueous solutions, J. Hazard. Mater. **152** (2008) 1073–1081.

[35] S.S. Ahluwalia, D. Goyal, Removal of heavy metals by waste tea leaves from aqueous solution, Eng. Life Sci. **5** (2005) 158–162.

[36] M.C. Ncibi, B. Mahjouba, M. Seffen, Kinetic and equilibrium studies of methylene blue biosorption by *Posidoniaoceanica* (L.) fibres, J. Hazard. Mater., B **139** (2007) 280–285.

[37] G. Annadurai, R.S. Juang, D.J. Lee, Use of cellulose-based wastes for adsorption of dyes from aqueous solutions, J. Hazard. Mater. **92** (2002) 263-274.

[38] Z.P. Gao, Z.F. Yu, T.L. Yue, S.Y. Quek, Adsorption isotherm, thermodynamics and kinetics studies of polyphenols separation from kiwifruit juice using adsorbent resin, J. Food Eng. **116** (2013) 195–201.

[39] J. Shah, M.R. Jan, A. Ul-Haq, M. Zeeshan, Equilibrium, kinetic and thermodynamic studies for sorption of Ni (II) from aqueous solution using formaldehyde treated waste tea leaves, J. Saudi Chem. Soc. (2012), http://dx.doi.org/10.1016/j.jscs.2012.04.004.

[40] K. Vijayaraghavan, M.H. Han, S.B. Choi, Y.S. Yun, Biosorption of Reactive black 5 by Corynebacterium glutamicum biomass immobilized in alginate and polysulfone matrices, Chemosphere **68** (2007) 1838–1845.

[41] R. Sivaraj, C. Namasivayam, K. Kadirvelu, Orange peel as an adsorbent in the removal of Acid violet 17 (acid dye) from aqueous solutions, Waste Manage. **21** (2001) 105––110.

[42] D.H.K. Reddy, K. Seshaiah, A.V.R. Reddy, M. Madhava Rao, M.C. Wang, Biosorption of Pb^{2+} from aqueous solutions by Moringa oleifera bark: Equilibrium and kinetic studies, J. Hazard. Mater. **174** (2010) 831–838.

IZVOD

ISKORIŠĆENJE SIROVOG OTPADA IZ RESTORANA ZA ADSORPCIJU BOJA

Marija D. Pavlović, Ivan R. Nikolić, Milica D. Milutinović, Suzana I. Dimitrijević-Branković, Slavica S. Šiler-Marinković, Dušan G. Antonović

Univerzitet u Beogradu, Tehnološko-metalurški fakultet, Katedra za biohemijsko inženjerstvo i biotehnologiju, Karnegijeva 4, 11000 Beograd, Srbija

(Naučni rad)

Metilen plavo je bazna boja sa strukturom heterocikličnog aromatičnog jedinjenja, koja se u dobu savremenog društva često koristi za bojenje raznih tipova materijala. Efluenti iz industrije boja predstavljaju jednu od najproblematičnijih vrsta otpadnih voda za tretiranje, usled njihove velike biološke i hemijske potrebe za kiseonikom. Pored toga, toksičnost i teško razgradiva priroda boja mogu značajno uticati na fotosintetičku aktivnost vodenog sveta. Adsorpcijom na čvrstim nosačima mogu se ukloniti, odnosno, svesti na minimum razni tipovi zagađivača, zbog čega ova tehnika ima široku primenu u kontroli zagađenja voda. S tim u vezi, ispitivana je mogućnost iskorišćenja sirovog otpada iz restorana za adsorpciju i uklanjanje boje metilen plavo iz vodenih rastvora. U radu su određivani adsorpcioni kapaciteti otpadnih sirovina najčešće konzumiranih namirnica, uključujući kafu, čaj, zelenu salatu i mešavinu citrusnog voća (citrusa). Proces adsorpcije izveden je u šaržnom režimu, uz mešanje na tresilici, u uslovima ambijentalne temperature. Efikasnost procesa praćena je u zavisnosti od promene koncentracije boje u radnim rastvorima. Pokazano je da otpadna kafa ispoljava najviši adsorpcioni kapacitet, a za njom otpadni čaj, zelena salata i citrusi, redom. Nakon 30 min odigravanja reakcije, na kafi se vezalo gotovo 90%, dok na čaju 80%, zelenoj salati 60% i citrusima 30% od početne koncentracije rastvora boje. Vezivanje boje na adsorbentima bilo je efikasnije u slučajevima kada je koncentracija rastvora boje rasla od 5 do 60 mg/L. Na osnovu ispitivanja najčešće primenjivanih modela izotermi za definisanje adsorpcione ravnoteže, pronađeno je da su ravnotežni podaci, u slučajevima svih vrsta adsorbenata, bili u skladu sa Frojndlihovom adsorpcionom izotermom. S tim u vezi, smatra se da je proces odigravanja reakcije baziran na interakcijama između molekula boje i funkcionalnih grupa na heterogenoj površini adsorbenata. Kinetika i mehanizam reakcija opisani su po principu modela pseudo-drugog reda, koji se zasniva na pretpostavci da hemisorpcija, odnosno stvaranje hemijskih veza između adsorbenta i adsorbata, kontroliše celokupan tok reakcija. Iskorišćenjem sirovog otpada iz restorana može se doći do ekonomski isplativog rešenja za brzo i efikasno uklanjanje toksičnih i teško razgradivih boja iz vodenih rastvora. Smatra se da ova vrsta otpadnog materijala može naći svoju primenu u brojnim adsorpcionim procesima, u prvom redu onim koji se zasnivaju na tretmanima prečišćavanja otpadnih i pijaćih voda.

Ključne reči: Adsorpcija • Boja • Otpad iz restorana • Izoterme • Kinetika

Development and validation of an RP-HPLC method for quantification of *trans*-resveratrol in the plant extracts

Zika S. Cvetkovic, Vesna D. Nikolic, Ivan M. Savic, Ivana M. Savic-Gajic, Ljubisa B. Nikolic

Faculty of Technology, University of Niš, Leskovac, Serbia

Abstract

New, simple, cost effective, accurate and reproducible RP-HPLC method was developed and validated for the quantification of *trans*-resveratrol in the extracts of grape exocarp and seeds. The method has proved to be simpler and faster than available methods. Methanol was used as a mobile phase with a flow rate of 1.0 cm^3 min^{-1}, while the quantification was effected at 306 nm. The separation was performed at 35 °C using a C_{18} column. The results showed that the peak area response was linear in the concentration range of 1–40 μg cm^{-3}. The values of *LOD* and *LOQ* were found to be 0.125 and 0.413 μg cm^{-3}, respectively. The antioxidant activity of the extracts was determined using DPPH assay. The ability of DPPH radicals inhibition decreases in the following order: the extract of grape exocarp > *trans*-resveratrol standard > the extract of grape seeds.

Keywords: validation, RP-HPLC, *trans*-resveratrol, grape extract, antioxidant activity.

Available online at the Journal website: http://www.ache.org.rs/HI/

SCIENTIFIC PAPER

UDC 543.544:634.8

Hem. Ind. **69** (6) 679–687 (2015)

doi: 10.2298/HEMIND140917004C

Resveratrol (3,5,4'-trihydroxystilbene) presents a bioactive compound that was extracted as a white powder from the roots of *Veratrum grandiflorum* in 1940 [1]. Then, it was detected in more than seventy species of plants, including grapes [2], blueberries, cranberries, mulberries, peanuts, white pine and corn. Although the two isomeric forms of resveratrol can be found in the nature (Fig. 1), *trans*-resveratrol is the most commonly used isomer during investigation, because *cis*-isomer is not commercially available due to its stability. After effect of UV light or natural daylight, *trans*-isomer is transformed to *cis*-isomer [3].

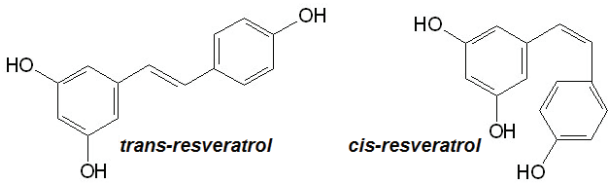

Fig. 1. The structures of trans- and cis-resveratrol.

Based on the pharmacological studies, it can be concluded that resveratrol act as: antioxidant [4], inhibitor of cyclooxygenase and lipid modifications [5], inhibitor of LDL oxidation and platelet aggregation, vasodilator [6, 7] and antiviral agent [8]. Furthermore, resveratrol is able to inhibit transcriptional activation of carcinogen-activating enzyme CIP1A1, thereby preventing the occurrence of cancer in the initiation stage [9].

Correspondence: I.M. Savic-Gajic, Faculty of Technology, University of Nis, Bulevar oslobodjenja 124, 16000 Leskovac, Serbia.
E-mail: vana.savic@yahoo.com
Paper received: 17 September, 2014
Paper accepted: 26 December, 2014

For the determination of *trans*-resveratrol in wines, there are many described analytical methods, such as gas chromatography-mass spectrometry (GC–MS) [10], capillary electrophoresis (CE) [11] and high performance liquid chromatography-mass spectrometry (HPLC-MS) method [12,13]. GC-MS coupled methods commonly require derivatization with bis(trimethylsilyl) trifluoroacetamide in order to improve the evaporation of analyzed compounds [14,15]. The extraction and derivation procedures require a considerable time and may cause the conversion of *trans*- to *cis*-resveratrol. Additionally, the lack of these methods is a low sensitivity. The content of resveratrol was also determined in the biological samples by GC–MS methods [16,17]. An advantage of HPLC analysis in compared with other methods is due to detection of lower concentrations of resveratrol and its metabolites [18–24]. Also, the separation of resveratrol isomers in wine is possible using HPLC method [25]. Based on the literature search, the HPLC method for simultaneous determination of the resveratrol content and other compounds (*e.g.*, phenolic compounds in the plant extracts or metabolites in the biological samples) are mainly developed. The combined solvents such as methanol, acetic acid, water, acetonitrile, etc. were used as the mobile phase in many cases [26–29].

Given the state of the literature, the aim of this study was to develop simple, precise, accurate and validated RP-HPLC method for the determination of the *trans*-resveratrol content in the extracts of grape exocarp and seeds in the presence of other bioactive compounds. These plant materials were used because they represent the main source of this bioactive compound. The developed analytical method was validated in

accordance with ICH guidelines and USP requirements [30,31].

EXPERIMENTAL

Chemicals and reagents. *trans*-Resveratrol (>99.4%) (Dr. Ehrenstorfer GmbH, Augsburg, Germany), methanol HPLC grade (LGC Standards, Merkatorstabe, Wesel, Germany), ethanol (96%) analytical grade (Zorka Pharma-Hemija d.o.o., Šabac, Serbia), 2,2-diphenyl-1--picrylhydrazyl (DPPH, Sigma Chemical Company, Saint Louis, USA).

Plant materials. The used red grape was of variety "Cardinal" from Southeastern Serbia. Plant materials (exocarp and seeds) were dried at room temperature and then disintegrated in laboratory mill.

Procedure of resveratrol extractions. About 2 g of the disintegrated plant materials (grape exocarp and seeds) were transferred into the round-bottom flask of 100 cm^3. After adding 96% ethanol in the solid to liquid ratio of 1:15 (*m*/*V*), the mixture was put under reflux at the boiling temperature of solvent for 90 min. The extraction temperature was maintained using a water bath. After extraction, the solid matrix was separated from the liquid by vacuum filtration. Then, the extract was evaporated under reduced pressure on the rotary evaporator at 60 °C until semi-solid consistency. The extract was dried to constant mass in a desiccator.

HPLC analysis. The development of method was performed using an Agilent 1100-Series HPLC system. It consisted of a DAD detector and Agilent 1100-Series autosampler (Waldbronn, Germany). The system was controlled and data analyses were tested by Agilent HPLC Data Analysis software. The assays were reproduced using another LC system for repeatability. This system contained an Agilent 1100-Series binary pump and Agilent 1100-Series DAD detector (Waldbronn, Germany). The detector was set and the peak areas were integrated automatically by the computer using the Agilent HPLC Data Analysis software program. RP-HPLC analysis was performed by isocratic elution with a flow rate of 1.0 cm^3 min^{-1}. Methanol was used as a mobile phase, which was filtered through a 0.45 μm millipore filter (Econofilters, Agilent Technologies, Germany) before injecting into the system. The injected volume of samples was 20 μL, and the detection wavelength was 306 nm. The separation was carried out at 35 °C using a Supelco C_{18} column (250 mm×4.6 mm, 5 μm), Agilent Technologies, USA.

Preparation of samples. The stock solutions of *trans*-resveratrol and extracts were prepared by dissolving 12.5 mg of standard and 50 mg of the dried extracts in 25 cm^3 of methanol, respectively. From these solutions, the aliquot of 1 cm^3 was transferred into the flask of 10 cm^3 and filled to the mark with mobile phase. The samples were sonificated for 15 min, filtered through a cellulose membrane of 0.45 μm (Econofilters, Agilent Technologies, Germany). The volume sample of 20 μl was injected into the HPLC system. The identification of *trans*-resveratrol in the extracts was performed by comparison of the retention times and UV spectra with *trans*-resveratrol standard. The samples of standard solution and extracts were stored in the dark to avoid oxidative degradation and isomerization of *trans*-resveratrol to *cis*- form.

Analytical method validation

Linearity. The series of *trans*-resveratrol standard solutions were prepared in the range from 1–100 μg cm^{-3} to establish a linearity of the proposed method.

Accuracy. The different concentrations of *trans*-resveratrol (10, 20 and 30 μg cm^{-3}) were prepared from independent stock solution and then analyzed (n = 10). Accuracy was assessed as a percentage accuracy and mean recovery (%). In order to provide an additional support to the accuracy of the developed assay method, the method of standard addition was employed. It involves the addition of different concentrations of pure *trans*-resveratrol (1, 3 and 5 μg cm^{-3}) to the known pre-analyzed sample.

Precision. Inter-day, intra-day and inter-instrument variation were studied to determine the intermediate precision of the proposed analytical method. Three different concentrations of *trans*-resveratrol (10, 20 and 30 μg cm^{-3}) were analyzed for three days (three times, n = 3) to study the intra-day variation. The same procedure was followed for three different days to study the inter-day variation (n = 10). One set of different concentrations was reanalyzed by proposed method using another HPLC Agilent 1100-Series system to study inter-instrument variation (n = 10).

Limit of detection (*LOD*) and limit of quantitation (*LOQ*). *LOD* and *LOQ* were determined based on the solutions of *trans*-resveratrol used to construct the calibration curve. *LOD* and *LOQ* were calculated as 3.3 σ/S and 10σ/S, respectively, where S is the slope of the calibration curve and σ is the standard deviation of regression equation intercept (n = 10).

Robustness. A full factorial design was used for investigation of method robustness, where the temperature and flow rate of mobile phase were used as the independent variables. The temperature and the flow rate were in the range of 33–37 °C, *i.e.,* 0.8–1.2 cm^3 min^{-1}, respectively. In accordance with the design matrix 9 experimental runs were performed and repeated 3 times. Statistica version 8.0 (StatSoft Inc., Tulsa, OK, USA) was used to generate the experimental designs, statistical analysis and regression model.

DPPH assay. The series of different concentrations of the extracts and *trans*-resveratrol standard were prepared by dissolving the stock solutions (2.0 mg cm^{-3}). The ethanolic solution of DPPH radicals with the con-

centration of 3×10^{-4} mol dm^{-3} (1 cm^3) was added into the investigated solution (2.5 cm^3). The absorbance of samples was measured at 517 nm in compared to 96% ethanol after incubation of 30 min with DPPH radicals. The incubation was performed in the dark at room temperature. Under the same conditions, the absorbance of the diluted ethanolic solution of DPPH radical (1 cm^3 was diluted with 2.5 cm^3 of ethanol) was determined. The inhibition of DPPH radicals was calculated using the following equation:

$$\text{Inhibition of DPPH radicals (\%)} = \\ = 100 - \left[\left(A_U - A_B \right) \left(\frac{100}{A_K} \right) \right] \quad (1)$$

where A_U – absorbance of the sample treated with the solution of DPPH radicals, A_B – absorbance of the untreated sample with the solution of DPPH radicals, A_K – absorbance of the diluted ethanolic solution of DPPH radicals [32,33].

RESULTS AND DISCUSSION

Optimization of HPLC method

RP-HPLC method was developed and validated for the quantification of *trans*-resveratrol in the plant extracts. The chromatographic conditions were optimized to provide a good performance of the assay. The different stationary phases like C_{18} and C_8 were tested during method optimization. The satisfactory separation was achieved on a Supelco C_{18} column (250 mm×4.6 mm, 5 µm) using methanol as a mobile phase. The effects of various organic modifiers on the peak properties (peak height, peak area, peak symmetry, retention time, etc.) and response function were observed. A maximum absorption of *trans*-resveratrol was detected at 306 nm, and this wavelength was chosen for monitoring its content in the samples. A chromatogram of the *trans*-resveratrol solution at 20 µg cm^{-3} is presented in Fig. 2. The peak of *trans*-resveratrol at the retention time of 2.535 min was confirmed based on the UV spectrum.

The column efficiency was considered based on peak asymmetry (*As*), height equivalent to a theoretical plate (*HETP*), number of theoretical plates (*N*) and retention time (t_r). The calculated value of *HETP* was 0.042, *i.e.*, the value of *N* was 5958. The asymmetry peak of 1.4 indicates that the peak is not ideally symmetric and that it is not a Gauss's peak. Having in mind the fact that W_{ab} is lower than W_{bc}, there is the presence of some interactions between the stationary phase and the investigated compound. Most practical researchers strive that the asymmetry peak to be lower than 1.5.

Validation

The obtained results for construction of the calibration curve can be fitted as follows: A_{306} = 111.75*c* (µg cm^{-3}) + 123.95. The linearity of the constructed curve was noticed in the concentration range of 1–40 µg cm^{-3} (r = 0.9994). The high value of regression coefficient indicates a good fitting of the curve. The precision of fitting was further confirmed based on standard error (*S.E.*) at 95% confidence interval for the values of intercept (0.114) and slope (0.456).

In order to determine the accuracy of the proposed method, the different levels of *trans*-resveratrol concentrations: lower concentration (*LC*, 10 µg cm^{-3}), intermediate concentration (*IC*, 20 µg cm^{-3}) and higher concentration (*HC*, 30 µg cm^{-3}) were prepared from independent stock solutions and analyzed (n = 10). Accuracy was assessed as the percentage relative error and mean recovery (Table 1).

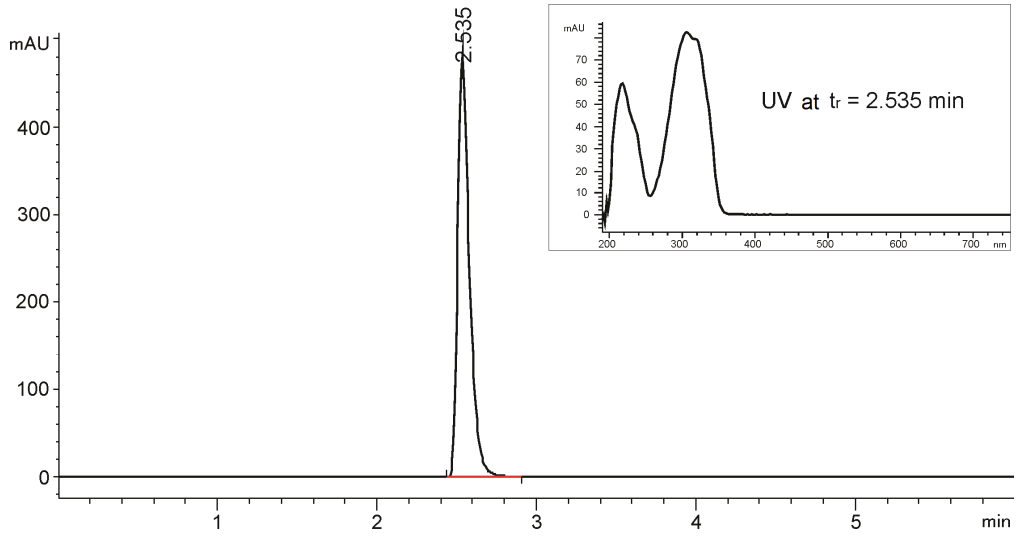

Fig. 2. Chromatogram of the standard solution of trans-resveratrol (20 µg cm^{-3}) at 306 nm.

Table 1. Accuracy and precision data for the developed method (n = 10)

Level, μg cm^{-3}	Predicted concentration, μg cm^{-3}		Mean recovery, %	Accuracy, %
	Mean (±*SD*)	*RSD* / %		
10	10.29±0.24	0.71	102.90	2.90
20	19.47±0.51	0.62	97.35	–2.70
30	29.39±0.41	0.49	97.96	–2.03

The excellent mean recovery values, close to 100%, and their low standard deviation values (*RSD* < 1.0) represent high accuracy of the analytical method. The validity and reliability of the proposed method were further assessed by recovery studies *via* standard addition method. The mean recoveries (*RSD*) for the concentration of 20 μg cm^{-3} are shown in Table 2.

These results revealed that any small change in *trans*-resveratrol concentration in the solution could be accurately determined by the proposed analytical method.

Precision was determined by studying the repeatability and the intermediate precision. The precision was determined using the same *trans*-resveratrol concentration levels taken in the accuracy study.

The results of repeatability studies (Table 3) indicate the precision under the same operating conditions over a short interval of time and the inter-assay precision. The intermediate precision expresses within-laboratory variations in different days and with different instruments. In the intermediate precision study, *RSD* values were not more than 2.0% in all cases (Table 3). *RSD* values of the proposed analytical method were well within the acceptable range. These values indicate the excellent repeatability and intermediate precision of the method.

The calculated *LOD* and *LOQ* values of *trans*-resveratrol were 0.125 and 0.413 μg cm^{-3}, respectively.

Stability of solution. The different concentrations of *trans*-resveratrol (10, 20 and 30 μg cm^{-3}) were used to determine the stability of the test solution (20 μg cm^{-3}). The change in *trans*-resveratrol concentration was monitored during 24 and 48 h. Test and standard solutions were stored in autosampler vials at ambient temperature. The obtained results for test and standard solutions are shown in Table 4.

Robustness of method. The robustness of method is investigated in the framework of method development as a concept of quality by design. The aim of the robustness of the developed RP-HPLC method is to examine the variation which might be expected in routine use of this method. A full factorial design with two variables at three levels was used for monitoring the robustness of the developed method [34–37]. The peak area (Y_1), retention time (Y_2), number of theoretical plates (Y_3) and peak asymmetry (Y_4) were defined as the response, while the column temperature (x_1) and flow rate of mobile phase (x_2) were used as the independent variables. The column temperature and flow rate of mobile phase were analyzed in the range of 33–37 °C, *i.e.*, 0.8–1.2 cm^3 min^{-1}, respectively. A polynomial equation that can be used for investigation of the interaction between linear and quadratic terms in the equation was used for modeling the experimental data. The terms with p-values higher than 0.05 are the statistically insignificant and they were excluded from the polynomial equation. The equations that present the effect of the process variables on the observed response, it can be presented in the following way:

Table 2. Determination of trans-resveratrol by standard addition method (n = 10); concentration: 20 μg cm^{-3}

Pure drug added, μg cm^{-3}	Total drug found ± *SD*, μg cm^{-3}	*RSD* / %
0	20.17±0.3	100.85±0.6
1	20.89±0.3	99.47±0.5
3	23.11±0.4	100.48±0.6
5	24.91±0.4	99.64±0.5

Table 3. System precision study (n = 10)

Concentration, μg cm^{-3}	Estimated concentration, intra-day reproducibility (*RSD* / %, *n* = 10)			Intra-instrument reproducibility (*RSD* / %, *n* = 10)
	Day 1	Day 2	Day 3	
10	8.15 (0.81)	10.74 (0.57)	10.41 (0.44)	9.09 (0.89)
20	20.86 (0.05)	20.32 (0.30)	19.78 (0.10)	20.83 (1.43)
30	29.59 (0.10)	28.66 (0.84)	30.13 (0.12)	28.99 (1.58)

Peak area: $Y_1 = 2531.2 - 510.6x_2 - 52.1x_2^2$
(r^2 = 1.000) (2)

Retention time: $Y_2 = 2.6 - 0.004x_1 - 0.5x_2 - 0.05x_2^2$
(r^2 = 1.000) (3)

Number of theoretical plates:
$Y_3 = 6825 - 784.6x_1^2 - 3173.8x_2 - 949.4x_2^2 +$
$+1151.2x_1x_2 + 928.3x_1x_2$
(r^2 = 0.998) (4)

Peak assymetry:
$Y_4 = 1.87 - 0.11x_2 - 0.15x_2^2 -$
$-0.15x_1x_2 - 0.07x_1x_2$ (r^2 = 0.921) (5)

Table 4. Stability of trans-resveratrol solutions

Time elapsed, h	Sample	c / μg cm^{-3}	Recovery, %
Initial	st	20.00	100.0
24		19.51	97.55
48		20.42	102.1
Initial	1	10.00	100.0
24		9.81	98.1
48		10.34	103.4
Initial	2	20.00	100.0
24		20.88	104.4
48		19.20	96.0
Initial	3	30.00	100.0
24		29.01	96.7
48		30.57	101.9

The high values of correlation coefficient indicate a good agreement between experimental and predicted values. In all case this value is almost equal to 1. The highest impact on the peak area has the flow rate of mobile phase, while the effect of column temperature is statistically insignificant. The retention time, number of theoretical plates and peak asymmetry mainly depend on the flow rate of mobile phase. Based on the obtained data, it can be concluded that unlike the change in column temperature, the significant change in flow rate can be impact the performance of the system.

A functional dependency between flow rate of mobile phase and column temperature is presented in Fig. 3. In this case, a number of theoretical plates were used as a response. The previous conclusion that the flow rate of mobile phase most impacts the number of theoretical plates was confirmed based on that three-dimensional diagram. Also, it can be noticed that the column temperature is not a statistically significant parameter and does not impact the system performance.

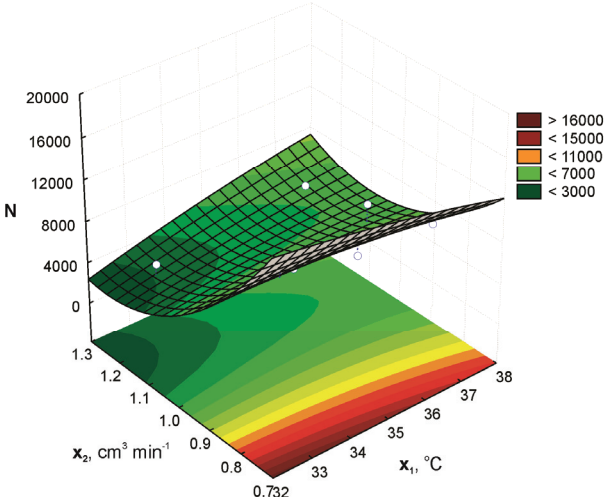

Fig. 3. The effect of column temperature (x_1) and flow rate of mobile phase (x_2) on number of theoretical plates (N).

Application of the method for analysis of the plant extracts

In order to apply the developed and validated RP-HPLC method, the ethanolic extracts of red grape exocarp and seeds were prepared. The two solutions of the obtained extracts were dissolved and two solutions were analyzed in order to identify and quantify *trans*-resveratrol. The chromatograms of the extracts solutions are presented in Fig. 4. The presence of *trans*-resveratrol in the extracts of seeds and exocarp was identified at the retention times of 2.523 and 2.525 min, respectively. The peaks of *trans*-resveratrol were confirmed by comparison of the UV spectra at these retention times with the UV spectrum of *trans*-resveratrol standard. Based on the regression equation of calibration curve, the content of *trans*-resveratrol in the extracts of exocarp and seeds was found to be 208.88 mg and 277.63 mg calculated per 100 g of the dried extracts, respectively.

The RP-HPLC method was presented as suitable for analysis of *trans*-resveratrol in the plant extracts due to simpler composition of the mobile phase and shorter time of analysis in compared with available methods [26–29].

Antioxidant activities of *trans*-resveratrol and grape extracts

In this study, DPPH assay was used for determination of antioxidant activities of *trans*-resveratrol standard and grape extracts. The incubation time has the impact on inhibition of DPPH radicals and thereby the antioxidant activity is better observed. Due to this reason, all samples were incubated for 30 min before the absorbance measurement.

The effect of concentration of the samples on inhibition of DPPH radicals is presented in Fig. 5. It can be noticed that the inhibition of DPPH radicals increases

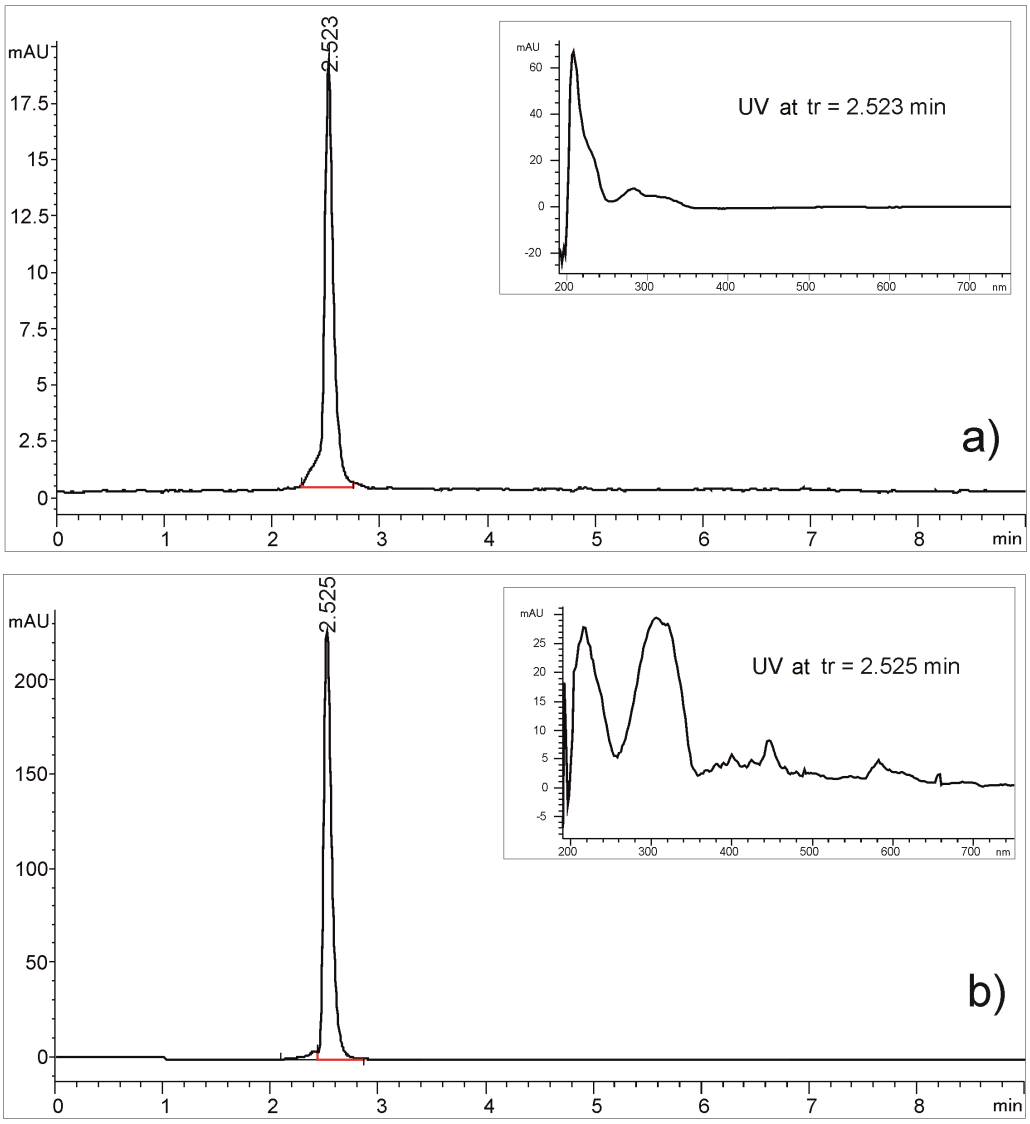

Fig. 4. Chromatogram of the extracts of: grape seeds (a) and grape exocarp (b) at 306 nm.

with increasing the concentration of *trans*-resveratrol standard (6.25–800 μg cm^{-3}). The maximum inhibition of DPPH radicals (93.48%) was achieved at the concentration of *trans*-resveratrol standard of 0.4 mg cm^{-3} after incubation of 30 min. In the literature, the inhibition of DPPH radicals of 14% was achieved at the concentration 250 μM [38], while the concentration of 5.7 mM inhibited 21.16% of DPPH radicals in this study.

The obtained results indicate that the extract of grape seeds has better antioxidant activity compared to the extract of grape exocarp at similar concentrations of the samples. The inhibition of DPPH radicals of 96.06% for the grape seeds extract was achieved at the concentration of 0.125 mg cm^{-3}, while the inhibition of 99.47% was at 2.000 mg cm^{-3} of the extract of grape exocarp. Thus, the antioxidant activity of the extract of grape seeds is lower about 16 times in compared with the extract of grape exocarp, *i.e.*, about 3 times lower in compared with *trans*-resveratrol standard.

EC_{50} values of the samples were determined empirically from diagrams given in Fig. 5. The highest value (EC_{50} = 0.44 mg cm^{-3}) was obtained for the extract of grape exocarp, and something lower value (EC_{50} = = 0.066 mg cm^{-3}) for *trans*-resveratrol standard. The lowest value (EC_{50} = 6.77 μg cm^{-3}) was calculated for the extract of grape seeds. The obtained values indicate that the extract of grape exocarp has the lowest ability of DPPH radicals inhibition in compared with the extract of grape seeds and *trans*-resveratrol standard. The ability of the extract of grape seeds to better "scavenge" DPPH radicals than *trans*-resveratrol standard and the extract of grape exocarp is probably the result of the presence of other additional compounds that also show the antioxidant activity. The flavonoids and

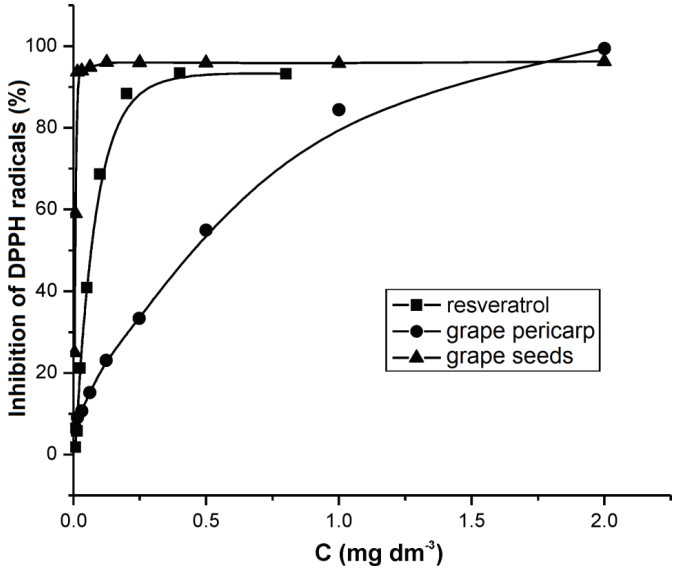

Fig. 5. Antioxidant activity of trans-resveratrol standard (■), the extract of grape exocarp (●) and the extract of grape seeds (▲).

phenolic acids commonly belong to the group of these compounds.

CONCLUSION

The proposed RP-HPLC method is presented as a simple, rapid, accurate, precise and economic analytical method. It can be used for the routine analysis of *trans*--resveratrol in the red grape extracts and other plant extracts containing *trans*-resveratrol. This method has advantages due to fast analysis and simpler composition of the mobile phase in compared with the other HPLC methods for monitoring the content of *trans*-resveratrol in the plant extracts. The results of robustness study indicate that the proposed method stays stable even after the nominal changes in the column temperature. The antioxidant activity of the extract of grape seeds was higher than the extract of grape exocarp probably due to the presence of additional bioactive compounds with expressed activity.

Acknowledgments

The financial support was provided by the Ministry of Education, Science and Technological Development of the Republic of Serbia, under the project TR-34012.

REFERENCES

[1] M. Takaoka, Of the phenolic substances of white hellebore (*Veratrum grandiflorum* Loes. Fil.), J. Faculty Sci. Hokkaido Imperial Univ. **3** (1940) 1–16.

[2] M. Ndiaye, C. Philippe, H. Mukhtar, N. Ahmad, The grape antioxidant resveratrol for skin disorders: promise, prospects, and challenges, Arch. Biochem. Biophys. **508** (2011) 164–170.

[3] T.S. Figueiras, M.T. Neves-Petersen, S.B. Petersen, Activation energy of light induced isomerization of resveratrol, J. Fluoresc. **21** (2011) 1897–1906.

[4] I. Gulcin, Antioxidant activity of food constituents: an overview, Innov. Food Sci. Emerg. **11** (2010) 210–218.

[5] J.E. Torres-Lopez, M.I. Ortiz, G. Castaneda-Hernandez, R. Alonso-Lopez, R. Asomoza-Espinosa, V. Grandos-Soto, Comparison of the antinociceptive effect of celecoxib, diclofenac and resveratrol in the formalin test, Life Sci. **70** (2002) 1669–1676.

[6] C. Alarcon de la Lastra, I. Villegas, Resveratrol as an antioxidant and pro-oxidant agent: mechanisms and clinical implications, Biochem. Soc. T. **35** (2007) 1156––1160.

[7] Z.R. Wang, Y.Z. Huang, J.C. Zou, K.J. Cao, Y.N. Xu, J.M. Wu, Effects of red wine and wine polyphenol resveratrol on platelet aggregation in vivo and in vitro, Int. J. Mol. Med. **9** (2002) 77–79.

[8] M. Campagna, C. Rivas, Antiviral activity of resveratrol, Biochem. Soc. T. **38** (2010) 50–53.

[9] T. Walle, F. Hsieh, M.H. DeLegge, J.E. Oatis, J.U. Kristina Walle, High absorption but very low bioavailability of oral resveratrol in humans, Drug Metab. Dispos. **32** (2004) 1377–1382.

[10] R. Montes, M. Garcia-Lopez, I. Rodriguez, R. Cela, Mixed-mode solid-phase extraction followed by acetylation and gas chromatography mass spectrometry for the reliable determination of *trans*-resveratrol in wine samples, Anal. Chim. Acta **673** (2010) 47–53.

[11] R.G. Peres, G.A. Micke, M.F. Tavares, D.B. Rodriguez-Amaya, Multivariant optimization, validation, and application of capillary electrophoresis for simultaneous determination of polyphenols and phenolic acids in Brazilian wines, J. Sep. Sci. **32** (2009) 3822–3828.

[12] L. Vlase, B. Kiss, S.E. Leucuta, S. Gocan, A rapid method for determination of resveratrol in wines by HPLC-MS, J. Liq. Chromatogr. R. T. **32** (2009) 2105–2121.

[13] M. Ji, Q. Li, H. Ji, H. Lou, Investigation of the distribution and season regularity of resveratrol in Vitis amurensis via HPLC–DAD–MS/MS, Food Chem. **142** (2014) 61–65.

[14] F. de Souza Dias, M.F. Silva, J.M. David, Determination of Quercetin, Gallic Acid, Resveratrol, Catechin and Malvidin in Brazilian Wines Elaborated in the Vale do Sao Francisco Using Liquid–Liquid Extraction Assisted by Ultrasound and GC-MS, Food Anal. Method **6** (2013) 963–968.

[15] P. Vinas, N. Campillo, N. Martinez-Castillo, M. Hernandez-Cordoba, Solidphase microextraction on-fiber derivatization for the analysis of some polyphenols in wine and grapes using gas chromatography–mass spectrometry, J. Chromatogr. A **1216** (2009) 1279–1284.

[16] G.J. Soleas, J. Yan, D.M. Goldberg, Measurement of *trans*-resveratrol, (+)-catechin, and quercetin in rat and human blood and urine by gas chromatography with mass selective detection, Method Enzymol. **335** (2001) 130–145.

[17] G.J. Soleas, J. Yan, D.M. Goldberg, Ultrasensitive assay for three polyphenols (catechin, quercetin and resveratrol) and their conjugates in biological fluids utilizing gas chromatography with mass selective detection, J. Chromatogr. B Biomed. Sci. Appl. **757** (2001) 161–172.

[18] D.M. Goldberg, J. Yan, G.J. Soleas, Absorption of three wine-related polyphenols in three different matrices by healthy subjects, Clin. Biochem. **36** (2003) 79–87.

[19] X. Meng, P. Maliakal, H. Lu, M.J. Lee, C.S. Yang, Urinary and plasma levels of resveratrol and quercetin in humans, mice, and rats after ingestion of pure compounds and grape juice, J. Agric. Food Chem. **52** (2004) 935–942.

[20] L. Almeida, M. Vaz-da-Silva, A. Falcao, E. Soares, *et al*., Pharmacokinetic and safety profile of trans-resveratrol in a rising multiple-dose study in healthy volunteers, Mol. Nutr. Food Res. **53** (2009) S7–S15.

[21] T. Walle, F. Hsieh, M.H. DeLegge, J.E. Oatis, U.K.Walle, High absorption but very low bioavailability of oral resveratrol in humans, Drug Metab. Dispos. **32** (2004) 1377–1382.

[22] P. Vitaglione, S. Sforza, G. Galaverna, C. Ghidini, *et al*., Bioavailability of trans-resveratrol from red wine in humans, Mol. Nutr. Food Res. **49** (2005) 495–504.

[23] A. Burkon, V. Somoza, Quantification of free and proteinbound *trans*-resveratrol metabolites and identification of trans-resveratrol-C/O-conjugated diglucuronides – two novel resveratrol metabolites in human plasma, Mol. Nutr. Food Res. **52** (2008) 549–557.

[24] E. Wenzel, T. Soldo, H. Erbersdobler, V. Somoza, Bioactivity and metabolism of *trans*-resveratrol orally administered to Wistar rats, Mol. Nutr. Food Res. **49** (2005) 482–494.

[25] M.A. Vian, V. Tomao, S. Gallet, P.O. Coulomb, J.M. Lacombe, Simple and rapid method for *cis*- and *trans*-resveratrol and piceid isomers determination in wine by high-performance liquid chromatography using chromolith columns, J. Chromatogr., A **1085** (2005) 224–229.

[26] L. Paulo, F. Domingues, J.A. Queiroz, E. Gallardo, Development and validation of an analytical method for the determination of *trans*-and *cis*-resveratrol in wine: analysis of its contents in 186 Portuguese red wines, J. Agr. Food Chem. **59** (2011) 2157–2168.

[27] R.M. Lamuela-Raventos, A.I. Romero-Perez, A.L. Waterhouse, M.C. De La Torre-Boronat, Direct HPLC analysis of *cis*-and *trans*-resveratrol and piceid isomers in Spanish red *Vitis vinifera* wines, J. Agr. Food Chem. **43** (1995) 281–283.

[28] A.A. Souto, M.C. Carneiro, M. Seferin, M.J. Senna, A. Conz, K. Gobbi, Determination of *trans*-resveratrol concentrations in brazilian red wines by HPLC, J. Food Compos. Anal. **14** (2001) 441–445.

[29] V.S. Sobolev, R.J. Cole, *trans*-Resveratrol content in commercial peanuts and peanut products, J. Agr. Food Chem. **47** (1999) 1435–1439.

[30] International Conference on Harmonisation (ICH) of Technical Requirements for Registration of Pharmaceuticals for Human Use, Topic Q2 (R1): Validation of Analytical Procedures: Text and Methodology, 2005, www.ich.org.

[31] United States Pharmacopoeia, Validation of Compendial Methods, 26th ed., Pharmacopoeial Convention Inc., Rockville, MD, 2003. pp. 2439–2442.

[32] R. Aquino, S. Morelli, A. Tomaino, M. Pellegrino, A. Saija, L. Grumetto, C. Pugli, D. Ventura, F. Bonina, Antioxidant and photoprotective activity of a crude extract of *Culcitium reflexun* HBK leaves and their major flavonoids, J. Ethnopharmacol. **79** (2002) 183–191.

[33] C.W. Choi, S.C. Kim, S.S. Hwang, B.K. Choi, H.J. Ahn, M.Y. Lee, S.H. Park, S.K. Kim, Antioxidant activity and free radical scavenging capacity between Korean medicinal plants and flavonoids by assay-guided comparison, Plant Sci. **163** (2002) 1161–1168.

[34] I. Savic, V. Nikolic, I. Savic, Lj. Nikolic, M. Stankovic, Development and validation of a new RP-HPLC method for determination of quercetin in green tea, J. Anal. Chem. **68** (2013) 906–911.

[35] I. Savic, V. Nikolic, I. Savic, Lj. Nikolic, M. Stankovic, Development and validation of HPLC method for the determination of amygdalin in the plant extract of plum kernel, Res. J. Chem. Environ. **16** (2012) 80–86.

[36] R. Ragonese, M. Mulholland, J. Kalman, Full and fractionated experimental designs for robustness testing in the high-performance liquid chromatographic analysis of codeine phosphate, pseudoephedrine hydrochloride and chlorpheniramine maleate in a pharmaceutical preparation, J. Chromatogr., A **870** (2000) 45–51.

[37] E. Hund, D.L. Massart, S. Verbeke, Robust regression and outlier detection in the evaluation of robustness tests with different experimental designs, J. Anal. Chim. Acta **463** (2002) 53–73.

[38] S. Selvaraj, A. Mohan, S. Narayanan, S. Sethuraman, U.M. Krishnan, Dose-dependent interaction of *trans*-resveratrol with biomembranes: effects on antioxidant property, J. Med. Chem. **56** (2013) 970–981.

IZVOD

RAZVOJ I VALIDACIJA RP-HPLC METODE ZA KVANTIFIKACIJU *TRANS*-RESVERATROLA U BILJNIM EKSTRAKTIMA

Žika S. Cvetković, Vesna D. Nikolić, Ivan M. Savić, Ivana M. Savić-Gajić, Ljubiša B. Nikolić

Tehnološki fakultet, Univerzitet u Nišu, Bulevar oslobođenja 124, 16000 Leskovac, Srbija

(Naučni rad)

U ovom radu razvijena je i validirana nova, jednostavna, isplativa i ponovljiva RP-HPLC metoda za kvantifikaciju *trans*-resveratrola u ekstraktima egzokarpa i semena grožđa. Metoda se pokazala jednostavnijom i bržom u odnosu na ostale dostupne metode. Kao mobilna faza korišćen je metanol pri protoku 1,0 cm^3 min^{-1}. Separacija je postignuta na 35 °C primenom C_{18} kolone. Kvantifikacija *trans*-resveratrola vršena je na 306 nm. Rezultati su pokazali da je konstruisana kalibraciona kriva linearna u opsegu koncentracija 1–40 μg cm^{-3}. Sračunate vrednosti *LOD* i *LOQ* iznosile su 0,125 i 0,413 μg cm^{-3}, redom. Antioksidativna aktivnost ektrakata određena je primenom DPPH testa. Sposobnost inhibicije DPPH radikala smanjuje se sledećim redosledom: ekstrakt egzokarpa grožđa > standard *trans*-resveratrola > ekstrakt semena grožđa.

Ključne reči: Validacija • RP-HPLC • *trans*-Resveratrol • Ekstrakt grožđa • Antioksidativna aktivnost

Cloning of the gene for a carbohydrate oxidase from *Lactuca sativa* in the yeasts *Saccharomyces cerevisiae* and *Pichia pastoris*

Vojin M. Tadić[1], Ana Marija J. Balaž[2], Marija P. Petrić[1], Snežana M. Milošević[1], Nevena D. Zelenović[3], Martin Z. Raspor[1], Jovan M. Tadić[4], Radivoje M. Prodanović[2]

[1]*Department for Plant Physiology, Institute for Biological Research "Siniša Stanković", University of Belgrade, Belgrade, Serbia*
[2]*Department for Biochemistry, Faculty of Chemistry, University of Belgrade, Belgrade, Serbia*
[3]*Institute for Chemistry, Technology and Metallurgy, University of Belgrade, Belgrade, Serbia*
[4]*Department of Global Ecology, Carnegie Institution for Science, Stanford, CA, USA*

Abstract

We have cloned the gene for carbohydrate oxidase (CHO) from *Lactuca sativa* in two species of yeasts (*Saccharomyces cerevisiae* and *Pichia pastoris*). The synthetic gene for the carbohydrate oxidase (1821 bp) from *L. sativa* cloned into the vector pUC57 and inserted into plasmids pYES2 and pGAP using *Escherichia coli* DH5α strain. The *P. pastoris* strain X-33 and the *S. cerevisiae* strain InvSC1 were used for extracellular expression of CHO. After transformation of *P. pastoris* X-33 with CHO-pGAP construct none of the colonies showed CHO activity. Two samples displayed a band which did not exist in the sample with the empty vector similar to the molecular weight of CHO. The *S. cerevisiae* strain InvSC1 has been also transformed with CHO-pYES constructs. Three colonies grew on the plate with cells transformed with the construct. One of the samples showed a band corresponding to about 110 kDa, but no CHO activity was recorded in this case either. Cloning of the foreign genes and heterologous expression in yeasts is widely used in biotechnology, but sometimes can be very dependent on the gene sequence and strain used. In order to obtain active CHO enzyme the further studies on purification and refolding of expressed protein are necessary.

Keywords: *Saccharomyces cerevisiae*, *Pichia pastoris*, carbohydrate oxidase, glycosylation.

Available online at the Journal website: http://www.ache.org.rs/HI/

SCIENTIFIC PAPER

UDC 635.52:575:577:663

Hem. Ind. **69** (6) 689–701 (2015)

doi: 10.2298/HEMIND140823003T

Carbohydrate oxidase (CHO) from lettuce (*Lactuca sativa*) is an enzyme that has not been examined in detail. Very little is known about its structure and function. CHO belongs to the large family of carbohydrate oxidases which oxidize sugars. Length of the polypeptide sequence varies depending on the source. Some carbohydrate oxidases have long polypeptide chains (418 to 475 amino acids), while some authors mention up to 540 amino acids polypeptide sequences [1–3]. One of the domains is a flavin cofactor binding domain, and the second is a substrate binding domain. Most of substrate oxidation occurs through a so-called ping-pong mechanism [4]. The Michaelis–Menten constant and V_{max} vary depending on the substrate used, and on the natural source from which enzyme was obtained. K_m may be from 0.175 mM for glucose up to 11 mM for lactose and 50 mM for galactose. According to some authors, the K_m for lactose is 0.066 mM [1,3––5]. The temperature and pH optimum of the enzyme are also diverse. The most common data in the studies mention a temperature optimum of around 38 °C [4]. The pH optimum displays two peaks, the first one located at pH 6.0-6.5, and the other one at pH 9–10.5 [6,7].

All the carbohydrate oxidases have found great application in various fields of industry. Examples of such enzymes are glucose oxidase, L-glucono lactone oxidase, hexose oxidase, lactose oxidase, glucoologosaccharide-oxidase and pyranose oxidase. All of mentioned enzymes, except glucose oxidase and pyranose oxidase, belong to the family of vanillyl alcohol oxidases.

Data on CHO relative molecular mass are also diverse depending on the source of the enzyme. Moreover, recombinant proteins have higher molecular weight. Proteins derived from expression vectors such as yeasts *S. cerevisiae* or *P. pastoris*, have a higher degree of glycosylation. The recombinant enzyme, expressed in *P.pastoris*, contains up to 14 *N*-linked mannose residues [8]. The relative molecular weight of the carbohydrate oxidase from various species of fungi, bacteria and plants has been found to vary between 45 and 65 kDa [1–4]. CHO catalyzes the oxidation of the primary alcohol groups in monosaccharides and oligosaccharides, with the reduction of molecular oxygen to

Correspondence: V.M. Tadić, Department for Plant Physiology, Institute for Biological Research "Siniša Stanković", University of Belgrade, Bulevar despota Stefana 142, 11000 Belgrade, Serbia.
E-mail: vojin.tadic@ibiss.bg.ac.rs
Paper received: 23 August, 2014
Paper accepted: 10 December, 2014

hydrogen peroxide. The enzyme is capable of generating hydrogen peroxide using cellobiose as substrate. However, this enzyme does not oxidize fructose. Essential substrate structure is a six-member pyranose monosaccharide ring and the OH group on the second carbon atom in the equatorial position [1,8,9].

CHO may be applied to the diagnosis, particularly in biosensors for the determination of glucose in the blood, in the food industry, agriculture, production of bread and detergents and in various other industrial areas. The drawback of this enzyme is the low concentrations in natural sources [10]. Also, natural enzymes often do not meet industrial requirements. Various methods of recombinant technology have been developed for the synthesis of these enzymes. Apart from the necessary quantities, the enzyme must have a high stability and activity, particular substrate specificity and high selectivity.

Very little is known about the structure and activities of CHO from lettuce and its role in nature can be easily described through examples of related enzymes. All members of the large family of CHO's have the same role: oxidation of sugar. Today, the best known and most widely applied enzymes are glucose oxidase, galactose oxidase and hexose oxidase.

The yeast *P. pastoris* has become one of the most used eukaryotic organisms for the production of recombinant proteins. Many authors emphasize that *P. pastoris* is easy to grow and can reach a high density of cells, which is of great industrial interest. In addition, this system has strong regulated promoters and has the ability of secreting foreign proteins. Also, it has the possibilities of posttranslational modifications in the form of glycosylation and formation of disulfide bonds [11,12]. However, the high density of cells raises several problems such as transfer of oxygen, which is the main limiting factor. The high cell density is a source of stress which could lead to a decrease in cell viability and productivity and increase cell lysis. Another problem associated with the secretion of heterologous protein is the retention of a certain amount of product in the cells [13].

Most *P. pastoris* expression systems use the methanol-induced alcohol oxidase (AOX1) promoter. Upon induction by methanol, the relative amount of AOX in total soluble proteins can typically rise up to 30%. AOX1 and AOX2 genes encode a functional enzyme, except that the AOX1 makes 95% of the AOX expressed due to the strength of its promoter. Therefore, systems that use pAOX1 take priority in the expression of foreign proteins [12].

Unlike the AOX1 system, where the production is limited by the availability of the protein in the methanol induction phase, the glyceraldehyde 3-phosphate dehydrogenase constitutive promoter (GAP) system of biomass and protein synthesis occurred simultaneously without methanol. While conditions during the induction phase of the AOX1 system must be strictly controlled, the GAP system has minimum requirements. For extracellular expression, a vector derived from *S. cerevisiae* α-factor is used, that contains a sequence encoding a secretion signal linked to the foreign gene [11]. Several studies have shown that pGAP is more efficient of pAOX1 for the production of proteins [12,14].

One of the main disadvantages of the *P. pastoris* expression system is a post-secretory proteolytic degradation of the recombinant products. Reducing the number of cells during the induction phase is correlated with the accumulation of intracellular reactive oxygen species, especially of formaldehyde and hydrogen peroxide, which are by-products of the metabolism of methanol [12,15].

The yeast *S. cerevisiae* is the most important eukaryotic model organism for molecular genetic studies. It is used in the production of bread and beer, and it is considered safe for the production of proteins for use in medicine or in the food industry. It is easy for genetic manipulation, which makes it popular for cloning and expression of eukaryotic proteins [12,16,17]. Beside *P. pastoris* and *Hansenula polymorpha*, *S. cerevisiae* is the most commonly used expression system due to the high amount of expressed proteins [18]. *S. cerevisiae* allows correct folding and glycosylation of heterologous eukaryotic proteins. The recombinant proteins were expressed in *S. cerevisiae* to a high level. Enzymes expressed in *S. cerevisiae* have a much greater molecular mass than in their natural host, due to extensive *N*-hyperglycosylation [19].

The aim of this study was cloning of CHO in yeast *S. cerevisiae* and *P. pastoris*, as well as its expression in these, nowadays, widely applied expression systems. We tried to obtain an enzyme that could be applied to enzymatic assays, biosensors, or as a supplement to the food industry and in the industry for bleaching detergents.

MATERIAL AND METHODS

Genes for CHO

The synthetic gene for the CHO (1821 bp) from the *L. sativa* was obtained from GenScript Company, USA, and cloned into the vector pUC57.

Strains and vectors

E. coli strain DH5α was used for cloning of genes and maintenance of the plasmid. *P. pastoris*, strain X-33, and the *S. cerevisiae* strain InvSC1 were used for extracellular expression of the carbohydrate oxidase. PGAPZαA vector, used for the expression of the carbohydrate oxidase in *P. pastoris* strain X-33, as well as the expression vector pYES2 carbohydrate oxidase in *S.*

cerevisiae strain InvSC1, were supplied by the company Invitrogen, Carlsbad, CA, USA.

Media for the growth of microorganisms

Luria Broth medium (LB)

LB medium was used for the growth of bacteria. The LB medium contained: yeast extract, 5 g L^{-1}; NaCl, 5 g L^{-1}; tryptone, 10 g L^{-1}; agar, 20 g L^{-1} (for solid medium) and antibiotics: zeocin (25 mg mL^{-1}) or ampicillin (100 mg mL^{-1}). Antibiotics have been added to the media after adjusting pH to 7.4, autoclaving and cooling to 40–50 °C.

Liquid medium for optimal growth of the bacteria (SOC)

SOC medium is primarily used for recovery of transformed *E. coli* competent cells. This medium improves the productivity of transformation of competent cells and contains: tryptone, 20 g L^{-1}, yeast extract, 5 g L^{-1}, NaCl, 0.5 g L^{-1}, 10 mM $MgCl_2$, 10 mM $MgSO_4$, glucose, 4 g L^{-1}. The media were autoclaved prior to addition of sterile solutions of $MgCl_2$, $MgSO_4$ and glucose through filter sterilization.

YPDS medium for P. pastoris growth

This medium was used for growing *P. pastoris* cells after transformation. The medium contains: yeast extract 10 g L^{-1}, peptone 20 g L^{-1}, 1 M sorbitol, agar 20 g L^{-1} (for solid medium), zeocin 100 mg mL^{-1} and glucose 20 g L^{-1}. The media were adjusted to pH 7.4 and autoclaved prior to addition of sterile solutions of glucose and zeocine through filter sterilization.

Rich liquid medium for growth of yeasts (2xYPAD)

2xYPAD is used for culture growing to log phase before transformation. The medium contains: yeast extract, 20 g L^{-1}, peptone, 40 g L^{-1}, adenosine sulfate, 80 mg L^{-1} and glucose, 40 g L^{-1}.

YNB-CAA medium

YNB-CAA medium was used for the selection of transformed yeast *S. cerevisiae* and consists of: $(NH_4)_2SO_4$, 5.1 g L^{-1}, YNB (yeast nitrogen base) without amino acids and ammonium sulfate (1.6 g L^{-1}), bacto casamino acid, 5 g L^{-1}, agar, 20 g L^{-1} (for solid medium), adenine, 20 mg L^{-1}, tryptophan, 20 mg $L^{-1}$and either glucose (2%, for selective media) or galactose (2%, for inducible media). Glucose or galactose have been added to the media from a sterile solution, after adjusting the pH to 5–6 and autoclaving.

Preparation of competent cells

Preparation of chemically competent E. coli DH5α cells

A single colony of *E. coli* DH5*α* was inoculated from a LA agar plate into 5 mL of LB liquid medium and grown in a shaker (250 rpm) over night at 37 °C. 1 mL of the overnight culture was transferred in 100 mL of LB liquid medium and cells were grown in a shaker (250 rpm) at 37 °C until the optical density reached a value between 0.3–0.5 at 600 nm (about 2–3 h). When the cells have reached the appropriate optical density, they were transferred on ice for 10 min and then centrifuged for 5 min at 3000 rpm at 4 °C. The precipitate was resuspended in 10 mL sterile cold $CaCl_2$ solution (60 mM $CaCl_2$, 15% glycerol, 10 mM TRIS, pH 7.0) and incubated on ice for 30 min. Cells were centrifuged for 5 min at 3000 rpm at 4 °C, then resuspended in 2 mL of sterile cold $CaCl_2$ solution, aliquoted at 100 µL, immediately frozen in liquid nitrogen and stored at –80 °C [20].

Preparation of electrocompetent cells of Pichia pastoris X-33

A single colony of *P. pastoris* X-33 was inoculated from YPD agar plate into 3 mL of YPD liquid medium containing 12.5 µg/mL chloramphenicol and grown in a shaker (250 rpm) over night at 30 °C. The overnight culture was transferred into 50 mL of YPD medium and the optical density was measured at 600 nm. Cells were grown in a shaker (250 rpm) at 30 °C until the optical density increased to 1–2. After reaching the appropriate optical density, cells were centrifuged for 10 min at 3000 rpm, resuspended in 10 mL of DTT/LiAc solution, and incubated for 30 min at room temperature. Then the cells were centrifuged again for 5 min at 3000 rpm, resuspended in 1 mL of cold 1 M sorbitol, transferred to a mini tube (1.5 mL) and centrifuged 5 min at 5000 rpm/min. The cells were then washed three times in cold 1 M sorbitol, resuspended in 500 µl of cold 1 M sorbitol and frozen at –80 °C.

Preparation of competent S. cerevisiae cells InvSC1

A single colony of *S.cerevisiae* InvSC1 was inoculated from YPD agar plate into 2.5 mL 2xYPAD liquid media containing 12.5 µg/mL chloramphenicol and grown in a shaker (250 rpm) over night at 30 °C. The overnight culture was transferred to 50 mL of 2xYPAD medium and the optical density was measured at 600 nm. Cells were grown in a shaker (250 rpm) at 30 °C until the optical density increased 4 times (about 4 h). After the cells have reached the appropriate optical density, they were centrifuged for 5 min at 3000 rpm, resuspended in 25 mL of sterile water and then centrifuged again for 5 min at 3000 rpm. After that, cells were resuspended in 500 µl of sterile water, centrifuged for 5 min at 6000 rpm, resuspended in 500 µl of a sterile solution of the FCC (5% glycerol, 10% DMSO) and frozen at –80 °C.

Cloning of CHO

Cloning of CHO in pGAPZαA vector

Restriction of CHO-pUC and pGAPZαA vectors. CHO--pUC57 was checked for restriction before cloning into the vector pGAPZ*α*A EcoRI. CHO-pUC and pGAPZ*α*A

vector were subjected to a double restriction with enzymes XbaI and XhoI. Restriction mixture contained components shown in Table 1.

Table 1. Components for restriction mixture for CHO-pUC and pGAPZαA vector double restriction with enzymes XbaI and XhoI

Component	CHO-pUC	pGAPZαA vector (μL)
10x Tango buffer	4	4
XhoI resriction enzyme (10U/μL)	2	2
XbaI resriction enzyme (10 U/μL)	1	1
Plasmid	10	10
MiliQ water	3	3
Total volume, mL	20	20

Restriction mixture was incubated for 16 h at 37 °C. After 16 h the reaction was stopped by incubating for 20 min at 80 °C. The digested pGAPZαA vector was purified with *GeneJet* PCR Purification Kit (Fermentas, Canada). Digested CHO-pUC was subjected to dephosphorylation. Mixture of dephosphorylation contained: 2 μL 10x buffer for alkaline phosphatase, 0.5 μL alcaline phosphatase (1 U/μL), 15 μL of sample and 2.5 μL MiliQ water. Total volume of the reaction mixture was 20 μL.

The mixture was incubated at 37 °C for 10 min and after that at 75 °C. After dephosphorylation and purification of restricted CHO-pUC and pGAPZαA vectors, the samples were checked by agarose electrophoresis.

Ligation of CHO pGAPZαA vectors and transformation of E. coli DH5α

After the successful restriction of CHO-pUC and pGAPZαA vectors, the gene for CHO was ligated into the pGAPZαA vector. Ligation mixture contained: 2 μL 10x T4 buffer for ligation, 0.5 μL ligase (10 U/μL), 3 μL dephosphorilated CHO (12 ng/μL), 10 μL pGAPZαA (1 ng/μL), 4.5 μL MiliQ water. Total volume of the reaction mixture was 20 μL.

Ligation mixture was incubated for 16 h at 16 °C, and then at 70 °C for 5 min. 2 μL of this mixture was added to 100 μL of frozen electrocompetent *E. coli* DH5α cells. The entire mixture was then transferred to a cold cuvette (which was pre-incubated on ice for 5 min) for transformation. The mixture was incubated on ice in cuvettes for 1 min. 1 mL of SOC medium was added and the mixture was transferred to a sterile tube and incubated for 1 h at 37 °C (250 rpm).

After 1h 200 μL of transformation mixture was plated on solid LB medium with zeocin. The plates were incubated overnight at 37 °C. The next day, colonies were transferred to a fresh solid LB medium with zeocin and individually placed in 1 mL of liquid LB medium with zeocin. Liquid cultures were incubated overnight at 37 °C and 250 rpm. After two days, plasmids were isolated from the growing colonies. Before transformation of *P. pastoris* X-33, linearized plasmids were isolated. The mixture for linearization contained: 2 μL 10x Tango buffer, 0.5 μL XmajI restricted enzyme (10 U/μL), 1 μL CHO-pGAP and 16.5 μL MiliQ water. Total volume of the reaction mixture was 20 μL. The mixture was incubated for 12 h at 37 °C and then at 80 °C for 20 min. Linearized plasmids were tested by agarose electrophoresis.

Transformation of P. pastoris X-33

Cuvettes for the transformation were pre-incubated on ice for 5 min. 10 μL of linearized plasmid was added to 100 μL of competent cells. The mixture was supplemented with 1 mL of sterile sorbitol, transferred to a sterile tube and incubated for 1 h at 30 °C without mixing. After 1 h, 500 μl of YPD medium was added and the mixture was incubated for 3 h at 30 °C, 250 rpm. After 3 h, 200 μL of transformation mixture was transferred to solid YPDS medium with zeocin at a final concentration of 100 mg/mL.

Cloning of carbohydrate oxidase into the pYES2 vector

Restriction of CHO-pUC and pYES2 vectors. CHO--pUC57 and pYES2 vectors were subjected to double digestion in the presence of XbaI and EcoRI restriction enzymes. Restriction mixture contained components shown in Table 2.

Table 2. Components for restriction mixture for CHO-pUC57 and pYES2 vector double restriction with enzymes XbaI and XhoI

Component	CHO-pUC57 (μL)	pYES2 vector (μL)
10xTango buffer	4	4
EcoRI (10 U/μL)	1	1
XbaI (10 U/μL)	2	2
Plasmid	6	13
MiliQ water	7	0
Total volume	20	20

Restriction mixtures were incubated at 37 °C overnight and then at 80 °C for 20 min. Digested CHO--pUC57 was subjected to dephosphorylation, in a mixture containing: 2 μL 10x buffer for alcaline phosphatase, 1 μL alcaline phosphatase, 15 μL sample and 2 μL MiliQ water. Total volume of reaction mixture was 20 μL. The reaction was running for 10 min at 37 °C, followed by 5 min at 75 °C. After double digestion with GeneJet PCR Purification Kit (Fermentas, Canada), pYES2 was purified and then checked by agarose electrophoresis.

Ligation of CHO and pYES2 and transformation of E. coli DH5α

After the successful restriction of CHO-pUC and pYES2 vector, the CHO gene was ligated into the vector

pYES2. The ligation mixture contained: 2 μL10x T4 ligation buffer, 0.5 μL ligase (10 U/μL), 1 μL dephosphorilated CHO (65 ng/μL), 10 μL pYES2 (2 ng/μL), 6.5 μL MiliQ water. Total volume of reaction mixture was 20 μL.

Ligation mixture was incubated for 16 h at 16 °C, followed by 10 min at 70 °C. 2 μL of this mixture was added into 100 μL frozen electrocompetent *E. coli* DH5α cells. The mixture was incubated on ice cuvettes for 1 min. 1 mL of SOC medium was added and the mixture was transferred to a sterile tube and incubated for 1 h at 37 °C (250 rpm).

After 1 h 200 μL of transformation mixture was plated on solid LB medium with ampicillin. The plates were incubated overnight at 37 °C. The next day growing colonies were tranferred on a fresh solid LB medium with ampicillin. Liquid cultures were incubated overnight at 37 °C and 250 rpm. The next day, plasmids were isolated from growing colonies and then checked with EcoRI restriction. Restriction mixture was incubated for 3 h at 37 °C, and contained: 1 μL 10xEcoRI buffer, 0.5 μL EcoRI (10 U/μL), 4 μL plasmid and 4.5 μL MiliQ water. Total volume of the reaction mixture was 10 μL.

Three of the constructs displayed the bands corresponding to the expected molecular mass. To determine if constructs have the gene for CHOx inserted into pYES2 expression vector, another double digestion with EcoRI and XbaI enzymes was performed. The reaction mixture contained: 4 μL 10x Tango buffer, 1 μL EcoRI (10 U/μL), 2 μL XbaI (10 U/μL), 5 μL plasmid and 8 μL MiliQ water. Total volume of the reaction mixture was 20 μL. The mixture was incubated for 3 h at 37 °C, then 20 min at 80 °C and DNA was analyzed by agarose electrophoresis.

Transformation of *S. cerevisiae* InvSC1

Chemically competent cells InvSC1 were centrifuged for 2 min at 13000 rpm. Then the cells were transferred to a solution containing 260 μL of PEG, 36 μL Li acetate, 50 μL SS DNA (which was previously heated for 5 min at 100 °C) and 14 μL of the plasmid. The mixture was vortexed and incubated for 1 h at 42 °C, with occasional mixing. 1 mL YNB-CAA-Glc-A-T was added to the mixture. Plates with cells were incubated for 2 days at 30 °C.

Isolation of plasmid

A single colony from the LA medium supplemented with antibiotics was inoculated into 3 mL of medium and grown in a shaker (250 revolutions/min) at 37 °C overnight. The culture was transferred to a 1.5 mL eppendorf tube and centrifuged for 1 min at 13000 rpm. The supernatant was removed and the cells were resuspended in 150 μL of cold GTE+ solution (25 mM TRIS, 10 mM EDTA, 50 mM glucose, 100 mg/mL of ribonuclease, pH 8.0) + 300 μL of freshly prepared P2 solution (200 mM NaOH, 1% SDS) and slowly mixed until the solution became clear. After that 450 μL of cold potassium acetate solution (4 M CH_3COOK, pH 6.3) was added and slowly mixed. The suspension was centrifuged for 4 min at 13000 rpm. The supernatant was transferred to a new eppendorf tube with 400 μL isopropanol. The content was mixed several times and centrifuged for 4 min at 13000 rpm. The supernatant was removed and 1 mL of ice-cold 75% ethanol was added to the residue. The solution was centrifuged for 2 min at 13000 rpm. The supernatant was removed and the precipitate (plasmid DNA) was dried in a vacuum evaporator.

Yeast fermentation

Production of carbohydrate oxidase in P. pastoris X-33

Colonies, which grew after transformation of *P. pastoris* on YPDS medium containing zeocin, were plated in 1 mL of YPD medium with zeocin and incubated for two days at 30 °C and 250 rpm. After two days, the colonies were tested under the microscope, in order to determine contamination. Non-contaminated colonies were tested in the ABTS assay for detection of carbohydrate oxidase activity. As none of the colonies showed CHO activity, all were centrifuged and dissolved respectively in 0.1 M sodium acetate buffer pH 5.5 and then tested with SDS PAGE.

After silver staining, seven colonies were selected which were re-tested in SDS PAGE after precipitation of trichloroacetic acid (TCA). Three of these colonies were placed into 10 mL YPD medium with zeocin, in a final concentration of 100 mg/mL. The colonies were incubated at 30 °C and 250 rpm for 4 days.

After fermentation, all samples were TCA precipitated and then tested on SDS PAGE. The samples were tested with native PAGE and zymogram.

Production of carbohydrate oxidase in S. cerevisiae InvSC1

Colonies were grown after 24 h on YNB + CAA-Glc + T + A solid medium, inoculated with 1 mL of the same liquid medium and incubated for 24 h at 30 °C and 25 rpm. After 24 h, 3 mL of the liquid YNB + CAA-Gal + A + T medium was added to each of the colonies and they were incubated at 30 °C and 250 rpm for 12 h, after which the colonies were concentrated from 100 to 10 mL by ultrafiltration on a membrane of 50 kDa. Finally, samples were tested on SDS PAGE.

Determination and expression of CHO

ABTS assay

The mixtures for determining the activity of glucose oxidase contained 60 mM sodium acetate buffer pH 5.5, 333 mM glucose, 1 mM ABTS, 1 U/mL HRP in a volume of 990 μL. Change in absorbance was measured

at 405 nm after addition of 10 µL of sample with carbohydrate oxidase. 1 U of CHO is defined as the quantity of the enzyme producing 1 µmol hydrogen peroxide in 1 min. The amount of hydrogen peroxide was determined by the concentration of the oxidized ABTS whose extinction coefficient at 405 nm is 36.8 mL μmol^{-1} cm^{-1} [21].

Precipitation of the protein with TCA

TCA precipitation of the proteins was performed in cold conditions. 250 µL TCA (50% TCA in dH2O) was added into 500 µl of sample. The tubes were vortexed and centrifuged for 10 min at 4 °C. The supernatant was removed and sample was mixed with 200 µL acetone. After another centrifugation, the supernatant was again removed, and the side walls of the tube were washed with another 100 µL of acetone. The supernatant was removed and the sample was dried at room temperature. The sample was resuspended in a small volume of the 0.1 M sodium acetate buffer pH 5.5.

Electrophoretic techniques

DNA agarose electrophoresis

For DNA agarose electrophoresis, 1% agarose in TBE buffer (89 mM TRIS, 89 mM boric acid, 20 mM EDTA, pH 8.0) was used and 5 µL of DNA sample was mixed with the color in 1:5 proportion. DNA markers for electrophoresis (Fermentas, Canada) were applied in an amount of 3 µL. Electrophoresis started at a voltage of 80 V until the dye reached the end of the gel. After completion of electrophoresis, the gel was immersed for 5 min in a solution of ethidium bromide 0.5 mg/mL and filmed under UV light.

SDS polyacrylamide gel electrophoresis (SDS PAGE)

For the analysis of glucose oxidase, the reductive polyacrylamide electrophoresis was used [22]. The gels contained the components as shown in Table 3.

Table 3. The gels for SDS-PAGE

Solutions	8% Separating gel	4% Gel for concentration
Acrylamide monomer solution (30% T, 2,7% C)	3,33 mL	0,50 mL
1.5 M TRIS pH 8,8	2,50 mL	–
0.5 M TRIS pH 6,8	–	0,94 mL
Water	4 mL	2,25 mL
10% SDS	0,10 mL	38 mL
TEMED	4 µL	2 µL
10% Ammonium persulfate (APS)	50 µL	25 µL
Total volume	10 mL	4 mL

Samples for SDS electrophoresis were mixed with preparation buffer (60 mM TRIS pH 6.8, 25% glycerol, 2% SDS, 14.4 mM β-mercaptoethanol, 0.1% bromophenol blue) at a ratio of 1:4. The resulting solution was boiled for 5 min at 95 °C. Protein markers for electrophoresis (Fermentas, Canada) were applied in 5 µL volume.

Electrophoresis was done for 2 h at constant voltage of 150 V in a water bath containing electrophoresis buffer (0.025 M Tris pH 8.3, 0.192 M glycine, 0.1% SDS). Electrophoresis was stopped when bromophenol blue dye reached the edge of the gel. The gel was fixed and stained with CBB (Coomassie brilliant blue) G-250 (0.1% CBB and 50% methanol, 10% acetic acid) overnight. Bleaching of the gel was carried out in 7% acetic acid solution until the appearance of stained protein bands on the gel.

Native gel electrophoresis

Solutions for native electrophoresis were identical to solutions for SDS-PAGE electrophoresis, except that no SDS was added to the gel and no β-mercaptoethanol was added to the buffer. Electrophoresis was done in the same order as in the SDS-PAGE electrophoresis. After completion of the electrophoresis gel was colored with silver. The protocol for the silver staining of gel is given in the Table 4.

Table 4. The protocol for the silver staining of gel

Solution	Time, min
1. Rinse with dH2O	1
2. 50% methanol, 20 % TCA, 2% $CuCl_2$	15
3. 10% ethanol, 5 % acetic acid	10
4. 0.01% $KMnO_4$	10
5. Rinse 2× with dH_2O	1
6. 10% ethanol, 5% acetic acid	10
7. 10% ethanol	10
8. Rinse 2× with dH_2O	1
9. dist. H_2O	10
10. 0,1% $AgNO_3$	10
11. Rinse with dist. H_2O	20 sec
12. 10% K_2CO_3	1
13. 2% K_2CO_3, 0.01% formaldehyde	Untill the occurrence of strip
14. 10% ethanol, 5% acetic acid	20 sec
15. Rinse with dist. H_2O	20 sec
16. Stain in 0,02 % K_2CO_3	Unlimited

Zymogram

Zymogram was done identically to the native electrophoresis, only that instead of washing the gel with distilled water, the gel was dipped in the solution for activity determination. In contrast to the assay used to determine the activity of the solution, guaiacol was used instead of ABTS.

RESULTS AND DISCUSSION

The transformation of the bacteria and miniprep with the restriction mapping of the plasmid

After double digestion of CHO-pUC57 and pGAPZαA with restriction enzymes XhoI and XbaI, pGAPZαA vector was purified and each sample was checked on agarose gel electrophoresis to determine an approximate concentration of DNA (Fig. 1).

Comparing bands intensity of the digested samples with bands intensity of the molecular markers and quantities of DNA in each lane, the concentration of pGAPZαA was determined as 1 ng/μL, while the concentration of digested CHO-pUC57 was 12 ng/μL.

Six colonies grew the next day and they were transferred to a fresh solid LB medium with zeocin. Liquid cultures were incubated overnight at 37 °C and 250 rpm. After two days, the colonies 3 and 6 grew and plasmids were isolated from them. Before transformation of *P. pastoris* X-33, isolated plasmids were linearized (Fig. 2). Agarose electrophoresis of DNA showed that plasmids satisfied criteria of molecular weight (4.9 kbp), and these plasmids were used for further transformation of *P. pastoris* X-33.

Transformation of *E. coli* DH5α with gene CHOx cloned into an expression vector pYES2

After double digestion of CHO-pUC57 and pYES2 with restriction enzymes EcoRI and XbaI, samples were checked by agarose gel electrophoresis in order to determine the approximate concentration of DNA (Fig. 3).

Comparing the intensity of the bands of the digested samples to the intensity of the bands corresponding to molecular markers and quantities of DNA in each lane, the concentration of CHO-pUC57 was determined as approximately 65 ng/μL. The pYES2 plasmid was then purified and then checked by agarose gel electrophoresis (Fig. 4). Based on the intensity of molecular markers and quantities of DNA in each lane, it was determined that a concentration of pYES2 was approximately 2 mg/μL.

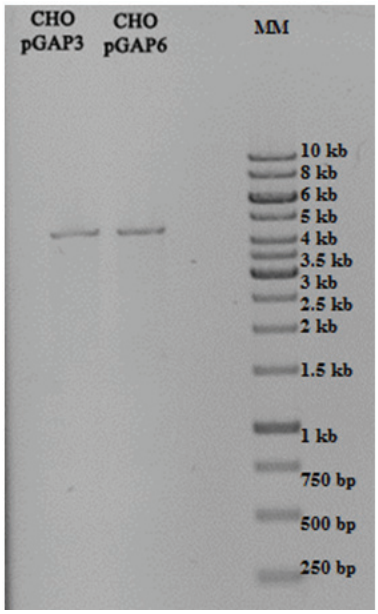

Fig. 2. DNA electrophoresis of linearized CHO-pGAP plasmids 3 and 6.

After dephosphorylation CHO-pUC57 the volume of reactants for ligation was calculated. Colonies that have

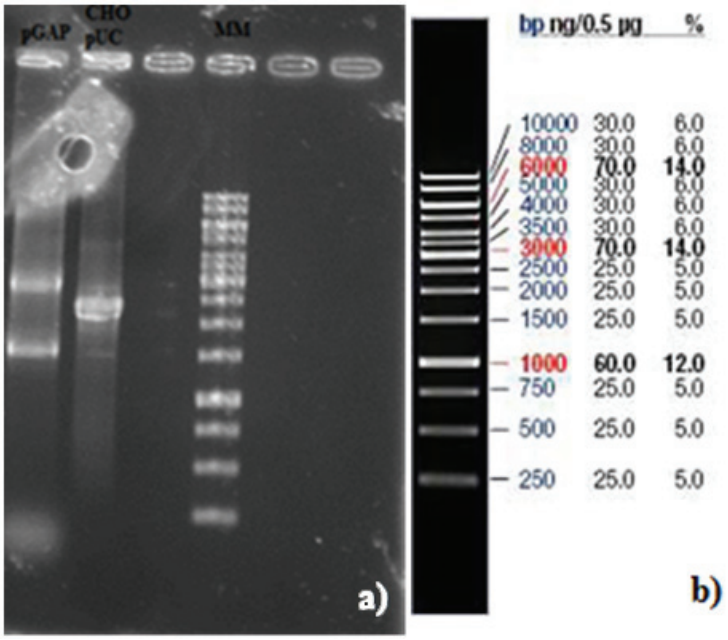

Fig. 1. DNA electrophoresis: a) digested pGAPZαA and CHO-pUC57; b) DNA molecular markers.

grown until the next day and plasmids were isolated from colonies that grew and then checked with EcoRI restriction (Fig. 5).

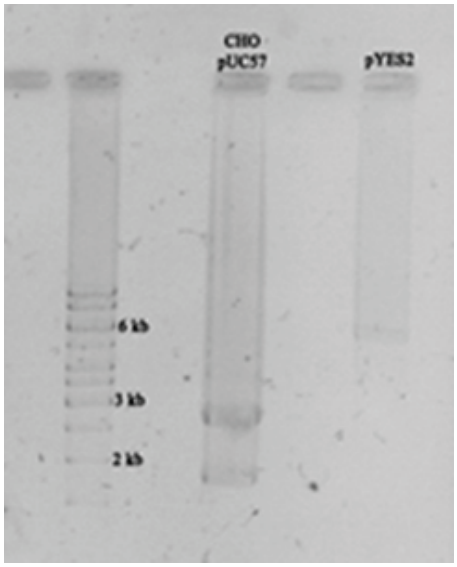

Fig. 3. DNA electrophoresis: digested pYES2 and CHO-pUC57.

The obtained results showed that constructs 14 and 15 displayed the expected size ~ 8kb (5.9kb +1.8 kb). However, the construct number 8 also showed a band of slightly below 8kb. Thus, the constructs 8, 14 and 15 were subjected to double digestion with EcoRI and XbaI restriction enzymes for further verification (Fig. 6).

DNA electrophoresis showed that the construct 8 does not display a band on 1.8 kb, which is the approximate length of CHO genes, while constructs 14 and 15 displayed two bands, corresponding to 1.8 and 5.9 kb. These constructs were used for the further transformation of *S. cerevisiae* InvSC1.

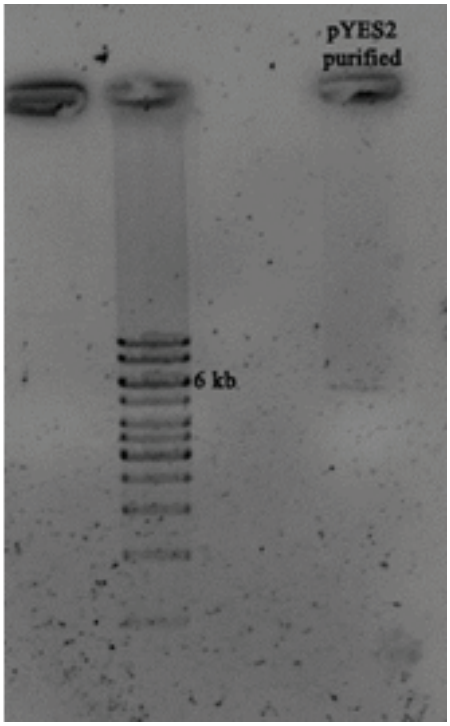

Fig. 4. DNA electrophoresis pYES2 after double digestion and purification.

Transformation of yeast and fermentation

Transformation of *P. pastoris* X-33 with pGAP-CHO construct

P. pastoris X-33 was transformed with linearized constructs 3 and 6. Twenty five colonies of cells transformed with the construct 3 grew on a solid YPDS medium with zeocin, while 11 colonies grew on a plate with cells transformed with the construct 6. After two days, colonies were tested under the microscope in order to determine the contamination. Colonies that were not contaminated were tested with the ABTS assay for detection of carbohydrate oxidase activity.

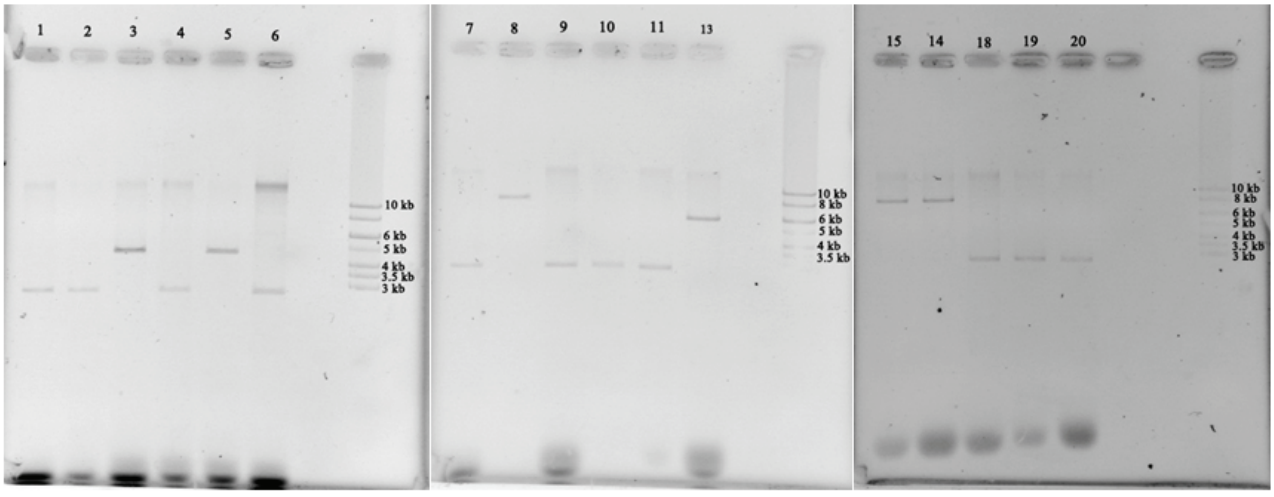

Fig. 5. DNA Electrophoresis of digested (EcoRI) constructs CHO-pYES.

None of the colonies showed activity and all were centrifuged and resuspended in 0.1 M sodium acetate buffer pH 5.5.

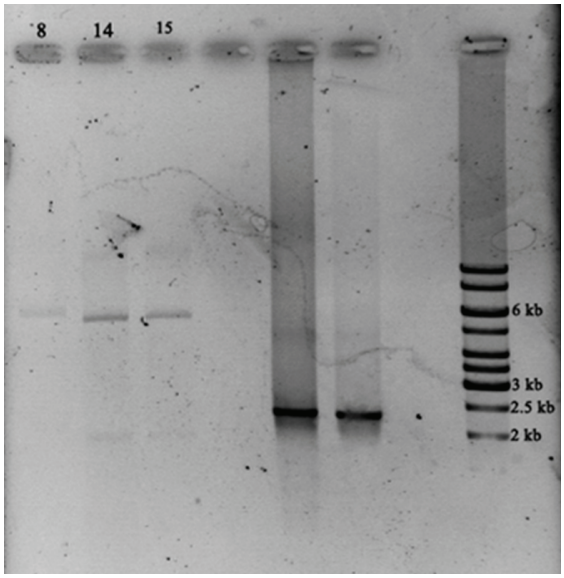

Fig. 6. DNA electrophoresis of CHO-pYES constructs with a number 8, 14 and 15.

Non-contaminated colonies were tested by SDS PAGE after the first fermentation. After electrophoresis, 4 selected samples (7, 14, 24 and 26) were precipitated with trichloroacetic acid (TCA) and tested by SDS PAGE (Fig. 7).

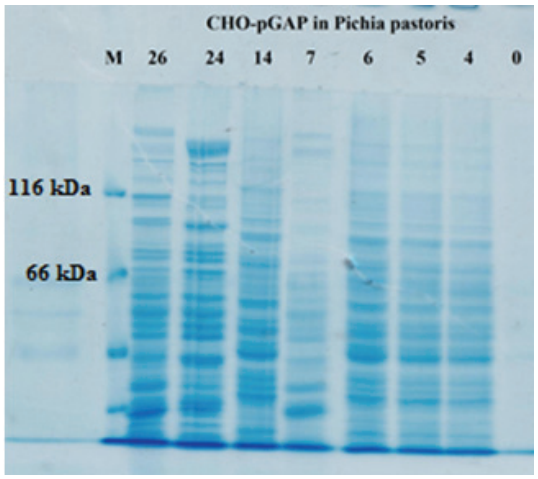

Fig. 7. SDS PAGE after TCA precipitation for 4 samples (7, 14, 24 and 26).

Based on these results, the samples with numbers 14, 24 and 26 were selected for monitoring the fermentation and time profile of the protein expression. These samples were selected because their protein bands on the electrophoresis were different from the others and from the empty pGAP (number 0). Three selected colonies were placed into 10 mL YPD medium with zeocin (100 mg mL^{-1}). The colonies were incubated at 30 °C and 250 rpm for 4 days. Aliquots were collected every 24 hours. After the fermentation, cells were centrifuged and the supernatants were precipitated with TCA again and tested on SDS PAGE (Fig. 8).

After the first day, the samples 24 and 26 displayed a band which did not occur in the sample derived from the empty vector, thus it is possible to assume that this band corresponded to the desired CHO. The band occurred on a molecular weight higher than the theoretical molecular weight of this enzyme (greater than 120 kDa), but since the enzyme can be glycosylated, it could have a higher molecular weight than its expected value. Samples from the first and second day were tested with native electrophoresis, and then with zymogram with guaiacol, hoping to detect CHO activity which has not been detected previously with the enzyme assay. However, even these tests did not yield positive results. Foumani *et al*. [8] claimed that GOOX from *Acremonium strictum* could have a novel substrate specificity and that occurred likely due to amino acid substitution in this enzyme. Most substitutions are located on the protein surface or far from the oxidation site, which may be a reason for the lack of the enzyme activity.

There is a possibility that the enzyme had misfolded upon synthesis, so refolding it might have resulted in recovering the activity. For *P. pastoris*, the oligosaccharide chains attached to proteins are shorter and more authentic than in *S. cerevisiae*. The average chain lenght of glycoproteins expressed by *P. pastoris* is only 8–14 mannose residues, whereas that by *S. cerevisiae* it is 40–150 residues [23]. Analysis of the carbohydrates coupled to recombinant enzymes indicated the predominant presence of N-linked, high mannose structure and Asn-X-Ser/Thr was found to be the site of glycolisation , same as that in mammalian cells [24]. Many glycosylated proteins have been expressed successfully in *P. pastoris*. Up to now, many heterologous proteins have been expressed in *P. pastoris* because the level of expression is equivalent to that of *E. coli* and significantly higher than that of *S. cerevisiae* [25]. Expression and secretion of these heterologous proteins, however, depends not only on gene dosage, but also on other factors, such as signal sequence recognition and processing, proteolysis, fermentation and glycosylation.

Salts were also proven necessary for the production of heterologous proteins in *Pichia*. The presence of at least 200 μM copper was needed for optimal laccase activity [26].

There are several reports on expressing heterologous proteins in *P. pastoris* at low temperatures [11]. Incubation temperatures of 30, 27, 25 and 23 °C have been examined in order to minimize extracellular proteolysis.

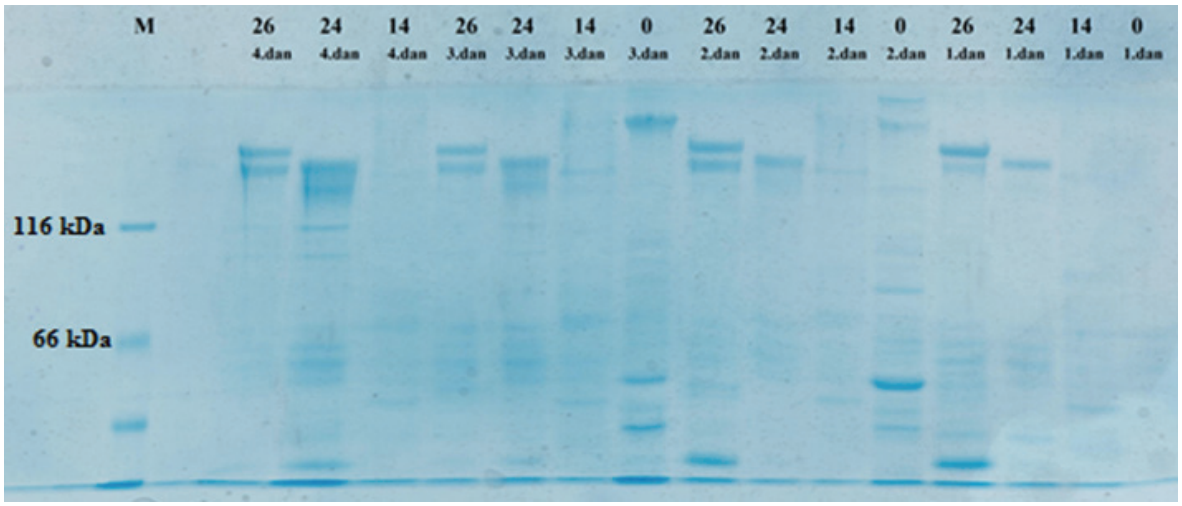

Fig. 8. SDS PAGE of fermentation liquid from samples after second fermentation of P.pastoris.

The kinetics of proteolytic reaction, in the presence or absence of cells, were shown to be influenced by pH. Jahic *et al*. [27] reported that decreasing the pH from 5.0 to 4.0 in bioreactor cultures resulted in an increase in the fraction of full-length product from 40 to 90% during expression of cellulose-binding module in *P. pastoris*. The optimal pH would be determined best by running a series of fermentations at different pH values, therefore controlling the medium pH during the fermentation process is necessary. Optimum pH depends on individual properties of the protein, especially stability.

Transformation of *S. cerevisiae* with the construct CHO- pYES

S. cerevisiae strain InvSC1 was transformed with constructs CHO-pYES 14 and 15. Only one colony had grown after 24 hours on the plate containing cells transformed with the construct 14, while on the plate containing the cells with construct 15, two colonies grew (marked as: 15-1 and 15-2). Activity of each sample was determined after concentration but samples did not show any activity. However, the samples were further tested with SDS PAGE (Fig. 9).

The sample 15-2 showed a band corresponding to a molecular mass of about 110 kDa. This value is higher than the theoretical one, but given that only this sample differed from the empty vector and showed a band that was absent from other samples, we assumed that the band may derive from the desired enzyme, CHO.

Glycosylation is one of the critical post-translation processing events in the synthesis of proteins. The role of glycosylation in protein folding, oligomer assembly, structural stability, specific signal transduction has been well documented [28]. Yeast and the highest eukaryotes utilize an evolutionarily conserved N-linked oligosaccharide biosynthetic pathway that involves the formation of a Glc3Man9GlcNAc2-PP-dolichol lipid-linked precursor [29]. Subsequently, glycohydrolases in

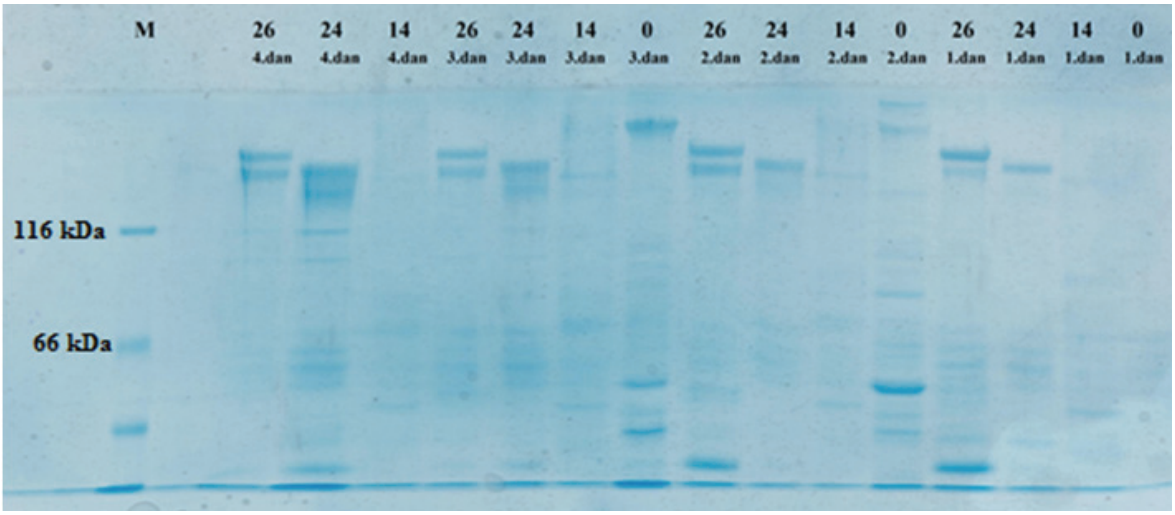

Fig. 9. SDS PAGE of samples obtained by fermentation of Saccharomyces cerevisiae.

the endoplasmic reticulum remove the three glucoses and (with the exception of *Schizosaccharomyces pombe*) one specific mannose residue. Processing sugar transferases in the Golgi leads to the fomation of core-sized structure ($Hex_{(<15)}GlcNac_{(2)}$) and cores with an extended poly–α1, 6-Man backbone [29]. The protein has to undergo all the mentioned post-translation modifications in order to obtain the correct conformation and any misstep in posttranslational modification pathway can cause the protein to be inactive.

Proteins may be susceptible to misfolding for a variety of reasons, including the formation of intermolecular disulfide bonds and exposure of their hydrophobic surfaces [11]. Intermolecular disulfide bonds are formed at higher temperatures when proteins are expressed in *E. coli* [30]. Lowering the cultivation temperature can be beneficial for reducing the proteolytic degradation of the recombinant proteins in the culture medium.

CONCLUSIONS

After cloning and heterologous expression of CHO in the *P. pastoris* expression system we have obtained several expressed protein bands with molecular weights over 116 kDa.

Cloning and heterologous expression of CHO in a *S. cerevisiae* expression system, gave a protein that showed on SDS PAGE a molecular weight of about 110 kDa.

Bands obtained on the SDS PAGE had a higher molecular weight than theoretical. It is known that recombinant proteins, expressed in yeast, have higher molecular weights than expected due to the higher degree of glycosylation.

The resulting protein has shown no enzymatic activity in the ABTS assay and this may be due to inadequate folding of the protein in the expression system of *S. cerevisiae*. Further experiments on recombinant protein purification and refolding studies are necessary.

Abbreviations

ABTS – 2,2'-azinobis(3-ethylbenzthiazoline-6-sulfonic acid); ADH – alcohol dehydrogenase; AOX – alcohol oxidase; APS – ammonium persulfate; CBB – Coomassie Briliant Blue; CHO – carbohydrate oxidase; EDTA – ethylenediamine-tetraacetic acid; FAD – flavin adenine dinucleotide; GAP – glyceraldehyde 3-phosphate dehydrogenase promoter; GOx – glucose oxidase; HOx – hexose oxidase; HPLC – high performance liquid chromatography; HRP – horseradish peroxidase; LB – Luria Broth medium; PAGE – polyacrylamide gel electrophoresis; SDS – sodium dodecyl sulfate; TCA – trichloroacetic acid; TEMED – 1,2-bis(dimethylamino)ethane; TRIS - tris(hydroxymethyl) aminomethane; YPD – yeast peptone dextrose.

REFERENCES

[1] J. Duskova, J. Dohnálek, T. Skálová, L. Henrik Østergaard, C. Crone Fuglsang, P. Kolenko, A. Štěpánková, J. Hašeka, Crystallization of carbohydrate oxidase from *Microdochium nivale*, Acta Crystallogr. Sect. F Struct. Biol. Cryst. Commun. **65** (2009) 638–640.

[2] D.P.H. Heuts, E.W. Van Hellemond, D.B. Janssen, M.W. Fraaije, Discovery, characterization, and kinetic analysis of an alditol oxidase from *Streptomyces coelicolor*, J. Biol. Chem. **282** (2007) 20283–20291.

[3] J.H. Custers, S.J. Harrison, M.B. Sela-Buurlage, E. Van Deventer, W. Lageweg, P.W. Howe, P.J. Van der Meijs, A.S. Ponstein, B.H. Simons, L.S. Melchers, M.H. Stuiver, Isolation and characterisation of a class of carbohydrate oxidases from higher plants, with a role in active defence, Plant J. **39** (2004) 147–160.

[4] M. Nordkvist, P.M. Nielsen, J. Villadsen, Oxidation of lactose to lactobionic acid by a *Microdochium nivale* carbohydrate oxidase: Kinetics and Operational Stability, Biotechnol. Bioeng. **97** (2006) 694–707.

[5] A. Ioannou, E. Cini, R.S. Timofte, S.L. Flitsch, N.J. Turner, B. Linclau, Heavily fluorinated carbohydrates as enzyme substrates: oxidation of tetrafluorinated galactose by galactose oxidase, Chem. Commun. **47** (2011) 11228––11230.

[6] B. Savary, K.B. Hicks, J.V. O'Connor, Hexose oxidase from *Chondrus crispus*: improved purification using perfusion chromatography, Enzyme Microb Techn. **29** (2001) 42–51.

[7] Z. Fan, G.B. Oguntimein, P.J. Reilly, Characterization of Kinetics an Thermostability of *Acremonium strictum* Glucooligosaccharide Oxidase, Biotechn. Bioeng. **68** (2000): 231–237.

[8] M. Foumani, T.V. Vuong, E.R. Master, Altered Substrate Specificity of the Gluco-Oligosaccharide Oxidase From *Acremonium strictum*, Biotech. Bioeng. **108** (2011) 2261–2269.

[9] S. Pricelius, L. Ludwig, N.J. Lant, D. Haltrich, G.M. Guebitz, *In situ* generation of hydrogen peroxide by carbohydrate oxidase and cellobiose dehydrogenase for bleaching purposes, Biotechnol. J. **6** (2011) 224–230.

[10] M.A. Wolff, O.C. Hansen, O. Poulsen, Optimization of the Production of *Chondrus crispus* Hexose Oxidase in *Pichia pastoris*, Protein Express. Purif. **22** (2001) 189––199.

[11] P. Li, A. Anumanthan, X.G. Gao, K. Ilangovan, V.V. Suzara, N. Düzgüneş, V. Renugopalakrishnan, Expression of recombinant proteins in *Pichia pastoris*. Appl. Biochem. Biotechnol. **142** (2007) 105–124.

[12] G. Potvin, A. Ahmad, Z. Zhang, Bioprocess engineering aspects of heterologous protein production in *Pichia pastoris*: A review, Biochem. Eng. J. **64** (2012) 91–105.

[13] H. Hohenblum, N. Borth, D. Mattanovich, Assessing viability and cell-associated product of recombinant protein producing *Pichia pastoris* with flow cytometry, J. Biotechnol. **102** (2003) 281–290.

[14] A.L. Zhang, J.X. Luo, T.Y. Zhang, Y.W. Pan, Y.H. Tan, C.Y. Fu, F.Z. Tu, Recent advances on the GAP promoter deri-

ved expression system of *Pichia pastoris*, Mol. Biol. Rep. **36** (2009) 1611–1619.

[15] S.M. Patrick, M.L. Fazenda, B. McNeil, L.M. Harvey, Heterologous protein production using the *Pichia pastoris* expression system, Yeast **22** (2005) 249–270.

[16] S. Shibasaki, M. Ueda, T. Iizuka, M. Hirayama, Y. Ikeda, N. Kamasawa, M. Osumi, A. Tanaka, Quantitative evaluation of the enhanced green fluorescent protein displayed on the cell surface of *Saccharomyces cerevisiae* by fluorometric and confocal laser scanning microscopic analyses, Appl. Microbiol. Biotechnol. **55** (2001) 471––475.

[17] Y. Nakamura, S. Shibasaki, M. Ueda, A. Tanaka, H. Fukuda, A. Kondo, Development of novel whole-cell immunoadsorbents by yeast surface display of the IgG-binding domain, Appl. Microbiol. Biotechnol. **57** (2001) 500–505.

[18] E.H. Park, Y.M. Shin, Y.Y. Lim, T.H. Kwon, D.H. Kim, M.S. Yang, Expression of glucose oxidase by using recombinant yeast, J. Biotech. **81** (2000) 35–44.

[19] J.H. Ko, M.S. Hahm, H.A. Kang, S.W. Nam, B.H. Chung, Secretory expression and purification of *Aspergillus niger* glucose oxidase in *Saccharomyces cerevisiae* mutant deficient in PMR1 gene, Protein Express. Purif. **25** (2002) 488–493.

[20] C.T. Chung, S.L. Niemela, R.H. Miller, One-step preparation of competent *Escherichia coli*: transformation and storage of bacterial cells in the same solution, Proc. Natl. Acad. Sci. USA **86** (1989) 2172–2175.

[21] L. Sun, I.P. Petrounia, M. Yagasaki, G. Bandara, F.H. Arnold, Expression and stabilization of galactose oxidase in *Escherichia coli* by directed evolution, Protein Eng. **14** (2001) 699–704.

[22] U.K. Laemmli, Cleavage of structural proteins during the assembly of the head of bacteriophage T4, Nature **227** (1970) 680–685.

[23] L. Grinna, J. F. Tschop, Size distribution and general structural features of N-linked oligosaccarides from the methyltrophic yeast *Pichia pastoris*, Yeast **5** (1989) 107––115.

[24] R.B. Trimble, P.H. Atkinson, J.F. Tschopp, R.R. Townsend, F. Maley, Structure of oligosaccharides on *Saccharomyces* SUC2 invertase secreted by the methylotrophic yeast *Pichia pastoris*, J. Biol .Chem. **266** (1991) 22807––22817.

[25] S.R. Hamilton, T.U. Gerngross, Glycosylation engineering in yeast: the advent of fully humanized yeast, Curr. Opin. Biotech. **18** (2007) 387–392.

[26] M. Jahic, M. Gustavsson, A.K. Jansen, M. Martinelle, S.O. Enfors, Stable linker peptides for a cellulose-binding domain-lipase fusion protein expressed in *Pichia pastoris*, J. Biotech. **102** (2003) 45–53.

[27] A. Wright, S.L. Morrison, Effect of glycosylation on antibody function: implications for genetic engineering, Trends Biotech. **15** (1997) 26–32.

[28] T.R. Gemmil, R.B. Trimble, Overview of *N*- and *O*-linked oligosaccharide structures found in various yeast species, Biochim. Biophys. Acta **1426** (1999) 227–237.

[29] C.H. Schein, M.N.R. Noteborn, Formation of Soluble Recombinant Proteins in *Escherichia coli* is Favored by Lower Growth Temperature, Biotechnology (NY) **6** (1988) 291–294.

[30] S.C. Makrides, Strategies for achieving high-level expression of genes in *Escherichia coli*, Microbiol. Rev. **60** (1996) 512–538.

IZVOD

KLONIRANJE GENA ZA UGLJENI HIDRAT OKSIDAZU IZ BILJKE *Lactuca sativa* U KVASCE *Saccharomyces cerevisiae* I *Pichia pastoris*

Vojin M. Tadić[1], Ana Marija J. Balaž[2], Marija P. Petrić[1], Snežana M. Milošević[1], Nevena D. Zelenović[3], Martin Z. Raspor[1], Jovan M. Tadić[4], Radivoje M. Prodanović[2]

[1]Odeljenje za fiziologiju biljaka, Institut za biološka istraživanja "Siniša Stanković", Univerzitet u Beogradu, Bulevar despota Stefana 142, 11000 Beograd, Srbija
[2]Odeljenje za biohemiju, Hemijski fakultet, Univerzitet u Beogradu, Studentski trg 12-16, 11000 Beograd, Srbija
[3]Institut za hemiju, tehnologiju i metalurgiju, Univerzitet u Beogradu, Njegoševa 12, 11000 Beograd, Srbija
[4]Odeljenje za globalnu ekologiju, Carnegie Institution for Science, Stanford, CA 94305, USA

(Naučni rad)

Ugljeni hidrat-oksidaza (CHO) iz zelene salate (*Lactuca sativa*) je enzim koji je do danas nedovoljno ispitan. Vrlo se malo zna o njegovoj strukturi i funkciji. CHO pripada velikoj familiji ugljenihidrat-oksidaza, koje oksiduju šećere. Svaki od članova ove velike familije dobio je ime po supstratu koji oksiduje. Oksidaze iz ove familije enzima imaju kako sličnu ulogu tako i sličnu strukutru. Sve ili većina ovih enzima su monomeri, čiji se polipeptidni lanac uvija u dva domena. Jedan od domena vezuje flavinski kofaktor, a drugi domen je supstrat vezujući. Većina njih oksidaciju supstrata vrši po takozvanom ping-pong mehanizmu. Sve oksidaze iz karbohidrat-oksidaza familije, pa među njima i enzim koji je predmet ove studije (CHO), danas su našle veliku primenu u industriji. CHO se može primenjivati kako u medicinskoj djagnostici, konkretno u biosenzorima za određivanje glukoze u krvi, u prehrambenoj industriji, poljoprivredi, proizvodnji hleba, deterdženata i u raznim drugim industrijskim oblastima. Problem sa ovim enzimom, kao i sa ostalim članovima ove familije, jeste niska koncentracija u prirodnim izvorima. Zato su danas razvijene različite metode rekombinantne tehnologije, kojima se dobijaju ovi enzimi. U ovom radu opisano je kloniranje gena za CHO iz zelene salate u dve vrste kvasaca (*Saccharomyces cerevisiae* i *Pichia pastoris*). Sintetički gen za CHO (1821 bp) iz zelene salate kloniran je u vektor pUC57. *Escherichia coli* soj DH5α korišćen je za kloniranje gena i održavanje plazmida. *P. pastoris* soj X-33 i *S. cerevisiae* soj InvSC1 korišćeni su za ekstracelularnu ekspresiju CHO. Aktivnost CHO određena je ABST esejom, a promena absorbance merena je na 405 nm. Potvrda prisustva enzima rađena je na DNK agaroznoj elektroforezi i SDS-PAGE. Posle transformacije *P. pastoris* X-33, nijedan od klonova nije pokazivao aktivnost CHO. Posle prve fermentacije, kolonije su testirane na SDS-PAGE. Kako su dva uzorka pokazala trake, koje ne postoje na praznom vektoru, ove trake bi mogle odgovarati željenom enzimu, CHO. Traka se nalazi na molekulskoj masi koja je veća od teoretske (više od 120 kDa). Enzim bi mogao biti glikolizovan i zbog toga pokazivati ovako velike vrednosti za molekulsku masu. *S. cerevisiae* soj InvSC1 transformisan je konstruktom CHO-pZES. Posle 24 sata, tri kolonije su porasle na ploči na kojoj su bile ćelije transformisane pomenutim konstruktom. Uzorci su testirani na SDS-PAGE. Jedan uzorak je pokazao traku na oko 110 kDa, ali aktivnost CHO nije potvrđena takođe. Cilj ove studije je bio kloniranje CHO u kvascima *S. cerevisiae* i *P. pastoris*, kao i njena ekspresija u ovim, danas široko primenjivanim ekspresionim sistemima.

Ključne reči: *Saccharomyces cerevisiae* • *Pichia pastoris* • Glikozilacija

Alkyl polyglucoside-stabilized emulsion as a prospective vehicle for *Usnea barbata* CO_2-supercritical extract: Assessing stability, safety and efficiency of a topical formulation

Ana R. Žugić[1], Milica Z. Lukić[2], Marija Z. Tasić Kostov[3], Vanja M. Tadić[1], Ivana A. Arsic[3], Dušan R. Mišić[4], Slobodan D. Petrović[5], Snežana D. Savić[2]

[1]*Institute for Medicinal Plant Research "Dr Josif Pančić", Department of Pharmaceutical Research and Development, Belgrade, Serbia*
[2]*University of Belgrade, Faculty of Pharmacy, Department of Pharmaceutical Technology and Cosmetology, Belgrade, Serbia*
[3]*University of Niš, Faculty of Medicine, Department of Pharmacy, Niš, Serbia*
[4]*University of Belgrade, Faculty of Veterinary Medicine, Department of Microbiology, Belgrade, Serbia*
[5]*University of Belgrade, Faculty of Technology and Metallurgy, Department of Organic Chemistry, Belgrade, Serbia*

Abstract

Antimicrobial activity of *Usnea barbata* especially against bacteria involved in pathogenesis of various skin conditions has been well documented in literature. Nevertheless, there are no papers dealing with formulation of its isolates into topical preparations for treatment of skin infections. In present study, alkyl polyglucoside (APG)-based vehicle was developed as carrier of *U. barbata* CO_2-supercritical extract (U-SE) that demonstrated the best antimicrobial potential in preliminary screening. For comparison, chosen extract in the same concentration and using the same procedure was incorporated into a pharmacopoeial vehicle. Comparative evaluation of physicochemical stability, efficiency and safety proved APG-based vehicle to possess certain preferential features as carrier of U-SE compared to the reference one, composing a topical formulation with potential clinical relevance in treatment of skin infections.

Keywords: alkyl polyglucosides, *Usnea barbata* supercritical CO_2-extract, skin infections, physicochemical stability, antimicrobial activity, skin performance.

Available online at the Journal website: http://www.ache.org.rs/HI/

SCIENTIFIC PAPER

UDC 582.282:615.2:54

Hem. Ind. **69** (6) 703–712 (2015)

doi: 10.2298/HEMIND140701002Z

Usnea barbata is one of the most studied lichens belonging to the genus *Usnea*, traditionally used in Asia, Africa and Europe for pain relief and fever control. According to literature data, *U. barbata* (UB) has allegedly been used by Hippocrates to treat urinary complaints and in folk medicine of South Africa for the treatment of wounds [1,2]. In addition to traditionally claimed properties of UB as a folk remedy, German Commission E approved its usage as an antimicrobial agent intended for the treatment of mild inflammation of the oral and pharyngeal mucosa in the form of lozenges [3].

Antimicrobial activity of UB has been fairly documented in several scientific studies [2,4,5]. Comparative testing of acetone, methanol and water extract of UB against 10 bacterial and 5 fungal strains using dilution method on solid agar medium revealed the best antimicrobial activity against Gram positive bacteria, with acetone extract being the most active among the investigated extracts [2]. Furthermore, an investigation of acetone extracts of several *Usnea* species including UB using agar disc diffusion method demonstrated antimicrobial activity to be proportional to usnic acid (UA) content in the investigative extracts [4]. Similar results were reported in a recent study screening nine plant extracts and isolated compounds for antimicrobial activity against bacteria and yeasts with dermatological relevance. Namely, supercritical CO_2-extract of UB in a form of a suspension with 4 mass% of UA and pure UA were the most active compounds, especially effective against anaerobic and Gram-positive bacteria as well as dimorphic yeast *Malassezia furfur*. Moreover, it was suggested that antimicrobial activity of the extract was mainly mediated by UA [5]. To the best of our knowledge, there are not papers regarding formulation of UB extracts into pharmaceutical preparations for the treatment of skin disorders.

Bearing in mind the above statements, the objective of our study was to develop and evaluate a pharmaceutical topical formulation with UB extract as an active ingredient for the treatment of skin infections. The current investigation consisted of two parts. The aim of the first part was screening of several UB ext-

Correspondence: S.D. Savić, University of Belgrade, Faculty of Pharmacy, Belgrade, Serbia.
E-mail: snexs@pharmacy.bg.ac.rs
Paper received: 1 July, 2014
Paper accepted: 19 December, 2014

racts prepared using different protocols and/or solvents, in terms of their UA content and antimicrobial activity, as well as correlation thereof. The extract with the best antimicrobial potential against bacteria that commonly cause skin infections was further chosen for the second part of the study. In this part, our objective was to formulate selected extract into oil-in-water (O/W) emulsion and evaluate its physicochemical stability, as well as efficiency and safety features. We aimed at developing a vehicle with emollient properties as carrier for UB extract, being prospective topical antimicrobial, considering the potential of emollients (moisturizers) to restore skin barrier function accompanying skin infections, while soothing its concomitant symptoms [6]. In this regard, for stabilization of investigated emulsion we used alkyl polyglucoside (APG) emulsifiers, prepared from natural renewable raw materials, which have been gaining increasing attention in recent years due to their favorable ecological, toxicological and dermatological properties [7,8]. For comparison with the developed emulsion, chosen UB extract in the same concentration and using the same preparation procedure was incorporated into widely used conventional (pharmacopoeial) vehicle, used as a reference.

EXPERIMENTAL

Preparation of UB extracts

Lichen UB was collected in the Former Yugoslav Republic of Macedonia (GPS N41 53.5764 E21 33.6348) on 15th of October, 2009. The lichen was identified at the Faculty of Biology, University of Belgrade (voucher of specimen No. 16390/10.04.2010.). Ethanol 96.3 vol.% was purchased from Vranje, Serbia and ether from Carlo Erba Reagents, France.

Investigated samples were following UB extracts: supercritical CO_2 extract (U-SE), Soxhlet extracts (ether fraction (U-SOX-E) and ethanol fraction (U-SOX-EtOH)) and macerate (U-MAC).

U-SE was purchased from Flavex, Germany. According to manufacturer's claims U-SE was obtained by the method of supercritical CO_2 extraction, and then purified in a second step to practical pure UA (drug:extract ratio (DER) 62–100:5). Samples U-SOX-E and U-SOX-EtOH were obtained by repeated continuous extraction using Soxhlet apparatus. 75.0 g of dried UB, grinded to the size of 180 mesh, was measured in each of five thimbles used, covered with appropriate amount of ether and extracted until ether discoloration. Thereafter, the same procedure as for U-SOX-E was utilized with ethanol 96.3 vol.% using thimbles with plant material already extracted with ether, in order to obtain U-SOX-EtOH. For the preparation of U-MAC, 93.91 g of dried UB grinded to the size of 180 mesh was covered with 600 mL of ethanol 70 vol.%, macerated for 24 h and then filtered. After all extractions, liquids were evaporated using rotary evaporator Buchi R 114, USA, yielding 2.04, 6.71 and 5.41 % residues for U-SOX-E, U-SOX-EtOH and U-MAC respectively, expressed as dry matter.

UA assay in UB extracts

UA was assayed using Hewlett Packard HPLC model 1200; column Zorbax Eclipse XDB-C18 600 Bar (4.6 mm×100 mm, 1.8 μm). The mobile phase A consisted of 99% H_2O and 1% H_3PO_4, while B was acetonitrile. Flow rate was 0.1 mL/min, and elution was as follows: 11–55% B, 0–5 min; 55–80% B, 5–10 min; 80% B, 10–12 min; 80–100% B, 12–20 min; 100% B, 20–35 min, 100––11% B, 35–40 min, 11% B, 40–55 min. Investigated samples (in triplicate) were prepared in a following procedure: 5.0, 7.1, 18.9 and 61.3 mg of U-SE, U-SOX-E, U-SOX-EtOH and U-MAC, respectively were dissolved in 50 mL methanol (analytical grade, purchased from Merck, Germany) then filtered through 0.45 μm PTFE syringe filters into glass HPLC vials and analyzed as described above. Commercially available UA, used as a reference standard was bought from Santa Cruz Biotechnology, USA, with the purity declared as > 98%.

Preparation of O/W creams

Test cream sample (labeled ML) was stabilized with mixed non-ionic APG emulsifier Montanov® L (INCI/$C_{12–14}$ glucoside and $C_{12–14}$ alcohol). A preliminary formulation study, conducted in accordance with manufacturer's recommendations, showed that the emulsifier concentration used (8 mass%) allowed the formation of creams with satisfactory organoleptic characteristics. For co-stabilization, a novel co-emulsifier Montanov® S (INCI/ cocoglucoside and coconut alcohol) was used in the concentration of 2 mass%, in accordance to manufacturer's recommendations. The emulsifiers were kindly provided by Seppic, France. The oil phase comprised caprylic-capric triglycerides (Sabo, Italy) and cetostearyl alcohol (Sabo, Italy), while the water phase was the mixture of 85% glycerol and water preserved using potassium sorbate.

Non-ionic hydrophilic cream (DAB 2011), used as a reference vehicle of pharmacopoeial quality (labeled P), was stabilized with mixed non-ionic emulsifier comprising Polysorbate 60 (Merck, Germany) and cetostearyl alcohol (Sabo, Italy). The oil phase contained white soft paraffin (Sigma Aldrich, Germany), while the water phase consisted of 85% glycerol and water preserved with potassium sorbate [9]. Detailed composition of investigated samples is given in Table 1.

Selection of the extract concentration was performed in the context of UA content, as a carrier of the stated biological activity of the extract. In accordance to our previous investigations (data not shown), chosen

concentration of the extract corresponded to 2 mass% of UA. In addition, selected extract concentration was supported by the literature data [10]. Upon the addition of extract, active samples were labeled ML-U and P-U. Double distilled water was used for the preparation of all samples. Compounds used were of pharmacopoeial quality (Ph. Eur.), whenever possible.

Table 1. Composition (mass%) of investigated vehicles (alkyl polyglucoside-stabilized vehicle (ML) and pharmacopoeial vehicle (P))

Component	ML	P
Caprylic-capric triglycerides	18.5	–
Cetearyl alcohol	1.5	10.0
C_{12-14} glucoside and C_{12-14} alcohol	8.0	–
Cocoglucoside and coconut alcohol	2.0	–
Polysorbate 60	–	5.0
White soft paraffin	–	25.0
Glycerol, 85%	5.0	10.0
Potassium sorbate	0.5	0.5
Water, double distilled	64.5	49.5

APG-stabilized vehicle was prepared by heating the emulsifiers and oil phase at 70-75 °C and then adding them to the preserved water phase at the same temperature by stirring (stirrer RW16 basic, IKA, Germany) at constant temperature for 3 min at 800 rpm and then 3 min at 500 rpm. Cooling was started at 500 rpm for 1 min and then at 300 rpm to the room temperature. Referent non-ionic hydrophilic cream was prepared according to DAB 2011 [9]. Briefly, white soft parrafin together with Polisorbate 60 and cetostearyl alcohol (oil phase) were heated to 70 °C. Components of the aqueous phase were heated to the same temperature, and then added to the oil phase and stirred until cooled to the room temperature. Active samples (ML-U and P-U) were prepared by suspending UB extract into appropriate vehicles. More precisely, the extract was rubbed with glycerol, using mortar and pestle, followed by addition of portions of vehicle. Prepared samples were allowed 7 days equilibration before being submitted to selected characterization techniques.

Rheological measurements

The rheological characterization was conducted in order to evaluate preliminary physical stability of investigated samples, especially in terms of the influence of UB extract addition to both types of investigated bases in a predetermined period of time. Additionally, flow properties were assessed as parameters known to exhibit influence on sensory properties of semisolids, crucial for patient acceptability [11].

Continual measurements were performed after 7, 30 and 90 days of storage at room temperature (Rheometer Rheolab MC 120, Paar Physica, Germany). All measurements were carried out using cone/ plate measuring system (diameter 50 mm, angle 1°), with 0.05 mm sample thickness, at 20±0.1 °C (in triplicate). Controlled shear rate procedure was applied (shear rate 0–200 s^{-1} and back again to the start point, each stage lasting 120 s).

Conductivity measurements

In order to assess both the emulsion type (mode of water distribution) and sample stability, conductivity measurements were performed in both placebo and active cream samples (conductivity meter CDM 230, Radiometer, Denmark). All measurements were performed after 7, 30 and 90 days of storage at room temperature.

pH Measurements

pH measurements were taken by direct immersion of pH meter glass electrode (Hanna instruments HI 9321, USA) in the investigated samples. In order to estimate impact of the extract addition to pH value of the placebo samples, pH value of the extract *per se* was assessed in its aqueous solution which was prepared by putting an excess amount of the extract into 100 mL of purified water in Erlenmeyer flasks, which were tightly closed and shaken on orbital shaker (KS 260 basic, IKA® Werke GmbH & Company KG Germany) at 250 rpm at 25 °C for 24 h. The samples were then centrifuged (Centrifuge MPW-56; MPW Med. Instruments, Poland) at 3000 rpm for 30 min to separate the undissolved extract. For the assessment of preliminary chemical stability, pH value of the tested cream samples was measured 7, 30 and 90 days after their preparation.

***In vitro* antimicrobial activity**

Antimicrobial activity was performed on Gram-positive (G+) and Gram-negative (G-) bacterial species––causative agents of skin infections in humans. Aside referential strains from American Type of Culture Collection (ATCC), investigated strains isolated from skin swabs taken from the diseased persons with skin infection symptoms were also used (clinical isolates, CI). The isolation was made from clinical material delivered to the Microbiology Department, Faculty of Veterinary Medicine, University of Belgrade, in accordance with conventional microbiological methods applied for the purpose of isolation and identification [12]. From the group of G+ microorganisms, *Staphylococcus aureus* ATCC 25923, Methicillin-resistant *Staphylococcus aureus* (MRSA) ATCC 33591, *Staphylococcus epidermidis* (clinical isolate) and *Enterococcus faecalis* (clinical isolate) strains were chosen. From the group of G- bacteria, *Klebsiella pneumoniae* (clinical isolate) and *Escherichia coli* ATCC 25922 strains were selected.

For the investigation of antimicrobial activity and the determination of minimal inhibitory concentrations (MICs) of UB extracts (U-SE, U-SOX-E, U-SOX-EtOH and

U-MAC), investigated creams (ML-U and P-U) and UA, broth microdillution method was applied in accordance with the Clinical and Laboratory Standards Institute (CLSI) prescriptions for antimicrobial susceptibility testing [13,14].

Experiments were performed in 96-well microplate with "U" bottom (Spektar, Serbia) using cation adjusted Mueller Hinton II broth, CAMHB (Becton Dickinson, USA) with the addition of 1.6% bromocresol purple (Merck, Germany) in final concentration at 0.2 mL/200 mL for G+ and 1% phenol red (Merck, Germany) at 1 mL/200 mL for G- bacteria. Bromocresol purple and phenol red were added to obtain bacterial growth visibility. Dimethyl sulfoxide, DMSO (Merck, Germany) was used as a solvent for both extracts and creams. For the complete dissolving of the creams, DMSO was heated in water bath at 60 °C until deposit of creams disappeared. Investigated concentrations of both extracts and creams were 2560, 1280, 640, 320, 160, 80, 40, 20, 10, 5, 2.5, 1.25 and 0.625 μg/mL. The final bacterial inoculum density of 5×105 CFU/mL was achieved by adding 5 μL of 1–2×107 CFU/mL suspension of investigated strain in microtiter plate wells with 100 μL of previously added CAMHB. Microplates were incubated for 18–24 h at 37 °C. For MIC values determination the broth with lowest sample concentration, with no visible bacterial growth, was used.

In vivo skin irritation/performance study

In vivo skin irritation potential of the investigated samples was assessed in a 24-h study under occlusion. Thirteen healthy volunteers (mean age 21.92±1.6), which participated in the study, were thoroughly informed about the possible treatment effects and the protocol of the examination prior to signing written consents, in accordance with the Helsinki Declaration. The study was approved by the Ethical Committee of the Faculty of Medicine, University of Niš, Serbia. The following parameters were evaluated: erythema index (EI), transepidermal water loss (TEWL) and electrical capacitance (EC) (quantifying the *stratum corneum* hydration) using Multi Probe Adapter MPA®9 (Courage & Khazaka Electronic GmbH, Germany). All measurements were conducted on flexor aspects of forearms at square application sites of 9 cm^2, leaving a site per each arm for untreated control under occlusion (UCO) and without occlusion (UC). After initial measurements, 0.016 g/cm^2 of investigative samples were applied, covered with silicone film and fixed with hypoallergenic adhesive tapes. Two hours upon removal of the 24-h occlusion, all parameters were reassessed.

Statistical analysis

Statistical analysis was carried out in OriginPro 9.0 (Electronic Arts, USA). Parameters of *in vivo* measurements were assessed with a one-way ANOVA followed by Tukey post hoc test, whenever appropriate.

RESULTS AND DISCUSSION

Results of chemical analysis of UB extracts are presented in Table 2. UA content ranged from 1.39 % in U--MAC to 81.41% in U-SE, which could be expected, bearing in mind that its solubility increases with solvent polarity decrease [15]. Namely, the lowest UA content was found in the extracts prepared with ethanol, which was the most polar solvent used (Table 2). However, application of non-polar ether in the extraction process led to notable increase in UA content in the sample U-SOX-E (Table 2). The highest UA content was detected in the sample obtained by supercritical CO_2 extraction, U-SE (Table 2), known to be appropriate method for the isolation of low polarity compounds [16].

All of investigated extracts and pure UA showed antimicrobial activity against G+ strains, whereas there was no activity against G– bacteria (*MIC*s greater than 2560 μg/mL), which is in line with previous reports [2,4,5]. As expected, MIC values for the G+ bacteria were inversely proportional to the UA content, *i.e*., antimicrobial potential increased with the upsurge of UA percentage, thus reasserting its mediating role in demonstrated antimicrobial activity of UB extracts [4,5]. Precisely, among the investigated extracts, U-MAC revealed the highest *MIC* values (representing the weakest antimicrobial activity) against investigated bacteria, followed by U-SOX-EtOH and U-SOX-E (Table 2). U-SE was the most effective extract, revealing the same *MIC* values as the pure UA with *S. epidermidis*

Table 2. Usnic acid content and minimal inhibitory concentrations (MIC values) of the investigated isolates of U. barbata, expressed as μg/mL (usnic acid (UA), supercritical CO_2 extract (U-SE), Soxhlet extract-ether fraction (U-SOX-E), Soxhlet extract-ethanol fraction (U-SOX-EtOH) and macerate (U-MAC))

Extract/isolate	Usnic acid content, %	*S. aureus* ATCC 25923	MRSA ATCC 33591	*S. epidermidis* (CI)	*E. faecalis* (CI)	*K. pneumoniae* (CI)	*E. coli* ATCC 25922
UA	98.00	10	5	1.25	2.5	no effect	no effect
U-SE	81.41	10	5	1.25	2.5	no effect	no effect
U-SOX-E	67.09	40	20	5	5	no effect	no effect
U-SOX-EtOH	2.43	320	320	40	160	no effect	no effect
U-MAC	1.39	640	320	160	320	no effect	no effect

and *E. faecalis* clinical isolates being the most sensitive among the tested bacterial strains (Table 2).

Thus, U-SE, as the extract with the best antimicrobial potential, was incorporated into the developed APG-based (ML) and pharmacopoeial (P) vehicle in the same concentration corresponding to 2 mass% of UA, as a carrier of stated biological activity, by suspending the extract using mortar and pestle, yielding samples ML-U and P-U, respectively. Thereafter, their physicochemical stability, efficiency and safety were evaluated and compared both mutually and to their corresponding placeboes, in the second part of the study.

Both placebo samples were shiny, white semisolids, with ML having a softer consistency in comparison to P. Active samples (ML-U and P-U) were yellowish creams, somewhat thicker in comparison to their matching placebo samples.

A preliminary physical stability of investigated creams was carried out using continual rheology and electrical conductivity measurements, while pH value measurements gave an insight into their preliminary chemical stability. All measurements were carried out 7, 30 and 90 days after preparation, and tested parameters were compared as a function of time.

Taking into account shear stress–shear rate curves, all samples exhibited shear-thinning flow behavior with moderate (ML and ML-U) to pronounced (P and P-U) thixotropy, considered desirable for topically applied preparations (Fig. 1a) [17]. In addition, rheological measurements accentuated distinct sensory characteristics of APG-based samples in comparison to the reference ones, observed visually. Upon U-SE addition into both APG-based and pharmacopoeial vehicle, samples' yield stresses and hysteresis loops were increased, as

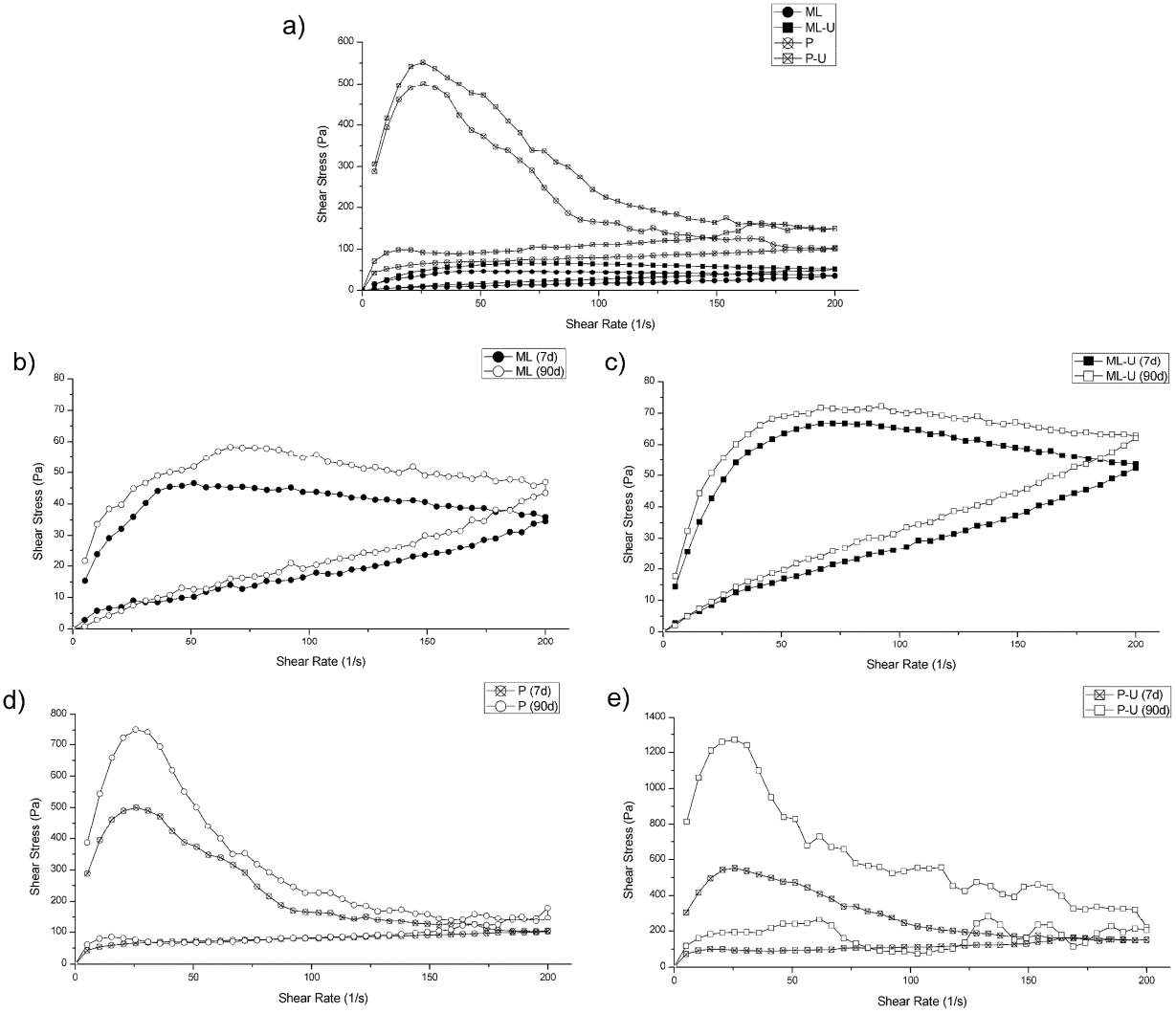

Figure 1. Flow curves of: a) all cream samples (alkyl polyglucoside-stabilized vehicle (ML) and pharmacopoeial vehicle (P)) and active cream samples with U. barbata supercritical CO_2 extract corresponding to 2 mass% of usnic acid in the final formulation incorporated into vehicle ML (ML-U and P (P-U)) 7 days after preparation, b) sample ML 7 days (ML(7d)) and 90 days (ML(90d)) after preparation; c) sample ML-U 7 days (ML-U(7d)) and 90 days (ML-U(90d)) after preparation, d) sample P 7 days (P(7d)) and 90 days (P(90d)) after preparation, e) sample P-U 7 days (P-U(7d)) and 90 days (P-U (90d)) after preparation.

expected, considering the fact that the extract was suspended in the investigated bases, substantiating findings of organoleptic inspection (Fig. 1a). It is a known fact that evolution of rheological properties can indicate instability of emulsions. Therefore, repeated measurements of rheological parameters may serve as a simple and convenient experimental method for estimating the state of an emulsion as a function of storage time [18]. In this accordance, samples ML, ML-U and P after 3 months did not show significant changes in rheological profiles (Fig. 1 b–d). More specifically, the lowest increase of hysteresis loop was recorded in APG-based samples, *i.e.*, in ML-U, followed by ML. On the other hand, a major upsurge of this rheological parameter for P-U, especially in respect to its corresponding placebo (P), could be connected to the dissatisfying preliminary physical stability, as well as unsatisfactory applicative characteristics of this sample (Fig. 1e) [19]. With this respect, continual rheological measurements indicated preferential physical stability of APG base, especially regarding U-SE incorporation potential, when compared to pharmacopoeial one. They also emphasized distinctively ameliorated sensory characteristics of APG-based samples, as an important property of topical preparations having a major impact on patients' compliance and consequent efficacy in the management of skin diseases [6].

Initial conductivity measurements of the placebo samples (ML and P) revealed the values being non-typical for the multiphase emulsion systems prepared with nonionic-mixed emulsifiers (0–50 μs/cm) and in the field of real O/W emulsions (Table 3). However, although conductivity measurements may indicate the degree of structuring and/or the type of emulsion, it is not possible to unequivocally interpret high conductivity solely as reduced structuring of the system, while it may also simply reflect the level of free ions present within the system [20,21]. Nevertheless, even though the only ionic moieties present in both systems originated from the preservative, potassium sorbate, used in the same concentration (Table 1) initially assessed specific conductivity detected in APG-based sample (ML) was notably higher in comparison to the pharmacopoeial one (P). This discrepancy might be attributed, at least partially, to the higher portion of water within the system and therefore probably higher percentage of free/bulk water (Table 1) but also the different time needed for achieving final microstructure of APG-based (ML) *versus* referent (P) emulsion [21,22]. Later assumption was broadly supported by conductivity measurements reasserted after 30 days of storage, that revealed discernible decrease in specific conductivity of APG-based vehicle (ML) pointing to its subsequent structuring [20], as opposed to pharmacopoeial one (P), having conductivity value at the same level as in initial measurements (Table 3). However, further measurement assessed 90 after preparation, disclosed an increase of conductivity for both placebo creams (ML and P). As for the active samples (ML-U and P-U), addition of the extract (U-SE) affected their matching vehicles (ML and P, respectively) in an inverse manner (Table 3). Namely, in the initial measurements, it led to certain decrease of specific conductivity in ML-U related to ML that is an increase in P-U connected to P (Table 3). In addition, both active creams followed the trend of conductivity change as the function of storage time pursuant to the corresponding vehicles (Table 3).

Conductivity increase could point to certain changes in physical characteristics of investigated systems and might be interpreted as a sign of physical instability, and it has been suggested that the later this rise occurred and the smaller the growth was, the stability of the cream increased [22]. In our experiments, all of the investigated cream samples, with the exception of ML, revealed an increase of conductivity after 90 days of storage at room temperature in comparison to the values assessed 7 days after their preparation (Table 3). However, when considering an initial decrease of specific conductivity of APG-based samples (ML and ML-U) within first 30 days of room temperature storage, an overall growth of conductivity may be considered more accentuated in these samples in relation to the reference ones (P and P-U, Table 3). It is well established that for the definitive evaluation of physical stability of an emulsion system, parameters assessed using different methods are considered relevant. In this regard, greater extent of conductivity increase in APG-based samples related to the reference ones was not in line with previously discussed rheological findings. On the other side, P-U was the only sample disclosing perm-

Table 3. Conductivity and pH values of placebo (alkyl polyglucoside-stabilized vehicle (ML) and pharmacopoeial vehicle (P)) and active cream samples (with U. barbata supercritical CO_2 extract corresponding to 2 mass% of usnic acid in the final formulation incorporated into vehicle ML (ML-U) and P (P-U)) assessed 7, 30 and 90 days after preparation

Sample	Conductivity, μS/cm			pH		
	7 days	30 days	90 days	7 days	30 days	90 days
ML	204.40	91.50	181.00	7.04	6.95	6.65
ML-U	199.50	107.30	248.00	6.96	6.98	6.90
P	73.70	73.30	110.70	7.37	7.15	7.47
P-U	83.60	85.90	131.60	7.30	7.32	7.47

anent increase of conductivity throughout 90-day period of storage at room temperature. Connected to previously discussed changes in rheological behavior of this sample as a function of the stated storage time, such observations should be taken into account in the long-term predictions of physical stability of this sample. Overall, on the basis of certain dissidences in findings of rheological and conductivity measurements, additional investigations are needed for the final assessment on physical stability of all investigated cream samples.

pH measurements showed all examined samples to be within ranges suitable for skin application (Table 3) [6]. Addition of the U-SE in the active samples (ML-U and P-U) led to a slight decrease in pH value in comparison to corresponding vehicle (ML and P, respectively), which could be expected considering the measured pH value of the extract *per se* (5.80). In addition, obtained values remained similar throughout the 3-month observation period, indicating satisfying preliminary chemical stability of investigated samples.

In accordance to the results obtained for the extract of UB incorporated into the investigative creams (U--SE), their antimicrobial activity assessment was performed only against G+ bacterial species (the same as used for the extracts). Results of antimicrobial activity are presented in Table 4. ML and P served as negative controls for the appropriate active creams (ML-U and P-U, respectively), while ampicillin was used as a positive control for UA. *MIC*s are presented for UA as a part of ML-U and P-U and as intact substance [23]. None of the placebo creams (neither ML nor P) showed activity against tested microorganisms (MICs greater than 2560 μg/mL), as seen in Table 4. On the other hand, both active creams (ML-U and P-U) revealed the potential to inhibit growth of investigated bacteria (Table 4). Accordingly, UA as the active substance of active creams followed the same pattern (Table 4). Moreover, obtained MIC values were consistent with the ones determined for UA *per se*, revealing strong antimicrobial activity against tested G+ strains, especially in the case of UA as a part of ML-U. With this respect, comparison of antimicrobial activity of ML-U *versus* P-U revealed the same inhibition spectrums of both creams against MRSA ATCC 33591 and clinical isolate of *E. faecalis*, whereas ML-U was more active against *S. aureus* ATCC 25923 and clinical isolate of *S. epidermidis* (Table 4). In contrast, ampicillin showed no effect against most of the tested strains. It was, however, more effective than UA against clinical isolate of *E. faecalis* (Table 4).

Investigated samples showed overall satisfying preliminary safety profiles (Fig. 2). Two hours after occlusion removal, there was no significant change in EI, which was even decreased for all investigated samples, indicating well-tolerated skin formulations (Fig. 2a). TEWL was increased for the samples ML and P-U related to corresponding baseline, but not the controls. Nevertheless, this increase might be attributed predominantly to the occlusion effect, regarding the fact that TEWL obtained for UCO was also significantly higher in comparison to the baseline (Fig. 2b). As for EC, all samples led to an increase of this parameter (Fig. 2c). The increase could be considered significant in the case of both APG-based samples (ML and ML-U) compared to baselines and both controls, revealing skin hydration potential probably related to the vehicle itself, considering that there was no statistically significant differences in EC increase between these two samples (Fig. 2c). The same finding regarding EC was noted for the pharmacopoeial vehicle (P), but not the active cream (P-U), which EC increase was statistically significant compared to UC, but not UCO.

Table 4. Minimal inhibitory concentrations (MIC values), expressed as μg/mL, for the investigated samples: placebo creams (alkyl polyglucoside-stabilized vehicle (ML) and pharmacopoeial vehicle (P), negative control); active creams (with U. barbata supercritical CO_2 extract corresponding to 2 mass% of usnic acid in the final formulation incorporated into vehicle ML (ML-U) and P (P-U)); active substance usnic acid (UA, as a part of active cream (ML-U and P-U) and per se) and ampicillin (positive control)

Sample	*S. aureus* ATCC 25923	MRSA ATCC 33591	*S. epidermidis* (CI)	*E. faecalis* (CI)
ML	No effect	No effect	No effect	No effect
ML-U	1280	320	40	80
UA (AP ML-U)[a]	25.6	6.4	0.8	1.6
P	No effect	No effect	No effect	No effect
P-U	2560	320	80	80
UA (AP P-U)[b]	51.2	6.4	1.6	1.6
UA (*per se*)	10	5	1.25	2.5
Ampicillin	No effect	No effect	No effect	0.125

[a]*MIC* of UA as a part of ML-U (AP ML-U) was calculated as the concentration of UA in the cream multiplied by *MIC* for ML-U; [b]*MIC* of UA as a part of P-U (AP P-U) was calculated as the concentration of UA in the cream multiplied by *MIC* for P-U

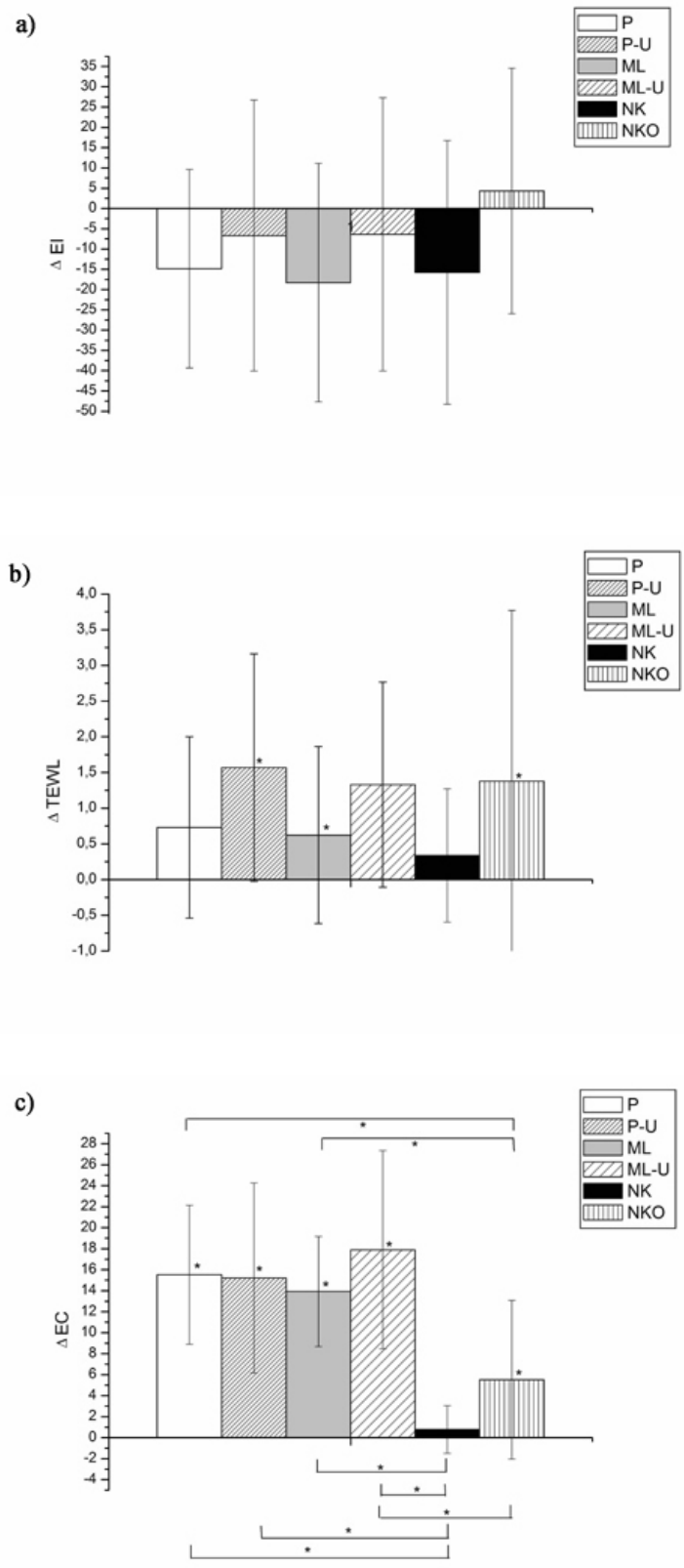

Figure 2. The effects of placebo (alkyl polyglucoside-stabilized vehicle (ML) and pharmacopoeial vehicle (P) and active cream samples (cream samples with U. barbata supercritical CO_2 extract corresponding to 2 mass% of usnic acid in the final formulation incorporated into vehicle ML (ML-U) and P (P-U)) on: a) erythema index (EI), b) transepidermal water loss (TEWL) and c) electrical capacitance (EC). The results are shown as absolute changes of mean values and standard error of mean to the baseline. The effects of tested formulations were compared mutually and to both controls (under occlusion, UCO and without occlusion, UC). Significant differences are marked with ($P < 0.05$).*

CONCLUSION

Results of our study proved the developed alkyl polyglucoside (APG)-based vehicle to be a promising carrier for *Usnea barbata* CO_2-supercritical extract (U--SE) in the concentration corresponding to 2 mass% of usnic acid, composing a topical formulation with potential clinical relevance in the treatment of skin infections. Investigations on rheological behavior of the investigated cream samples indicated APG-stabilized emulsion to possess highly satisfactory ability to remain physically stable upon the addition of U-SE, when compared to pharmacopoeial one. However, conductivity measurements revealed certain dissidences related to rheological findings, imposing the need for additional investigations for the final assessment on physical stability of the investigated emulsion systems. Satisfying preliminary chemical stability was shown for all tested cream samples. Further efficiency and safety evaluation revealed stronger antimicrobial potential of APG-containing pharmaceutical vehicle when compared to traditionally used pharmacopoeial base of proven quality. Overall satisfying preliminary safety profiles were demonstrated for both APG-based and reference cream samples.

In all, investigated APG base revealed certain preferential features as a vehicle for U-SE compared to the conventional one, especially considering its improved sensory characteristics (confirmed by organoleptic and rheological assessment), as a property often decisive for the patient compliance.

Acknowledgements

Authors wish to thank Serbian Ministry of Education, Science and Technological Development (Projects: III45017 and TR34031).

REFERENCES

[1] K. Ingolfsdottir, Molecules of Interest Usnic acid, Phytochemistry **61** (2002) 729–736.

[2] T. Madamombe, A.J. Afolyan, Evaluation of Antimicrobial Activity of Extracts from South African *Usnea barbata*, Pharm. Biol. **41** (2003) 199–202.

[3] J. Gruendwald, T. Brendler, C. Jaenicke, PDR for Herbal Medicines, 3rd ed., Thomson, Montvale, 2004.

[4] D. Cansaran, D. Kahya, E. Yurdakulola, O. Atakol, Identification and quantitation of usnic acid from the lichen Usnea species of Anatolia and antimicrobial activity, Z. Naturforsch., C **61** (2006) 773–776.

[5] S. Weckesser, K. Engel, B. Simon-Haarhaus, A. Wittmer, K. Pelz, C. M. Schempp, Screening of plant extracts for antimicrobial activity against bacteria and yeasts with dermatological relevance, Phytomedicine **14** (2007) 508–516.

[6] M. Loden, Role of Topical Emollients and Moisturizers in the Treatment of Dry Skin Barrier Disorders, Am. J. Clin.Dermatol. **4** (2003) 771–788.

[7] K. Holmberg, Natural surfactants, Curr. Opin. Colloid In. **6** (2001) 148–159.

[8] I. Johansson, M. Svensson, Surfactants based on fatty acids and other natural hydrophobes, Curr. Opin. Colloid In. **6** (2001) 178–188.

[9] Deutsches Arzneibuch 2011, Deutscher Apotheker Verlag, Stuttgart, 2011.

[10] C.M. Schempp, A. Jocher, K. Engel, C. Huyke, Pharmaceutical composition comprising old man's beard (*Usnea barbata*) and St. John's wort (*Hypericum perforatum*) and their use, US patent 7,687,083 B2 (2005).

[11] N. Dragicevic-Curic, S. Winter, M. Stupar, J. Milic, D. Krajisnik, B. Gitter, A. Fahr, Temoporfin-loaded liposomal gels: viscoelastic properties and in vitro skin penetration, Int. J. Pharm. **373** (2009) 77–84.

[12] I. Žižovic, J. Ivanović, D. Mišić, M. Stamenić, S. Đorđević, J. Kukić-Marković, S. Petrović, SFE as a superior technique for isolation of extracts with strong antibacterial activities from lichen *Usnea barbata* L., J. Supercrit. Fluid. **72** (2012) 7–14.

[13] Clinical and Laboratory Standards Institute, Performance standards for antimicrobial susceptibility testing, twentieth informational supplement, CLSI document M100-S20, Wayne, 2010.

[14] I. Arsić, A. Zugic, V. Tadic, M. Tasic-Kostov, D. Misic, M. Primorac, D. Runjaic-Antic, Estimation of Dermatological Application of Creams with St. John's Wort Oil Extracts, Molecules **17** (2012) 275–294.

[15] J. Jin, Y. Rao, X. Bian, A. Zeng, G. Yang, Solubility of (+)-Usnic Acid in Water, Ethanol, Acetone, Ethyl Acetate and n-Hexane, J. Solution Chem. **42** (2013) 1018–1027.

[16] M. Palma, L. Taylor, Fractional Extraction of Compounds from Grape Seeds by Supercritical Fluid Extraction and Analysis for Antimicrobial and Agrochemical Activities, J. Agric. Food Chem. **47** (1999) 5044-5048.

[17] L.E. Pena, B.L. Lee, J.F. Stearns, Structural Rheology of a Model Ointment, Pharm. Res. **11** (1994) 875–881.

[18] S.R. Derkach, Rheology of emulsions, Adv. Colloid Interf. **151** (2009) 1–23.

[19] I. Jaksic, M. Lukic, A. Malenovic, S. Reichl, C. Hoffmann, C. Müller-Goymann, R. Daniels, S. Savic, Compounding of a topical drug with prospective natural surfactant-stabilized pharmaceutical bases: Physicochemical and in vitro/in vivo characterization –A ketoprofen case study, Eur. J. Pharm. Biopharm. **80** (2012) 164–175.

[20] S. Tamburic, D.Q.M. Craig, G. Vuleta, J. Milic, A comparison of electrical and rheological techniques for the characterization of creams, Int. J. Pharmaceut. **137** (1996) 243–248.

[21] M. Korhonen, H. Niskanen, J. Kiesvaara, J. Yliruusi, Determination of optimal combination of surfactants in creams using rheology measurements, Int. J. Pharm. **197** (2000) 143–151.

[22] M. Korhonen, L. Hellen, J. Hirvonen, J. Yliruusi, Rheological properties of creams with four different surfactant combinations-effect of storage time and conditions, Int. J. Pharmaceut. **221** (2001) 187–196.

[23] M. Asterholm, N. Karami, J. Faergemann, Antimicrobial Activity of Topical Skin Pharmaceuticals – An *In vitro* Study, Acta Derm.-Venerol. **90** (2010) 239–245.

IZVOD

EMULZIJA STABILIZOVANA ALKIL POLIGLUKOZIDNIM EMULGATOROM KAO POTENCIJALNI NOSAČ ZA CO_2-NATKRITIČNI EKSTRAKT VRSTE *Usnea barbata*: PROCENA STABILNOSTI, BEZBEDNOSTI I EFIKASNOSTI TOPIKALNE FORMULACIJE

Ana R. Žugić[1], Milica Z. Lukić[2], Marija Z. Tasić Kostov[3], Vanja M. Tadić[1], Ivana A. Arsic[3], Dušan R. Mišić[4], Slobodan D. Petrović[5], Snežana D. Savić[2]

[1]*Institut za proučavanje lekovitog bilja "Dr Josif Pančić", Odsek za farmaceutska istraživanja i razvoj, Beograd, Srbija*
[2]*Univerzitet u Beogradu, Farmaceutski fakultet, Katedra za farmaceutsku tehnologiju i kozmetologiju, Beograd, Srbija*
[3]*Univerzitet u Nišu, Medicinski fakultet, IAS Farmacije, Niš, Srbija*
[4]*Univerzitet u Beogradu, Fakultet veterinarske medicine, Katedra za mikrobiologiju, Beograd, Srbija*
[5]*Univerzitet u Beogradu, Tehnološko-metalurški fakultet, Katedra za organsku hemiju, Beograd, Srbija*

(Naučni rad)

Antimikrobna aktivnost vrste *Usnea barbata* naročito protiv bakterija koje učestvuju u patogenezi različitih bolesti kože, dobro je dokumentovana u naučnoj literaturi. Uprkos tome, ne postoje radovi koji se bave formulacijom topikalnih preparata na bazi ovog lišaja namenjenih lečenju kožnih infekcija. U ovoj studiji, razvijena je podloga stablizovana alkil poliglukozidnim (APG) emulgatorom, kao potencijalni nosač za ekstrakt vrste *U. barbata* koji je pokazao najbolji antimikrobni potencijal u preliminarnom istraživanju nekoliko ekstrakata dobijenih upotrebom različitih ekstragenasa/postupaka. Radi poređenja, odabrani CO_2-natkritični ekstrakt je inkorporiran u istoj koncentraciji (koja odgovara 2 mas.% usninske kiseline) i istim postupkom izrade u često korišćenu podlogu farmakopejskog kvaliteta, a zatim je sprovedeno uporedno istraživanje fizičko-hemijske stabilnosti, efikasnosti i bezbednosti na obe grupe uzoraka. Rezulati našeg istraživanja pokazali su da se razvijena podloga stabilizovana APG emulgatorom može smatrati pogodnim nosačem za CO_2-natkritični ekstrakt vrste *U. barbata*, čineći topikalnu formulaciju sa potencijalnim kliničkim značajem u terapiji kožnih infekcija. Reološka istraživanja pokazala su zadovoljavajuću sposobnost emulzije stabilizovane APG emulgatorom da ostane fizički stabilna nakon dodatka CO_2-natkritičnog ekstrakta vrste *U. barbata*, u poređenju sa farmakopejskom. Međutim, konduktometrijska merenja su pokazala određena neslaganja sa reološkim nalazima, namećući potrebu za dodatnim istraživanjima radi konačne procene fizičke stabilnosti testiranih emulzionih sistema. Izmerene vrednosti pH tokom perioda od 90 dana čuvanja uzoraka na sobnoj temperaturi ukazale su na zadovoljavajuću preliminarnu hemijsku stabilnost svih uzoraka. Dalja istraživanja efikasnosti i bezbednosti pokazala su bolji antimikrobni potencijal uzoraka sa podlogom stabilizovanom APG emulgatorom u odnosu na tradicionalno upotrebljavanu farmakopejsku bazu poznatog kvaliteta. Zadovoljavajući preliminarni bezbedonosni profili su pokazani kako za uzorke stabilizovane APG emulgatorom tako i za referentne krem uzorke. Na osnovu navedenog, može se zaključiti da je istraživana podloga bazirana na APG emulgatoru pokazala određene povoljnije karakteristike kao nosač za CO_2-natkritični ekstrakt vrste *U. barbata* u poređenju sa konvencionalno korišćenom podlogom, naročito uzimajući u obzir njene poboljšane senzorne karakteristike, kao osobinu koja je često odlučujuća za komplijansu pacijenata.

Ključne reči: Alkil poliglukozidi • *Usnea barbata* natkritični CO_2-ekstrakt • Infekcije kože • Fizičko–hemijska stabilnost • Antimikrobna aktivnost • Performanse na koži

CFD and laboratory analysis of axial cross-flow velocity in porous tube packed with differently structured static turbulence promoters

Igor Gaspar[1], Predrag Tekic[2], Andras Koris[1], Albert Krisztina[1], Svetlana Popovic[2], Gyula Vatai[1]

[1]*Corvinus University of Budapest, Department of Food Engineering, H-1118 Budapest, Menesi St. 44, Hungary*
[2]*University of Novi Sad, Bulevar Cara Lazara 1, 21000 Novi Sad, Serbia*

Abstract

Computational fluid dynamics (CFD) was used for modeling flow regime in a porous tube. This tube is an ultrafiltration membrane filter made from zirconium-oxide which is very effective in the separation of stable oil-in-water micro-emulsions, especially when the tube is filled with static mixer. The results of the CFD analysis were used in the preliminary optimisation of the static mixer's geometry since it has significant effect on the energy requirement of this advanced membrane technology. The self-developed static mixers were tested "*in vitro*" from the aspect of separation quality and process productivity as well to validate CFD results and to develop a cost effective, green method to recover unmanageable oily wastewaters for sustainable development. In this work the results of computational simulation of the fluid velocity and membrane separation experiments are discussed.

Keywords: cross-flow ultrafiltration, oil-in-water emulsion, computational fluid dynamics, static mixers.

Available online at the Journal website: http://www.ache.org.rs/HI/

SCIENTIFIC PAPER

UDC 66.081.63:004:51

Hem. Ind. **69** (6) 713–718 (2015)

doi: 10.2298/HEMIND140312001G

Oil-in-water emulsion is common by-product in chemical-, food-, mechanical- and other type of industries. Nowadays these waste waters cannot be discharged directly into the natural environment to avoid creating a significant ecological problem. With treatment of such waste oil emulsions, fluid can be separated to its components: oil and water. This separation can be done by evaporation too, but this method is very energy-consuming. Furthermore, in case of stable nano- or micro-emulsions the traditional water cleaning technologies are not always enough efficient to ensure the limited oil values in the released water [1]. With ultrafiltration, concentration of the oil in permeate can be reduced below 50 mg L^{-1} (limiting value for discharge to the public sewer in Hungary [2]). After filtration, the concentrated wastewater may contain less than 1/5 of original volume, so final evaporation might need approximately one-fifth of the original energy requirement to separate the water from the oil.

Using Kenics® static mixer inside a tubular membrane during ultrafiltration of an oil-in-water emulsion has a positive effect to permeate flux, retention of the oil and fouling delay [3]. Originally the aim of Kenics® type turbulence promoter's geometry was the cost effective mixing two or more fluids. For this reason this kind of mixer causes big pressure drop along the membrane; due to this phenomena Kenics® mixer can be used only at lower recirculation flow rates for membrane separation to ensure cost-effectiveness [4]. The main aim of this work was to find new turbulence promoter geometry which will result in similar flux and retention improvement, raising tangential velocity, but keep pressure drop along membrane as low as possible.

In the first step, the new shapes were tested with "*in silico*" simulation experiments. Computational fluid dynamics (CFD) is a state-of-the-art numerical technique for solving fluid problems [5]. CFD calculations use a computational grid to solve the governing equations describing fluid flow, *e.g.*, the continuity equation and the set of Navier-Stokes equations, and any additional conservation equations, such as energy balance, across each grid cell by means of an iterative procedure in order to predict and visualize the profiles of velocity, pressure, temperature, etc. Early users of CFD are found in the automotive, aerospace and nuclear industries. With the enhancement of computing power and efficiency and the availability of affordable CFD packages applications of CFD have extended into the food industry for modeling industrial processes, thereby generating comprehensive analyses leading to designing more efficient systems [6].

Lattice Boltzmann methods which were used for CFD analysis in this work are numerical techniques for the simulation of fluid flows [7]. Their strength lies however in the ability to easily represent complex physical phenomena, ranging from multiphase flows to chemical interactions between the fluid and the borders. Indeed, the methods find their origin in a molecular description of a fluid and can directly incorporate physical terms stemming from knowledge of the inter-

Correspondence: I. Gaspar, Corvinus University of Budapest, Department of Food Engineering, H-1118 Budapest, Menesi St. 44, Hungary.
E-mail: igor.gaspar@uni-corvinus.hu
Paper received: 12 March, 2014
Paper accepted: 29 December, 2014

action between molecules. The methods are often regarded as particular discrete representations of the Boltzmann equation. The Boltzmann equation is analogue of the Navier–Stokes equation at a molecular level, where it describes the evolution of the probability distribution function for a molecule to be present at a given point in the space of positions and velocities, the 6-dimensional phase space. The amount of physical phenomena contained in the model at this molecular level of description is larger than at the hydrodynamic level of the Navier–Stokes equation. This is because the Boltzmann equation is not subject to a separation of time scales and has the ability to describe fluids in non-hydrodynamic regimes with large molecular mean free paths. Furthermore, the molecular model is able to capture transport phenomena such as friction, diffusion and temperature transport and derive the corresponding transport coefficients. Boltzmann equation acts on real-valued quantities, but it describes some dynamics in a discrete phase space which can be called lattice [8].

As result of this simulation, 5 new geometries have been found which should be interesting for real time experiments. After producing 5 new turbulence promoters their effect on initial flux and retention has been tested.

MATERIALS AND METHODS

For computational fluid dynamics (CFD) open source software based on lattice Boltzmann algorithm was used [8]. Input for this method was textual file with 3D matrix in it where rectangular space around membrane was divided into 0.1 mm cubes. Values in this matrix can be 1 (solid material) or 0 (means in that particle is fluid) (Eq. (1)):

$a_{i,j,k}$, where i = 1,2,...,72, j = 1,2,...,72, k = 1,2,...,500,
a = 0 or 1 (1)

Initial average flow velocity was also given as input parameter. After calculation vorticity and velocity norms are calculated for each particle and the output of this computation is also a matrix in textual (*.vti) file. This file can be visually represented with Paraview open source scientific visualization software [9].

The laboratory experiments were carried out in cross-flow mode, using a conventional ultrafiltration set-up with tubular single-channel module containing a ceramic zirconia (ZrO_2) membrane (Exekia, Pall, USA) (Fig. 1). The ceramic membrane had a nominal pore size of 50 nm, inner diameter of 6.8 mm and the effective membrane area of 50 cm^2.

Inside the tube, membrane static mixers were installed as shown in Fig. 2. Turbulence promoter used as origin for comparison was Kenics® static mixer (Omega, USA) made from polyacetate. Based on CFD simulation, for laboratory testing, 5 new static mixers were produced from stainless steel (Fig. 2).

A stable oil-in-water emulsion was prepared from a commercial cutting lubricant oil additive (Unisol, Mol, Hungary). The oil concentration in the emulsion was 5 mass%. The feed was pumped from a tank to the membrane module and then recirculated (Fig. 1). The recirculated flow rate (*RFR*) and transmembrane pressure (*TMP*) were controlled by means of regulation valves. The recirculated flow rate was 100 L h^{-1} and transmembrane pressure was 2 bar.

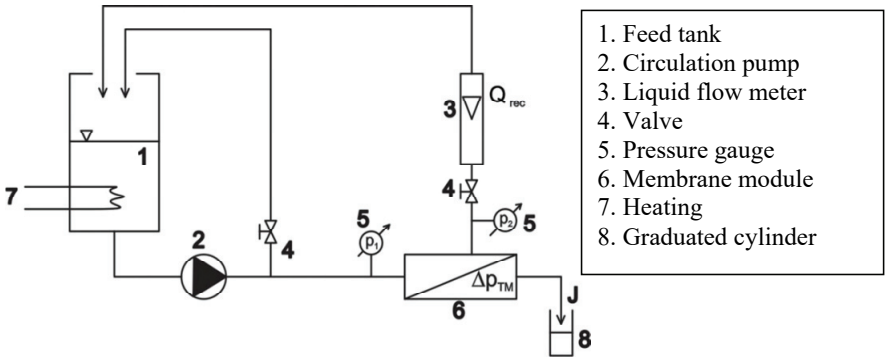

Figure 1. Schematic diagram of the experimental set-up.

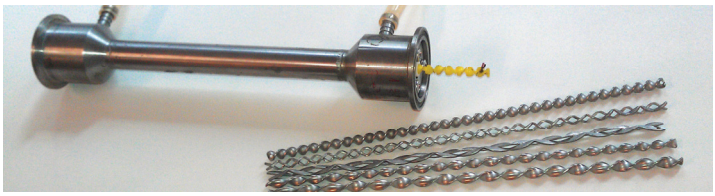

Figure 2. Kenics® static mixer in membrane module (left), 5 new turbulence promoters (right).

The membranes were cleaned according to the recommendations of the manufacturers prior to each experiment and the pure water fluxes of the cleaned membranes were measured. The cleaning procedure was repeated until the original water flux was restored.

Beside permeate flux, and retention of the oil, one of the most important parameter from an economical point is pressure drop along the membrane, because it has direct effect to specific energy consumption (E in (J m^{-3}) defined as the power dissipated per unit volume of permeate. The hydraulic dissipated power is directly related to the pressure drop along the membrane module (Δp in Pa) and the specific energy consumption can be calculated as:

$$E = \frac{RFR\Delta p}{J_p A} \tag{2}$$

where J_p (L m^{-2} h^{-1}) is the permeate flux, A (m^2) is the membrane surface area and RFR (L h^{-1}) represents the recirculated flow rate.

The permeate flux was calculated from the experimental data with the following classical equation:

$$J_p = \frac{V}{tA} \tag{3}$$

where V (L) is the volume of permeate and t (h) is for time.

The oil concentrations in the feed and the permeate solutions were analysed using UV spectrophotometer on 600 nm wave length. Measured absorbency was converted to concentration using calibration curve.

RESULTS

CFD Analysis

In Fig. 3 the CFD analysis of the 6 different packing is demonstrated, from 1 to 6. In each figure the vorticity norm (norm of the vorticity vector in 3D) distribution (based on discrete particle motion) can be found on the left, the matrix of the turbulence promoter is the middle one and on the left the structure of static mixer is illustrated. The green colour shows low vorticity values compared to blue surface where the vorticity is increased. In Figs. 3–7 it can be seen that Kenics® static mixer causes very big turbulence because of high friction of fluid with turbulence promoter. As a result this phenomenon causes enormous pressure drop along membrane. This pressure change has direct effect on specific energy consumption of ultrafiltration (Eq. (2)). Static mixers Nos. 1 and 2 on Fig. 3 doesn't ensure very intensive promotion of turbulence (compared to Kenics® type mixer), but the problem is still the high pressure drop caused by the geometry. Spiral-ribbon mixer (Fig. 3, No. 3) could be optimal solutions for turbulence promotion since the velocity increase caused by them does not results in higher pressure drop along the module. However the shaping is crucial with these types of mixers; when the spiral's pitch is too large and the size (diameter and thickness) is small the mixing efficiency is very limited.

Laboratory UF experiments

The method to simulate permeation through the pores of a given membrane with CFD is still under

Figure 3. CFD pictures generated with ParaView [8] static mixers: 1) zigzag h/d = 2, 2) zigzag .h/d = 1.2, 3) spiral h/d = 1, 4) spiral h/d = 1.5, 5) spiral h/d = 2, 6) Kenics® static mixer.

development thus the effect on the flux or retention of the membrane cannot be seen in the figures. Because of this the next step was the test of the turbulence promoters in real environment from the aspect of oil retention, but also flux and pressure-drop. The results of this ultrafiltration experiments with new static mixers are presented in Figs. 5–7. In Fig. 5 the flux increasing effect of inline static mixers can be seen. If the flux-enhancement is the standalone target, Kenics® type mixer (6.) and the dense spiral mixer (3.) are the best choices, but the zigzag mixer (2.) is very good as well. Noticeable fact, that the permeate flux of an ultrafilter could be raised up to 3–4 times higher with appropriate static turbulence promoter packing. In Fig. 6 it is well understood that mixer No. 6 causes great promotion in the fluid which generates flow resistance and leads to drastically increased energy requirement. The promoter No. 6 was developed for mixing reasons and due to this its application for membrane filtration enhancement is not advisable. Comparatively, the turbulence promoters which were developed for membrane applications behave more like the empty tube – except No. 2 zigzag mixer. From energy consumption point of view the No. 2 significantly increases the energy usage of the operation.

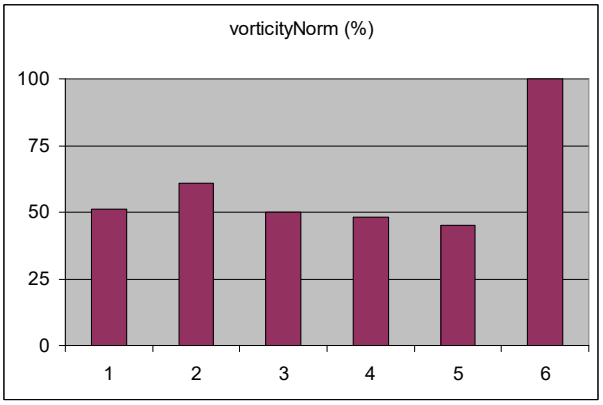

Figure 4. Vorticity Norm peaks in % compared to Kenics® static mixer.

In Fig. 7 oil retentions of the membrane are introduced. Consecutively the No. 3 promoter showed the best, industrially acceptable separation of emulsified oil droplets, especially on 100 L/h and 1 bar TMP. It is also

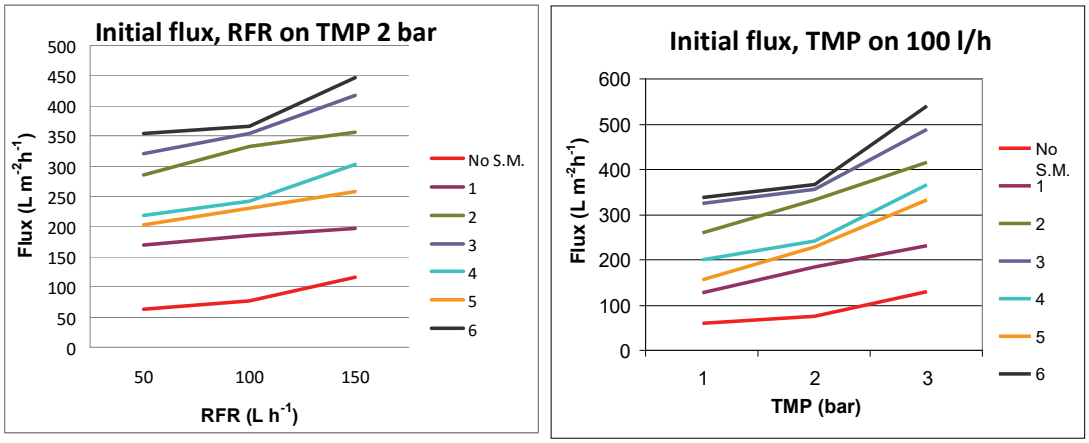

Figure 5. Initial flux vs RFR (left), Initial flux vs. TMP (right).

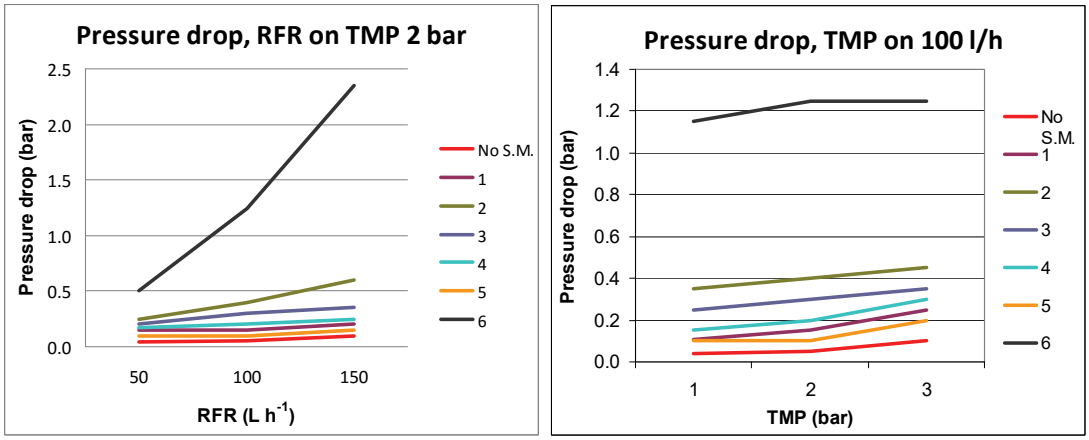

Figure 6. Pressure drop along membrane vs. RFR (left) and pressure drop vs. TMP (right).

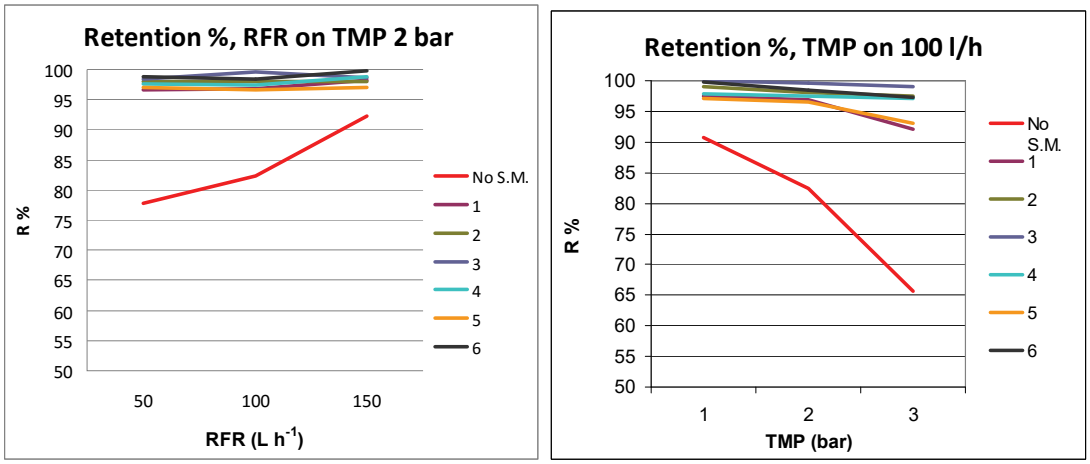

Figure 7. Retention % vs. RFR (left) and Retention % vs. TMP (right).

obvious that the traditionally used empty tube membrane could not ensure satisfying separation of the oil (No S.M.). It can be also seen in Fig. 7 that all of the package could greatly increase retention of the membrane, but since the environmental limit is very strict, some of the results are still not good enough.

Based on the above mentioned result, because of its high flux, low energy demand and high increase of oil retention, static mixer No. 3 is an ideal choice, if productive and sustainable technology is required for stable oil-in-water emulsion separation. The results of CFD analysis is validated with laboratory experiments.

CONCLUSIONS

Computational fluid dynamics is a method with great potential in the prediction of turbulence intensity inside a tubular membrane filter. In present work cross-flow velocity was modelled successfully within a tube packed with differently shaped static turbulence promoters. The model could help to better understand flow regime phenomena caused by different inline static mixers. The method pointed clearly out the advantage of Kenics® FMX type promoter in operations where mixing is a main target, but the simulation also suggested the solution for membrane separation purposes. As far as the CFD still not including the transport through the pores of the membrane, so this is an area with a need for further development in recent algorithms. In future work, the pressure analysis of the same problem with CFD is planned. In order to validate CFD results, the laboratory experiments were also carried out. Within the investigated range, using any of 5 new static mixers showed good improvement for permeate flux and retention of the oil and pressure drop along membrane was significantly reduced using optimised types of turbulence promoters compared with Kenics® static mixer and the empty tube. The experimental data suggests that, for ultrafiltration of stable oil-in-water microemulsion, turbulence promoter No. 3 has best performance (spiral, $d \cong h$).

REFERENCES

[1] A. Ezzati, E. Gorouhi, T. Mohammadi, Separation of water in oil emulsions using microfiltration, Desalination **185** (2005) 371–382.

[2] MSZ EN ISO 9377-2, Water quality – Determination of hydrocarbon oil index **(**2001) (Hungarian Standard – in Hungarian).

[3] D.M. Krstić, W. Höflinger, A. Koris, G. Vatai, Energy-saving potential of cross-flow ultrafiltration with inserted static mixer: Application to an oil-in-water emulsion, Sep. Purif. Technol. **57** (2007) 134-139

[4] I. Gaspar, A. Koris, C. Dechambre, S. Koskinen, G. Vatai, Effects of the static mixer's geometry on the intensified ultrafiltration of oil-in-water emulsions**,** Synergy in the Technical Development of Agriculture and Food Industry, Book of abstracts, 2011, pp. 26

[5] B. Xia, D.W. Sun, Application of CFD in the food industry: a review, Comput. Electron. Agric. **34** (2002) 5–24.

[6] D.W. Sun, Computational Fluid Dynamics in Food Processing, CRC Press Taylor & Francis Group, Boca Raton, FL, 2007.

[7] S. Sauro, The Lattice Boltzmann Equation for Fluid Dynamics and Beyond, Oxford University Press, Oxford, 2001.

[8] optilb.org Open Source Lattice Boltzmann Code, now on new web address: optilb.com.

[9] ParaView, www.paraview.org.

IZVOD

CFD I LABORATORIJSKA ANALIZA AKSIJALNE BRZINE PROTOKA KROZ POROZNE CEVI SA PROMOTERIMA TURBULENCIJE RAZLIČITE GEOMETRIJE

Igor Gaspar[1], Predrag Tekic[2], Andras Koris[1], Albert Krisztina[1], Svetlana Popovic[2], Gyula Vatai[1]

[1]*Corvinus University of Budapest, Department of Food Engineering, H-1118 Budapest, Menesi st. 44, Hungary*
[2]*University of Novi Sad, Bulevar Cara Lazara 1, 21000 Novi Sad, Serbia*

(Naučni rad)

Kompjuterska dinamika fluida (*computational fluid dynamics*, CFD) je primenjena za modelovanje režima protoka u poroznoj cevi. Porozna cev je membrana sa aktivnim slojem od cirkonijum-oksida, koja služi za razdvajanje stabilne mikroemulzije ulje-u-vodi, a čija se efikasnost povećava kada se u cev ubace statički mešači. Rezultati CFD analize su primenjeni za preliminarnu optimizaciju geometrije statičkog mešača, budući da ona ima značajan uticaj na količinu utrošene energije pri unakrsnoj ultrafiltraciji. Statički mešači razvijeni u našoj laboratoriji, eksperimentalno su testirani sa aspekta kvaliteta i efikasnosti procesa separacije i dobijeni rezultati su upoređeni sa rezultatima CFD analize, a sve sa ciljem da se razvije ekonomski efikasan i ekološki prihvatljiv način prečišćavanja otpadnih zauljenih voda. U radu se diskutuju rezultati dobijeni kompjuterskom simulacijom protoka i brzine fluida i eksperimentalni rezultati membranske separacije uz primenu statičkih mešača.

Ključne reči: Ultrafiltracija • Emulzija ulje-u-vodi • Kompjuterska dinamika fluida • Statički mešači

SADRŽAJ VOLUMENA 69.

Sveska 1

Sveska 2

Sveska 3

Sveska 4

Sveska 5

Sveska 6

INDEKS AUTORA 2015